



UNIVERSITA' DEGLI STUDI DI MILANO

Scuola di Dottorato in Scienze e Tecnologie Chimiche

Dipartimento di Scienze Farmaceutiche

Dottorato di Ricerca in Chimica del Farmaco

XXVII Ciclo

**HIGH RESOLUTION MASS SPECTROMETRIC STRATEGIES FOR
DETECTION OF PROTEINS AND PEPTIDES COVALENTLY
MODIFIED BY ELECTROPHILIC XENOBIOTICS AND
ENDOGENOUS INTERMEDIATES**

(CHIM/08)

Candidato

Dott. Davide Garzon

Matr. n. R09560

Docente Guida: Prof. Giancarlo ALDINI

Coordinatore: Prof. Ermanno VALOTI

(A.A. 2013/2014)

Index

1 Foreword	1
2 Introduction on β-lactam antibiotics protein haptentation	3
2.1 Adverse Drug Reaction	3
2.2 Idiosyncratic reactions (IDRs)	4
2.3 Hapten hypothesis	6
2.4 Danger hypothesis	8
2.5 Pharmacological interaction hypothesis	9
2.6 Review of the methodological approaches used to study the interaction between protein and β- lactams antibiotics	10
<i>2.6.1 From the first studies to immunoenzymatic techniques</i>	10
<i>2.6.2 The advent of mass spectrometry and chromatography hyphenated techniques</i>	19
2.7 References	27
3 Protein haptentation by amoxicillin: high resolution mass spectrometry analysis and identification of target proteins in serum	31
3.1 Introduction	33
3.2 Materials and Methods	37
3.2.1 Reagents	37
3.2.2 In vitro modifcaion of synthetic HSA peptides by AX	37

<i>3.2.3 In vitro modification of HSA or serum proteins by AX</i>	38
<i>3.2.4 SDS-PAGE electrophoresis and Western blot</i>	38
<i>3.2.5 Two-dimensional electrophoresis and protein identification</i>	39
<i>3.2.6 Mass spectrometry analysis of AX-modified HSA by MALDI-TOF</i>	41
<i>3.2.7 Direct infusion electrospray mass spectral analysis (ESI-MS): LTQ XL Orbitrap mass spectrometer</i>	42
<i>3.2.8 Liquid chromatography electrospray ionization mass spectrometry/mass spectrometry analysis (LC-ESI-MS/MS): LTQ Orbitrap XL mass spectrometer</i>	43
<i>3.2.9 Bioinformatics</i>	45
<i>3.2.10 Molecular modelling</i>	46
3.3 Results	48
<i>3.3.1 Detection of AX-HSA adducts by western blot</i>	48
<i>3.3.2 Immunological detection of AX-modified HSA with various anti-β-lactam antibodies</i>	49
<i>3.3.3 Detection of AX candidate target proteins in human serum</i>	50
<i>3.3.4 AX reaction with His, Lys and Cys containing peptides from HSA</i>	54
<i>3.3.5 AX reaction with HSA: top-down experiments</i>	60
<i>3.3.6 Identification of the HSA sites modified by amoxicillin: bottom-up experiment</i>	63
<i>3.3.6.1 Identification of the sites modified by AX in purified HSA</i>	66
<i>3.3.6.2 Identification of the sites modified by AX in HSA in complete human serum</i>	68
<i>3.3.7 Peptide consumption</i>	68
<i>3.3.8 Molecular modelling</i>	71

3.4 Discussion	76
3.5 References	80
4 Mass spectrometric strategies for the identification and characterization of Human Serum Albumin covalently adducted by Amoxicillin: ex vivo studies	83
4.1 Introduction	86
4.2 Material and methods	89
<i>4.2.1 Reagents</i>	89
<i>4.2.2 AX administration, serum collection and HSA isolation</i>	89
<i>4.2.3 HSA isolation</i>	90
<i>4.2.4 In vitro modification of serum proteins by AX</i>	90
<i>4.2.5 HSA protein digestion for LC-ESI-MS analysis</i>	91
<i>4.2.6 Multiple Reaction Monitoring and Precursor Ion Scan analyses</i>	92
<i>4.2.7 Liquid chromatography electrospray ionization mass spectrometry/mass spectrometry analysis (LC-ESI-MS/MS): LTQ Orbitrap XL mass spectrometer</i>	94
<i>4.2.8 Bioinformatics</i>	97
4.3 Results	99
<i>4.3.1 Detection of AX-HSA adducts in human serum by Multiple Reaction Monitoring and Precursor Ion Scan: LC-ESI-MS/MS studies</i>	99
<i>4.3.2 Detection of AX-HSA adducts by LC-MS/MS Orbitrap</i>	104
<i>4.3.2.1 Customized targeted MS/MS mode</i>	104

4.3.3 <i>Comparing MS approaches with immunological methods</i>	111
4.4 Discussion	113
4.5 References	116
5 Carnosine and derivatives as inhibitors of protein covalent modifications induced by reactive carbonyl species	119
5.1 Reactive carbonyl species and protein covalent modification	120
5.1.1 <i>α,β-unsaturated aldehydes</i>	123
5.1.2 <i>Di-aldehydes</i>	125
5.1.3 <i>Keto-aldehydes</i>	127
5.2 Biological implications of RCS induced protein covalent modifications	129
5.2.1 <i>Protein function derangement</i>	129
5.2.2 <i>The antigenic properties of RCS protein adducts</i>	130
5.2.3 <i>The damaging AGEs-RAGE axis</i>	131
5.2.4 <i>The amyloidogenic properties of RCS protein adducts</i>	131
5.3 Endogenous detoxification of RCS	132
5.3.1 <i>phase I metabolism</i>	132
5.3.2 <i>phase II metabolism</i>	134
5.3.3 <i>Carnosine and histidine dipeptides as RCS sequestering agents</i>	134
5.4 In vitro studies	136
5.4.1 <i>α,β-unsaturated aldehydes</i>	137
5.4.2 <i>Di-aldehydes and ketoaldehydes</i>	142

5.5 In vivo studies	143
5.6 Carnosine derivatives as a novel class of bioactive compounds	151
5.7 Conclusions	154
5.8 Summary points	155
5.9 Definitions of words and terms	156
5.10 References	158
6 Intervention study of Carnosine in obese volunteers: bioavailability and reactive carbonyls species sequestering effect	165
6.1 Introduction	166
6.2. Materials and Methods	169
6.2.1. Chemicals and Reagents	169
6.2.2 Biological samples used as the matrix for calibration curves	170
6.2.3 Supplementation study design	170
6.2.4 Carnosine-RCS adducts quantification in urine	171
6.2.4.1 Carnosine-RCS adducts preparation	171
6.2.4.2 Carnosine-RCS calibration curves	173
6.2.4.3 Ex vivo urine samples preparation for CAR-RCS adducts detection and quantification	173
6.2.4.4 Liquid chromatography electrospray ionization mass spectrometry/mass spectrometry analysis (LC-ESI-MS/MS): LTQ Orbitrap XL mass spectrometer	174
6.2.4.4.1 Orbitrap data-dependent scan and targeted scan	175
6.2.5 Carnosine quantification in urine and plasma	177

<i>6.2.5.1 Calibration curves in urine and plasma</i>	177
<i>6.2.5.2 Ex vivo sample preparation for CAR quantification in urine and plasma</i>	178
<i>6.2.5.3 Liquid chromatography electrospray ionization multiple reaction monitoring analysis (LC-ESI-MRM): TSQ mass spectrometer</i>	178
6.2.6 Intact protein analysis of plasma to profile human plasma albumin	180
<i>6.2.7 Fluorescence and UV-vis assays for urine samples quantification of total protein, Advanced Glycation End products (AGE) and creatinine</i>	181
<i>6.2.8 Fluorescence and UV-vis assays for plasma samples quantification of total protein, Advanced Glycation End products (AGE), Advanced Oxidation Protein Products (AOPP), Protein Carbonyls (PCO) and Carboxy Methyl Lysine (CML)</i>	182
<i>6.2.9 informatics</i>	183
6.3 Results	186
<i>6.3.1 Carnosine-RCS-adducts preparation and quantification</i>	186
<i>6.3.2 Preliminary LC-Orbitrap-MS/MS analysis for adduct identification</i>	191
<i>6.3.3 Carnosine propanal and Carnosine propanol calibration curves in urine</i>	198
<i>6.3.4 Carnosine propanal and Carnosine propanol determination in urine samples of overweight/obese individuals</i>	203
<i>6.3.5 Carnosine determination in urine and plasma</i>	205

6.3.6 Top down ESI-MS analysis of albumin's isoforms	212
6.3.7 Creatinine determination in urine	215
6.3.8 Advanced Glication End products (AGE) in urine and plasma	216
6.3.9 Carboxymethyl lysine (CML)in plasma	218
6.3.10 Advanced Oxidation Protein Products (AOPP) in plasma	219
6.3.11 Protein Carbonyl (PCO) in plasma	220
6.3.12 Statistical Analysis: T test	221
6.3.12.1 Free carnosine t test results	222
6.3.12.2 CAR-propanal t test results	225
6.3.12.3 Correlation between CAR-ACR adducts and CAR concentration in urine	228
6.3.13 Statistical analysis: Principal Component Analysis (PCA)	229
6.3.13.1 PCA on urinary analytes before carnosine administration	230
6.3.13.2 PCA on urinary analytes after carnosine administration	234
6.4 Discussion and conclusions	237
6.5 References	242
7 Conclusions	245
7.1 References	249
8 Scientific activity during the Ph.D course	250

1 Foreword

Protein covalent modification and the consequent protein function modulation represent a key molecular mechanism for several drugs, belonging to different therapeutic classes, such as anti-inflammatory, antibiotic and chemotherapeutic agents. Indeed, protein covalent adducts formation is involved in the toxic mechanisms of electrophilic xenobiotics as well as of endogenous cytotoxic mediators. For instance, both the beneficial effects and the adverse drug reaction of beta-lactams involve protein covalent binding. In particular, the β -lactam nucleus acylates the Ser403 residue of the peptidoglycan layer of bacterial cell walls thus blocking the cell wall synthesis. Moreover, β -lactam nucleus can covalently react with lysine residues of albumin and generate haptens able to induce an immune-mediated adverse reaction. Identification and characterization of protein adducts also represents a promising approach for the identification of novel drug target. In particular, several endogenous harmful agents such as electrophilic prostaglandins or lipid-glucose oxidation products, react with some target proteins inducing a cascade of toxic effects. Hence the identification of protein targets as well as of the electrophilic agents represent a promising strategy for the discovery of novel bioactive compounds. Based on these premises, it is well clear that the identification and characterization of covalent protein adduct, especially when formed in biological matrices, is a very stimulating analytical challenge, and of great importance in the different branches of the drug discovery program, such as the elucidation of reaction mechanisms, prediction of potential idiosyncratic agents and identification of novel drug targets.

1 Foreword

Among the different analytical techniques so far employed, mass spectrometry has attained a central role because of the wealth of structural and molecular information that can be obtained. Regarding protein covalent binding, the MS approach not only reveals the identity of the adducted protein but also clarifies the stoichiometry of reaction, the aminoacidic site undergoing biotransformation, the reaction products and hence the mechanism of reaction. More recently, the advent of high resolution MS analyzer such as the orbitrap, characterized by a significant increase of resolution and accuracy in respect to the well established MS analyzers such as ion trap, quadruple or time of flight, together with novel stationary phases and column dimension which have significantly improved the efficacy and resolution of chromatographic separation, has opened novel frontiers in the identification and characterization of covalently modified proteins also when present in trace amount and in crude biological systems such as cells or tissues.

Considering these issues, aim of my Ph.D work was to set-up MS methods for the identification, characterization and quantification of non-enzymatic covalently modified proteins and peptides in biological matrices. To reach this goal both tandem MS and high resolution approaches were employed due to the wealth of structural and molecular information that these techniques can provide. As a first step the MS methods were applied for understanding in both in vitro and ex vivo conditions the mechanism of protein haptention induced by amoxicillin (AX). The MS approach was then focused to study in ex vivo condition the covalent reaction between histidine dipeptides, such as carnosine, and toxic endogenous intermediates like reactive carbonyl species (RCS)

2 Introduction on β -lactam antibiotics protein haptentation

2.1 Adverse Drug Reaction

Adverse drug reactions (ADRs) are a major problem in clinical practice. These are defined by the World Health Organization (WHO) as any noxious, unintended and undesired effect of a drug that occurs at doses used for prevention, diagnosis and treatment of a given disease.

In addition, any drug may be harmful to the organism. It has been estimated that 3-5% of all hospital admissions are caused by adverse drug reactions, and this results in 300,000 people hospitalized each year in the USA. The most serious cases in which the patient's life is in danger are around 3% concerning in hospital therapy and around 0.4% in the classical therapy at home. It should be emphasized that the side effects are the primary cause of iatrogenesis. [1]

Drug reactions are frequently classified as type A and type B reactions, however in the last years a more detailed classification system have been drawn. Type A reactions stand for “augmented” and are reactions resulting from an exaggeration of the drug pharmacological effect and are normally dose-dependent, for example respiratory depression with opioids or bleeding with warfarin. These reactions account for the 80% of the all ADRs and are usually identified by toxicological preclinical test [2].

Type B reactions stand form “bizzare” and concern novel adverse drug reactions that happen rarely, they are not predictable by preclinical and clinical studies and can take place at any therapeutic dose. These are usually defined also as idiosyncratic. Examples includes anaphylaxis with penicillin or skin rashes with antibiotics, or angioedema caused by ACE inhibitors.

The new classification includes also type C reaction, or continuing reactions that persist for a relatively long time as jaw osteonecrosis caused by bisphosphonates.

Then there are type D reactions that are delayed reactions that become apparent some time after the use of a medicine, for example leucopenia which can occur up to six weeks after a dose of lomustine. Finally there are type E reactions, or end of use reaction that are provoked by the withdrawal of the medicine as in the case of the insomnia and anxiety following the withdrawal of benzodiazepines.

Since the first part of this thesis will concern the interaction between amoxicillin and serum proteins, type B idiosyncratic reaction will be deeper examined.

2.2 Idiosyncratic reactions (IDRs)

The idiosyncratic reactions to drugs pose a major problem in clinical practice, the main adverse effects are: hepatotoxicity, mild or severe skin reactions, anaphylactic reactions, blood dyscrasia. Clinical evidence suggests that the idiosyncratic reactions are caused by reactive metabolites and are mostly immune-mediated; However the scientific community is still far from understanding the chemical and molecular processes involved in the idiosyncratic reactions. Specifically, among all adverse drug reactions, those based on immunological or allergic basis account for 6-10% of all ADRs [3].

The IDRs are the hardest obstacles to overcome in order to achieve the full development and market success of a drug. The 10.2% of the drugs approved from 1975 to 2000 have been withdrawn from the market or put in the black box warning [1].

The most significant problem is that many idiosyncratic reactions cannot be detected even in meticulous trials with a large number of subjects; and these are usually found in the monitoring phase after approval, even at long distance of time after the market introduction of the drug.

Since the IDRs are based on an immunological reaction to drug, these reactions require a sensitization period, during which the patient is exposed to the drug that stimulates the immune system by producing antibodies, sensitized T cells or both.

2 Introduction on β -lactam antibiotics protein haptentation

Allergic drug reactions are reproduced with a new drug exposure and are elicited at drug doses far below the therapeutic range, usually subsiding after drug discontinuation. As with hypersensitivity reactions in general, drug allergic reactions can be classified according to the categories defined by Gell and Coombs [4] which have been updated [5] and are as follows: type I or immediate hypersensitivity reactions mediated by drug-specific immunoglobulin Ig E antibodies; type II or cytolytic or cytotoxic reactions; type III or immune complex-mediated reactions and type IV or delayed hypersensitivity reactions (mediated by drug-specific T lymphocytes). Most of the allergic reactions to drug are IgE (type I) or T-cell mediated (type IV).

Even if any drug can induce an immune response, the drugs most affected by IDRs are antibiotics, in particular the IgE mediated immediate hypersensitivity reactions to β -lactams. Then there are many cases that involve NSAIDs especially used for inflammatory chronic pathologies where in particular it is still too difficult to identify the best tolerated therapy. Furthermore, there are allergic drug reactions also for anaesthetics and radiological contrast fluids; although less frequent, this IDRs constitute an important risk in surgical and diagnostic procedures.

Mechanistically, three main types of hypothesis attempt to explain immunological reactions to drugs. These are a) the hapten hypothesis, b) the danger hypothesis and c) the pharmacological interaction hypothesis.

These three main hypotheses are not to be considered distinct from the other one, as in the same context of allergic reaction they may act in a cooperative manner, giving as a final result a immunological reaction to that particular drug.

2.3 Hapten hypothesis

The formation of a drug-protein adduct plays generally an important role in its toxicity, especially concerning the immunological reactions to the drugs. Already in 1935 Karl Landsteiner stated that a small molecule is not able to induce an immune response unless already is or become chemically reactive and capable of binding to protein [6]. The classical theory states that the modified protein by the drug is seen as foreign agent (antigen) by the immune system.

The immune system in the early stages of development is able to differentiate "self" from "not-self" [7] and the drug itself is not recognized by the immune system due to the low molecular weight. On the contrary, the formation of a covalent adduct with the protein is recognized by the immune system as "not-self" and triggers the immune response. The drug modified protein is processed (hydrolyzed into peptide fragments) by antigen presenting cell (APC) and presented by the major histocompatibility complex (MHC) to T helper lymphocytes that will and activate CD8⁺ T cells (killer) and B lymphocytes that will start the immune response, as shown in figure 1.

The first mechanism of idiosyncratic reaction studied was the penicillin allergic reactions.[8] The β -lactam ring of penicillin irreversibly reacts with the free amino groups or sulfhydryl groups present in proteins. In some patients, this leads to an immune response against the penicillin-protein adduct. If the response produces a sufficient amount of IgE an anaphylactic reaction may be triggered. The mechanism of penicillin allergic reaction fits very well with the hapten hypothesis since the β -lactam group is an hapten itself, due to its high reactivity towards nucleophilic groups.

One of the major results of this theory is the use of prick test for the detection of patients prone to drug allergic reactions. In case of β -lactams, few drops of a polymer of lysine covalently linked to penicillin (BPO-Poly-Lys) is introduced in

2 Introduction on β -lactam antibiotics protein haptentation

skin by a needle: if the patient is allergic, it will form local redness and inflammation and in some worse cases also anaphylaxis.

In many cases, however, only the active metabolite of the drug can form covalent adducts with proteins, so the role of biotransformation is important in protein haptentation. As an example we can cite the case of anti-epileptic drug felbamate: the reactive metabolite 2-phenylpropenal form covalent adducts with human serum albumin (HSA), which is potentially involved in the formation of antigens [9].

Ultimately the understanding of the penicillin allergic reactions and the study of the haptent hypothesis are cornerstones for the study of other IDR.

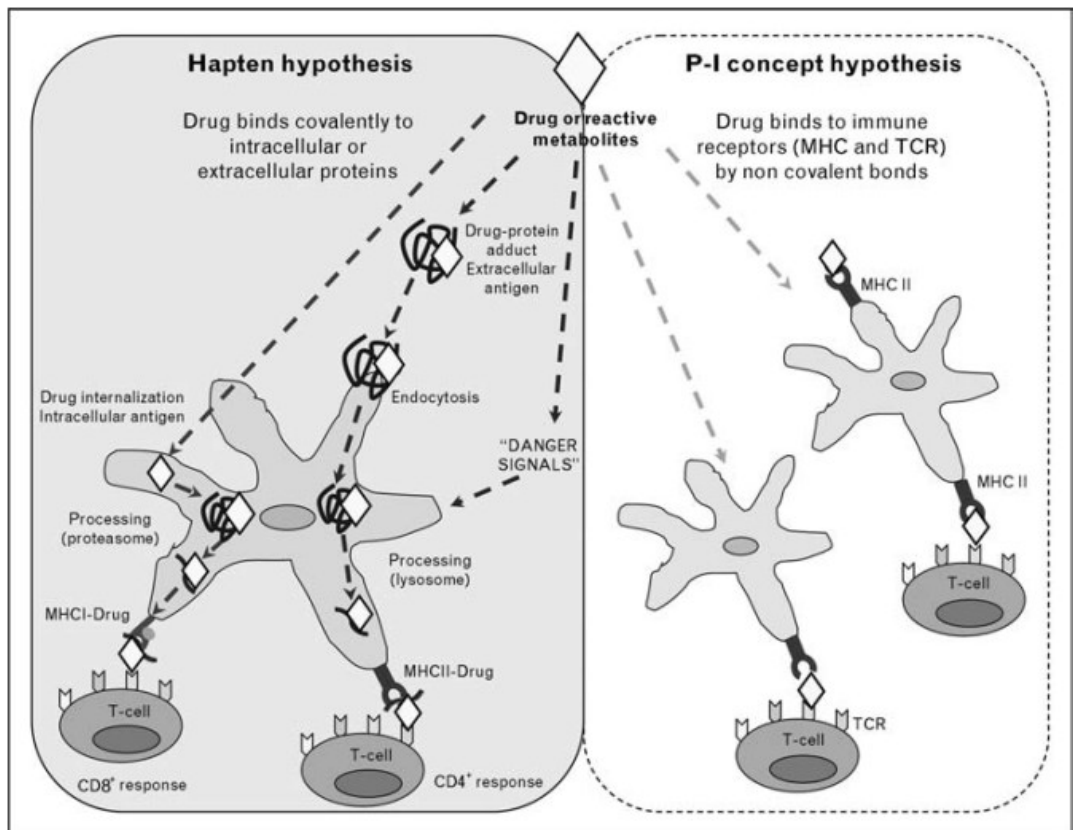


Fig. 1. On the right panel it is depicted the haptent hypothesis, instead on the left PI concept hypothesis is shown The picture is taken from Ariza et al [10].

2.4 Danger hypothesis

Although the hapten hypothesis is convincing, it should be noted that drug-protein adducts are often detected in tolerant patients, making the mechanism of develop drug allergy still a matter of debate. It was thought then that co-stimulatory signals are required to activate the immune system. These signals may be infections, exposure to endotoxin, stimulation by cytokines, metabolic alterations or drug toxicity. All of these have been called "danger signals"[11].

Matzinger et al proposed that the primary determiner of an immune response is not the "not self" condition of the antigen but rather the "damage" that this antigen can induce [12]. Fearon et al described that foreign proteins usually do not cause a significant immune response if they are not administered with an adjuvant; the first purpose of the adjuvant is the activation of the antigen presenting cell (APC). So without APC activation, the immune response can't be elicited [13].

The basis of the theory of Matzinger is that an organism cannot trigger an immune response against any "not self" protein, unless it's dangerous. For example human organism tolerate different bacteria that live in symbiosis with its body and moreover many proteins don't appear in the human organism until puberty [14].

Furthermore the theory states that, in case of a damage, the tissue itself will determine the nature of the immune response. The wound tissue will release danger signals that will activate the APC and trigger the immune response [15]. Several molecules have been proposed as a "danger signal" hydrophobic molecules (Hypos) and also proteins such as heat shock proteins (HSP) [16]

Extending this theory to the idiosyncratic reaction, it could happen that the drug itself or its metabolite causes cellular damage and then the release of "danger signal" can elicit an immune response [17, 18]. It is possible that other factors may contribute to the onset of idiosyncratic reaction such as infection or post-surgical

periods, however a linear correlation between a particular health conditions and increased incidence of IDRs have not been found.

The hapten and damage hypotheses can play a synergistic role in the formation of IDRs. In case of anaphylactic reactions induced by penicillins the hapten hypothesis is convincing, however it seems that the "danger signals" could have a primary role in stimulating the formation of a co-signal (B7) exposed by the APC on the cell surface: this co-signal eventually bind the T-helper lymphocyte (CD28) giving an indispensable contribution to its activation [17, 18].

2.5 Pharmacological interaction hypothesis

The pharmacological interaction hypothesis states that non-covalent interactions may be involved in the pathophysiology of immunological reactions: as shown in figure 1, right panel, the activation of the immune system would be mediated by the direct binding of drugs to typical receptors of the lymphocytes, such as the TCR, main receptor of the T cell and the major histocompatibility complex receptors (MHC). The binding is non-covalent therefore it is mediated by Van Der Waals forces, electrostatic forces and hydrogen bonds [19].

It is reported in literature that Pichler generated clones of T lymphocytes from patients having a history of IDRs to sulfamethoxazole and noticed that the cells proliferated in the presence of the drug. He proposed that some drugs may reversibly bind to the MHC complex of T helper cells, and in some cases this can lead to IDRs. Furthermore it is known that many metals such as nickel or beryllium can cause allergic reactions, by reversibly binding to the MHC [20].

2.6 Review of the methodological approaches used to study the interaction between protein and β - lactams antibiotics

2.6.1 From the first studies to immunoenzymatic techniques

The first clinical cases of allergy induced by β - lactam antibiotics, in particular by penicillin G, were firstly published around 1945 [21], but in the sixties the scientific community began to study the identity of the antigenic determinants responsible for hypersensitivity to penicillin G.

In a paper published in 1961 Levine and Ovary incubated γ -globulin, human serum albumin (HSA) and poly-L-Lysine with an excess of penicillin G [22]. The purpose was to show that human proteins could be covalently modified by the β - lactam antibiotic and elicit hypersensitivity reactions against penicillin G, based on Landsteiner hapten hypothesis [23].

They showed that these proteins were modified by means of alkaline hydrolysis of the penicilloyl group to get the benzyl-penicilloic acid. Afterwards the hydrolyzate was analyzed with thin layer chromatography (TLC) together with the benzyl-penicilloic acid standard. In order to confirm that the hydrolyzate contained benzyl-penicilloic acid (BPA) the authors relied on BPA retention factor and on the blue coloration that is created by adding mercury chloride and arsenic molibdate. Furthermore, after a purification step, the penicillin G treated proteins were incubated with anti-penicillin G antibodies: the formation of a precipitate confirmed the covalent modification of the proteins.

More modern techniques like electrophoresis and radio immunological assay (RIA) began to be used since the end of the sixties. In 1968 Arvan et al [24] reported that in patients treated with high concentrations of penicillin was observed a transient bisalbuminemia. The bisalbuminemia occurs when there are two types of serum albumin that differ in mobility during serum electrophoresis. The techniques used

were the electrophoresis on paper, electrophoresis on cellulose acetate and finally electrophoresis on agar gel. Figure 2 shows the paper electrophoresis (panel A), cellulose acetate electrophoresis (panel B) and agarose gel electrophoresis (panel C): it was clearly shown a definite separation between the faster and slower albumin. It was thought, therefore, that this effect was due to a covalent interaction between albumin and penicillin. In particular, it was suggested that it was caused by the covalent modification of the basic amino acidic residues by the penicilloyl group.

In 1979, Wal and Lapresle repeated [25] the experiment and confirmed that the fast albumin is covalently modified by penicillin. Two patients were treated with a high dose of penicillin G and then their serum was analyzed by agarose gel electrophoresis, resulting in the detection of the bisalbuminemia. Afterwards the fast and slow albumins were separated by chromatography with DEAE-Sephadex stationary phase. So the two albumins were analyzed using a radioimmunoassay (RIA) with antibodies specific for the penicilloyl group. The radioimmunoassay (RIA) used in this paper was developed in the article of the same Wal in collaboration with other researchers in 1975 [26].

In Wal method it was used as a labeled antigen I^{125} bovine albumin modified by penicilloyl groups (BPO-BSA- I^{125}). This labeled antigen was made to react in known quantity with a known and limiting amount of rabbit antibody, that recognize the penicilloylated-protein. Consequently there was a specific binding between the rabbit antibody and the the penicilloylated-protein. Then in the same tube the patient albumins, suspected to contain an unknown quantity of penicilloyl groups, were added. Hence the not labelled (cold) antigens of the patient compete with labeled (hot) antigens for the binding to the antibodies. The antigens bound to antibody are precipitated by means of a secondary sheep antibody that recognized the complex between rabbit antibody a the penicilloylated-protein. After 4 hours of incubation at 4 degrees, the mixture is centrifuged. Hence a pellet is obtained that is constituted by the antigen-antibody complex; instead the supernatant is formed by

the unbound antigen. In the method developed by Wal et al the radioactivity of the pellet is measured, hence the antigen-antibody complex: more albumin of the patient is modified by penicilloyl group, less the complex is radioactive. A calibration curve was set up by using known amounts of reagents and therefore the modified albumin present in the serum of patients were quantified. A calibration curve used to develop the analytical method is shown in fig 3. By means of this RIA, the authors proved that the penicilloyl modifications were on the fast albumin.

Wal examined in depth these studies and in 1980 published an article [27] in which the pronase B was used to partially degrade albumin and to expose penicilloyl groups making them more accessible to specific antibodies against this antigen. Thanks to this work Wal proved the existence of two different types of penicilloyl residues, characterized by a different accessibility to antibodies, different quantities and elimination kinetics. Wal thus opened new questions about the site and about the mechanism in which the albumin was modified by penicillin. Wal also started to examine the toxicological and pharmacological significance of penicilloyl groups localized within the albumin molecule.

At the same time Lapresle and Lafaye set up one of the first ELISA [28] test for the measurement of the penicilloyl groups. In this technique the alkaline phosphatase enzyme, linked to penicilloyl residues, was made to react with anti-penicilloyl antibodies fixed on a polystyrene plate. The plate was washed to remove non-specific binding. Then the alkaline phosphatase substrate was added, that is the p-nitrophenylphosphate. Hence the enzyme catalyzed a colorimetric reaction whose intensity is directly proportional to the amount of labelled penicilloyl groups bounded to the antibodies fixed on the plate. If in the serum some penicilloyl modified proteins were present, the reaction just described was inhibited and then there was a reduction in signal intensity directly proportional to the amount of penicilloyl groups present in human serum. By means of a calibration curve the penicilloyl groups were quantified up to a picomolar concentration. The authors

focused also the penicilloyl residue covalently bound to albumin, and they showed once again that after the treatment of albumin with a proteolytic enzyme, the amount of detected penicilloyl group increased.

The studies described up to now allowed to identify the isoform of albumin covalently modified by penicillin as well as to prove the presence of different modified residues within albumin, while it was not yet been identified nor the region of modification, nor the aminoacidic residues involved.

In 1987 Lafaye and Lepresle [29] identified what fragments of human albumin, obtained by digestion with CNBr, were modified by penicilloyl groups. In their paper the serum from a patient treated with high concentrations of penicillin G for 40 days were analyzed using a DEAE-Sephadex chromatography to separate the two albumin isoform. Then both the albumins were treated with CNBr to obtain the fragments that were subsequently reduced with 2-mercaptoethanol. The fragments that typically are obtained with the CNBr digestion of albumin are from N-terminal to C-terminal: B₁₋₁₂₃, C₁₂₄₋₂₉₈, A₂₉₉₋₅₈₅. In order to identify which one of the three fragments was modified by penicilloyl groups an ELISA test was used. It resulted that only the fragments C₁₂₄₋₂₉₈ and A₂₉₉₋₅₈₅ were identified as modified because they showed an inhibition and thus reducing the intensity of the ELISA test: by using a calibration curve the authors calculated that each fragment was modified by a penicilloyl residue. Moreover it resulted that the 2-mercaptoethanol treatment improved the detection of the penicilloyl residue and hence they deduced that disulfide bridge have an important role considering the inaccessibility of the modified residue.

This preliminary work was deepened by Yvon and Wal in 1988 [30]. Their paper focused on the identifying the penicilloylated residues on the C₁₂₄₋₂₉₈ fragment. Hence the albumin isolated from a patient treated with high concentration of penicillin was digested by CNBr and the resulting three fragments were separated by preparative chromatography. Hence the C₁₂₄₋₂₉₈ fragment was isolated and then reduced and alkylated on the Cys residues by 2-mercaptoethanol and then digested

by trypsin. The resulting peptide mixture was separated by preparative chromatography and each fraction was tested with a dedicated ELISA assay. The positive fraction was further separated by chromatography and once again each fraction was tested by ELISA. The new positive fraction was then sequenced by an automatic analyzer Biotronik LC 5000. The modified peptide was identified because the modified aminoacid was not recognized by the sequencer and moreover the possible modified peptide was tested again by ELISA, confirming the penicilloylation. Thanks to this analytical platform the researchers identified one modified residue on fragment C₁₂₄₋₂₉₈, that was Lys 199: this was the first time that a penicilloylated residue was identified.

Furthermore the authors emphasized the importance of the low pKa of the amino group of the Lys ϵ 199 that is approximately 7.9, unlike the other residues Lys in which typically the same amino group has a pKa of 11. The lower pKa facilitates the nucleophilic attack of the amine on the β -lactam ring: it is necessary that the amine is not charged because this reaction is favored. So more the pKa of the amine is close to the value of pH of the buffer and more the reaction is favored.

The same authors in 1989 published an article [31] in which they analyzed again fragment C₁₂₄₋₂₉₈, by applying a similar analytical platform of the previous article, but adding a further step of ionic exchange chromatography after the reverse phase preparative chromatography, as explained in fig.4. Hence the residues Lys 190, 195 and 199 were identified as penicilloylated. It is important to notice that each modified Lys is near to a Ser residue, spaced by two or three other aminoacids. For example Lys 190 is near to Ser 193, Lys 195 has Ser 192 and Lys 199 is near Ser 202. Moreover all these aminoacids are placed on an α -helix motif in which Lys and Ser are very near in the three dimensional space. All these findings supported the adduction mechanism proposed by Yamana [32], concerning the formation of penicilloylamidic determinants. This mechanism requires that the penicilloylation of the hydroxyl group of serine occurs very quickly, assisted by an acid-base catalysis towards the penicillin β -lactam to get the corresponding penicilloyl ester,

which is rapidly converted to a stable penicilloylamide thanks to the nucleophilic attack of a near Lys ϵ amino group. Furthermore the identified residues were placed on a very short fragment of 10 aminoacids localized in a junction between albumin domain 1 and domain 2. This flexible junction contains also high affinity binding site for salicylates, glucose and warfarine [33].

Finally in 1990 the authors completed the identification of the penicilloylated residues by analyzing the other fragment A₂₉₉₋₅₈₅, found positive for penicillin modification to the ELISA test. By means of the same analytical platform (fig. 4) used for the previous papers Lys, 432, 451 and 545 were found as modified. Moreover also the C₁₂₄₋₂₉₈ was analysed again and Lys 190, 195 and 199 were confirmed as penicilloylated. Hence finally the albumin of a patient, treated with high concentration of penicillin G, was found to have six lysine as modified [34].

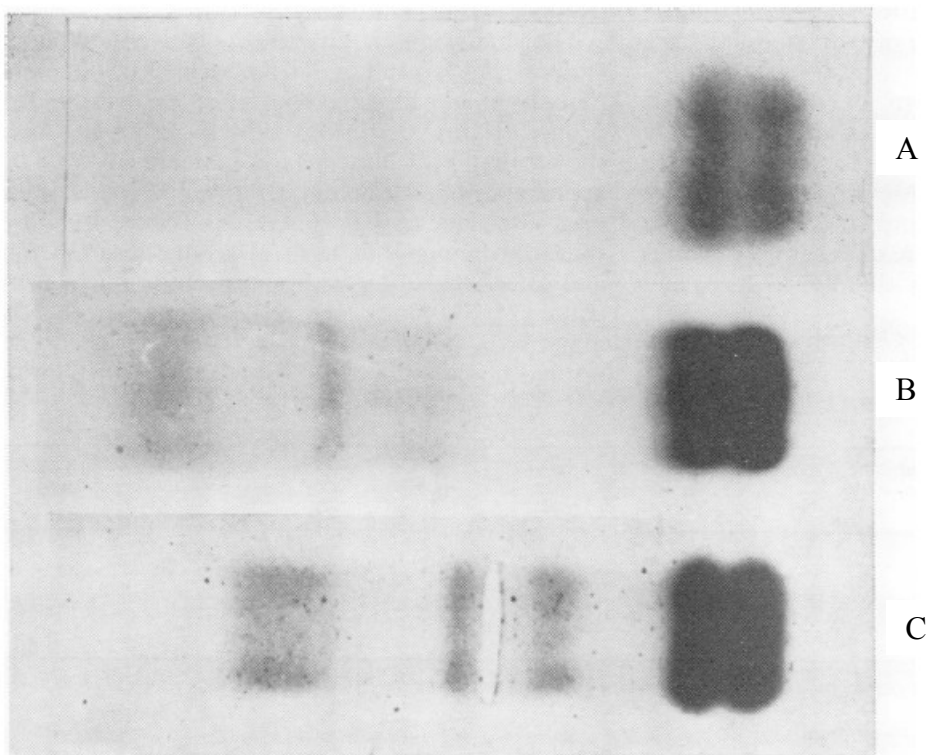


Fig. 2. Penicillin induced bisalbuminemia (25.000 units / mL). A) Paper electrophoresis B) Cellulose acetate electrophoresis C) Agar gel electrophoresis. The picture is taken from Arvan et al paper [24]

2 Introduction on β -lactam antibiotics protein haptentation

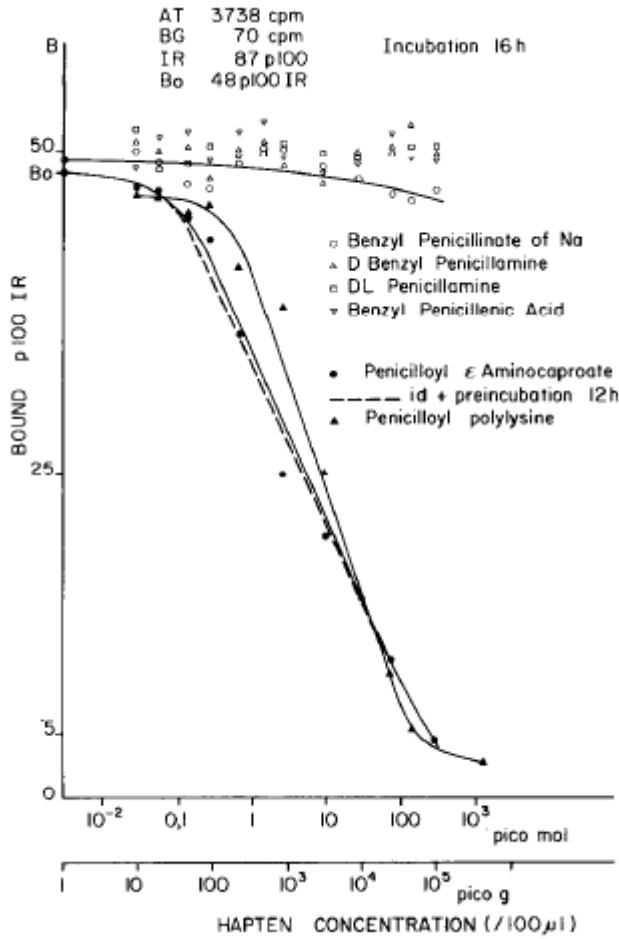


Fig. 3. Standard curves generated by RIA. The concentration of cold antigens are reported on the x axis, instead the radioactivity (cpm) of the antigen-antibody complex is reported on the y axis. Penicillin G and derivatives were used as cold antigens. It can be noticed that penicilloyl-aminocaproate and penicilloyl-polylysine displaced efficiently the labelled antigen BPO-BSA-I¹²⁵. Picture taken from Wal et al [26]

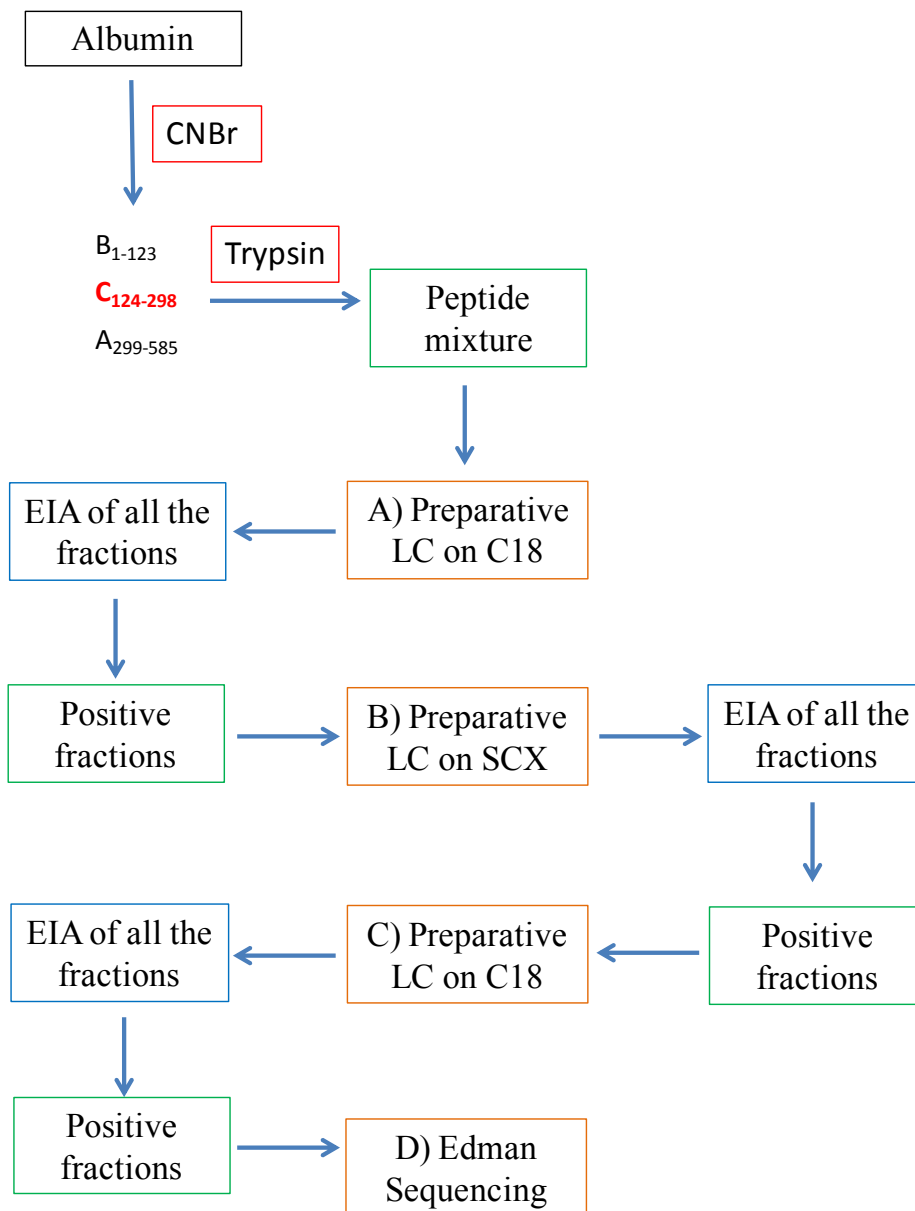


Fig. 4. Analytical platform used by Yvon et al. [31, 34]

2.6.2 The advent of mass spectrometry and chromatography hyphenated techniques

Until the late 80s mass spectrometry (MS) was rarely used for the analysis of protein and peptide mixtures, although these techniques could easily measure the molecular weight of a compound. Since the MS separates and detects ions in the gaseous phase it is necessary that the compounds to be analyzed may be ionized and converted into the gas phase by various ionization sources. In those days there weren't sources that could ionize and carry large and polar molecules in the gas phase without sample degradation.

Since 1982 the only ionization technique available was the Fast Atom Bombardment (FAB) and the analyzer used was a magnetic field. This instrumentation was rarely used given the high cost and the low sensitivity which required considerably higher amount of protein in respect to the automatic Edman degradation, routinely used at that time.

At the end of the 80s two new techniques of "soft" ionization were developed: the Electrospray Ionization (ESI) and Matrix Assisted Laser Desorption Ionization (MALDI) which enabled the acquisition of mass spectra of proteins and peptides with a quantity used in the order of picomoles. The MALDI sources were usually coupled to time of flight analyzers (TOF), while the analyzers coupled to ESI source were various: quadrupole, triple quadrupole, ion trap. The two last analyzers also permit to acquire the MS/MS spectra of any peptide and based on the fragmentation pattern, to identify the sequence. Thanks to these new mass spectrometers, the use of this technique grew rapidly in the field of proteomics, becoming the technique which is used routinely. In particular, nowadays, it is the standard technique in order to identify and sequence proteins, as well as to study the physiological post-translational modifications or induced by xenobiotic or endogenous electrophilic compounds. Mass spectrometry also allows to thoroughly

2 Introduction on β -lactam antibiotics protein haptentation

characterize the type of modification and the site of modification on protein: this information is of crucial importance in many fields of proteomics and drug development research.

Regarding the protein haptentation induced by β -lactam, one of the first paper employing mass spectrometry is that reporting the metabolism of the benzylpenicilloyl residues bound to albumin. The MS spectrometer was equipped with a FAB source and it was used to analyze the metabolites of benzyl penicilloyl group excreted in the urine, indicating that penicillin G conjugated to albumin was excreted as benzyl penicilloic acid more slowly than the free penicillin G.[19].

Only in 2000 human albumin treated with penicillin G was analyzed by ESI-MS: Bertucci et al in their paper used MS along with circular dichroism in order to assess if the penicilloylation of albumin modifies the secondary structure of the protein and the binding properties towards other drugs. The deconvoluted spectra of control albumin and treated albumin are reported in fig 5: panel a) shows the deconvoluted spectrum of control albumin characterized by a base peak relative to the mercapto-albumin characterized by a mass of 66463 Da. Panel b) shows the deconvoluted spectra of albumin incubated with penicillin G for 24 hours with a stoichiometric ratio albumin:penicillin G of 1:25. Compared to the control albumin, the spectrum is characterized by the presence of an additional peak with a relative abundance of about 50 % and characterized by a mass increment of 330 Da in respect to the mercaptoalbumin, due to the adduction of one molecule of penicillin G. As shown in panel c) and d) the increase of the incubation time is related to an increase of the relative content of the protein adducts. Moreover, although circular dichroism studies did not find differences regarding the secondary structure of penicilloylated albumin in respect to control albumin, it was observed that the binding affinity of the modified albumin towards a series of known ligands such as warfarin, diazepam and bilirubin, was drastically reduced compared to control albumin [35].

Ten years later, mass spectrometry was used to obtain novel important information concerning β -lactams haptentation. In 2011 Meng et al [36] reported the use of MS to evaluate the mechanism of reaction between human serum albumin and penicillin G and to identify the sites of modification. They isolated the albumin from the serum of patients treated with high concentration of penicillin G, then the protein was digested with trypsin and the peptides mixture was analyzed by reverse phase liquid chromatography coupled to a triple quadrupole in multiple reaction monitoring (MRM) analysis. Fourteen lysines were found modified by penicillin G, as listed in table 1. Moreover it was shown that penicillin G and benzyl-penicillenic acid formed diastereoisomers when bound to the albumin Lys residues. The different diastereoisomers were identified on the basis of their different interaction with the column stationary phase, leading to well distinguishable chromatographic peaks characterized by different retention times. This finding is significant because the immune system can discriminate between penicillin stereoisomers [37] and the authors suggested that this could be important in the diversity of immunogenic responses among different patients.

In 2009, the same research group [38] characterized the haptentation of human albumin by flucloxacillin both in vitro and in vivo. The flucloxacillin is an antibiotic resistant to penicillinases, especially used in infections with staphylococci. Similar to all β -lactam antibiotics, flucloxacillin can cause idiosyncratic reactions, and therefore, already in 2005, the consequent protein haptentation was studied with immunochemical techniques [39], which did not permit a complete structural characterization of the adducted moiety. By means of an analytical platform, already reported in the previous article, it was found that Lys 190 and 212 were the most reactive Lys residues, and that up to ten Lys residues were modified after incubating albumin with an higher concentration of flucloxacillin. When the albumin of patients treated with high doses of flucloxacillin was analyzed, nine Lys were found modified (table 2). It was evidenced that since the ϵ amino group of Lys 190 is characterized by a pKa of

7.42, it is not completely charged at physiological pH thus explaining its nucleophilic reactivity to the β -lactam ring. The pKa of the ϵ amino group of Lys 212 is 10.5, hence due to the fact that it is charged at physiological pH it should be not reactive: however on the basis of molecular modeling studies, the authors proposed that Lys 212 is reactive because the surrounding residues form a hydrophobic pocket where flucloxacillin non-covalently binds therefore becoming more available for the nucleophilic attack.

The research group extended the analytical strategy to study the haptentation of albumin isolated by patients treated with this flucloxacillin; the following four Lys were found to be modified: Lys 190, Lys 195, Lys 432 and Lys 541.

Figure 6 summarizes the data so far reported, showing a 3D model of human albumin where the main aminoacidic residues identified as target of the antibiotic covalent modification are highlighted: it can be noticed that among the nucleophilic residues, potential target of covalent modification and including His, Ser and Cys, only Lys was found to be modified. A possible explanation could be that only Lys forms stable reaction products, as suggested by Yvon et al.[34]

Based on the above reported review on the papers reporting the β -lactam protein haptentation, it can be noticed that penicillin G is the most studied antibiotic and albumin the protein target mostly considered and that only recently the interaction with other antibiotics was considered and among this amoxicillin whose detailed haptentation mechanism represents one of the aim of the PhD thesis.

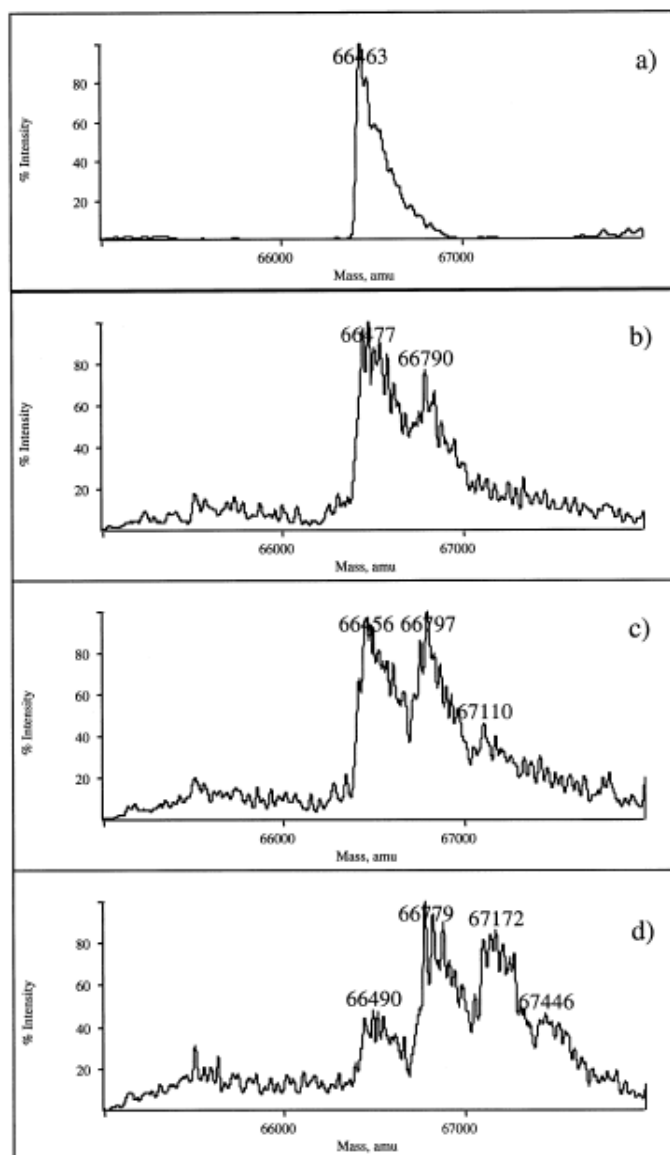


Fig. 5. Deconvoluted ESI mass spectra of defatted samples of HSA. a) After 4 days of incubation with an equimolar amount of penicillin G. b) After 1 day of incubation with 25:1 molar excess of penicillin G c) After 2 days of incubation with 25:1 molar excess of penicillin G. d) After 4 days of incubation with 25:1 molar excess of penicillin G. The number of adducts is directly proportional to penicillin G concentration and the period of incubation. Picture taken by Bertucci et al [35]

TABLE 1
Penicilloylated tryptic peptides of HSA identified in vitro and in vivo

Lysine	Peptide ^a	PA ^b	BP ^c	In patient
20	FK*DLGEENFK	+	+	+
137	K*YLYEIAR	+	+	+
159	HPYFYAPELLFFAK*R	+	+	+
162	YK*AAFTECCQAADK	+	-	-
190	LDEL RDEGK*ASSAK	+	+	+
195	ASSAK*QR	+	+	+
199	LK*CASLQK	+	+	+
212	AFK*AWAVAR	+	+	+
351	LAK*TYETTLEK	+	+	+
372	VFDEFK*PLVEEPQNLIK	+	-	+
432	NLGK*VGSK	+	+	+
436	VGSK*CCK	+	-	+
475	VTK*CCTESLVNR	+	-	-
525	K*QTALVELVK	+	+	+
541	ATK*EQLK	+	+	+
545	EQLK*AVMDDFAAFVEK	+	+	+

^a *indicates modification site.

^b Incubation at PA HSA molar ratio of 1:1.

^c Incubation at BP HSA molar ratio of 10:1.

Tab. 1. The penicilloylated tryptic peptides found by Meng et al are reported [36]

A	Lysine	Peptide	Patient (no prefractionation)							
			1	2	3	4	5	6	7	8
	K137	KYLYEIAR	X	X	X	X	X	X	X	X
	K162	YK*AAFTECCQAADK	X	X	X	X	X	X	X	X
	K190	LDEL RDEGK*ASSAK	√	√	√	√	√	√	√	√
	K195	ASSAK*QR	X	X	X	X	X	X	X	X
	K199	LK*CASLQK	X	X	X	X	X	X	X	X
	K212	AFK*AWAVAR	√	√	√	√	√	√	√	√
	K351	LAK*TYETTLEK	X	X	X	X	X	X	X	X
	K432	NLGK*VGSK	X	√	X	X	√	X	X	X
	K525	K*QTALVELV K	X	X	X	X	X	X	X	X
	K541	ATK*EQLK	X	X	√	X	X	X	X	X

B	Lysine	Peptide	Patient (+CEX of peptides)							
			1	2	3	4	5	6	7	8
	K137	KYLYEIAR	√	X	√	X	√√	X	X	√√
	K162	YK*AAFTECCQAADK	X	√	X	X	X	X	X	X
	K190	LDEL RDEGK*ASSAK	√√	√√	√√	√	√√	√√	√√	√√
	K195	ASSAK*QR	√	X	√	X	√	√	√	√
	K199	LK*CASLQK	√√	√	√	X	√√	√	√√	√
	K212	AFK*AWAVAR	√√	√	√√	√	√√	√√	√	√√
	K351	LAK*TYETTLEK	√	√	√	X	√√	√	√√	√√
	K432	NLGK*VGSK	√	√	√	√	√√	√	√√	√√
	K525	K*QTALVELVK	√	X	√√	X	√√	√√	√√	√√
	K541	ATK*EQLK	√√	√	√√	X	√√	√√	√√	√√

Tab. 2. In table A the flucloxacillin modified peptides found with no pre fractionation are reported, instead in table B there are the modified peptides found after pre fractionation on cationic exchange column. [38]

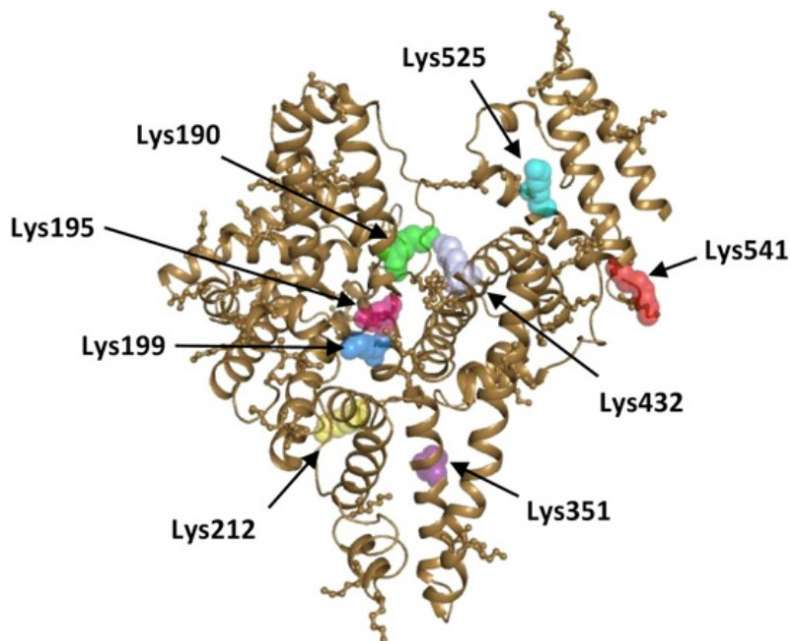


Fig. 6. Main aminoacid residues found modified in the studies regarding penicillin G, flucloxacillin and piperacillin haptentation.

2.7 References

1. Brunton L, Chabner B, Knollman B. Goodman & Gilman's The Pharmacological basis of Therapeutics. 12th ed; 2011.
2. Olson H, Betton G, Robinson D, Thomas K, Monro A, Kolaja G, et al. Concordance of the toxicity of pharmaceuticals in humans and in animals. *Regul Toxicol Pharmacol*. 2000 Aug;32(1):56-67.
3. Bates DW, Spell N, Cullen DJ, Burdick E, Laird N, Petersen LA, et al. The costs of adverse drug events in hospitalized patients. Adverse Drug Events Prevention Study Group. *JAMA*. 1997 1997 Jan 22-29;277(4):307-11.
4. Coombs RR. The basic types of allergic reactivity producing disease. *Triangle*. 1969;9(2):43-7.
5. Pichler WJ. Delayed drug hypersensitivity reactions. *Ann Intern Med*. 2003 Oct;139(8):683-93.
6. Landsteiner K, Jacobs J. STUDIES ON THE SENSITIZATION OF ANIMALS WITH SIMPLE CHEMICAL COMPOUNDS. *J Exp Med*. 1935 Apr;61(5):643-56.
7. Langman RE, Cohn M. Self-nonsel self discrimination revisited. Introduction. *Semin Immunol*. 2000 Jun;12(3):159-62.
8. PARKER CW, THIEL JA. STUDIES IN HUMAN PENICILLIN ALLERGY: A COMPARISON OF VARIOUS PENICILLOYL-POLYLYSINES. *J Lab Clin Med*. 1963 Sep;62:482-91.
9. Roller SG, Dieckhaus CM, Santos WL, Sofia RD, Macdonald TL. Interaction between human serum albumin and the felbamate metabolites 4-Hydroxy-5-phenyl-[1,3]oxazinan-2-one and 2-phenylpropenal. *Chem Res Toxicol*. 2002 Jun;15(6):815-24.
10. Ariza A, Montañez MI, Pérez-Sala D. Proteomics in immunological reactions to drugs. *Curr Opin Allergy Clin Immunol*. 2011 Aug;11(4):305-12.
11. Lavergne SN, Wang H, Callan HE, Park BK, Naisbitt DJ. "Danger" conditions increase sulfamethoxazole-protein adduct formation in human antigen-presenting cells. *J Pharmacol Exp Ther*. 2009 Nov;331(2):372-81.
12. Matzinger P. Tolerance, danger, and the extended family. *Annu Rev Immunol*. 1994;12:991-1045.

13. Fearon DT. Seeking wisdom in innate immunity. *Nature*. 1997 Jul;388(6640):323-4.
14. Matzinger P. An innate sense of danger. *Ann N Y Acad Sci*. 2002 Jun;961:341-2.
15. Harris HE, Raucchi A. Alarmin(g) news about danger: workshop on innate danger signals and HMGB1. *EMBO Rep*. 2006 Aug;7(8):774-8.
16. Seong SY, Matzinger P. Hydrophobicity: an ancient damage-associated molecular pattern that initiates innate immune responses. *Nat Rev Immunol*. 2004 Jun;4(6):469-78.
17. Pirmohamed M, Naisbitt DJ, Gordon F, Park BK. The danger hypothesis--potential role in idiosyncratic drug reactions. *Toxicology*. 2002 Dec;181-182:55-63.
18. Séguin B, Uetrecht J. The danger hypothesis applied to idiosyncratic drug reactions. *Curr Opin Allergy Clin Immunol*. 2003 Aug;3(4):235-42.
19. Christie G, Kitteringham NR, Park BK. Drug-protein conjugates--XIII. The disposition of the benzylpenicilloyl hapten conjugated to albumin. *Biochem Pharmacol*. 1987 Oct;36(20):3379-85.
20. Pichler WJ. Pharmacological interaction of drugs with antigen-specific immune receptors: the p-i concept. *Curr Opin Allergy Clin Immunol*. 2002 Aug;2(4):301-5.
21. MACEY HB, HAYS TG. Allergic reactions to penicillin therapy; report of cases. *U S Nav Med Bull*. 1945 Dec;45:1143-6.
22. LEVINE BB, OVARY Z. Studies on the mechanism of the formation of the penicillin antigen. III. The N-(D-alpha-benzylpenicilloyl) group as an antigenic determinant responsible for hypersensitivity to penicillin G. *J Exp Med*. 1961 Dec;114:875-904.
23. Landsteiner K, Harte RA. ON GROUP SPECIFIC A SUBSTANCES : IV. THE SUBSTANCE FROM HOG STOMACH. *J Exp Med*. 1940 Mar;71(4):551-62.
24. Arvan DA, Blumberg BS, Melartin L. Transient "bisalbuminemia" induced by drugs. *Clin Chim Acta*. 1968 Oct;22(2):211-8.
25. C L, JM W. The binding of penicillin to albumin molecules in bisalbuminemia induced by penicillin therapy. In: *Service d'Immunochimie des Protéines IP, Paris 75015, France, editor. Biochim Biophys Acta; 1979. p. 6.*
26. Wal JM, Bories G, Mamas S, Dray F. Radioimmunoassay of penicilloyl groups in biological fluids. *FEBS Lett*. 1975 Sep;57(1):9-13.

27. Wal JM. Enzymatic unmasking for antibodies of penicilloyl residues bound to albumin. *Biochem Pharmacol.* 1980 Feb;29(2):195-9.
28. Lapresle C, Lafaye P. Enzyme-linked immunosorbent assay for measurement of penicilloyl groups. *Ann Inst Pasteur Immunol.* 1985 May-Jun;136C(3):375-82.
29. Lafaye P, Lapresle C. Location of penicilloyl groups on CNBr fragments of the albumin from penicillin-treated patients. *FEBS Lett.* 1987 Aug;220(1):206-8.
30. Yvon M, Wal JM. Identification of lysine residue 199 of human serum albumin as a binding site for benzylpenicilloyl groups. *FEBS Lett.* 1988 Nov;239(2):237-40.
31. Yvon M, Anglade P, Wal JM. Binding of benzyl penicilloyl to human serum albumin. Evidence for a highly reactive region at the junction of domains 1 and 2 of the albumin molecule. *FEBS Lett.* 1989 Apr;247(2):273-8.
32. Yamana T, Tsuji A, Miyamoto E, Kiya E. The reaction of benzylpenicillin with amines containing hydroxyl groups. *J Pharm Pharmacol.* 1975 Oct;27(10):771-4.
33. Kragh-Hansen U, Chuang VT, Otagiri M. Practical aspects of the ligand-binding and enzymatic properties of human serum albumin. *Biol Pharm Bull.* 2002 Jun;25(6):695-704.
34. Yvon M, Anglade P, Wal JM. Identification of the binding sites of benzyl penicilloyl, the allergenic metabolite of penicillin, on the serum albumin molecule. *FEBS Lett.* 1990 Apr;263(2):237-40.
35. Bertucci C, Barsotti MC, Raffaelli A, Salvadori P. Binding properties of human albumin modified by covalent binding of penicillin. *Biochim Biophys Acta.* 2001 Jan;1544(1-2):386-92.
36. Meng X, Jenkins RE, Berry NG, Maggs JL, Farrell J, Lane CS, et al. Direct evidence for the formation of diastereoisomeric benzylpenicilloyl haptens from benzylpenicillin and benzylpenicillenic acid in patients. *J Pharmacol Exp Ther.* 2011 Sep;338(3):841-9.
37. Nagata N, Hurtenbach U, Gleichmann E. Specific sensitization of Lyt-1+2-T cells to spleen cells modified by the drug D-penicillamine or a stereoisomer. *J Immunol.* 1986 Jan;136(1):136-42.
38. Jenkins RE, Meng X, Elliott VL, Kitteringham NR, Pirmohamed M, Park BK. Characterisation of flucloxacillin and 5-hydroxymethyl flucloxacillin haptentated HSA in vitro and in vivo. *Proteomics Clin Appl.* 2009 Jun;3(6):720-9.

39. Carey MA, van Pelt FN. Immunochemical detection of flucloxacillin adduct formation in livers of treated rats. *Toxicology*. 2005 Dec;216(1):41-8.
40. Ariza A, Garzon D, Abánades DR, de los Ríos V, Vistoli G, Torres MJ, et al. Protein haptentation by amoxicillin: high resolution mass spectrometry analysis and identification of target proteins in serum. *J Proteomics*. 2012 Dec;77:504-20.

3 Protein haptention by amoxicillin: high resolution mass spectrometry analysis and identification of target proteins in serum

Adriana Ariza^{a,b,1}, Davide Garzon^{c,1}, Daniel Ruiz-Abánades^{a,b}, Vivian de los Ríos^a, Giulio Vistoli^c, María J. Torres^b, Marina Carini^c, Giancarlo Aldini^{c*}, Dolores Pérez-Sala^{a*}

^aDepartment of Chemical and Physical Biology, Centro de Investigaciones Biológicas, C.S.I.C., Ramiro de Maeztu, 9, 28040 Madrid, Spain.

^bResearch Unit for Allergic Diseases, Fundación IMABIS-Hospital Carlos Haya, Málaga, Spain

^cDepartment of Pharmaceutical Sciences, Università degli Studi di Milano, via Mangiagalli 25, 20133, Milan, Italy

¹Contributed equally to this work

3 Protein haptentation by amoxicillin: high resolution mass spectrometry analysis and identification of target proteins in serum

ABSTRACT

Allergy towards wide spectrum antibiotics such as amoxicillin (AX) is a major health problem. Protein haptentation by covalent conjugation of AX is considered a key process for the allergic response. However, the nature of the proteins involved has not been completely elucidated. Human serum albumin (HSA) is the most abundant protein in plasma and is considered a major target for protein haptentation by various drugs, including β -lactam antibiotics. Here we have developed a procedure for immunological detection of AX-protein adducts with antibodies recognizing the lateral chain of the AX molecule. With this approach we detected human serum proteins modified by AX in vitro and identified HSA, transferrin and heavy and light chains of immunoglobulins as prominent AX-modified proteins. Since HSA was the major AX target, we characterized AX-HSA interaction using high resolution LTQ orbitrap mass spectrometry. At 0.5 mg/ml AX, we detected one main AX-HSA adduct involving residues Lys 190, 199 or 541, whereas higher AX concentrations elicited a more extensive modification. In molecular modelling studies Lys190 and Lys 199 were found the most reactive residues towards AX, with surrounding residues favouring adduct formation. These findings provide novel tools and insight for the study of protein haptentation and of the mechanisms involved in AX-elicited allergic reactions.

Keywords: drug allergy, β -lactam antibiotics, protein haptentation, amoxicillin binding, high resolution mass spectrometry, amoxicillin targets

Abbreviations: AX, amoxicillin; HSA, human serum albumin; ECL, enhanced chemiluminiscence

3.1 Introduction

The widely prescribed β -lactam antibiotics are among the drugs most frequently eliciting allergic reactions, thus posing an important clinical problem. In the most severe cases allergic reactions may be life-threatening and reduce the therapeutic options against infections. Protein haptentation plays a key role in immunological reactions to β -lactams. This process occurs through the nucleophilic opening of the β -lactam ring, generally by the attack of free amino groups in proteins, and gives rise to a penicilloyl-protein adduct which is able to elicit an immune response (reviewed in [1]). See Fig.1 for a schematic representation of the formation of an amoxicilloyl-protein adduct. Important efforts have been devoted towards the understanding of the pathogenic role of protein haptentation by β -lactams, the identification of the adducts formed and their ability to activate the immune system. Because human serum albumin (HSA) is the most abundant protein in serum, most works have attempted the characterization of penicilloyl-HSA adducts. The first pioneering studies on these aspects, employing HPLC separation of tryptic peptides and EDMAN degradation sequencing, were published by Yvon et al. [2, 3] and reported the sites of adduct formation in albumin obtained from a penicillin-treated patient or prepared by in vitro conjugation. More recently, mass spectrometry (MS) has been applied to the study of adducts of HSA with various β -lactam antibiotics, including benzylpenicillin [4], flucloxacillin [5] and piperacillin [6] formed either in vitro or in the serum of patients. Noteworthy, there seems to exist a high degree of variability among the adducts detected and the factors that influence this process are not completely understood.

3 Protein haptention by amoxicillin: high resolution mass spectrometry analysis and identification of target proteins in serum

Unlike the other investigated penicillins, amoxicillin (AX) is a zwitterionic molecule which possesses a primary amino group and belongs to the class of aminopenicillins characterized by a greater activity against gram-negative bacteria and a better pharmacokinetic profile [7]. This unique feature of AX can heavily influence its reactivity towards nucleophilic centers.

The detection and characterization of the amoxicilloyl-HSA (AX-HSA) adducts formed could be very helpful for the understanding of the pathogenic role of protein haptention in the allergic reaction, as well as for the design of more relevant antigens to be used in diagnostic tests. HSA modified in the presence of high concentrations of β -lactam antibiotics, including benzylpenicillin, ampicillin or AX has been widely used in the development of diagnostic assays to detect penicillin-reactive IgE antibodies in the serum of patients, to evaluate cross-reactivity and as immunogens for the development of anti- β -lactam antisera [8-11]. However there is little information on the structural features of HSA modified by AX concentrations close to those occurring during treatment with this antibiotic. Pharmacokinetic studies of AX in human and animal models reveal that the plasma concentrations after oral or intravenous administration may be in the order of 20 or 250 $\mu\text{g/ml}$, respectively [12, 13], whereas HSA concentration in plasma is approximately 30 mg/ml. Therefore, the molar ratio of antibiotic to protein in vivo is not expected to exceed 2:1.

Here we have undertaken the study of the formation of covalent adducts of low AX concentrations with HSA and potentially with other serum proteins, as a first step to understand the processes that govern protein haptention, resulting in the identification of a novel set of serum proteins as potential targets for modification by AX. Moreover, in the present study we explored the potentialities of a novel MS approach based on a high resolution MS analyzer (orbitrap) coupled to nanoscale capillary liquid chromatography for

3 Protein haptention by amoxicillin: high resolution mass spectrometry analysis and identification of target proteins in serum

the full elucidation of the covalent binding of AX to HSA and in particular to obtain the following information: stoichiometry of reaction, chemical nature of the covalent adduct and the sites of modification. LTQ Orbitrap mass spectrometry is emerging as a powerful tool for protein identification and characterization due to its capabilities of high resolution (up to 100,000 for small molecules), and excellent mass accuracy (<5 ppm with external calibration) in a robust manner even within HPLC time scales [14]. Orbitrap has been successfully applied to investigate post-translational modifications as well as to fully elucidate protein modifications induced by xenobiotics [15]. However, to our knowledge, no applications of orbitrap and in general of high resolution MS analyzers have been reported for the study of penicillin binding to proteins and for this reason a top-down and an innovative bottom-up MS approach is here reported to fully elucidate the covalent binding of AX towards HSA.

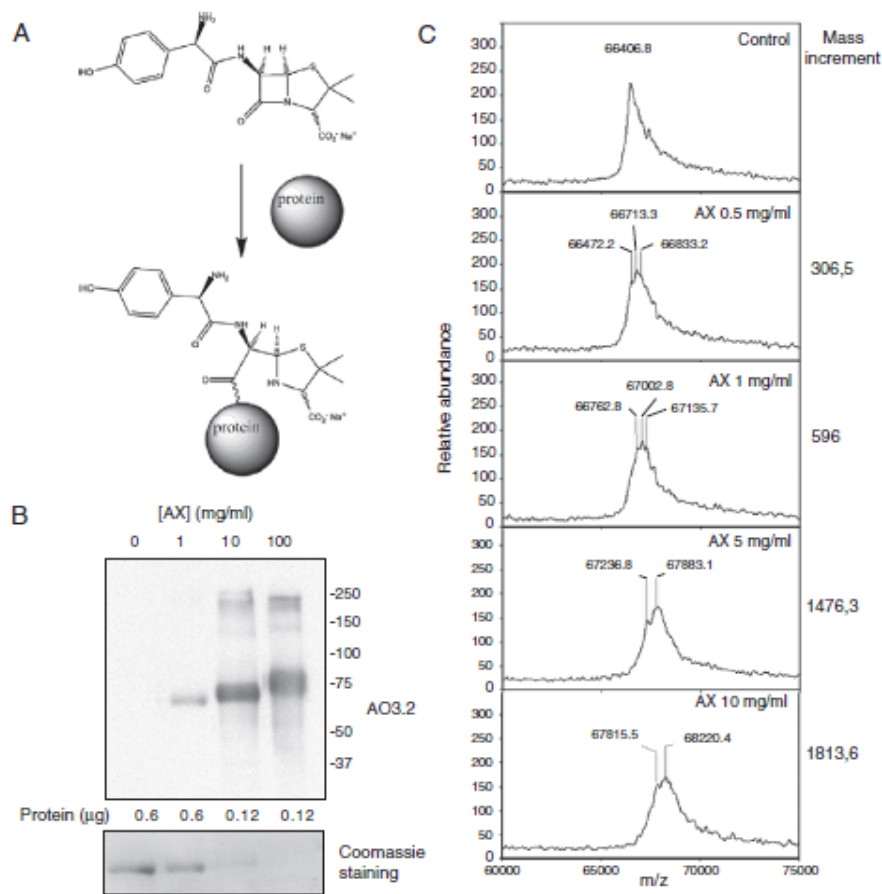


Fig. 1. Interaction of AX with HSA as detected by immunological and MALDI-TOF MS approaches. (A) Structure of AX and the adduct formed with a protein (amoxicilloyl-protein adduct) through a non-specified residue. The main nucleophilic sites from the protein potentially able to react with the β -lactam ring of AX include lysine, histidine, cysteine and the amino terminal group. (B) Immunological detection of AX-modified HSA by western blot with the AO3.2 monoclonal antibody. HSA was incubated in the presence of increasing concentrations of AX under the conditions used for antibody generation (see methods) and analyzed by SDS-PAGE followed by western blot and ECL detection. Aliquots of the incubations containing decreasing amounts of protein (indicated at the bottom) were loaded in each lane to avoid saturation of the signal. The Coomassie staining of the blot is shown in the lower panel. The protein amount of the two lanes on the right was close to the detection level. (C) MALDI-TOF MS analysis of HSA incubated with the indicated concentrations of AX for 16 h at 37°C. The mass increment observed in every condition is indicated on the right. Results are representative of at least 4 assays with similar results

3.2 Materials and Methods

3.2.1 Reagents

Amoxicillin was from GlaxoSmithKline. Human serum was obtained from Sigma-Aldrich or prepared from blood samples (male healthy donors) collected by venipuncture and allowed to clot at room temperature for no longer than 30 min and centrifuged for 10 min at 1500 g. Serum aliquots were stored in liquid nitrogen until their use. Iodoacetamide, (D)-threo-1,4-dimercapto-2,3-butanediol (DTT), tris(hydroxymethyl)aminomethane, sodium phosphate dibasic and LC-grade and analytical-grade organic solvents were from Sigma-Aldrich. Anti-AX monoclonal antibodies, raised against HSA modified in the presence of high concentrations of AX prepared in 50 mM Na₂CO₃/NaHCO₃ pH 10.2, have been previously described [10]. Anti-penicillin antibody was from AbD Serotec. Reagents for enhanced chemiluminescence (ECL) detection were from GE Healthcare. Human serum albumin was obtained from Sigma or purified from serum from young healthy donors, as previously described [16]. Custom-synthesized LQQCPF, HPYFYAPELLFFAK, LKCASLQK, LVNEVTEF peptides, with 90% purity were supplied by Sigma-Aldrich (Milan Italy). Sequence grade modified trypsin was obtained from Promega (Milan, Italy) and chymotrypsin from Roche Diagnostics S.p.A. (Monza, Italy).

3.2.2 *In vitro* modification of synthetic HSA peptides by AX

Synthetic HSA peptides containing nucleophilic sites such as LQQCPF (Cys34), HPYFYAPELLFFAK (His146), LKCASLQK (Lys199), and LVNEVTEF (ctrl) were dissolved in 10 mM PBS (pH 7.4) and diluted to

3 Protein haptation by amoxicillin: high resolution mass spectrometry analysis and identification of target proteins in serum

reach a final concentration of 150 μ M. Aliquots of an AX solution in PBS pH 7.4 were then mixed with each peptide to reach a final concentration of 14 mM. In another set of experiments AX (14 mM final concentration) was incubated in the presence of the mixed peptides (150 μ M each peptide). After an overnight incubation at 37°C, an aliquot of each sample was analyzed by ESI-MS as described below. Stability analyses were carried out by incubating the AX-peptide mixtures in the presence of trypsin and/or by freezing at -20 °C and thawing.

3.2.3 In vitro modification of HSA or serum proteins by AX

AX was freshly prepared in 50 mM Na₂CO₃/NaHCO₃ pH 10.2 or 10 mM PBS pH 7.4, as indicated. For modification by AX, HSA at 10 mg/ml in PBS was incubated with AX at the indicated concentrations, for most assays the concentration of AX used was 0.5 mg/ml. Mixtures were incubated overnight at 37°C. For modification of serum proteins, human serum was incubated with the indicated concentrations of AX for 16 h at 37°C.

3.2.4 SDS-PAGE electrophoresis and Western blot

Samples from incubations containing 1-4 μ g of protein were separated in 12.5% polyacrylamide gels. Proteins were transferred to Immobilon-P membranes using a three buffer system according to the manufacturer instructions on a semi-dry Western blot system (Bio-Rad). Proteins of interest were detected using various primary antibodies typically at 1:500 dilution followed by incubation with HRP-conjugated secondary antibodies (Dako) at 1:2000 dilution and ECL detection. Coomassie staining of blots was used as a control for protein loading and transfer.

3 Protein haptentation by amoxicillin: high resolution mass spectrometry analysis and identification of target proteins in serum

3.2.5 Two-dimensional electrophoresis and protein identification

For two-dimensional electrophoresis, aliquots of control and AX-treated human serum containing 100 µg of protein were precipitated with 10% TCA, and the pellet was washed once with 80% ethanol and twice with acetone. The dried pellet was resuspended in 140 µl of IEF sample buffer (4% CHAPS, 2 M thiourea, 7 M urea, 100 mM DTT, and 0.4% Bio-lyte ampholytes) and loaded on ReadyStrip IPG Strips (pH 3-10, Bio-Rad) for isoelectric focusing on a Protean IEF cell (Bio-Rad), following the instructions of the manufacturer. Before the second dimension strips were equilibrated in 6 M urea, 2% SDS, 0.375 M Tris pH 8.8, 20% glycerol, containing 130 mM DTT for the first equilibration step and 135 mM iodoacetamide for the second step. Strips were then placed on top of 12.5% polyacrylamide SDS gels. Gels were run in duplicate. One of the gels was subsequently transferred to Immobilon P membrane (Millipore) and used for localization of AX-positive spots by Western blot. The duplicate gel was stained for total protein with Simplyblue stain (Invitrogen) or SYPRO Ruby (Bio Rad) and it was used for spot excising and identification. The EXQuest Spot Cutter (BIO-RAD) was used for gel imaging and picking the selected spots. Excised spots were deposited in 96-well plates and digested automatically using a DigestPro MS (Intavis AG). The digestion protocol used was based on Schevchenko et al., [17] with minor variations: gel pieces were washed first with 50 mM ammonium bicarbonate (Sigma-Aldrich) and secondly with acetonitrile (Scharlau). Trypsin (Promega), at a final concentration of 12.5 ng/µl in 50 mM ammonium bicarbonate solution, was added to the gel pieces for 8 h at 37 °C. Finally, 70% acetonitrile containing 0.5% TFA (Sigma-Aldrich) was added for peptide extraction. Tryptic eluted

3 Protein haptention by amoxicillin: high resolution mass spectrometry analysis and identification of target proteins in serum

peptides were dried by speed-vacuum centrifugation and resuspended in 4 μ l of 30% acetonitrile - 0.1% TFA. One μ l of each peptide mixture was deposited onto an 800 μ m AnchorChip (Bruker-Daltonics) and dried at RT. One μ l of matrix solution (3 mg/ml α -cyano-4-hydroxycinnamic acid) in 33% acetonitrile - 0.1% TFA was then deposited onto the digest and allowed to dry at RT. Samples were analyzed with an Autoflex III TOF/TOF mass spectrometer (Bruker-Daltonics). Typically, 1000 scans for peptide mass fingerprinting (PMF) and 2000 scans for MS/MS were collected. Automated analysis of mass data was performed using FlexAnalysis software (Bruker-Daltonics). Internal calibration of MALDI-TOF mass spectra was performed using two trypsin autolysis ions with m/z 842.510 and m/z 2211.105; for MALDI-MS/MS, calibrations were performed with fragment ion spectra obtained for the proton adducts of a peptide mixture covering the m/z 800–3200 region. The typical error observed in mass accuracy for calibration was usually below 20 ppm. MALDI-MS and MS/MS data were combined through the BioTools 3.0 program (Bruker-Daltonics) to interrogate the NCBI non-redundant protein database (NCBI: 20100306) using MASCOT software 2.3 (Matrix Science). Relevant search parameters were set as follows: enzyme, trypsin; fixed modifications, carbamidomethyl (C); oxidation (M); 1 missed cleavage allowed; peptide tolerance, 50 ppm; MS/MS tolerance, 0.5 Da. Protein scores greater than 75 were considered significant ($p < 0.05$).

3 Protein haptention by amoxicillin: high resolution mass spectrometry analysis and identification of target proteins in serum

3.2.6 Mass spectrometry analysis of AX-modified HSA by MALDI-TOF

For MALDI-TOF MS analysis, HSA incubated in the presence of various AX concentrations was purified by ZipTip (C4) from Millipore as indicated by the manufacturer. The 2,5-Dihydroxy-acetophenone (2,5-DHAP) matrix solution was prepared by dissolving 7.6 mg (50 μmol) in 375 μl ethanol followed by the addition of 125 μl of 80 mM diammonium hydrogen citrate aqueous solution. For sample preparation, 2.0 μl the sample (reconstituted in water) were diluted with 2.0 μl of 2% trifluoroacetic acid aqueous solution and 2.0 μl of matrix solution. A volume of 1.0 μl of this mixture was spotted onto the 800 mm AnchorChip MALDI probe (Bruker-Daltonics) and allowed to dry at room temperature. The MALDI experiments were performed on an Autoflex III MALDI-TOF-TOF instrument (Bruker Daltonics, Bremen, Germany) with a smartbeam laser. The spectra were acquired using a laser power just above the ionization threshold. Samples were analysed in the positive ion detection and delayed extraction linear mode. Typically, 1000 laser shots were summed into a single mass spectrum. External calibration was performed, using bovine albumin from Sigma, covering the range from 20000 to 70000 Da.

3 Protein haptention by amoxicillin: high resolution mass spectrometry analysis and identification of target proteins in serum

3.2.7 Direct infusion electrospray mass spectral analysis (ESI-MS): LTQ XL Orbitrap mass spectrometer

Peptide analysis: peptides incubated in the absence and presence of AX as described above were analyzed by direct infusion on a LTQ XL Orbitrap mass spectrometer (Thermo Scientific, Milan, Italy) equipped with a Electrospray Finnigan Ion Max source. An aliquot of each sample was diluted 300 fold with CH₃CN/H₂O/HCOOH (30:70:0.1 v/v/v) for the MS analysis and infused into the mass spectrometer at a flow rate of 5 µL/min. Analyses were carried out under the following instrumental conditions: full scan mode, mass range m/z 200-2000, positive-ion mode, AGC target 5×10^5 , 500 ms maximum inject time, 1 microscan, scan time 1.9 s, resolving power 100,000 (FWHM at 400 m/z), capillary temperature 275°C, spray voltage applied to the needle 3.5 kV; capillary voltage 40 V; tube lens voltage 100 V; nebulizer gas (nitrogen) flow rate set 2 a.u.; acquisition time 0.5 min. A list of 20 common inquilants of ESI background were used for internal mass calibration, i.e. protonated phthlates [dibutylphthlate (plasticizer), m/z 279.159086; bis(2-ethylhexyl)phthalate, m/z 391.284286] and polydimethylcyclosiloxane ions [(Si(CH₃)₂O)₆ + H]⁺; m/z 445.120025]. MS/MS experiments were performed in collision induced dissociation (CID) and high energy collision dissociation (HCD) modes (isolation width, 3 m/z ; normalized collision energy, 30 to 50 CID arbitrary units, 25 to 35 HCD arbitrary units).

HSA infusion: Prior to infusion HSA incubated in the presence or absence of AX was filtered and desalted by Amicon filter devices, 30 KDa MWCO (Millipore S.p.A., Milan, Italy). Three different aliquots were withdrawn from each sample and washed using three different procedures: the first aliquot was washed four times with 0.3 ml of H₂O, the second one twice with

3 Protein haptention by amoxicillin: high resolution mass spectrometry analysis and identification of target proteins in serum

0.3 ml H₂O and twice with 0.3 ml of a 1:1 (v:v) H₂O:EtOH, the third one four times with 1:1 (v:v) H₂O:EtOH. Then the retained aliquots were dried using speedvac and kept frozen at -20°C until analysis. To detect changes in protein mass and to determine the stoichiometry of the reaction, undigested native, and AX-treated HSA were analyzed by direct infusion on a linear ion trap LTQ Orbitrap™ XL mass spectrometer (Thermo Scientific, Milan, Italy) equipped with a an Electrospray Finnigan Ion Max source. An aliquot of the dried protein (96 µg) prepared as above described was dissolved with 10 µL of H₂O, diluted with 200 µL of H₂O and 200 µL of CH₃CN/H₂O/HCOOH (60:40:0.4 v/v/v) and infused into the mass spectrometer at a flow rate of 5 µL/min. The linear ion trap was set under the following instrumental conditions: mass range m/z 800-2000, positive-ion mode, capillary temperature 300°C, spray voltage applied to the needle 3.5 kV; capillary voltage 48 V; tube lens voltage 190 V; nebulizer gas (nitrogen) flow rate set 8 a.u.; acquisition time 5 minutes.

3.2.8 Liquid chromatography electrospray ionization mass spectrometry/mass spectrometry analysis (LC-ESI-MS/MS): LTQ Orbitrap XL mass spectrometer

All digested peptide mixtures were separated by online reversed-phase (RP) nanoscale capillary liquid chromatography (nanoLC) and analyzed by electrospray tandem mass spectrometry (ESI-MS/MS). For sample preparation, the lipohylized protein (30 µg) was dissolved in 30 µl 50 mM Tris-HCl (pH 7.8) and digested with trypsin and trypsin/chymotrypsin according to the manufacturer's procedure. The tryptic mixtures were acidified with formic acid up to a final concentration of 10%. One microliter of tryptic digest was injected into a nano chromatographic system, UltiMate

3 Protein haptention by amoxicillin: high resolution mass spectrometry analysis and identification of target proteins in serum

3000 RSLCnano System (Dionex). The peptide mixtures were loaded on a fused silica reversed-phase column (PicoFrit™ Column, HALO, C18, 2.7 μm, 100 Å, 75 μm i.d. x 10 cm, New Objective). The peptides were eluted with a 30 min gradient from 4% buffer A (0.1% formic acid in water) to 60% buffer B (0.1% formic acid in acetonitrile) at a constant flow rate of 300 nL/min. The liquid chromatography system was connected to an LTQ XL-Orbitrap mass spectrometer (Thermo Scientific, Milan, Italy) equipped with a nano spray ion source (dynamic nanospray probe, Thermo Scientific, Milan, Italy) set as follows: spray voltage 1.7 Kv; capillary temperature 220 °C, capillary voltage 30 V; tube lens offset 100 V, no sheath or auxiliary gas flow. During analysis, the mass spectrometer continuously performed scan cycles in which first a high-resolution (resolving power 60000, fwhm at m/z 400) full scan (200-1500 m/z) in profile mode was made by the Orbitrap, after which MS2 spectra were recorded in centroid mode for the 3 most intense ions, using both CID and HCD modes (isolation width, 3 m/z ; normalized collision energy, 35 CID arbitrary units, 30 HCD arbitrary units). Protonated phthalates [dibutylphthalate (plasticizer), m/z 279.159086; bis(2-ethylhexyl)phthalate, m/z 391.284286] and polydimethylcyclsiloxane ions [(Si(CH₃)₂O)₆ + H]⁺; m/z 445.120025] were used for real time internal mass calibration. Dynamic exclusion was enabled (repeat count, 3; repeat duration, 10 s; exclusion list size, 50; exclusion duration, 120 s; relative exclusion mass width, 5 ppm). Charge state screening and monoisotopic precursor selection was enabled, singly and unassigned charged ions were not fragmented.

Identification of the adduct-bearing peptides and the sites of modification was carried out by a novel MS strategy based on two different steps: the first step consists of the analyses of the MS/MS spectra recorded in HCD mode, in order to identify the precursor ions of those found to be diagnostic in this

3 Protein haptention by amoxicillin: high resolution mass spectrometry analysis and identification of target proteins in serum

work, namely, ions at m/z 160.04 and 349.08 (see Results). In more detail, a list of precursor ions is extracted from the parent ion map displayed by setting as product mass the ions at m/z 160.04 (tolerance 0.01). A second ion map is then generated by setting as product ion that at m/z 349.08 (tolerance 0.01). The two lists of parent ions are then exported to Excel and analyzed using the following Boolean logic: if $\text{value1} > \text{ts}$, $\text{value2} > \text{ts}$, $\text{value\$} = \text{value1} + \text{value2}$ or else $\text{value\$} = 0$, where value1 , value2 are the relative abundances of the precursor ions setting the product ions at m/z 160 (value 1) and 349 (value 2) and ts is the threshold relative abundance (Fig. 2). Thus, by using this approach, each precursor ion is confirmed only when it is present in both the ion maps reconstituted by setting the two diagnostic precursor ions, otherwise it is discarded. The second step consists in matching the precursor ions with a list of theoretical modified ions generated by an *in silico* digestion of albumin carried out by considering the following parameters: trypsin/chymotrypsin as enzymes, two missed cleavages and the addition of the amoxicilloyl moiety.

3.2.9 Bioinformatics

Direct infusion ESI-MS spectra were deconvoluted using the software packages Bioworks 3.1.1 (Thermo-Quest, Milan, Italy) and the software MagTran 1.02 [18]. Peptide sequences were identified using the software turboSEQUEST (Bioworks 3.1, ThermoQuest, Milan, Italy), and using a database containing only the protein of interest and assuming trypsin and trypsin/chymotrypsin digestion. The protein sequence of HSA was obtained from the Swiss-Prot database (primary accession number P02768). Sequence fragments calculator (Bioworks 3.1.1) was used to obtain the theoretical digested masses setting trypsin and trypsin/chymotrypsin as enzymes, all the

3 Protein haptention by amoxicillin: high resolution mass spectrometry analysis and identification of target proteins in serum

Cys residues as carbamidomethyl-cysteine and considering the oxidation of methionine residues and the formation of amoxicilloyl-Lys adducts as variable modifications. The predicted y and b series ions were determined using the Peptide Sequence Fragmentation Modeling, Molecular Weight Calculator software program (ver. 6.37), <http://come.to/alchemistmatt>.

3.2.10 Molecular modelling

The starting structure of human serum albumin was retrieved by PDB Database (PDB Id: 1AO6) [19]. The experimental structure was completed by adding the hydrogen atoms using VEGA software [20] and underwent preliminary minimizations keeping fixed the backbone atoms to preserve the experimental folding. The optimized structure was then used to predict the ionization constants for lysine residues using PropPka [21] and in the following docking simulations. AX was considered in its zwitterionic form and its conformational profile was explored by a clustered MonteCarlo simulation to generate 1000 minimized conformers. The so obtained lowest energy structure was used in the docking analyses. For each identified site of addition, a docking search was performed using the AutoDock 4.0 software and considering a 12 Å sphere around the adducted lysine, which was considered in its neutral form. AX was docked into this grid with the Lamarckian algorithm and the ligand flexible bonds were left free to rotate. The genetic-based algorithm generated 100 poses with 2,000,000 energy evaluations and a maximum number of generations of 27,000. The crossover rate was increased to 0.8, and the number of individuals in each population to 150. All other parameters were left at the AutoDock default settings [22]. The obtained complexes were ranked considering both the docking scores and the distance between the lysine's amino group and the AX β -lactam carbonyl

3 Protein haptention by amoxicillin: high resolution mass spectrometry analysis and identification of target proteins in serum

group. The chosen complexes were finally minimized keeping fixed the atoms outside a 15 Å radius sphere around the bound substrate and then used to recalculate docking scores.

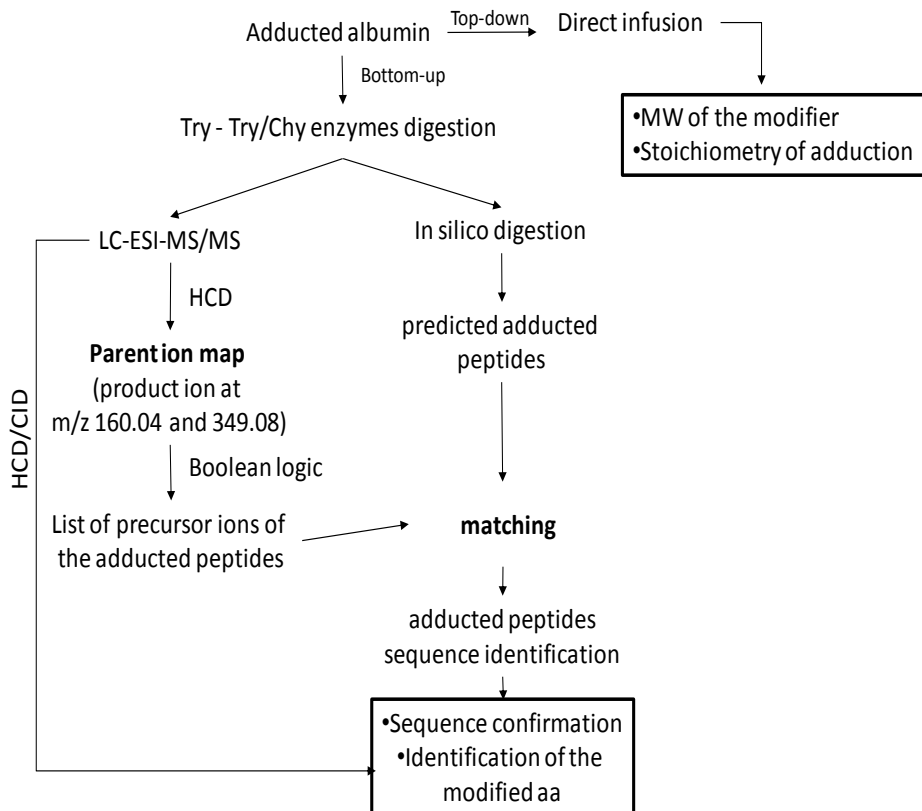


Fig. 2. Mass spectrometric strategies employed to identify AX modified residues.

3.3 Results

3.3.1 Detection of AX-HSA adducts by western blot

Anti-AX antibodies have been previously used for a variety of applications. However, the detection of AX-protein adducts by Western blot has not been previously documented. To explore this possibility, we incubated HSA with AX concentrations close to those used to generate AX-HSA for immunological studies or for the generation of antibodies (1 to 100 mg/ml) [8-11]. Interestingly, analysis of HSA incubated with high concentrations of AX by western blot with an anti-AX antibody, previously used for ELISA (AO3.2), showed a clear immunoreactive signal. Moreover, an increase in the apparent molecular weight of the HSA band was observed, as expected from the increment of mass produced by the incorporation of several AX molecules. In addition, higher molecular weight species appeared suggestive of the formation of HSA aggregates during incubation with the antibiotic. As a control for this assay, AX-modified HSA samples were analysed by MALDI-TOF MS. Incubation of HSA in the presence of increasing concentrations of AX induced a concentration-dependent increase in the mass of the protein as detected by MALDI-TOF MS (Fig. 1). A displacement of the centroid of the HSA peak was evident even with the lowest concentration of AX tested (0.5 mg/ml). In the spectrum of HSA treated with 5 mg/ml of AX, two poorly defined peaks could be observed showing m/z increments of 830 and 1476 with respect to the native protein, compatible with the incorporation of 2 and 4 molecules of AX, respectively. Finally, the spectrum of HSA treated with 10 mg/ml AX, conditions which are close to those routinely used for obtaining the AX-HSA complex for immunological applications, showed a major peak with at 68220.4, representing a m/z

3 Protein haptentation by amoxicillin: high resolution mass spectrometry analysis and identification of target proteins in serum

increment of approximately 1813.6 with respect to control HSA. This increment could be due to the incorporation of up to five AX molecules and/or to the occurrence of other modifications in the HSA molecule during incubation in the presence of the β -lactam, as suggested by the western blot assay (Fig. 1).

3.3.2 Immunological detection of AX-modified HSA with various anti- β -lactam antibodies

In previous works several monoclonal antibodies were obtained using HSA treated with high concentrations of AX as immunogen [10]. Competition studies with various moieties of the AX molecule in ELISA indicated that the antibodies obtained were directed towards different parts of the molecule. Therefore, we assessed the ability of several of these monoclonal antibodies to detect AX-modified HSA by western blot. As it can be observed in Fig. 3, two monoclonal antibodies, AO3.2 and AO19.1, effectively detected the AX-HSA adduct. The AO3.2 antibody, which recognizes the lateral chain plus a part of the nuclear region of AX, allowed the detection of an immunoreactive signal above the background even after incubation of HSA in the presence of 0.025 mg/ml AX, which is in the range of the concentrations expected to occur in vivo [12, 13] and indicates that this procedure shows high sensitivity. The AO19.1 antibody, which recognizes the lateral chain plus the open β -lactam ring, also gave a positive signal although it showed less sensitivity. In contrast, several monoclonal antibodies reportedly recognizing the lateral chain of AX (with a β -lactam ring absent or open), including AO24.1 (Fig. 3), AO14.1 and AO18.2 (results not shown), gave no signal in this assay, although they previously showed immunoreactivity in direct and inhibition ELISA [10] using exhaustively modified protein as antigen.

3 Protein haptention by amoxicillin: high resolution mass spectrometry analysis and identification of target proteins in serum

Finally, we used a commercial anti-penicillin antibody for comparison. This antibody showed much lower sensitivity towards AX-modified HSA than the AO3.2 antibody and, used at the same concentration, only detected HSA modified by high concentrations of AX after long exposures.

3.3.3 Detection of AX candidate target proteins in human serum

HSA is the most abundant protein in human plasma and therefore it is considered the main target for protein haptention. However, as binding of haptens to proteins depends on their structure, other plasma proteins may result covalently modified by AX to a significant proportion and therefore, may also be good candidates for mediating the immunological reactions towards this antibiotic. To assess this possibility we incubated human serum with AX and applied immunological detection. This allowed the observation of multiple positive bands, even with the lowest concentration of amoxicillin used (Fig. 4). In order to get insight into the nature of these proteins we carried out two-dimensional electrophoresis followed by peptide fingerprint analysis by tryptic digestion and MALDI-TOF MS (Fig. 4, Table 1). Protein identification was confirmed by MALDI-TOF-TOF MS/MS analysis of selected peptides from every protein. Identified proteins included HSA, several forms of transferrin, and heavy and light immunoglobulin chains. In contrast, other abundant proteins, like apolipoprotein or haptoglobin were negative in this assay. It should be noted that according to the signal given by the antibody, the relative modification of transferrin under these conditions was more extensive than that of HSA, thus suggesting that this and other serum protein(s) may play an important role in AX-induced reactions. Of particular interest is the modification of immunoglobulins, which could have functional consequences related to the immune response.

Table 1 – Protein identification by mass spectrometry.										
Spot number ^a	Protein name	Accession code ^b	Total score ^c	Ion score ^d	MW (Da) ^e	pI ^f	Matched peptides ^g	Cover (%) ^h	Identif. TOF/TOF/LTQ ⁱ	AO3.2 signal ^j
1	Human serum albumin	gi 168988718	570	41, 19, 91, 84, 81	67,690	5.63	21	37	Yes	(+)
2	Apo-human serum transferrin (chain A)	gi 110590599	524	55, 93, 84	76,988	6.85	22	42	Yes	(+)
3	Human serum albumin	gi 168988718	363	36, 79	67,690	5.63	19	39	Yes	(+)
4	Immunoglobulin G heavy chain	gi 185362	115	52	52,687	8.6	4	13	Yes	(+)
5	Immunoglobulin G heavy chain	gi 185363	150	52, 19	52,687	8.6	5	16	Yes	(+)
6	Haptoglobin 2	gi 47124562	280	18, 28, 58, 61	31,647	8.48	7	26	Yes	(-)
7	Haptoglobin 2	gi 47124562	270	18, 28, 58, 61	31,647	8.48	7	26	Yes	(-)
8	Apolipoprotein A1	gi 90108664	121	24, 42	28,061	5.27	4	16	Yes	(-)
9	Immunoglobulin kappa4 light chain	gi 170684480	187	94	24,507	6.1	5	35	Yes	(+)
10	Immunoglobulin kappa4 light chain	gi 170684480	313	94, 80, 60	24,507	6.0	5	48	Yes	(+)

Data under superscripts c through h are from MASCOT.
^a Spot numbering as shown in 2-DE Coomassie gel in Fig. 3.
^b Protein accession code from NCBI database.
^c Mascot total score.
^d Mascot ion score.
^e Theoretical molecular weight (Da).
^f Theoretical pI.
^g Number of matched peptides.
^h Protein sequence coverage for the most probable candidate as provided by Mascot.
ⁱ Proteins identified by MALDI-TOF/TOF (TOF-TOF) and proteins identified by nano-LC coupled to LTQ.
^j Results of Western blot analysis with AO3.2 antibody indicated.

Tab. 1: Protein identification by MALDI TOF/TOF and LTQ mass spectrometers

3 Protein haptentation by amoxicillin: high resolution mass spectrometry analysis and identification of target proteins in serum

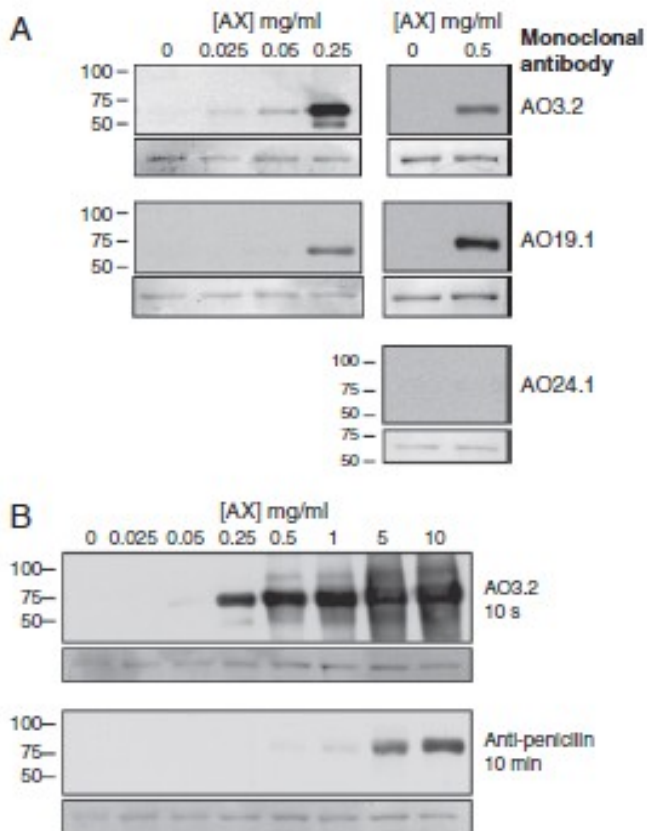


Fig. 3. Immunological detection of AX-modified HSA by western blot with various antibodies. HSA was incubated in the presence of increasing concentrations of AX. Aliquots of the incubations containing 2 μ g of protein were analyzed by SDS-PAGE followed by western blot with the indicated antibodies and ECL detection. In panel B, the times of exposure of films for signal detection is indicated on the right. Results are representative of four assays. Panels underneath each blot show the corresponding Commassie staining.

3 Protein haptentation by amoxicillin: high resolution mass spectrometry analysis and identification of target proteins in serum

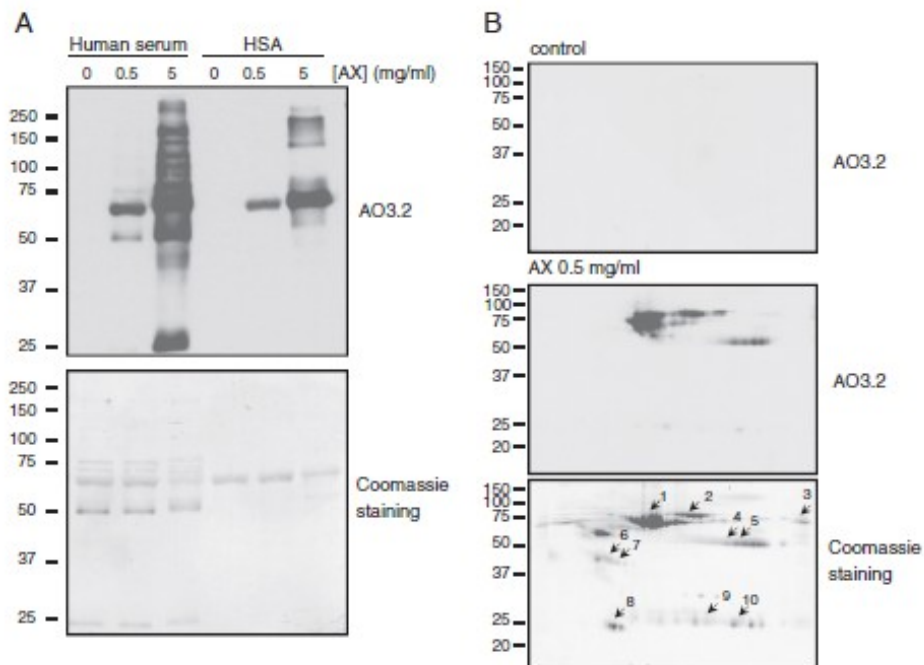


Fig. 4. Immunological detection of adducts of AX and serum proteins and identification of targets. (A) Human serum or HSA was incubated with the indicated concentrations of AX for 16 h at 37°C and analyzed by western blot. AX-modified proteins were detected with the AO3.2 antibody. Lower panel shows the Coomassie staining of the blot. (B) Samples of serum incubated in the absence or presence of 0.5 mg/ml AX were subjected to 2D-electrophoresis on duplicate gels, after which, one of the gels was used for detection of modified proteins by western blot and the other one was used for protein staining with Coomassie staining. Matched spots were excised from the gel and used for tryptic digestion and peptide fingerprint analysis. Results are representative of multiple assays.

3.3.4 AX reaction with His, Lys and Cys containing peptides from HSA

As reported above, HSA is the main plasma protein target of AX, and for this reason, we undertook a detailed characterization of the AX-HSA interaction, including the elucidation of the reactivity and the reaction mechanism, and identifying and characterizing the reaction products of AX towards the main nucleophilic sites of HSA potentially able to covalently react with the β -lactam ring, namely Lys, Cys, and His residues and the amino terminal group. As a first approach to achieve a detailed characterization of AX-HSA adducts, peptides containing the most reactive HSA nucleophilic residues, as determined by previous studies [16], were used for the in vitro reactions and in particular: Lys199 ($^{198}\text{L}\underline{\text{K}}\text{CASLQK}^{205}$), His146 ($^{146}\text{H}\underline{\text{P}}\text{YFYAPELLFFAK}^{159}$), Cys34 ($^{31}\text{LQQC}\underline{\text{P}}\text{F}^{36}$).

The reactivity of the amino terminal group was tested by considering $^{42}\text{LVNEVTEF}^{49}$ as model peptide, since it does not contain any nucleophilic amino acid residue. The MS spectra of each peptide incubated in the absence of AX showed the corresponding $[\text{M}+\text{H}]^+$ and $[\text{M}+2\text{H}]^{2+}$ ions (data not shown). When AX was added at a 1:90 molar ratio and incubated for 18 hours, all the adduct-bearing peptides were characterized by an increase of 365.10454 Da, compatible with the addition of the amoxicilloyl moiety (empirical formula $\text{C}_{16}\text{H}_{19}\text{N}_3\text{O}_5\text{S}$), with respect to the native forms and they were easily determined in the case of peptides containing Lys199, His146 and to a lesser extent (<0.5% relative abundance), but still detectable, for the peptide LVNEVTEF and that containing Cys34 (Fig. 5). If we consider that the amoxicilloyl modification impacts the response factors of the adducts to a similar extent, the relative abundance of the adducts can be considered as a good index of the chemical reactivity of the peptide towards AX. The relative

3 Protein haptention by amoxicillin: high resolution mass spectrometry analysis and identification of target proteins in serum

abundances of the adduct-bearing with respect to the native peptides were found to be different: the Lys199-containing peptide was the most reactive (12%) followed by the His146-containing peptide (3%), while LVNEVTEF and the Cys34-containing peptide were modified to a negligible extent (<0.5%). The modification site of each peptide was then identified by MS/MS experiments. The peptide $^{198}\text{L}\underline{\text{K}}\text{CASLQK}^{205}$ contains three potential nucleophilic sites: Lys199, the C-terminal Lys205 and the amino terminal group. MS/MS fragmentation pathway of the native peptide was carried out by selecting the $[\text{M}+2\text{H}]^{2+}$ as precursor ion at m/z 445.76 Da. The peptide sequence agrees well with the y and b ions series as determined by MS/MS experiments carried out in CID and HCD modes (data not shown). The fragmentation of the amoxicilloyl-peptide adduct was then analyzed by selecting the $[\text{M}+2\text{H}]^{2+}$ ion at m/z 628.31 (365.1 Da increase) as precursor ion (Fig. 6). The MS/MS fragment ions as detected in CID mode show an unmodified y ion series from y_2 to y_6 , excluding the formation of an amoxicilloyl-Lys205 adduct and this is well explained by considering that the amino group forms a salt bridge with the carboxyl group; by contrast the b-ion series (from b_2 to b_7) increased by 365.1 Da although their relative abundance is very low, excluding the amino terminal involvement and confirming Lys199 as main site for adduct formation. As a further confirmation, the y ion series was found to be modified from y_7 to y_8 (see the abundant ion at m/z 619.8 relative to $y_8^{*++}\text{-NH}_3$). By comparing the MS/MS spectrum of the adducted with respect to the native peptide, several other abundant fragment ions were observed and in particular the ion at m/z 553.78 (base peak) which can be attributed to the y_8^{*2+} ion adducted by the amoxicilloyl moiety with the loss of the 4-hydroxybenzylamine group (M_1 ion series). Two other diagnostic abundant ions were then observed at m/z

3 Protein haptentation by amoxicillin: high resolution mass spectrometry analysis and identification of target proteins in serum

548.79 and 540.28 which were assigned to the y_8^{*2+} and $y_8^{*2+}-NH_3$ of the amoxicilloyl group with the loss of the thiazolidinic group (M_2 ion series).

As shown in Fig. 6, the main differences between the MS/MS spectra of the adducted peptide recorded in CID and HCD is that the spectrum recorded in the latter mode is characterized by the presence of the ions at m/z 160.04222 (AX_1) and 349.08467 (AX_2), corresponding to the thiazolidinic moiety of AX and to AX minus the aminic residue, respectively.

The $^{146}H\underline{P}YFYAPELLFFAK^{159}$ peptide contains three potential nucleophilic residues, the amino terminal group, His146 and the C-terminal Lys159, although the latter should be excluded since it forms a salt bridge with the terminal carboxyl group as reported above. The MS/MS spectrum recorded in CID mode shows the unmodified y ion series from y_4 to y_{13} as well as the b ion series from b_5 to b_{13} to indicate that the modification is unstable and is lost during the collision. No diagnostic y and b fragment ions of the AX-adducted peptide were found (M_0 series). The comparison of the MS spectra of the native and adducted peptides indicates that the latter is characterized by intense ions at m/z 980.47 and 975.48 relative to the y_{14}^{2+} of the M_1 and M_2 series, accompanied by the corresponding $-NH_3$ ions. HCD spectrum shows a similar fragmentation pattern and in contrast to that observed for Lys199 no ions relative to the thiazolidinic ring of AX or to AX minus the aminic residue of the R group were detected (data not shown).

Taken together, these data indicate that among the nucleophilic sites present in HSA and potentially able to covalently react with the β -lactam ring, lysine residues are the most reactive sites towards AX and that the amoxicilloyl adduct represents the main reaction product. It should be noted that the order of reactivity as determined using HSA peptides takes into account only the intrinsic reactivity of the nucleophilic amino acid as well as the effect of the vicinal amino acids, while it does not consider other parameters related to the

3 Protein haptenation by amoxicillin: high resolution mass spectrometry analysis and identification of target proteins in serum

arrangement of the amino acid in the three-dimensional protein structure which can increase or reduce the reactivity, for example surface exposure or the presence of surrounding residues that can affect the nucleophilicity of the residues. The determined reactivity appears to be roughly proportional to the basicity of the nucleophilic site. This result is in line with other reported studies and confirms the key role of general acid catalysis exerted by the protonated amine to promote the breakdown of the tetrahedral intermediate by donating a proton to the β -lactam nitrogen atom [23]. The unexpected lack of reactivity of the cysteine residue, which is in contrast with several studies reporting the thiolysis of penicillins [24], could be justified by considering the effect of the protonated amine which attracts the reactive thiolate function hampering its proper attach to the β -lactam carbonyl group.

From an analytical point of view we found that the fragmentation patterns of the adduct-bearing peptides differ on the basis of the modified amino acid. In the case of Lys, both CD and HCD are characterized by diagnostic y and b fragment ions bearing fragmented AX and in particular the AX moiety arising by the loss of the 4-hydroxybenzylamine group (M_1 ion series) and the thiazolidine ring (M_2 ion series). Moreover, HCD but not CID spectra are characterized by the cleaved thiazolidine ring at m/z 160 and by the fragment at m/z 349.08 arising from the cleavage of the AX moiety and concomitant loss of the amino group.

We then evaluated the effect of trypsin incubation as well as sample freezing-thawing (both procedures used for the bottom-up analysis of the HSA sites modified by AX, *vide infra*) on the stability of the AX-peptide adducts. Trypsin digestion, freezing-thawing, as well as both the procedures did not affect the stability of adducts since the relative abundances were unchanged with respect to control samples before and after sample treatment.

3 Protein haptention by amoxicillin: high resolution mass spectrometry analysis and identification of target proteins in serum

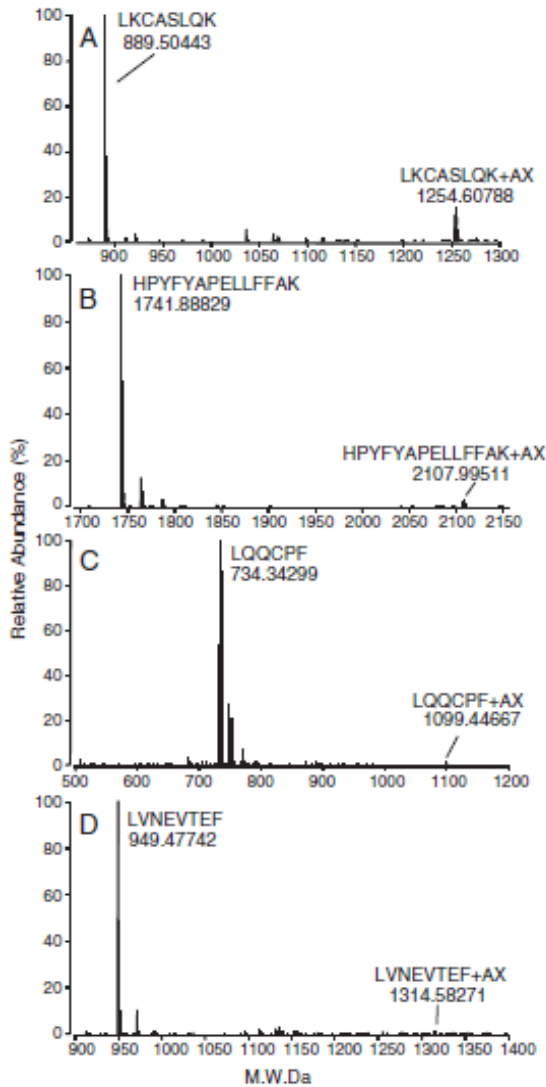
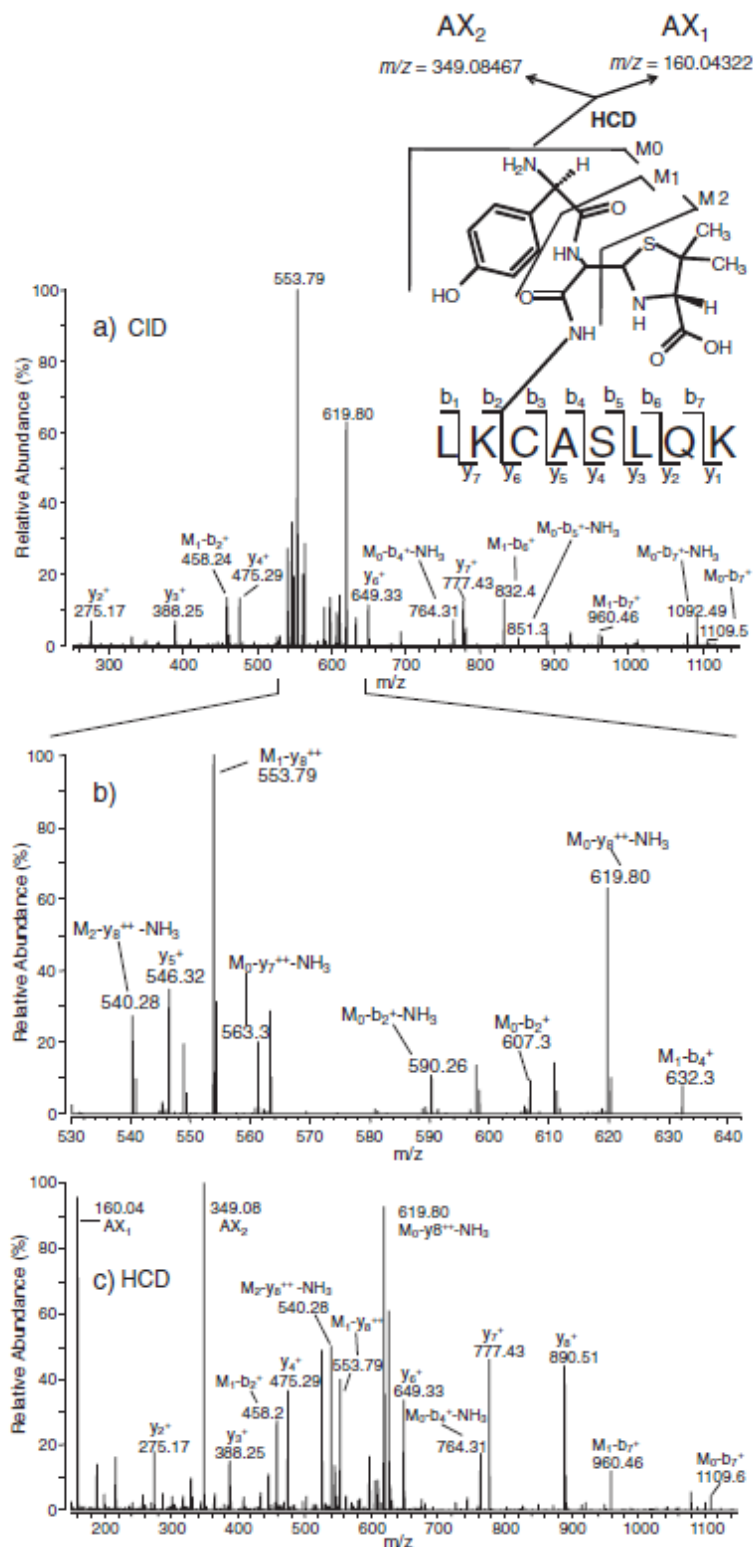


Fig. 5. *In vitro* modification of HSA peptides by AX. Deconvoluted MS spectra obtained by ESI-MS direct infusion experiments of HSA peptides incubated overnight at 37°C with AX. See material and methods for experimental details. Native and AX-modified peptides are labeled in each spectrum.

3 Protein haptention by amoxicillin: high resolution mass spectrometry analysis and identification of target proteins in serum



3 Protein haptention by amoxicillin: high resolution mass spectrometry analysis and identification of target proteins in serum

Fig. 6. ESI-MS/MS spectra and fragmentation pathway of the AX-modified peptide LK#CASLQK. Panels (a) and (b) show the ESI-MS/MS spectrum recorded in CID mode and with a mass range 250-1100 m/z and 530-640, respectively. Panel (c) shows the ESI-MS/MS spectrum recorded in HCD mode. In the upper part is shown the fragmentation pathway of the adducted peptide LKCASLQK leading to the M_0 , M_1 and M_2 ion series as well as the two diagnostic fragment ions at m/z 160 and 349 generated in HCD mode.

3.3.5 AX reaction with HSA: top-down experiments

A summary of the MS strategy used to characterize the AX-HSA adduct, including top-down and bottom-up approaches is shown in Fig. 2. The ability of AX to covalently react with HSA and the stoichiometry of the reaction were firstly evaluated by top-down experiments, consisting of directly infusing the AX-HSA reaction mixture. Fig. 7, panel (a) shows the deconvoluted MS spectrum of HSA incubated in absence of AX, which is characterized by the main peak at 66439 Da relative to the mercaptoalbumin and by two minor peaks at 66559 Da (+120 Da) and 66603 Da (+164 Da) which are attributed to the cysteinylated and glycosylated forms, respectively, as previously reported [16]. Fig. 7 panels (b) and (c) show the deconvoluted MS spectra of HSA incubated at pH 7.4 for 18 hours in the presence of AX at a molar ratio HSA:AX 1:9 (AX 0.5 mg/ml) and 1:90 (AX 5 mg/ml), respectively. When HSA was incubated with the lowest concentration of AX, an easily detectable single adduct at 66804 Da was observed, shifted by 365 Da with respect to mercaptoalbumin and referred to as the amoxicilloyl derivative. This adduct represented 20% of the native protein. By increasing AX concentration to 5 mg/ml, the relative abundance of the three native isoforms of albumin was drastically reduced and three main HSA adducts

3 Protein haptention by amoxicillin: high resolution mass spectrometry analysis and identification of target proteins in serum

appeared at 66804, 67169 and 67534 Da, shifted by 365, 730 and 1095 Da, respectively, with regard to the native forms, which can be attributed to AX-HSA adducts with the following stoichiometric ratios: 1:1, 1:2; 1:3 (Fig. 7 panel c). The cysteinylated and glycated HSA forms were also found to be modified to a similar extent than mercaptoalbumin, thus indicating that Cys34 (the site of cysteinylation) as well as Lys525 (the main glycation site) are not involved in the reaction with AX. It should be underlined that all samples were washed several times with an EtOH:H₂O mixture before MS analysis, until the relative abundances of the adducts were constant. This procedure was adopted in order to remove non-covalent protein-AX adducts that could be maintained in the gas-phase, although the sample is sprayed under denaturing conditions. In fact, when HSA was incubated with AX at a molar ratio of 1:9 and injected after a washing step carried out only with water, apart from mono-adduct, adducts with stoichiometric ratios 1:2 and 1:3 were observed due to the presence of non-covalent interactions which disappeared upon extensive washing with the EtOH:H₂O mixture (data not shown).

3 Protein haptention by amoxicillin: high resolution mass spectrometry analysis and identification of target proteins in serum

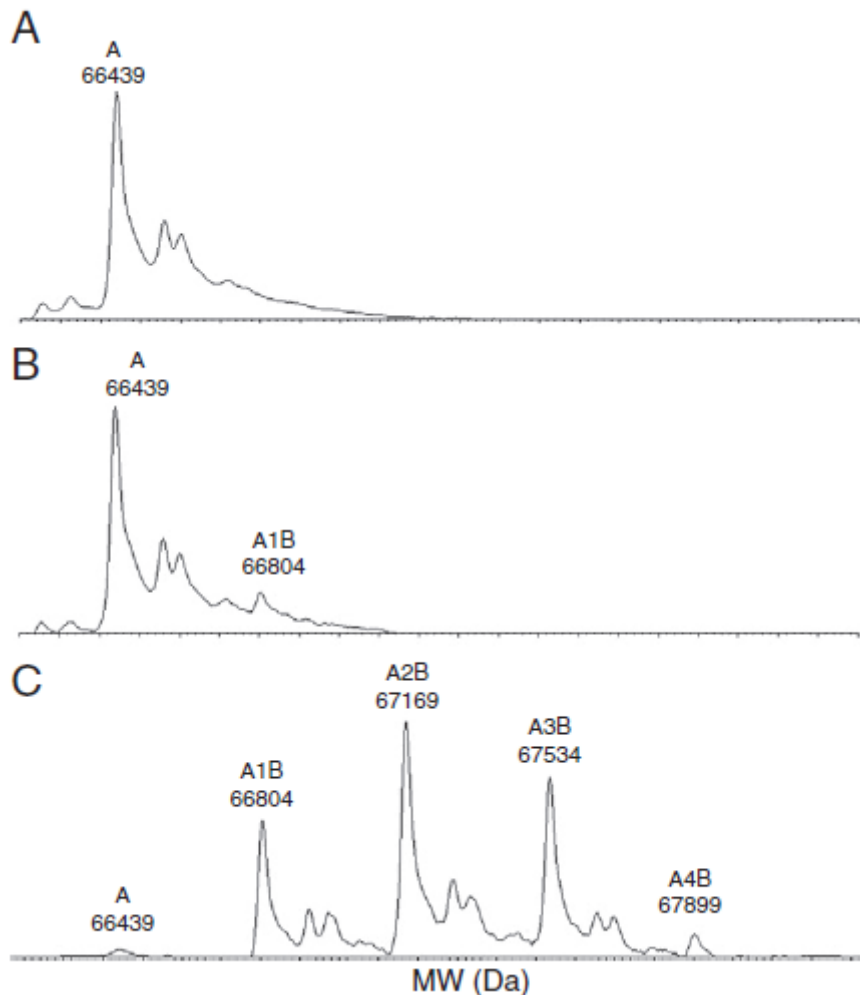


Fig. 7. Top-down approach for characterization of HSA modification by AX. Deconvoluted MS spectra of HSA incubated in the presence of AX. Deconvoluted MS spectra recorded by direct infusion experiments of HSA incubated in absence (a) and presence of 0.5 mg/ml (b) and 5 mg/ml (c) of AX. Mercaptoalbumin isoform is at 66439 (peak A). The peaks A1B, A2B, A3B and A4B are referred to the HSA:AX adducts at the following stoichiometric ratio: 1:1, 1:2, 1:3, 1:4.

3.3.6 Identification of the HSA sites modified by amoxicillin: bottom-up experiment

Identification of the HSA sites modified by the amoxicilloyl residue was carried out by a bottom-up approach using trypsin and trypsin plus chymotrypsin for protein digestion (Fig. 2). Double digestion with trypsin plus chymotrypsin was used since the modified Lys residues are not recognized by trypsin and this would increase the MW and the length of the adduct-bearing peptides to values not suitable for the LC-ESI-MS analysis. The protein coverages of both native and AX-modified HSA were always higher than 90% and 85% for trypsin and trypsin/chymotrypsin digestions, respectively (see Fig. 8). It should be noted that the most reactive Lys residues as reported in the literature and predicted by molecular modelling studies were covered.

The first attempt to identify the AX-modified peptides and the corresponding sites of modification was based on the Sequest algorithm search by setting the amoxicilloyl modification (+365 Da) as a variable modification on Lys, His, Cys and Ser. Such an automatic approach is of great value for the identification of the amino acids covalently modified by different xenobiotics as well as by post-translational modifications. However, this approach was not suitable to identify the AX-modified peptides and this can be clearly explained by considering the typical MS/MS pathways of the AX-peptide adducts, which are characterized, as reported above, by the cleavage of the amoxicilloyl moieties, leading to the formation of unpredictable y and b ion series.

The MS approach was then optimized on the basis of the fragmentation pathway of the peptides adducted on the Lys residue as described above and summarized in Fig. 2. As shown above, using model peptides we found that

3 Protein haptention by amoxicillin: high resolution mass spectrometry analysis and identification of target proteins in serum

the MS/MS spectra of the AX-Lys adducts recorded in HCD mode are characterized, besides by the y and b fragment ions, by the cleaved thiazolidine ring at m/z 160 and by the fragment at m/z 349.08, which arises from the cleavage of the amoxicilloyl moiety and the concomitant loss of the amino group. Therefore, such specific and diagnostic fragments were then set as product ions to generate the maps of precursor ions. The ion map relative to the sample of HSA incubated in presence of AX at the higher molar ratio (1:90) reported 11 precursor ions and 8 of them were attributed to 6 adducted peptides which were reduced to 3 peptides (five precursor ions) at the lowest molar ratio, as reported in Table 2. The method was found highly specific since no precursor-ions were detected in the control sample. To further confirm that the precursor ions are referred to the adducted peptides, SIC traces were then reconstituted for each of them by setting a 5 ppm tolerance. A well detectable peak was identified for each of the precursor ions selected and whose area dose dependently increased by increasing AX concentration in the reaction mixture, while it was absent in the control.

3 Protein haptentation by amoxicillin: high resolution mass spectrometry analysis and identification of target proteins in serum

Sequence coverage obtained by using chymotrypsin/trypsin digestion= 86%

DAHKSEVAHRFKDLGEENFKALVLI AFAQYLQQCPFEDHVKLVNEV
TEFAKTCVADESAENCDKSLHTLFGDKLCTVATLRETYGEMADCCA
KQEPERNECFLQHKDDNP NLPRLVRPEVDVMCTAFHDNEETFLKKY
LYEIARRHPYFYAPELLFFAKRYKAAFTECCQAADKAAACLLPKLDEL
RDEGKASSAKQRLKASLQKFGERAFKAWAVARLSQRFPKAEFAEV
SKLVTDLTKVHTECCHGDLLECADDRADLAKYICENQDSISSKLKEC
CEKPLLEKSHCIAEVENDEMPADLPSLAADFVESKDVCKNYAEAKDV
FLGMFLYEYARRHPDYSVVL LRLAKTYETTLEKCCAAADPHECYA
KVFDEFKPLVEEPQNLIKQNC ELFQ LGEYKFNALLVRYTKKVPQV
STPTLVEVSRNLGKVGSKCCKHPEAKRMPCAEDYLSVVLNQLCVLH
EKTPVSDRVTKCCTESLVNRRPCFSALEVDETYVPKEFNAETFTFHAD
ICTLSEKERQIKKQTALVELVKHKPKATKEQLKAVMDDEAAAFVEKCC
KADDKETCFAEEGKKLVAASQAALGL

Sequence coverage obtained by using trypsin digestion= 91%

DAHKSEVAHRFKDLGEENFKALVLI AFAQYLQQCPFEDHVKLVNEV
TEFAKTCVADESAENCDKSLHTLFGDKLCTVATLRETYGEMADCCA
KQEPERNECFLQHKDDNP NLPRLVRPEVDVMCTAFHDNEETFLKKY
LYEIARRHPYFYAPELLFFAKRYKAAFTECCQAADKAAACLLPKLDEL
RDEGKASSAKQRLKASLQKFGERAFKAWAVARLSQRFPKAEFAEV
SKLVTDLTKVHTECCHGDLLECADDRADLAKYICENQDSISSKLKEC
CEKPLLEKSHCIAEVENDEMPADLPSLAADFVESKDVCKNYAEAKDV
FLGMFLYEYARRHPDYSVVL LRLAKTYETTLEKCCAAADPHECYA
KVFDEFKPLVEEPQNLIKQNC ELFQ LGEYKFNALLVRYTKKVPQV
STPTLVEVSRNLGKVGSKCCKHPEAKRMPCAEDYLSVVLNQLCVLH
EKTPVSDRVTKCCTESLVNRRPCFSALEVDETYVPKEFNAETFTFHAD
ICTLSEKERQIKKQTALVELVKHKPKATKEQLKAVMDDEAAAFVEKCC
KADDKETCFAEEGKKLVAASQAALGL

Fig. 8. Sequence coverage of native HSA after chymotrypsin/trypsin (upper sequence) and trypsin (bottom sequence) digestion and LC-MS/MS analyses. The covered sequence is highlighted in yellow and the amoxicillin adducted peptides are underlined.

3 Protein haptention by amoxicillin: high resolution mass spectrometry analysis and identification of target proteins in serum

3.3.6.1 Identification of the sites modified by AX in purified HSA

By matching the precursor ions with a list of theoretical adducted ions, 8 precursor ions, relative to 6 adducted peptides, were identified and the sequence as well as the sites of adduct formation were then determined by analysing the MS/MS spectrum and attributing the y and b ions. In particular, Lys190, 199, 351, 432, 541 and 545 were found adducted when purified HSA was incubated with AX at 5 mg/ml and Lys 190, 199 and 541 when incubated in the presence of AX at 0.5 mg/ml (Table 2).

As an example of peptide matching and identification of the modified site, here below is described the approach we used to identify Lys 541 as adduction site. The ion map and Boolean logic identified two multi-charged precursor ions at m/z 591.79474 and m/z 394.86562 referred to the $z=2$ and $z=3$ of the adducted peptide. The SIC ion trace relative to the sample incubated with 0.5 mg of AX was characterized by a well detectable peak at RT of 8 min and whose area increased by almost ten-fold in the presence of 5 mg of AX and was absent in the control sample (Fig. 9). Matching such precursor ions with a list of theoretical AX-modified precursor ions, permitted to identify the peptide with the sequence $^{539}\text{ATK}\#\text{EQLK}^{545}$ and whose identity and the site of modification were determined by analyzing the MS/MS spectrum as reported in Fig. 9.

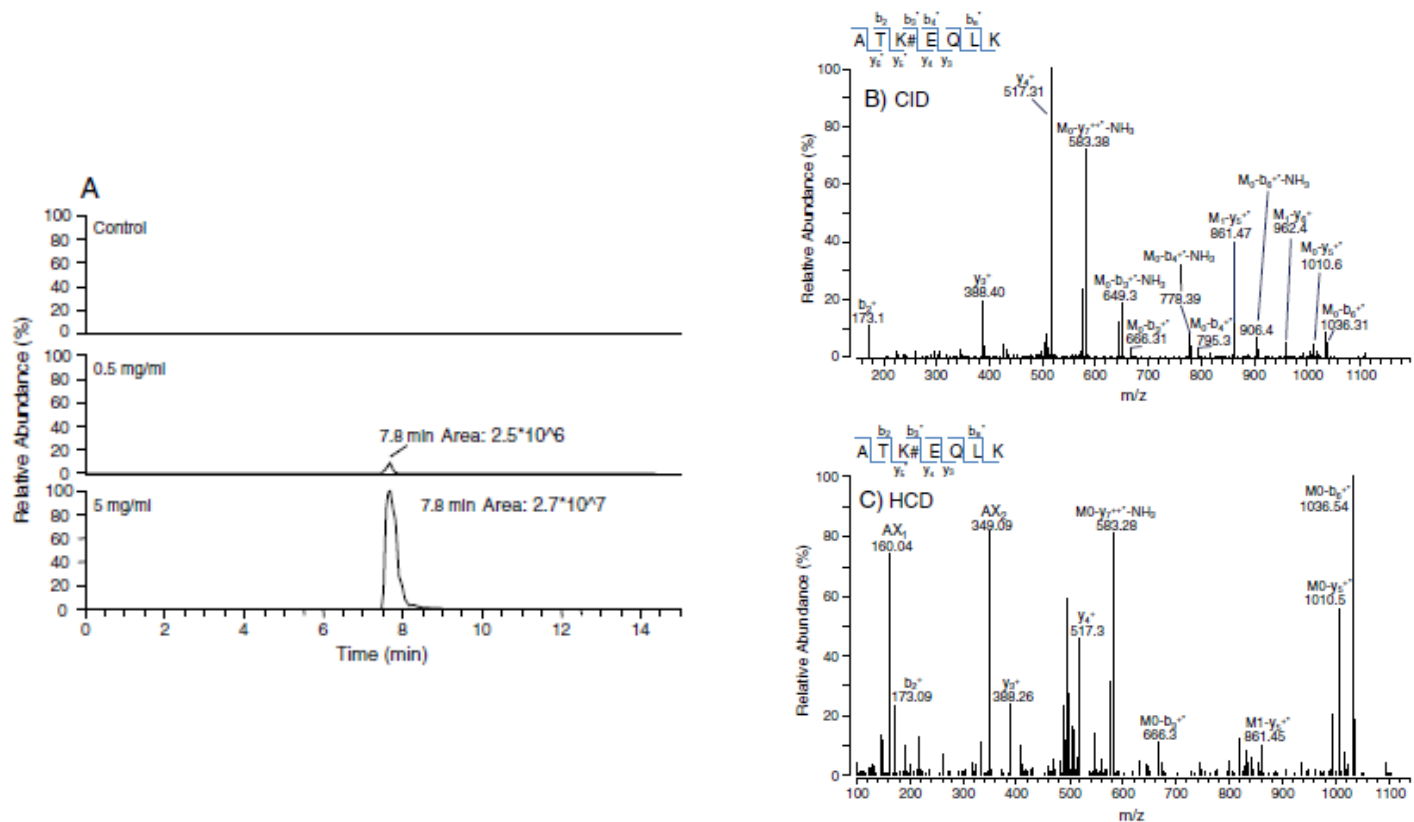


Fig. 9. Bottom-up approach for the study of HSA modification by AX showing the identification of the adduct at Lys541. Panel A: SIC ion traces reconstituted by setting the ion at m/z 591.79474 relative to the z=2 of the adducted peptide $^{539}\text{ATK}\#\text{EQLK}^{545}$ as filter ion. SICs are referred to HSA incubated in absence, and presence of AX 0.5 mg/ml and 5 mg/ml. Panels B and C show the MS/MS spectra of the adducted peptide $^{539}\text{ATK}\#\text{EQLK}^{545}$ in CID and HCD mode, respectively.

3 Protein haptention by amoxicillin: high resolution mass spectrometry analysis and identification of target proteins in serum

3.3.6.2 Identification of the sites modified by AX in HSA in complete human serum

We then analysed the AX-HSA adducts formed when complete human serum was incubated in the presence of the antibiotic. For this, after incubation, HSA was purified as described in Methods and subjected both to immunological detection of the modification and to proteomic analysis following the same approach described above. In general, adducts identified when using isolated HSA were confirmed in these experiments. In particular, when serum was incubated with AX at 5 mg/ml, the following HSA Lys residues were found to be modified by AX: Lys 190, 199, 351, 432, 541 and 545. At 0.5 mg/ml AX, a slight difference in the modification sites was observed with respect to the experiments carried out with purified HSA, since Lys 190 and Lys 432 but not Lys199 or Lys541 were found to be modified.

3.3.7 Peptide consumption

The relative consumption of the peptides undergoing AX modifications were determined as here below reported and compared to that calculated for peptides not covalently modified. The ion responses of the selected peptides were determined by measuring the peak areas in the selected ion chromatograms (SICs) reconstituted by using the $[M+nH]^{n+}$ as filter ions. The peptide responses were normalized with respect to peptide LVAASQAALGL, chosen as reference peptide because it does not contain nucleophilic residues and hence represents an off-target of AX. Relative consumption of the adducted peptides in AX-treated HSA with respect to native HSA was determined by using the following equation: peptide consumption (%) = $100 - [(A-AX)/(A-native) * 100]$ where A-AX and A-native

3 Protein haptentation by amoxicillin: high resolution mass spectrometry analysis and identification of target proteins in serum

are the normalized peptide ion response of the target peptide from HSA incubated in the presence and absence of AX, respectively.

As shown in Table 3 the peptides containing the Lys residues modified by AX and in particular P18-19 (Lys190), P21-22 (Lys 199), P39 (Lys 351), P60 (Lys 541) and P61 (Lys 545) were found to be concentration-dependently consumed. In particular, when AX was added at 0.5 mg/ml the peptide P18-19 underwent the highest consumption (85%), followed by P21-22 (54%). By considering the peptide consumption as an index of reactivity the following rank can be drawn: Lys 190 > Lys 199 > Lys 541 \approx Lys 351 > Lys 545. The consumption of the native peptide containing Lys 432 (⁴²⁹NLGK⁴³²) was not determined because it was not covered due to its small length. The method was then validated by calculating the peptide consumption of four peptides containing Lys residues but not undergoing AX adduction as determined by MS studies (negative controls). As summarized in Table 3, the consumption of the peptides considered as negative controls at either of the two AX concentrations was well below 20%, a value selected as the threshold level. At the highest AX concentration (5 mg/ml), the consumption of other peptides, namely, those containing Lys12, Lys73, Lys402 and Lys525, was higher than the threshold level. However, as the corresponding AX adducts were not found by either the precursor ion scanning approach or the manual search, their modification cannot be confirmed

3 Protein haptentation by amoxicillin: high resolution mass spectrometry analysis and identification of target proteins in serum

Table 2 – Matched precursor ions.

Peptide adduct I.D.	Precursor ion (m/z)	Charge (z)	Predicted adducted ions	Accuracy (ppm)	Sequence	Adducted site	0.5 mg/mL amoxicillin	5 mg/mL amoxicillin
P1	628.63147	3	628.63163	0.25	¹⁸² LDEL RDEGK#ASSAK ₁₉₅	Lys 190	X	X
	471.72574	4	471.72554	0.4	¹⁸² LDEL RDEGK#ASSAK ₁₉₅	Lys 190	X	X
P2	528.74624	2	528.74626	0.04	¹⁹⁸ LK#C*ASL ₂₀₃	Lys 199	X	X
P3	480.72837	2	480.72839	0.04	³⁴⁹ LAK#TY ₃₅₃	Lys 351	O	X
P4	584.29468	2	584.29496	0.48	⁴²⁹ NLGK#VGSK ₄₃₆	Lys432	O	X
P5	591.79474	2	591.79481	0.12	⁵³⁹ ATK#EQLK ₅₄₅	Lys 541	X	X
	394.86562	3	394.86563	0.02	⁵³⁹ ATK#EQLK ₅₄₅	Lys 541	X	X
P6	780.83907	2	780.83891	-0.20	⁵⁴² EQLK#AVMDDF ₅₅₁	Lys 545	O	X

#Amoxicilloyl adduct, *Carbamidomethyl-cysteine.

Tab. 2: Matched precursor ions by means of bottom up experiments

3 Protein haptention by amoxicillin: high resolution mass spectrometry analysis and identification of target proteins in serum

Table 3 – Peptide consumption for the peptides undergoing modification by AX and for four selected peptides not modified by AX and considered as negative controls.

Residue	Peptide	Peptide consumption	
		AX 0.5 mg/mL	AX 5 mg/mL
Peptides undergoing AX adduction			
P18-P19	¹⁸² LDEL ¹⁹⁰ DEGK	85	97
P21-P22	²⁰⁰ C*ASLQK ²⁰⁹ FGER	54	92
P39	³⁵³ TYETTLEK ³⁶⁰	29	63
P60	⁵⁴² EQLK ⁵⁴⁵	31	66
P61	⁵⁴⁶ AVMDDFAAFVEK ⁵⁵⁷	19	54
Peptides not modified by AX (negative controls)			
P5	⁴² LVNEVTEFAK ⁵¹	10	12
P24	²¹³ AWAVAR ²¹⁸	8	7
P37	³³⁸ HPDYSVWLLR ³⁴⁸	6	9
P42	³⁹⁰ QNC*ELFEQLGEYK ⁴⁰²	12	11

* Carbamidomethyl-cysteine.

Tab. 3: Peptides consumption for the peptides undergoing modification by AX and for four selected peptides not modified by AX and considered as negative control. Lys 190 containing peptide (P18-P19) is the most reactive, followed by Lys 190 containing peptide (P21-P22).

3.3.8 Molecular modelling

With a view to rationalizing in-depth the reactivity of the adducted lysine residues, molecular modelling studies were performed investigating the intrinsic reactivity of albumin Lys residues as well as the specific recognition between AX and the regions surrounding the modified residues. Analysis of some relevant physicochemical properties of all HSA Lys residues indicated that the reactivity of the modified Lys residues can be rationalized in terms of exposure and abundance of neutral form (Table 4). In particular, the

3 Protein haptention by amoxicillin: high resolution mass spectrometry analysis and identification of target proteins in serum

comparison of all the 58 Lys residues of HSA emphasizes that the adducted Lys residues are characterized either by a very low basicity which render them extremely reactive regardless of their accessibility (as in the case of Lys190 and Lys 199), or by a significant accessibility which markedly facilitates their approach by AX (as seen for Lys351, Lys541 and Lys545). Yet again, Table 4 evidences that the adducted residues are surrounded by other positively charged residues whose abundance appears in line with the reported reactivity. This finding has two explanations. First, positively charged residues contribute to low basicity of the adducted lysine; second, they can act as general acid catalysts breaking down the tetrahedral intermediates.

Furthermore, docking simulations were utilized to investigate whether the region surrounding the adducted Lys residues can stabilize convenient complexes with AX so further promoting adduct formation. Firstly, it should be noted that the docking scores for the minimized complexes are in agreement with the reported reactivity thus suggesting that the capacity to suitably harbour AX is another key factor which influences the reactivity of Lys towards AX for adduct formation. As an example, Fig. 10 illustrates the minimized complexes showing the interactions stabilizing AX in the proximity of Lys190 (Fig. 10A) and Lys199 (Fig. 10B), two residues that are modified under all experimental conditions used in this study. It is worth noting that in both complexes the adducted lysine is clearly close to the β -lactam carbonyl carbon atom with an arrangement favourable for adduct formation. In both cases, the β -lactam carbonyl oxygen atom elicits a H-bond (with Arg186 for Lys190 and with His242 for Lys199) which polarizes the carbonyl group favouring the aminolysis and mimicking the effect of the oxyanion hole of hydrolases. Moreover, Fig. 10A and 10B show that the AX ionizable groups are always involved in salt bridges (with Arg186 and

3 Protein haptation by amoxicillin: high resolution mass spectrometry analysis and identification of target proteins in serum

Glu425 for Lys190 and with Arg257 and Glu292 for Lys199) which play a pivotal stabilizing role and should minimize electrostatic interferences with adduct formation. Additional polar interactions involving the AX phenol ring characterize both complexes, which are also stabilized by apolar contacts between the dimethyl thiazolidinic ring and surrounding aliphatic residues. Beside the conducive distance between the adducted lysine and the β -lactam ring, all AX complexes obtained for the other reactive sites share similar salt bridges involving at least the AX carboxylate group, thus suggesting a third role for the basic residues surrounding the adducted lysine, namely attracting the AX negative center to reduce its interference with adduct formation

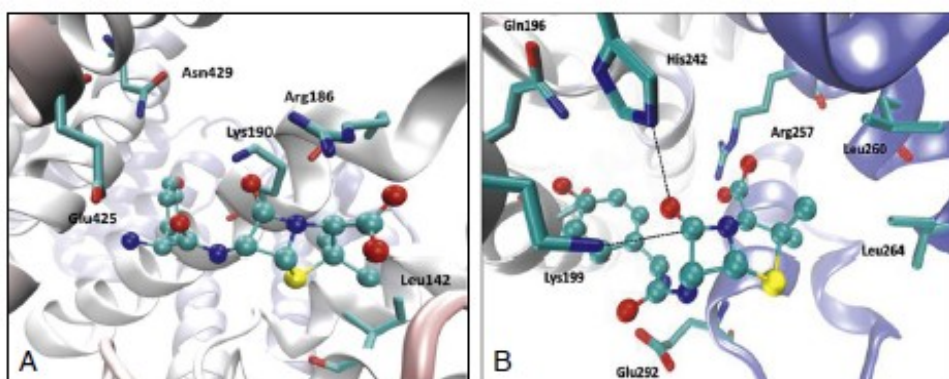


Fig. 10. Main interactions stabilizing the AX molecule in the proximity of the target residues. The residues potentially establishing interactions with AX in the region surrounding Lys190 (A) and Lys199 (B) are shown.

3 Protein haptention by amoxicillin: high resolution mass spectrometry analysis and identification of target proteins in serum

Table 4: Physicochemical descriptors for the 58 lysine residues of serum albumin

Lysine	pK	SAS (Å ³)	Lys/Arg	Score
12	10.58	138.8	1	----
20	10.5	138.8	2	----
41	11.15	110.1	1	----
51	10.74	102.9	1	----
64	10.45	72.2	0	----
73	10.82	53	1	----
93	10.36	96.1	1	----
106	7.36	17.6	0	----
136	9.68	45.6	2	----
137	10.51	103.5	1	----
159	10.87	87.6	2	----
162	10.62	81.1	2	----
174	11.24	67.9	0	----
181	10.62	69.7	1	----
190	8.71	63.3	3	-9.92
195	9.99	88.4	3	----
199	6.78	27	3	-10.42
205	10.5	148.9	2	----
212	10.67	78.3	1	----
225	10.94	99.1	2	----
233	11.17	87.5	0	----
240	10.93	123.8	0	----
262	10.83	127.9	2	----
274	11.12	48	2	----
276	10.73	132.4	1	----
281	10.4	107.4	1	----
286	10.09	43.8	2	----
313	10.51	171.9	1	----
317	11.45	163.1	1	----
323	10.62	103.3	1	----
351	9.86	116.3	2	-7.20
359	10.41	169.4	0	----
372	10.62	136.8	2	----

3 Protein haptention by amoxicillin: high resolution mass spectrometry analysis and identification of target proteins in serum

Lysine	pK	SAS (Å³)	Lys/Arg	Score
378	10.7	138.2	2	----
389	10.46	130.5	1	----
402	10.44	117.3	1	----
413	9.5	45.3	4	----
414	8.47	10.6	4	----
432	9.24	53	3	----
436	9.5	99.2	4	----
439	10.5	201.7	2	----
444	10.34	116.8	1	----
466	10.88	102.9	1	----
475	10.39	129.7	0	----
500	10.43	159.9	1	----
519	10.5	122.9	1	----
524	10.27	99.7	5	----
525	9.96	11.2	3	----
534	9.16	21.5	2	----
536	9.51	36.4	2	----
538	11.51	214.3	2	----
541	10.03	181.9	3	-8.26
545	10.12	110.1	2	-7.53
557	10.47	131.3	2	----
560	10.54	172.4	1	----
564	10.47	194.2	1	----
573	10.42	141.7	0	----
574	10.48	173.9	1	----

3.4 Discussion

Drug allergy constitutes an important clinical problem the molecular basis of which is not fully understood. AX is among the drugs most frequently eliciting allergic reactions. Untangling the mechanisms underlying allergy to β -lactam antibiotics will require multidisciplinary approaches. Here we have set up an *in vitro* model that may shed light into the process of protein haptention. Our results show that HSA can be modified *in vitro* by concentrations of AX in the range of those expected to occur *in vivo*. Moreover, we have detected this modification by high resolution MS, proteomic and immunological methods with high sensitivity. Using these approaches we have identified other potential candidates for protein haptention in human serum. Moreover, we have highlighted the structural features of the protein and of the antibiotic that would be important for the interaction. These findings may help to design and interpret *in vivo* studies addressing the mechanisms of drug allergy.

Immunological methods have been previously used to detect adducts of proteins and β -lactam antibiotics [25], and HSA and transferrin were identified as target proteins for binding of ampicillin [26]. Our results show that, in addition to these major targets, other serum proteins are modified by AX. Therefore, the potential involvement of these newly identified adducts in the immune response to AX deserves further study. In particular, modification of immunoglobulins by AX will surely need to be taken into account in the context of the immune response. In addition, covalent AX binding to serum proteins including immunoglobulins will need to be considered for the interpretation of the results of immunoassays aimed at detecting anti-AX antibodies in patients.

3 Protein haptentation by amoxicillin: high resolution mass spectrometry analysis and identification of target proteins in serum

Importantly, it is clear that the extent of AX addition is protein-specific. Transferrin appears to be modified by AX in a high proportion, which, taking into account the plasma concentration of this protein, could represent a modification 10-fold higher than that of HSA. Therefore, although HSA is the most abundant protein in serum, contribution of adducts of AX with other proteins may play an important role as providers of haptens. Interestingly, other relatively abundant serum proteins do not form detectable adducts under our experimental conditions. Therefore, factors other from protein abundance may influence AX binding.

In the early works by Yvon and co-workers, six major penicilloyl binding sites were identified in HSA, namely Lys 190, 195, 199, 432, 541 and 545 [2, 3]. Recently, using proteomic approaches, the formation of adducts between HSA and flucloxacillin, piperacillin and benzylpenicillin has been characterized [4-6]. In this case, the MS approach applied consisted of generating multiple reaction monitoring (MRM) transitions, specific for drug-modified peptides by selecting the m/z values calculated for all the possible peptides with a missed cleavage at a Lys residue plus specific fragments such as that at m/z 160 attributed to the cleaved thiazolidine ring, combined with MS/MS sequencing of the identified peptides. Interestingly, the nature of the residues modified appears to vary widely between subjects, and adducts with residues Lys190, 195, 432 and 541 have been detected in the plasma of patients treated with piperacillin, whereas multiple adduct-bearing peptides have been detected in patients treated with benzylpenicillin or flucloxacillin. Under our experimental conditions, both covalent and non-covalent modes of interaction of AX with HSA were detected, the latter being evidenced by their reversal by extensive washing of AX-incubated HSA. Our data indicate that the covalent coupling takes place by amide bond formation between primary amines from Lys residues and the carboxylic group from the β -

3 Protein haptention by amoxicillin: high resolution mass spectrometry analysis and identification of target proteins in serum

lactam ring, to afford the amoxicilloyl moiety. This is in agreement with what has been described for other β -lactams and it is also supported by data from the NMR characterization of an AX-butylamine complex (Montañez, M.I., personal communication). The major sites for addition of AX at low concentrations in isolated HSA were Lys 190, 199 and 541. Modelling studies were able to rationalize the marked reactivity of the targeted Lys residues confirming that their reactivity can be vastly influenced by the surrounding microenvironment and that residue accessibility, albeit relevant, cannot be seen as the sole factor governing the reactivity. The microenvironment can enhance the intrinsic reactivity of the Lys residues and it can contribute to the binding of AX through a sort of recognition process which can stably constrain AX in a pose conducive to adduct formation thus explaining the fine selectivity of the modification sites. Nevertheless, at high AX concentrations other sites of modification were found. Moreover, the modification of other residues *in vivo* cannot be excluded. Indeed, we noted that the main HSA sites modified by low AX concentrations when incubation was carried out in complete serum were Lys190 and Lys 432. The differences found in the residues modified by AX depending on the incubation conditions, either purified HSA or complete serum, suggest that the protein context may influence the nature of the adducts formed. This raises the possibility that changes in serum composition occurring in pathophysiological situations may influence protein haptention. It should be noted that β -lactam-peptide adducts will be formed both in non-allergic subjects and in subjects developing allergic reactions, the factors determining the development of allergy not being currently understood.

The so-called danger signals are thought to play an important role in allergic reactions. It has been shown that sulfamethoxazole forms adducts with proteins in antigen presenting cells and that the amount of adducts formed

3 Protein haptention by amoxicillin: high resolution mass spectrometry analysis and identification of target proteins in serum

increases when cells are exposed to bacterial endotoxin, cytokines or a variety of inflammatory or stress-inducing stimuli [27]. This underlines the importance of concomitant factors for protein haptention. It is known that HSA is the target of various modifications by reactive lipids generated under situations of inflammation or oxidative stress, including 4-hydroxy-2-nonenal and cyclopentenone prostaglandins [16, 28, 29]. Moreover, HSA is sensitive to various oxidative modifications [30]. It has been reported that HSA modification may drastically alter its binding properties and even its immunogenic and proinflammatory potential [31]. In preliminary experiments we have observed that pretreatment of HSA in vitro in the presence of certain oxidative agents alters its modification by amoxicillin, as evidenced by immunological detection (Ruiz-Abánades et al., unpublished observations). Further studies are needed to assess the biochemical basis of these effects.

In summary, this study sets the basis for the highly sensitive detection and identification of AX-protein adducts. Future studies will allow the identification of AX binding sites in other proteins as well as in vivo thus broadening the information on protein haptention by AX and hopefully contributing to the development of diagnostic tools and to the characterization of the pathogenic mechanisms of allergic reactions towards AX.

3.5 References

1. Ariza A, Montañez MI, Pérez-Sala D. Proteomics in immunological reactions to drugs. *Curr Opin Allergy Clin Immunol.* 2011;11:305-12.
2. Yvon M, Anglade P, Wal JM. Identification of the binding sites of benzyl penicilloyl, the allergenic metabolite of penicillin, on the serum albumin molecule. *FEBS Lett.* 1990 Apr 24;263(2):237-40.
3. Yvon M, Wal JM. Identification of lysine residue 199 of human serum albumin as a binding site for benzylpenicilloyl groups. *FEBS Lett.* 1988 Nov 7;239(2):237-40.
4. Meng X, Jenkins RE, Berry NG, Maggs JL, Farrell J, Lane CS, et al. Direct evidence for the formation of diastereoisomeric benzylpenicilloyl haptens from benzylpenicillin and benzylpenicillic acid in patients. *J Pharmacol Exp Ther.* 2011 Sep;338(3):841-9.
5. Jenkins RE, Meng X, Elliott VL, Kitteringham NR, Pirmohamed M, Park BK. Characterisation of flucloxacillin and 5-hydroxymethyl flucloxacillin haptentated HSA in vitro and in vivo. *Proteomics Clin Appl.* 2009 Jun;3(6):720-9.
6. Whitaker P, Meng X, Lavergne SN, El-Ghaiesh S, Monshi M, Earnshaw C, et al. Mass spectrometric characterization of circulating and functional antigens derived from piperacillin in patients with cystic fibrosis. *J Immunol.* 2011 Jul 1;187(1):200-11.
7. Acton G. *Aminopenicillins: Advances in research and application.* Atlanta, USA: Scholarly Editions; 2012.
8. Zhao Z, Batley M, D'Ambrosio C, Baldo BA. In vitro reactivity of penicilloyl and penicillanyl albumin and polylysine conjugates with IgE-antibody. *Journal of immunological methods.* 2000 Aug 28;242(1-2):43-51.
9. Audicana M, Bernaola G, Urrutia I, Echechipia S, Gastaminza G, Munoz D, et al. Allergic reactions to betalactams: studies in a group of patients allergic to penicillin and evaluation of cross-reactivity with cephalosporin. *Allergy.* 1994 Feb;49(2):108-13.
10. Mayorga C, Obispo T, Jimeno L, Blanca M, Moscoso del Prado J, Carreira J, et al. Epitope mapping of beta-lactam antibiotics with the use of monoclonal antibodies. *Toxicology.* 1995 Mar 31;97(1-3):225-34.

3 Protein haptention by amoxicillin: high resolution mass spectrometry analysis and identification of target proteins in serum

11. Fujiwara K, Shin M, Miyazaki T, Maruta Y. Immunocytochemistry for amoxicillin and its use for studying uptake of the drug in the intestine, liver, and kidney of rats. *Antimicrob Agents Chemother.* 2011 Jan;55(1):62-71.
12. Hoizey G, Lamiable D, Frances C, Trenque T, Kaltenbach M, Denis J, et al. Simultaneous determination of amoxicillin and clavulanic acid in human plasma by HPLC with UV detection. *Journal of pharmaceutical and biomedical analysis.* 2002 Oct 15;30(3):661-6.
13. Serrano JM, Hita J, Ponferrada CJ, López MC, Cárceles CM. Intravenous Pharmacokinetics and binding to plasmatic proteins of Amoxicillin and Clavulanic acid in sheeps. *AN VET.* 1989;5:75-87.
14. Makarov A, Denisov E, Kholomeev A, Balschun W, Lange O, Strupat K, et al. Performance evaluation of a hybrid linear ion trap/orbitrap mass spectrometer. *Analytical chemistry.* 2006 Apr 1;78(7):2113-20.
15. Perry RH, Cooks RG, Noll RJ. Orbitrap mass spectrometry: instrumentation, ion motion and applications. *Mass spectrometry reviews.* 2008 Nov-Dec;27(6):661-99.
16. Aldini G, Gamberoni L, Orioli M, Beretta G, Regazzoni L, Maffei Facino R, et al. Mass spectrometric characterization of covalent modification of human serum albumin by 4-hydroxy-trans-2-nonenal. *J Mass Spectrom.* 2006 Sep;41(9):1149-61.
17. Shevchenko A, Tomas H, Havlis J, Olsen JV, Mann M. In-gel digestion for mass spectrometric characterization of proteins and proteomes. *Nat Protoc.* 2006;1(6):2856-60.
18. Zhang Z, Marshall AG. A universal algorithm for fast and automated charge state deconvolution of electrospray mass-to-charge ratio spectra. *Journal of the American Society for Mass Spectrometry.* 1998 Mar;9(3):225-33.
19. Sugio S, Kashima A, Mochizuki S, Noda M, Kobayashi K. Crystal structure of human serum albumin at 2.5 Å resolution. *Protein engineering.* 1999 Jun;12(6):439-46.
20. Pedretti A, Villa L, Vistoli G. VEGA: a versatile program to convert, handle and visualize molecular structure on Windows-based PCs. *Journal of molecular graphics & modelling.* 2002 Aug;21(1):47-9.

3 Protein haptention by amoxicillin: high resolution mass spectrometry analysis and identification of target proteins in serum

21. Olsson MHM, Sondergard CR, Rostkowski M, Jensen JH. PROPKA3: Consistent treatment of internal and surface residues in empirical pKa predictions. *J Chem Theory Comput.* 2011;7:525-37.
22. Morris G, Goodsell D, Halliday R, Huey R, Hart W, Belew R, et al. Automated docking using a Lamarckian genetic algorithm and an empirical binding free energy function. *J Comput Chem.* 1998;19:1639-62.
23. Llinas A, Page M. Intramolecular general acid catalysis in the aminolysis of beta-lactam antibiotics. *Org Biomol Chem.* 2004;2:651-4.
24. Llinas A, Vilanova B, Page M. Thiol-catalysed hydrolysis of cephalosporins and possible rate-limiting amine anion expulsion. *J Phys Org Chem.* 2004;17:521-8.
25. Carey MA, van Pelt FNAM. Immunochemical detection of flucloxacillin adduct formation in livers of treated rats. *Toxicology.* 2005;216(1):41-8.
26. Magi B, Marzocchi B, Bini L, Cellesi C, Rossolini A, Pallini V. Two-dimensional electrophoresis of human serum proteins modified by ampicillin during therapeutic treatment. *Electrophoresis.* 1995 Jul;16(7):1190-2.
27. Lavergne SN, Wang H, Callan HE, Park BK, Naisbitt DJ. "Danger" conditions increase sulfamethoxazole-protein adduct formation in human antigen-presenting cells. *J Pharmacol Exp Ther.* 2009 Nov;331(2):372-81.
28. Aldini G, Vistoli G, Regazzoni L, Gamberoni L, Facino RM, Yamaguchi S, et al. Albumin is the main nucleophilic target of human plasma: a protective role against pro-atherogenic electrophilic reactive carbonyl species? *Chem Res Toxicol.* 2008 Apr;21(4):824-35.
29. Yamaguchi S, Aldini G, Ito S, Morishita N, Shibata T, Vistoli G, et al. Delta(12)-Prostaglandin J(2) as a Product and Ligand of Human Serum Albumin: Formation of an Unusual Covalent Adduct at His146. *J Am Chem Soc.* 2010;132:824-32.
30. Oettl K, Stauber RE. Physiological and pathological changes in the redox state of human serum albumin critically influence its binding properties. *Br J Pharmacol.* 2007 Jul;151(5):580-90.
31. Kormoczi GF, Wolfel UM, Rosenkranz AR, Horl WH, Oberbauer R, Zlabinger GJ. Serum proteins modified by neutrophil-derived oxidants as mediators of neutrophil stimulation. *J Immunol.* 2001 Jul 1;167(1):451-60.

4 Mass spectrometric strategies for the identification and characterization of Human Serum Albumin covalently adducted by Amoxicillin: ex vivo studies

Davide Garzon^a, Adriana Ariza^{b,c}, Luca Regazzoni^a, Riccardo Clerici^a, Alessandra Altomare^a, Federico Riccardi Sirtori^{a^}, Marina Carini^a, María José Torres^d, Dolores Pérez-Sala^b and Giancarlo Aldini^{a*}

^aDepartment of Pharmaceutical Sciences, Università degli Studi di Milano, via Mangiagalli 25, 20133, Milan, Italy

^bDepartment of Chemical and Physical Biology, Centro de Investigaciones Biológicas, C.S.I.C., Ramiro de Maeztu, 9, 28040 Madrid, Spain.

^cResearch Laboratory, IBIMA – Hospital Regional Universitario de Málaga - UMA, Málaga, Spain

^dAllergy Unit, IBIMA – Hospital Regional Universitario de Málaga – UMA, Málaga, Spain

[^] present address: Oncology Business Unit, Nerviano Medical Sciences, Viale Pasteur 10, 20014 Nerviano (MI), Italy

ABSTRACT

This study addresses the detection and characterization of the modification of human serum albumin (HSA) by amoxicillin (AX) in *ex vivo* samples from healthy subjects under oral amoxicillin administration (acute intake of 1 g every 8 h for 48 h). To reach this goal we have used an analytical strategy based on targeted and untargeted mass spectrometric approaches. Plasma samples withdrawn before AX oral intake represented the negative control samples to test the method selectivity, while HSA incubated *in vitro* with AX was the positive control. Different MS strategies were developed and in particular: 1) Multiple Reaction Monitoring (MRM) and Precursor Ion Scan (PIS) using a HPLC system coupled to a triple quadrupole MS analyser; 2) a dedicated data-dependent scan and a customized targeted MS/MS analysis carried out using a nano-LC system coupled to a high resolution MS system (LTQ Orbitrap XL).

Lys 190 was identified as the only modification site of HSA in the *ex vivo* samples. The AX adduct was identified and fully characterized by complementary targeted approaches based on triple quadrupole (MRM mode) and orbitrap (SIC mode) as mass analyzers. The SIC mode also permitted to measure the relative amount of AX adducted HSA, ranging from 1 to 2% (6-12 μM) after 24 and 48 hours from the oral intake. No adduct in any *ex vivo* sample was identified by the untargeted methods (PIS and data dependent scan mode analysis).

The results on one hand indicate that MS and in particular high resolution MS analyser represents a suitable analytical tool for the identification/characterization of covalently modified proteins/peptides; on the other hand they give a deeper insight into the AX-induced protein haptentation, which is required for a better understanding of the mechanisms involved in AX-elicited allergic reactions.

4 Mass spectrometric strategies for the identification and characterization of Human Serum Albumin covalently adducted by Amoxicillin: ex vivo studies

Keywords: Amoxicillin, human serum albumin (HSA), haptentation, Lys 190, protein covalent binding, Multiple Reaction Monitoring, Orbitrap.

Abbreviations: AX, amoxicillin; CID collision induced dissociation; HCD high energy collision induced dissociation HSA, human serum albumin; MRM, Multiple Reaction Monitoring; MS, mass spectrometry; PIS, Precursor Ion Scan; SIC, single ion chromatogram; TQ, triple quadrupole, TSQ, triple stage quadrupole.

4.1 Introduction

Allergy to β -lactam antibiotics poses important clinical problems *per se* and reduces the therapeutic possibilities in a time when bacterial infections are again rising as important causes of morbidity and mortality.[1, 2] Covalent binding of drugs to protein structures, in a process known as haptentation, is believed to be essential to give rise to a stable structure capable of eliciting an immune response.^{3,[3]} Identification and characterization of the protein targets for modification by drugs may help delineate the mechanisms involved in drug sensitization.[4] Amoxicillin (AX) is a wide spectrum β -lactam antibiotic, the use of which has been increasing steadily during the past decades becoming the most commonly consumed betalactam in many countries.[5, 6] Incidence of allergy to AX has increased in parallel with its consumption in such a way that nowadays it is the antibiotic eliciting a higher frequency of allergic reactions.[7, 8] A recent data analysis on 333 cases of allergy reaction shows that the 50% of hypersensitivity reactions are due to β -lactam antibiotics and among them AX was incriminated in 65 % of the patients.[9]

Patients who have developed an allergic reaction to AX are evaluated and diagnosed on the basis of either: *i*) the presence of AX-reactive IgE in serum detected by *in vitro* immunoassays, *ii*) the responsiveness of their basophil cells or the specific lymphocyte proliferation in presence of the antibiotic by *in vitro* basophil activation test or lymphocyte transformation test, respectively *iii*) the responsiveness of their mast cells and T cells by skin test and, *iv*) provocation tests by oral administration of AX.[10] Nevertheless, skin and oral provocation tests imply higher risks than *ex vivo* testing and have to be carried out in a hospital setting.[11] Therefore, diagnosis through *ex vivo* tests is preferable. Strategies for these tests include, besides the use of AX, AX-derivatized dendrimeric structure or extensively modified homopolymers and proteins such as poly-L-lysine and serum

4 Mass spectrometric strategies for the identification and characterization of Human Serum Albumin covalently adducted by Amoxicillin: ex vivo studies

albumin, respectively.¹⁵[12] However, the sensitivity of the present diagnostic tools is still limited and oral drug administration is required in a considerable percentage of patients in order to confirm the diagnostic.[10, 13-15] A current interpretation of this phenomenon postulates the contribution of endogenous protein structures to the formation of the antigenic determinant(s) important for antibody recognition. Identification of endogenous targets for haptation could therefore render a battery of new tools that could be explored to increase diagnostic efficiency.

With a view to fully elucidating the target protein of AX haptation, we recently described the *in vitro* modification of various serum proteins by AX and characterized the modification of HSA both by immunological and mass spectrometric (MS) approaches. Under the conditions of the previous study, several lysine residues in HSA, in particular Lys 190 and 199, were found to be the most reactive to AX. In addition, we observed that Lys 190 was modified by AX either using the isolated protein or whole serum.[16] Figure 1 reports the reaction mechanism between AX and Lys 190 together with the diagnostic fragment ions that were used for the adduct characterization by MS studies.[16] In the current study we have addressed the detection and characterization of the modification of HSA by AX in *ex vivo* samples from subjects under oral administration of AX. To reach this goal we used both immunological and MS methods. The MS approach we used is based on the most suitable techniques and MS analyzers (triple quadrupole and orbitrap) applied to identify and characterize peptide/protein covalent adducts. Using this approach we have been able to detect the addition of AX to Lys 190 of HSA and to determine the relative content in respect to the native peptide. These findings set the basis for the study of this structure as antigenic determinant and the development of novel diagnostic tools.

4 Mass spectrometric strategies for the identification and characterization of Human Serum Albumin covalently adducted by Amoxicillin: ex vivo studies

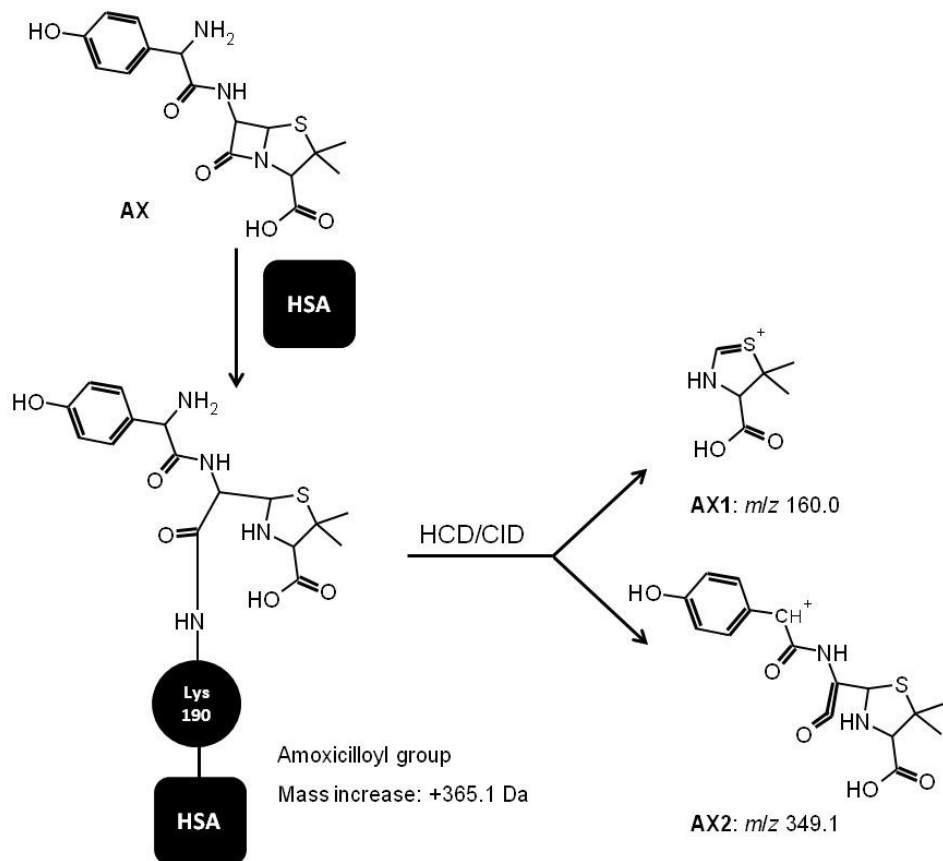


Fig.1. Reaction mechanism between Lys 190 and AX and chemical structure of AX diagnostic fragment ions. The amoxicilloyl modification induces a mass increase of +365.1 Da. HCD or CID fragmentation of the Lys 190 AX modified peptide generates two diagnostic fragment ions : AX1 referred to the thiazolidinic ring and AX2, attributed to the cleavage of AX from Lys 190 and by the concomitant loss of the amine group. The two fragment ions structure were predicted by Mass Frontier software.

4.2 Material and methods

4.2.1 Reagents

AX was from Glaxo SmithKline (Madrid, Spain). Iodoacetamide (IAA), (D)-threo-1,4-dimercapto-2,3-butanediol (DTT), tris (hydroxymethyl) aminomethane, sodium phosphate dibasic and LC-grade and analytical-grade organic solvents were from Sigma-Aldrich. Sequence grade modified trypsin was obtained from Promega (Milan, Italy).

The monoclonal antibody anti-amoxicillin (AO3.2) was the generous gift of Dr. Cristobalina Mayorga (Research Laboratory, IBIMA – Hospital Regional Universitario de Málaga - UMA, Málaga, Spain).[16]

4.2.2 AX administration, serum collection and HSA isolation

AX (Glaxo Smithkline, Madrid, Spain) was orally administered (1 g every 8 h for 48 h) to two healthy volunteers, not allergic to this antibiotic and identified as subject A and B within the manuscript. The extraction of peripheral blood using tubes with gel (Vacuette Greiner Bio-One, Kremsmünster, Austria) immediately before (T0) the intake of the first pill and 24 (T24) and 48 h (T48) after the intake of the first pill (with an accumulated dose of 3 and 6 g) was done at the Regional University Hospital of Malaga (Spain). Serum was obtained by centrifugation of the samples at 4000 rpm for 5 min and it was frozen in aliquots at -80°C until their analysis. The study was conducted according to the Declaration of Helsinki principles and was approved by the Malaga Research Ethics Committee (Spain). All subjects included in the study were informed orally about the study and signed the corresponding informed consent form.

4.2.3 HSA isolation

HSA was isolated from the serum by affinity chromatography using Affi-Gel[®] blue gel (Bio-Rad, Segrate, Italy). An aliquot of 50 μ L of serum was diluted with 150 μ L of sodium phosphate dibasic 20 mM, pH 7.1 (buffer A) and kept at room temperature for 15 minutes. In the meanwhile a Sigma Prep Spin column was filled with 500 μ L of BlueGel Affigel and the gel was activated as indicated by the protocol. Aliquots of 200 μ L of the diluted serum were pipetted in the column and washed three times with buffer A. Albumin was eluted by pipetting two aliquots of 250 μ L of NaCl 1.4 M (buffer B) in the column. For each step the columns were centrifuged by means of a mikro 120 Hettich centrifuge for one minute at 20 g. The recovery of HSA and of AX modified HSA ranged from 85 to 92% and did not changes significantly. HSA concentration was determined spectrophotometrically at 280 nm.

4.2.4 In vitro modification of serum proteins by AX

AX was freshly prepared in 50 mM Na₂CO₃/NaHCO₃ pH 10.2. For western blot analysis, HSA was incubated in the presence of 0.5 mg/ml AX for 16 h at 37°C. AX incorporation into serum proteins was assessed by SDS-PAGE followed by western blot and detection with anti-AX monoclonal antibody AO3.2, as previously described.[16] AX-modified HSA as positive control for MS study was prepared by incubating 150 μ M HSA (10 mg/mL) with 13.5 mM AX (5 mg/mL) in PBS overnight at 37°C (stoichiometric ratio HSA:AX of 1:90)

4.2.5 HSA protein digestion for LC-ESI-MS analysis

Aliquot of 30 µg of HSA was dissolved in 30 µL 50 mM Tris-HCl (pH 7.8) and digested with trypsin according to the manufacturer's procedure. Firstly DTT was added at a final concentration of 2 mM and the sample was incubated for 60 min at 37 °C; then IAA was added to the solution at a final concentration of 4 mM and the sample was incubated for 45 min at 37 °C in the dark. In order to quench the excess of IAA, DTT was added again at a final concentration of 4 mM and the sample was incubated for 60 min at 37 °C degrees. CaCl₂ was spiked at a final concentration of 1 mM and then trypsin was added to the sample at a trypsin to protein ratio of 1:30. After an overnight period at 37 °C the tryptic mixtures were acidified with formic acid up to a final concentration of 10%. The digested HSA was then analyzed by triple quadrupole and orbitrap mass spectrometer, using both targeted and untargeted approaches, as summarized in Figure 2.

4.2.6 Multiple Reaction Monitoring and Precursor Ion Scan analyses

Aliquots of 5 µg of digested HSA were dissolved in 20 µL of buffer A (0.1% formic acid in water) and injected onto a reversed-phase Agilent Zorbax SB-C18 column (4 mm i.d., particle size 3.5 µm, CPS Analytica, Milan, Italy) protected by an Agilent Zorbax RP guard column. The peptides were eluted with a 55 min gradient from 98% buffer A (0.1% formic acid in water) to 60% buffer B (0.1% formic acid in acetonitrile) at a constant flow rate of 200 µL/min. The triple quadrupole TSQ Quantum Ultra (ThermoQuest, Milan, Italy) was set in positive ion mode and with the following ion source parameters: capillary temperature 275° C; spray voltage 4.5 kV; capillary voltage 35 V; tube lens voltage 120 V. The flow rate of the nebulizer gas (nitrogen) was 50 a.u.

MRM of each of the AX adducted peptides previously identified under in vitro conditions[16] was carried out by setting as diagnostic fragments the ions at m/z 160.0 and 349.1, corresponding to the thiazolidinic moiety of AX and to AX minus the aminic residue, respectively. The AX modified peptides and the corresponding transitions are summarized in Table 1.

The parameters influencing these transitions were optimized as follows: argon gas pressure in the collision Q2, 1.5 mbar; peak full width at half-maximum (FWHM), 0.70 m/z at Q1 and Q3; scan width for all MRM channels, 1 m/z ; scan rate (dwell time), 0.05 s/scan. Data processing was performed by the Xcalibur 2.0 software. Fragmentation was done using CID mode (isolation width, 1 m/z ; normalized collision energy, 28 CID arbitrary units).

Precursor Ion Scan analysis was carried out by setting as diagnostic ions the ions at m/z 160.0 and 349.1 which are characteristic of the AX moiety.[16] MS parameters were set as follows: collisional voltage at 30 V, mass unit resolution, scan time of 1 s for both Q1 and Q3, m/z 300–1500 as Q1 scan range.

4 Mass spectrometric strategies for the identification and characterization of Human Serum Albumin covalently adducted by Amoxicillin: ex vivo studies

Multiple reaction monitoring: transition list			
Modified residue	Sequence	Precursor ion (m/z)	Product ions (m/z)
K 190	¹⁸² LDEL RDEGK#ASSAK ¹⁹⁵	628.6	160.0 +349.1
K 199	¹⁹⁸ LK#C\$ASLQK ²⁰⁵	656.8	160.0 +349.1
K 351	³⁴⁹ LAK#TYETTLEK ³⁵⁹	554.6	160.0 +349.1
K 432	⁴²⁹ NLGK#VGSK ⁴³⁶	584.3	160.0 +349.1
K 541	⁵³⁹ ATK#EQLK ⁵⁴⁵	591.8	160.0 +349.1
K 545	⁵⁴² EQLK#AVMDDFAAFVEK ⁵⁵⁷	736.0	160.0 +349.1

Table 1. AX modified peptides searched by MRM analysis. For each peptide the sequence and the m/z of the corresponding precursor ion and product ions used for the transition are reported. The symbol # indicates the modification site and \$ the carbamidomethylated Cys.

4.2.7 Liquid chromatography electrospray ionization mass spectrometry/mass spectrometry analysis (LC-ESI-MS/MS): LTQ Orbitrap XL mass spectrometer

Peptides from HSA digestion were then separated by reversed-phase (RP) nanoscale capillary liquid chromatography (nanoLC) and analyzed by electrospray tandem mass spectrometry (ESI-MS/MS). Digested peptides arising from 1.5 μg of HSA were dissolved in 10 μL of buffer A (0.1% formic acid in water) and injected into a trapping column in order to purify and concentrate the sample. The trapping column was a Acclaim PepMap 100, nanoviper C18, 100 \AA , 100 μm i.d. x 2 cm, Thermo Scientific. The flow rate was of 10 $\mu\text{L}/\text{min}$ for 4 minutes. After 4 minutes the valve switched and the peptide mixture was loaded onto a fused silica reversed-phase column (PicoFritTM Column, HALO, C18, 2.7 μm , 100 \AA , 75 μm i.d. x 10 cm, New Objective). The peptides were eluted with a 55 min gradient from 99% buffer A (0.1% formic acid in water) to 35% buffer B (0.1% formic acid in acetonitrile) at a constant flow rate of 300 nL/min. The nano chromatographic system, an UltiMate 3000 RSLCnano System (Dionex), was connected to an LTQ-Orbitrap XL mass spectrometer (Thermo Scientific, Milan, Italy) equipped with a nanospray ion source (dynamic nanospray probe, Thermo Scientific, Milan, Italy) set as follows: spray voltage 1.8 Kv; capillary temperature 220 $^{\circ}\text{C}$, capillary voltage 30 V; tube lens offset 100 V, no sheath or auxiliary gas flow.

The LTQ-Orbitrap XL mass spectrometer was set to perform scan cycles consisting, firstly, of recording a high-resolution (resolving power 60000, FWHM at m/z 400) full scan (200-1500 m/z) in profile mode, then by the acquisition of the MS/MS spectra of the three most intense ions in centroid mode, using both CID and HCD fragmentation (isolation width, 3 m/z ; normalized collision energy, 35 CID arbitrary units, 30 HCD arbitrary units). Protonated phthalates [dibutylphthalate (plasticizer), m/z 279.159086; bis(2-ethylhexyl)phthalate, m/z 391.284286] and polydimethylcyclosiloxane ions $[(\text{Si}(\text{CH}_3)_2\text{O})_6 + \text{H}]^+$; m/z

4 Mass spectrometric strategies for the identification and characterization of Human Serum Albumin covalently adducted by Amoxicillin: ex vivo studies

445.120025] were used for real time internal mass calibration. Dynamic exclusion was enabled (repeat count, 2; repeat duration, 45 s; exclusion list size, 50; exclusion duration, 80 s; relative exclusion mass width, 10 ppm). Charge state screening and monoisotopic precursor selection was enabled, singly and unassigned charged ions were not fragmented.

Identification of the peptides covalently modified by AX as well as the modification sites, was carried out by the MS strategy previously described and based on two different steps.[16] The first step consisted of identifying the precursor ions of diagnostic fragment ions at m/z 160.04 and 349.08. In more detail, the precursor ions were extracted from the two parent ion maps displayed by setting as product mass the ions at m/z 160.04 (tolerance 0.01) and the ion at m/z 349.08 (tolerance 0.01). The two lists of parent ions were then exported to Excel Microsoft and analyzed using the following Boolean logic: if $\text{value1} > \text{ts}$, $\text{value2} > \text{ts}$, $\text{value\$} = \text{value1} + \text{value2}$ or else $\text{value\$} = 0$, where value1 and value2 are the relative abundances of the precursor ions setting the product ions at m/z 160.04 (value 1) and 349.08 (value 2) and ts is the threshold relative abundance. By using this approach, each precursor ion was confirmed only when it was present in both the ion maps which were reconstituted by setting the two diagnostic precursor ions, otherwise it was discarded. The second step consisted of matching the precursor ions with a list of theoretical modified ions generated by an *in silico* digestion of albumin carried out by considering the following parameters: trypsin as enzyme, two missed cleavages and the addition of the amoxicilloyl moiety at the Lys residues.

Targeted MS/MS scan analyses were carried out by setting the LTQ-Orbitrap XL mass spectrometer to perform two scan cycles, one in full scan (200-1500 m/z), the other based on the inclusion list reported in Table 2:

MS/MS experiments were carried out in CID mode (isolation width, 3 m/z ; normalized collision energy, 33 CID arbitrary units). Protonated phthalates [dibutylphthalate (plasticizer), m/z 279.159086; bis(2-ethylhexyl)phthalate, m/z

4 Mass spectrometric strategies for the identification and characterization of Human Serum Albumin covalently adducted by Amoxicillin: ex vivo studies

391.284286] and polydimethylcyclosiloxane ions $[(\text{Si}(\text{CH}_3)_2\text{O})_6 + \text{H}]^+$; m/z 445.120025] were used for real time internal mass calibration.

Targeted Orbitrap MS/MS analysis: inclusion list			
Modified residue	Sequence	Exact mass (m/z)	Charge (z)
K 190	¹⁸² LDEL RDEGK#ASSAK ¹⁹⁵	628.63163	+3
K 199	¹⁹⁸ LK#C\$ASLQK ²⁰⁵	656.82303	+2
K 351	³⁴⁹ LAK#TYETTLEK ³⁵⁹	554.60787	+3
K 432	⁴²⁹ NLGK#VGSK ⁴³⁶	584.29496	+2
K 541	⁵³⁹ ATK#EQLK ⁵⁴⁵	591.79479	+2
K 545	⁵⁴² EQLK#AVMDDFAAFVEK ⁵⁵⁷	736.01134	+3

Table 2. Inclusion list used for targeted orbitrap MS/MS analysis. For each targeted peptide the sequence, the exact mass and the charge are reported. Mass tolerance was set at 10 ppm.

The symbol # indicates the modification site and \$ the carbamidomethylated Cys.

4.2.8 Bioinformatics

Peptide sequences were identified using the software turboSEQUEST (Bioworks 3.1, ThermoQuest, Milan, Italy), and using a database containing only HSA and assuming trypsin digestion. The protein sequence of HSA was obtained from the SwissProt database (primary accession number P02768). Sequence fragments calculator (Bioworks 3.1.1) was used to obtain the theoretical digested masses setting trypsin as enzyme, all the Cys residues as carbamidomethyl-cysteine and considering the oxidation of methionine residues and the formation of amoxicilloyl-Lys adducts as variable modifications. The predicted y and b series ions were determined using the Peptide Sequence Fragmentation Modeling, Molecular Weight Calculator software program (ver. 6.37), <http://come.to/alchemistmatt>. The chemical structure of amoxicillin diagnostic fragments were predicted by the software Mass Frontier 5.0 (HighChem ltd, Slovakia).

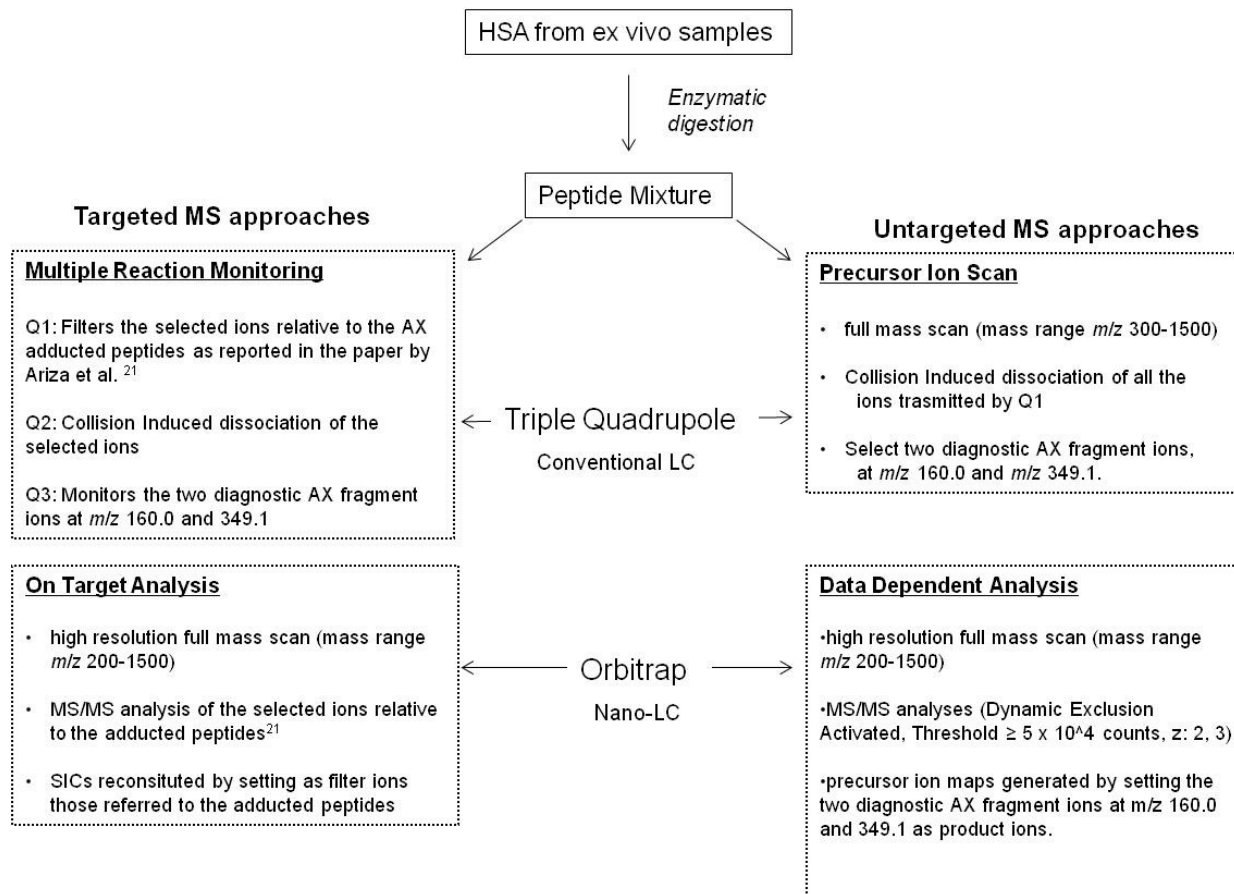


Fig. 2. Overview of the MS targeted and untargeted methods used to identify AX covalent adducts to HSA.

4.3 Results

4.3.1 Detection of AX-HSA adducts in human serum by Multiple Reaction Monitoring and Precursor Ion Scan: LC-ESI-MS/MS studies

Multiple Reaction Monitoring: development of allergy towards AX occurs most frequently after oral intake of the antibiotic. We were therefore interested in detecting AX-protein adducts under these conditions. Multiple Reaction Monitoring (MRM) is commonly used for targeted quantitative analyses.[17] Concerning β -lactams-induced protein haptentation, it was applied by Jenkins et al.[18] in order to identify the HSA residues modified by flucloxacillin in both in vitro and in vivo conditions.

Firstly, based on its well-established selectivity and sensitivity, the Multiple Reaction Monitoring scan mode was employed in order to identify the adducted peptides arising from the digested HSA isolated from subjects treated with AX. Transitions (fragment ions associated to the precursor ions) were set on the bases of the in vitro studies previously reported[17]¹ and are summarized in Table 1.

The method was firstly validated by identifying all the previously identified adducted peptides in the positive control sample (HSA incubated with AX)(Figure 3). Each adducted peptide was also identified on the basis of the retention time and the three most intense ions were K199-AX, K541-AX and K190-AX. Adducted peptides are named on the basis of the modified Lys: K190-AX, K199-AX, K351-AX, K541-AX, K545-AX and K432-AX. All the peptides monitored were not detected in the negative control samples T0A and T0B. The method was then applied to the ex vivo samples T1A, T1B, T2A and T2B. Only the peak corresponding to the Lys 190 adducted peptide ion (m/z 628.6 \rightarrow 160.0 + 349.1), and characterized by a retention time of 28 minutes, was detected in all ex vivo samples with comparable intensity. Figure 4 (left panel) shows the MRM traces of

4 Mass spectrometric strategies for the identification and characterization of Human Serum Albumin covalently adducted by Amoxicillin: ex vivo studies

Lys 190 adducted peptide relative to the negative and positive control and to the set of the *ex vivo* samples. The method was found to be selective since no peak of the adducted peptide ion was present in the negative control samples obtained by HSA isolated from samples collected before AX intake (T0A and T0B).

Although the MRM mode was found to be sensitive enough to identify the Lys 190 adducted peptide, it was unable to characterize the peptide or to identify the site of modification because of the lack of additional information such as accurate mass, isotopic pattern and MS/MS fragmentation pattern. To overcome this limitation, a mixed MRM-data-dependent scan was applied. The approach was effective for the positive control sample while in *ex vivo* samples the fragment ions did not reach suitable intensity values, even when concentrating the sample, so that no MS/MS spectra were recorded for the peptide characterization.

Another limitation of the MRM approach resides in the fact that it cannot perform a semi-quantitative analysis (the relative content of the adducted in respect to the native peptide) due to the fact that the product ions are characteristic only of the adducted peptides since they referred only to the AX moiety.

The PIS method was then used as an untargeted method in order to identify the unknown AX-modified peptides in addition to those already detected by using the MRM mode. However, as reported in Figure 5, this approach was not able to identify any AX modified peptides in the *ex vivo* samples.

By considering that the same set of samples were analysed in both MRM and PIS mode, we can confirm that the PIS mode is less sensitive in respect to the MRM mode and that in this study it was not useful for the untargeted identification due to the low abundance of the analytes.

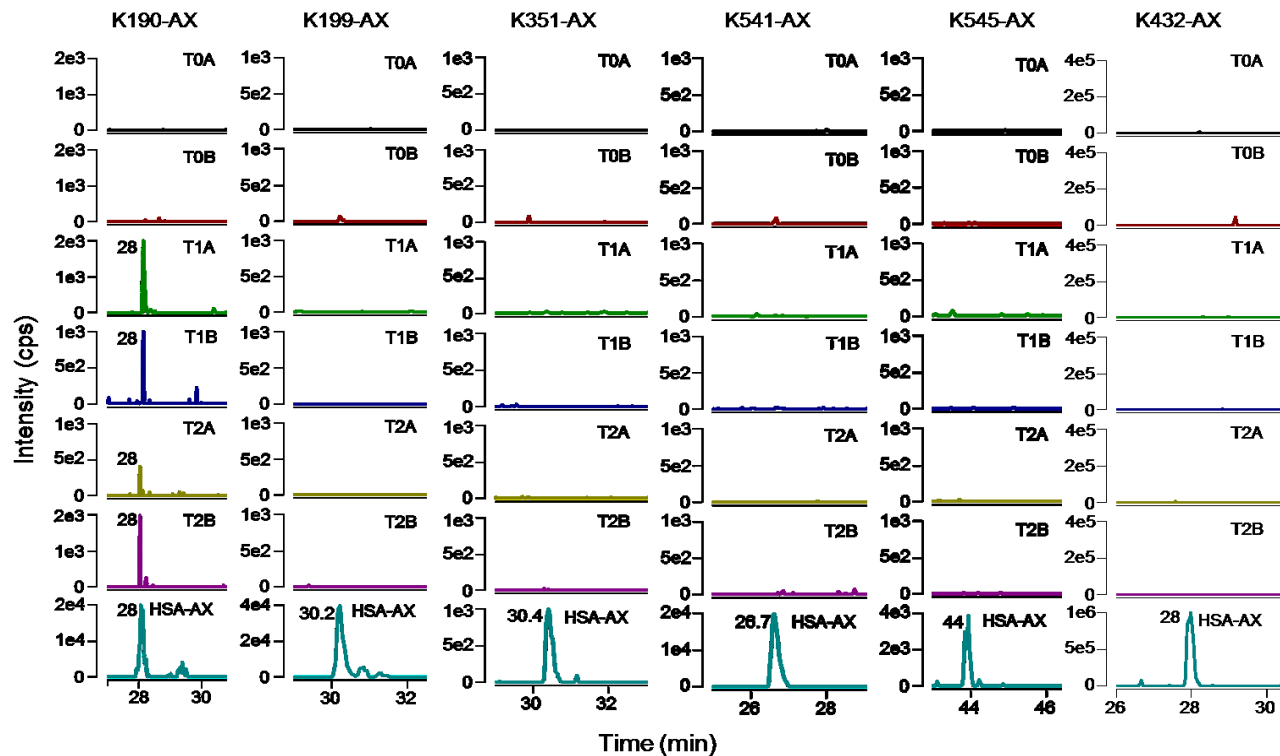


Fig. 3. Multiple Reaction Monitoring traces of the modified peptides were reconstituted by setting the transitions reported in table 1. Each column refers to a different adducted peptide ion and each row refers to a different sample, The method was found to be selective (no peak before AX administration; T0A and T0B) and able to identify the known adducted peptides formed under in vitro conditions (HSA-AX). In samples collected after AX administration (24 h for T1A, T1B and 48 h for T2A, T2B) only one peak at retention time 28 min was identified and attributed to K190-AX (m/z 628.6 \rightarrow 160.0+349.1).

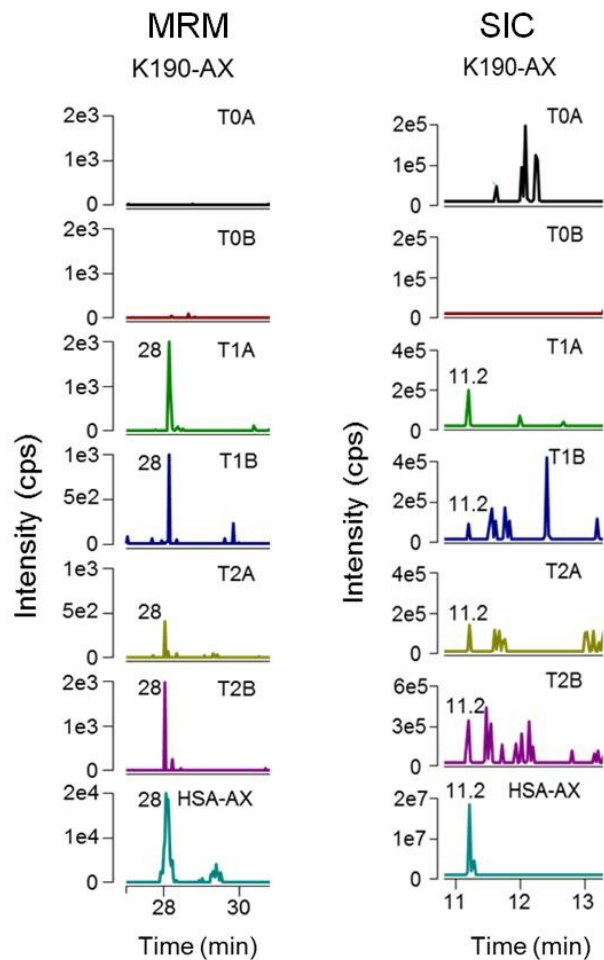


Fig. 4. Left panel: Multiple Reaction Monitoring. The Multiple Reaction Monitoring trace of the Lys 190 AX-modified peptide was reconstituted by setting the corresponding transition reported in table 1. The method was found to be selective (no peak before AX administration; T0A and T0B) and able to identify the Lys 190 AX modified peptide formed under in vitro conditions (HSA-AX). In samples collected after AX administration (24 h for T1A, T1B and 48 h for T2A, T2B) the peak at retention time 28 min was attributed to K190-AX (m/z 628.6 \rightarrow 160.0+349.1).

Right panel: Single Ion Chromatogram (SIC). Single Ion Chromatogram (SIC) of Lys 190 AX modified peptide was reconstituted by setting the $[M+3H]^{3+}$ of the modified peptide as filter ion. Orbitrap was used as MS analyser. The peak eluting at 11.2 min was attributed to K190-AX and it was identified in all the samples collected after AX administration (T1A, T1B, T2A, T2B) but not in samples T0A and T0B.

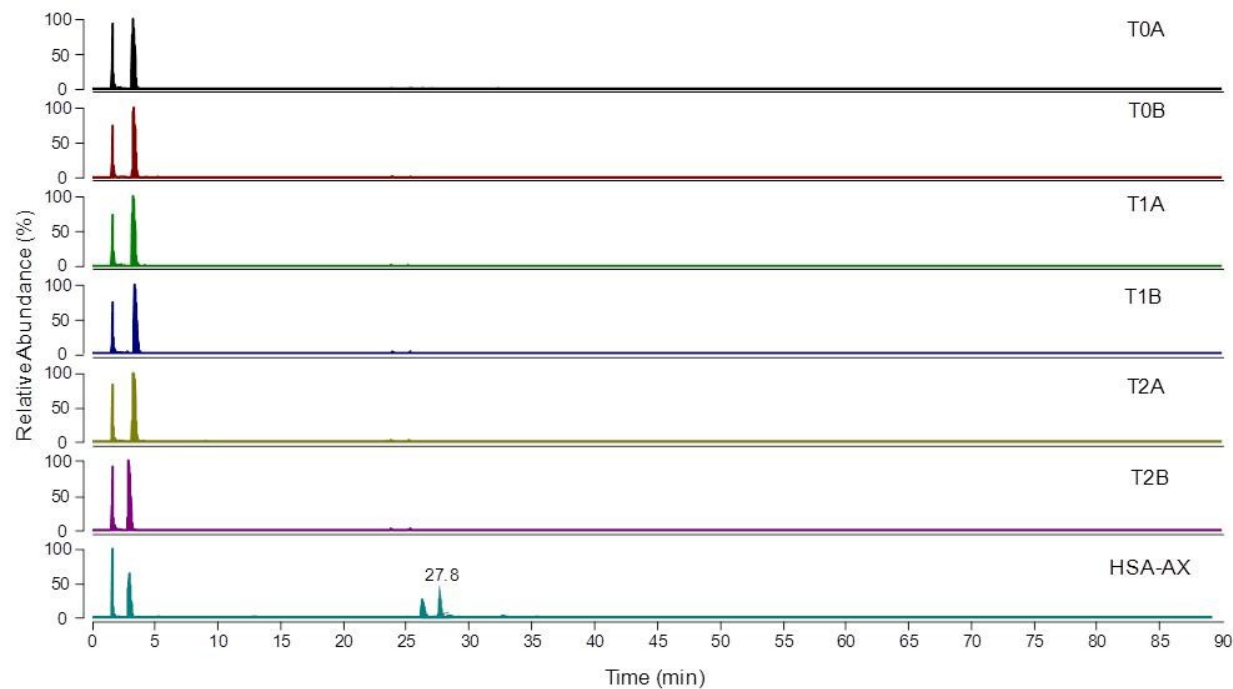


Fig. 5. Precursor Ion Scan analyses. No peak referred to the precursor ions of the diagnostic fragment ions at m/z 160.0+349.1 was identified either before (T0 A and B) or after AX administration (T1 A and B, T2 A and B). The approach only permitted identification of a peak with RT of 28 min in the positive control (HSA incubated with AX at a molar ratio of 1:90) which was attributed to K190-AX.

4.3.2 Detection of AX-HSA adducts by LC-MS/MS Orbitrap

The second step of the work was to apply a high resolution MS analyser coupled to a nano LC system in order to detect and identify the AX-adducted peptides. MS analyses were performed in two different scan modes, a data-dependent scan and a customized targeted MS/MS mode.

Data-dependent scan: The identification of AX-modified peptides was then carried out using a standard data-dependent scan as explained in the methods and in Figure 2. It should be noted that such an approach is *per se* not selective since it does not distinguish native and adducted peptides; hence when it was applied to the HSA digested samples, a large number of MS/MS spectra arising from the fragmentation of both native and adducted peptides was generated. Hence, the identification of AX-modified peptides was by necessity based on a post-run analysis. In particular for this analysis the same MS strategy described in our previous study[16] was employed in order to identify amoxicilloyl-modified peptides (+365.10454 Da).

Although this approach confirmed all the 6 different adducted peptides in the positive control sample (see supporting information Figure S3), it was not able to identify any modified peptide in the ex vivo samples. It should be noted that the lack of adduct identification is not due to a poor sequence coverage, since the protein coverage of both control and AX-treated HSA samples was always higher than 80% (see supplementary Figure 8) and the most reactive Lys residues, as reported in the literature and predicted by molecular modelling studies, were covered.

4.3.2.1 Customized targeted MS/MS mode

The next step was to search for the adducted peptides using a targeted method, based on reconstituting the single ion chromatograms (SIC) by extracting the

4 Mass spectrometric strategies for the identification and characterization of Human Serum Albumin covalently adducted by Amoxicillin: ex vivo studies

current ion relative to the m/z ion of each of the adducted peptides as previously identified, and setting a 5 ppm tolerance.

Figure 4 (right panel) shows the SICs relative to the positive control where only a single and well defined peak is observed for Lys 190 AX modified peptide. The retention time of the adducted peptide ion is clearly quite different from that observed in the MRM analysis, due to the different chromatographic configuration. By contrast, in the blank samples T0A and T0B, several peaks were detected but none at the RT of the analyte. SIC traces show the presence of the adducted peptide ion K190-AX, for all the ex vivo samples analysed (T1A, T1B, T2A, T2B). Regarding the peptide K190-AX, the method was found not to be highly selective since several peaks were present in the SIC trace, with a higher intensity compared to the adducted peptide although with a different RT. The adduct was assigned on the basis of the accurate mass and retention time and by considering the isotopic pattern of the multiply charged ion at m/z of 628.63184, overlapping the simulated data (Figure 6). These results also indicate that the failure to identify the K190-AX peptide by using the untargeted methods above reported (Sequest search algorithm and reconstituted precursor ion maps), is not due to the absence of the precursor ion, but to the fact that the target peptide was not fragmented. We then sought the reason for the lack of fragmentation. The first hypothesis was the poor intensity of the target ion. However a manual inspection of the SIC trace revealed that the intensity of the multiply charged ion relative to the target peptide was higher with respect to the ion threshold set in the data-dependent scan. We then found that several peptide ions eluted at the same retention time as the target peptide and that the dynamic exclusion did not succeed in excluding all the redundant ions.

In order to record the MS/MS spectrum of the target peptide, the threshold intensity was decreased and the dynamic exclusion modified. Although different attempts were made and the ion at m/z 628.63163 ion was always detectable in the full mass spectrum, the adducted peptide was never automatically fragmented (data not shown) and this prompted us to set-up a targeted MS/MS method. In this last

4 Mass spectrometric strategies for the identification and characterization of Human Serum Albumin covalently adducted by Amoxicillin: ex vivo studies

approach, the LTQ-Orbitrap XL mass spectrometer continuously performed scan cycles consisting of a high-resolution full scan (200-1500 m/z) followed by the MS/MS analysis of only those ions included in the list of AX adducted peptides as previously detected.[16]

This targeted-target approach was found to be highly informative since each adduct was identified not only by the accurate mass and isotopic pattern but also by the MS/MS fragmentation pattern.

This method identified the K190-AX adduct in all the ex vivo samples which was finally confirmed and fully characterized by the MS/MS spectrum (Figure 7), a result which was not achieved in the other MS approaches as above reported.

The peptide containing Lys190 ($^{182}\text{LDEL RDEGK}\#\text{ASSAK}^{195}$) contains three potential nucleophilic sites: Arg186, Lys190 and C-terminal Lys 195. The MS/MS fragment ions as detected in CID mode show an unmodified b series from b2 to b8 thus excluding the binding to Arg186. Moreover, in the spectrum there was an unmodified y series from y3 to y5 excluding the adduction on the C-terminal Lys 195. By contrast, the y series from y7 to y13 and the b series from b9 to b10 showed a mass increase of 365.1 Da due to the AX adduction, thus confirming that Lys190 is the modification site. As further confirmation of AX adduction, the spectrum showed the ion at m/z 349 which is a diagnostic fragment of modification by AX. The areas of the peaks relative to K190-AX and to the corresponding native peptide were determined by reconstituting the selected ion chromatograms (SICs), setting the filter ions at m/z 628.63163 $z=3$ and m/z 537.77492 $z=2$, respectively, and assuming that the ionic responses of the filter ions were similar. The relative content of the modified peptide with respect to the native one was then calculated and the results summarized in Table 3. The relative content of the modified peptides in the ex vivo samples obtained after either 24 or 48 h AX intake ranged from 1 to 2 % corresponding to a concentration range from 6 to 12 μM given that HSA is 600 μM

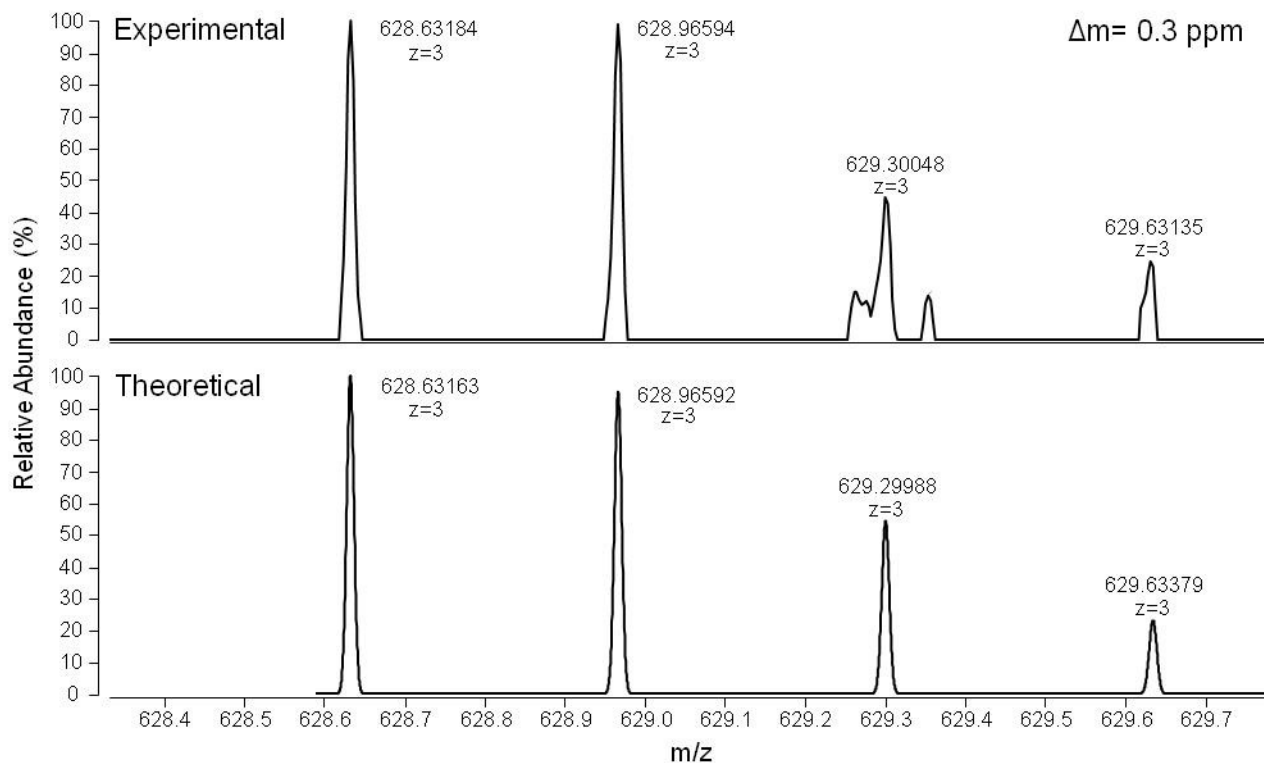


Fig. 6. Experimental and calculated isotopic pattern of K190-AX. The upper panel shows the experimental isotopic pattern of the ion at m/z 628.63184 ($z=3$) extracted from the peak eluting at 11.2 min for T1A and referred to as K190-AX. The lower panel shows the theoretical isotopic pattern of K190-AX calculated by considering the chemical formula $C_{78}H_{126}N_{22}O_{30}S$ and $z=3$.

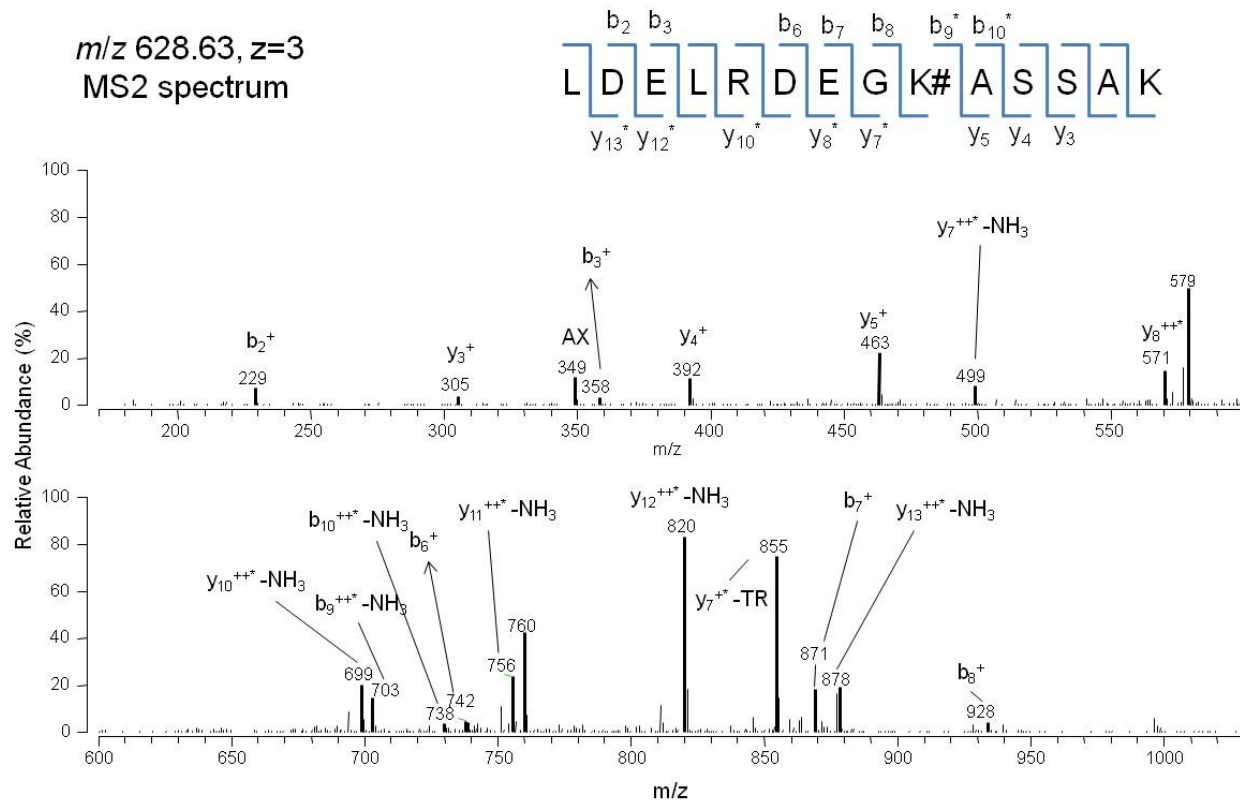


Fig. 7. MS/MS analysis of K190-AX. Tandem MS spectrum of the adducted peptide 182 LDEL RDEGK#ASSAK 195 (K190-AX) was recorded in CID mode and set a mass range 180-1020 m/z . The spectrum is characterized by the diagnostic y and b fragment ion series confirming the modification of Lys 190. AX adduction is further confirmed by the diagnostic ion fragment at m/z 349.

DAHKSEVAHRFKDLGEENFKALVLI AFAQYLQQCPFEDHVKLVNEVTEFAKTCV
ADESAENC DKSLHTLFGDKLCTVATLRETYGEMADCCAKQEPERNECFLQHKD
DNP NLPRLVRPEVDVMCTAFHDNEETFLKKYLYEIARRHPYFYAPELLFFAKRYK
AAFTECCQAADKAA CLLPKLDEL RDEG**KASSAKQRLK**CASLQKFGERAFKAWA
VARLSQRFPKAEFAEVSKLVTDLTKVHTECCHGDLLECADDRADLAKYICENQD
SISSKLKECCEKPLLEKSHCIAEVENDEMPADLPSLAADFVESKDVCKNYAEAK
DVFLGMFLYEYARRHPDYSVLLLRLAKTYETTLEKCCAAADPHECYAKVFDEF
KPLVEEPQNLIKQNC ELF EQLG EYKFQNAL LVRYTK**KVPQVSTPTLVEVSRNLG**
KVGSKCCKHPEAKRMPCAEDYLSVVLNQLCVLHEKTPVSDRVTKCCTESLVNR
RPCFSALEVD ETYVPKEFNAETFTFHADICTLSEKERQIKKQTALVELVKHKPKA
TKEQLKAVMDDFAAFVEKCCKADDKETCFAEEGK**KLVAASQAALGL**

Fig. 8. Sequence coverage of HSA after trypsin digestion and LC-MS/MS analyses. The covered sequence for the analyzed samples was >85%. As an example, the figure reports the covered sequence highlighted in yellow for the sample T1A which accounted for 86%. The peptides bearing the amoxicilloyl adduct and identified in vitro by incubating HSA with AX are underlined. The AX modified lysine residues are highlighted in bold type.

4 Mass spectrometric strategies for the identification and characterization of Human Serum Albumin covalently adducted by Amoxicillin: ex vivo studies

Sample	K190-AX Area (10⁶)	K190-native Area (10⁶)	Modification (%)
HSA-AX	146.0 ± 5.7	4.5 ± 0.6	97.0 ± 0.5
T0 A	0.0	11.1 ± 0.6	0.0
T0 B	0.0	11.0 ± 1.4	0.0
T1 A	0.5 ± 0.1	47.3 ± 1.8	1.1 ± 0.1
T1 B	0.13 ± 0.0	11.7 ± 0.6	1.5 ± 0.1
T2 A	0.3 ± 0.0	16.5 ± 0.6	1.8 ± 0.3
T2 B	0.9 ± 0.1	44.1 ± 2.2	1.9 ± 0.0

Tab. 3. Relative content of K190-AX in the in vitro and ex vivo samples. The relative content of K190-AX with respect to the native peptide (K190-native) was calculated by integrating the area of the peaks identified in the SICs traces as shown in Figure 4. The standard deviation of each value is calculated on three replicates for each sample. The following equation was used to calculate the % of adduction: $[K190-AX / (K190-AX + K190-native)] * 100$ where K190-AX and K190-native refer to the peak areas.

4.3.3 Comparing MS approaches with immunological methods

We have previously used immunological methods to detect AX-protein adducts formed *in vitro*. [16] For this reason we also explored the possibility of using immunological approaches for the detection of AX-protein adducts in *ex vivo* samples obtained after AX oral administration. Commercial human serum incubated with AX *in vitro* was used as a positive control. As described earlier, several adducts were detected under these conditions (Figure 9A). The major adducted proteins have been previously identified and can be assigned to transferrin (Trf), HSA, and heavy and light chains of immunoglobulins (Ig HC and Ig LC, respectively). Incubation of serum samples from healthy subjects with AX *in vitro* led to the detection of similar adducts (Figure 9B). However, analysis of serum from the same subjects after oral intake of AX for 24 or 48 h by this method did not allow the detection of signals above background levels (Figure 9C). Nor did the analysis of the same samples by 2D-electrophoresis using 100 µg of total protein allow the detection of specific signals (results not shown). Therefore, detection of AX-adducts formed *in vivo* by use of the available antibody may require enrichment steps. Alternatively, more sensitive methods, like the ones developed herein, need to be employed.

4 Mass spectrometric strategies for the identification and characterization of Human Serum Albumin covalently adducted by Amoxicillin: ex vivo studies

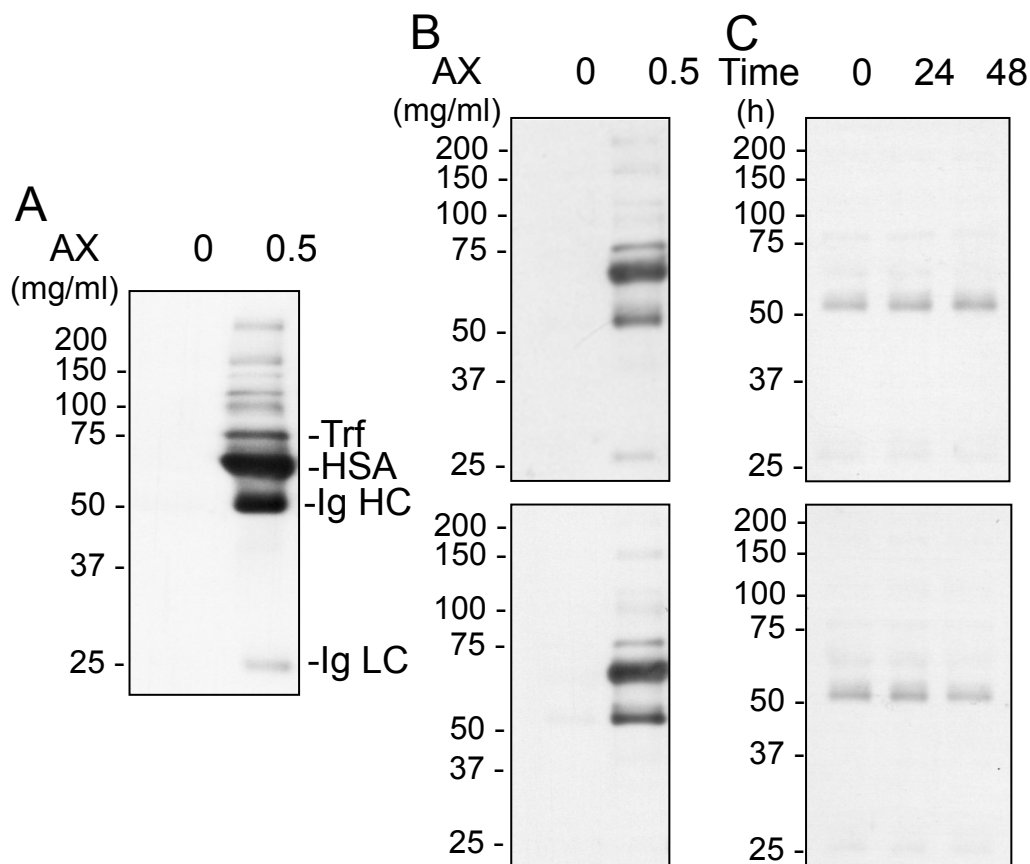


Fig. 9. Immunological detection of adducts of AX with serum proteins. Samples analyzed were: (A) commercial human serum or (B) serum from two different healthy subjects incubated *in vitro* with the indicated concentrations of AX for 16 h at 37°C, and (C) serum samples from healthy subjects before and after the intake of AX. Aliquots from all samples containing 2 µg of total protein were analyzed by SDS-PAGE and western blot with anti-AX AO3.2 monoclonal antibody. Exposure times were 10 s for (A) and (B) and 1 min for (C). Trf, transferrin; HSA, human serum albumin; Ig HC, immunoglobulin heavy chain; Ig LC, immunoglobulin light chain.

4.4 Discussion

As reported elsewhere, when AX is orally administered at a dose of 1 g, the plasma concentration of the antibiotic increases rapidly reaching at 2-3 hours a concentration peak of approximately 10-20 $\mu\text{g/ml}$. After this period, the AX plasma concentration decreases rapidly, reaching after 8 hours an almost negligible concentration. The kinetics of plasma AX levels upon repeated doses has been modeled and is thought to give rise to a series of peaks, not exceeding 20 $\mu\text{g/mL}$. [19] We have previously shown that immunological methods can detect HSA-AX adducts formed *in vitro* after incubation of HSA in the continuous presence of AX at 25 $\mu\text{g/mL}$ for 16 h at alkaline pH. [16] However, under these conditions, the extent of modification of HSA is higher than that occurring at neutral pH (not shown). As stated above, oral administration of AX results in the modification of only 1-2% of serum HSA, as detected in *ex vivo* samples by MS. Therefore, immunological methods using the AO3.2 antibody may not be suitable to detect AX-protein adducts in *ex vivo* serum samples withdrawn after AX oral administration, due to either the lower extent of HSA modification or the higher background given by serum samples.

We have previously reported MS strategies for the identification and characterization of the AX modifications. [16] Therefore, in this paper we turned to MS approaches in order to achieve high sensitivity. Figure 2 overviews the different targeted and untargeted approaches we used. None of the untargeted approaches considered (Precursor Ions Scan and data-dependent scan mode) were able to identify any AX-adducted peptides generated by the enzymatic digestion of isolated HSA and this is probably due to the lack of sensitivity of the PIS approach and to the limited scan rate of the orbitrap MS analyzer used in the present work. Moreover the limited amounts of the AX adducts present in the *ex vivo* samples with respect to the native peptides should also be considered. To overcome these

4 Mass spectrometric strategies for the identification and characterization of Human Serum Albumin covalently adducted by Amoxicillin: ex vivo studies

limitations a sample preparation method should be set-up in order to isolate HSA-AX adducts from unmodified-modified HSA. Moreover the use of a more sensitive MS analyzer for PIC analysis and of a HRMS characterized by a faster scan rate would facilitate the untargeted search.

The targeted approaches set-up on the basis of the known AX adducts previously identified in in vitro conditions, confirmed that AX only modifies Lys190 in vivo. The MRM approach was found to be highly selective and sensitive but limited with regard to the analyte structure confirmation. The SIC approach carried out in the HRMS orbitrap, although less selective, gave additional information concerning the accurate mass, the isotopic pattern and the MS/MS fragmentation pathway, leading to the structure confirmation of the AX adduct. The SIC approach also permitted the establishment of the relative content of the adduct with respect to the native peptide. Although the approach is limited since it assumes that the ionization efficiency of the native and adducted peptides overlaps, it represents the first attempt of measuring the formation of the adducted peptide in a semi-quantitative way. A MRM method based either on isotope labelled or unlabelled standards is needed to measure the absolute amount of native and modified peptides.

In conclusion, Lys 190 was identified as the modification site of AX orally given to human volunteers. The AX adduct was identified and fully characterized by complementary targeted approaches based on triple quadrupole (MRM mode) and orbitrap (SIC mode) as mass analyzers. The SIC mode also permitted the semi-quantitative measurement of AX-HSA amount, ranging from 1 to 2% (6-12 μM) of the total amount of HSA, 24 and 48 hours after the beginning of the oral intake.

It should be noted that several analytical methods have been developed towards the identification of the adducts formed between proteins and β -lactams. Because HSA is the most abundant protein in serum, most works have attempted the characterization of HSA adducts. The first pioneering studies employed the HPLC separation of tryptic peptides and Edman degradation sequencing coupled to the Enzyme Immuno Assay analysis (EIA).[20] Such strategies were able to identify 6

4 Mass spectrometric strategies for the identification and characterization of Human Serum Albumin covalently adducted by Amoxicillin: ex vivo studies

different Lys sites modified by penicillin. More recent works have studied the interaction between HSA and flucloxacillin, piperacillin and benzylpenicillin [21]:[22] by using different mass spectrometric strategies which permitted the characterization of the adducted peptides and the identification of the modification sites. As an example of MS strategy, the Accurate Inclusion Mass Screening[23] was developed to identify and characterize the penicilloyl-HSA adducts. It is interesting to note that, in contrast to our results, several adducted sites were detected in the previous works. Several possibilities could account for these differences. In some of the studies the routes of administration were different (i.e. intravenous or intramuscular). In addition, it is possible that if the modified proteins are stable, adduct accumulation at other sites of the protein or on other proteins could occur after prolonged administration of the antibiotic. Moreover, the presence of concomitant treatments or the pathophysiological conditions could affect plasma protein concentrations.

Accumulating evidence indicates that HSA adduction by AX occurs upon administration of the antibiotic in healthy subjects, not developing AX allergy. Therefore, other factors should intervene for the allergic reaction to occur. Apart from genetic predisposition, repeated administration, concurrent infections, inflammatory settings or other circumstances associated, known generically as “danger signals”, could potentiate the sensitization towards the antibiotic.[4] In addition, whether the nature or the amount of adducts formed are important factors for allergy development requires further study.

The methods so far reported together with the approaches herein described represent a starting point to stimulate further studies aimed at setting-up advanced MS strategies for untargeted identification and for the accurate quantitative analysis of penicillin protein adducts. The application of such methods would permit a better understanding of the haptentation pathways and the development of more specific allergy diagnostic tools.

4.5 References

1. Riedl MA, Casillas AM. Adverse drug reactions: types and treatment options. *Am Fam Physician*. 2003 Nov;68(9):1781-90.
2. Thong BY, Tan TC. Epidemiology and risk factors for drug allergy. *Br J Clin Pharmacol*. 2011 May;71(5):684-700.
3. Guengerich FP. Mechanisms of drug toxicity and relevance to pharmaceutical development. *Drug Metab Pharmacokinet*. 2011;26(1):3-14.
4. Ariza A, Montañez MI, Pérez-Sala D. Proteomics in immunological reactions to drugs. *Curr Opin Allergy Clin Immunol*. 2011 Aug;11(4):305-12.
5. Adriaenssens N, Coenen S, Kroes AC, Versporten A, Vankerckhoven V, Muller A, et al. European Surveillance of Antimicrobial Consumption (ESAC): systemic antiviral use in Europe. *J Antimicrob Chemother*. 2011 Aug;66(8):1897-905.
6. Versporten A, Coenen S, Adriaenssens N, Muller A, Minalu G, Faes C, et al. European Surveillance of Antimicrobial Consumption (ESAC): outpatient penicillin use in Europe (1997-2009). *J Antimicrob Chemother*. 2011 Dec;66 Suppl 6:vi13-23.
7. Blanca M. Allergic reactions to penicillins. A changing world? *Allergy*. 1995 Oct;50(10):777-82.
8. Doña I, Blanca-López N, Torres MJ, García-Campos J, García-Núñez I, Gómez F, et al. Drug hypersensitivity reactions: response patterns, drug involved, and temporal variations in a large series of patients. *J Investig Allergol Clin Immunol*. 2012;22(5):363-71.
9. Renaudin JM, Beaudouin E, Ponvert C, Demoly P, Moneret-Vautrin DA. Severe drug-induced anaphylaxis: analysis of 333 cases recorded by the Allergy Vigilance Network from 2002 to 2010. *Allergy*. 2013 Jul;68(7):929-37.
10. Blanca M, Romano A, Torres MJ, Fernández J, Mayorga C, Rodríguez J, et al. Update on the evaluation of hypersensitivity reactions to betalactams. *Allergy*. 2009 Feb;64(2):183-93.
11. García Núñez I, Barasona Villarejo MJ, Algaba Mármol MA, Moreno Aguilar C, Guerra Pasadas F. Diagnosis of patients with immediate hypersensitivity to beta-lactams using retest. *J Investig Allergol Clin Immunol*. 2012;22(1):41-7.
12. Blanca M, Mayorga C, Perez E, Suau R, Juarez C, Vega JM, et al. Determination of IgE antibodies to the benzyl penicilloyl determinant. A

4 Mass spectrometric strategies for the identification and characterization of Human Serum Albumin covalently adducted by Amoxicillin: ex vivo studies

comparison between poly-L-lysine and human serum albumin as carriers. *J Immunol Methods*. 1992 Aug;153(1-2):99-105.

13. Blanca M, Romano A, Torres MJ, Demoly P, DeWeck A. Continued need of appropriate betalactam-derived skin test reagents for the management of allergy to betalactams. *Clin Exp Allergy*. 2007 Feb;37(2):166-73.

14. Sanz ML, Gamboa PM, Antépara I, Uasuf C, Vila L, Garcia-Avilés C, et al. Flow cytometric basophil activation test by detection of CD63 expression in patients with immediate-type reactions to betalactam antibiotics. *Clin Exp Allergy*. 2002 Feb;32(2):277-86.

15. Torres MJ, Padial A, Mayorga C, Fernández T, Sanchez-Sabate E, Cornejo-García JA, et al. The diagnostic interpretation of basophil activation test in immediate allergic reactions to betalactams. *Clin Exp Allergy*. 2004 Nov;34(11):1768-75.

16. Ariza A, Garzon D, Abanades DR, de los Rios V, Vistoli G, Torres MJ, et al. Protein haptentation by amoxicillin: High resolution mass spectrometry analysis and identification of target proteins in serum. *Journal of Proteomics*. 2012 Dec;77:504-20.

17. Elschenbroich S, Kislinger T. Targeted proteomics by selected reaction monitoring mass spectrometry: applications to systems biology and biomarker discovery. *Mol Biosyst*. 2011 Feb;7(2):292-303.

18. Jenkins RE, Meng X, Elliott VL, Kitteringham NR, Pirmohamed M, Park BK. Characterisation of flucloxacillin and 5-hydroxymethyl flucloxacillin haptentated HSA in vitro and in vivo. *Proteomics Clin Appl*. 2009 Jun;3(6):720-9.

19. Chierakul W, Wangboonskul J, Singtoroj T, Pongtavornpinyo W, Short JM, Maharjan B, et al. Pharmacokinetic and pharmacodynamic assessment of co-amoxiclav in the treatment of melioidosis. *J Antimicrob Chemother*. 2006 Dec;58(6):1215-20.

20. Yvon M, Anglade P, Wal JM. Identification of the binding sites of benzyl penicilloyl, the allergenic metabolite of penicillin, on the serum albumin molecule. *FEBS Lett*. 1990 Apr;263(2):237-40.

21. Whitaker P, Meng X, Lavergne SN, El-Ghaiesh S, Monshi M, Earnshaw C, et al. Mass spectrometric characterization of circulating and functional antigens derived from piperacillin in patients with cystic fibrosis. *J Immunol*. 2011 Jul;187(1):200-11.

22. Meng X, Jenkins RE, Berry NG, Maggs JL, Farrell J, Lane CS, et al. Direct evidence for the formation of diastereoisomeric benzylpenicilloyl haptens from

4 Mass spectrometric strategies for the identification and characterization of Human Serum Albumin covalently adducted by Amoxicillin: ex vivo studies

benzylpenicillin and benzylpenicillenic acid in patients. *J Pharmacol Exp Ther.* 2011 Sep;338(3):841-9.

23. Jaffe JD, Keshishian H, Chang B, Addona TA, Gillette MA, Carr SA. Accurate inclusion mass screening: a bridge from unbiased discovery to targeted assay development for biomarker verification. *Mol Cell Proteomics.* 2008 Oct;7(10):1952-62.

5 Carnosine and derivatives as inhibitors of protein covalent modifications induced by reactive carbonyl species

Mara Colzani, Davide Garzon and Giancarlo Aldini

Department of Pharmaceutical Sciences, Università degli Studi di Milano, via Mangiagalli 25, 20133, Milan, Italy

Keywords: reactive carbonyl species, α,β -unsaturated aldehydes, AGEs, ALEs, carnosine, detoxifying agents, RCS sequestering agents, carnosinase, carnosine derivatives

Abbreviations:

15d-PGJ₂, 15-deoxy-delta 12,14-prostaglandin J₂; ACR, acrolein; AGEs, advanced glycation end-products; ALDH, aldehyde dehydrogenase enzymes; ALEs, advanced lipoxidation end-products; CEL, N^ε-(carboxyethyl)lysine; CN1, serum carnosinase; CN2, tissue carnosinase; CMC, S-(carboxymethyl)cysteine; CML, N^ε-(carboxymethyl)lysine; COPD, chronic obstructive pulmonary disease; GO, glyoxal; GSTs, glutathione transferases; HNE, 4-hydroxynonenal; L-FABP, liver fatty acid-binding protein; MGO methylglyoxal; MDA, malondialdehyde; ONE, 4-oxononenal; PEPT1, oligopeptide transporter 1; RCS, reactive carbonyl species;

5.1 Reactive carbonyl species and protein covalent modification

Reactive carbonyl species (RCS) are a class of exogenous and endogenous reactive compounds that can covalently react with nucleophilic targets such as proteins, phospholipids and nucleic acids, forming damaging adducts [1]. Proteins represent the most studied target of RCS and the corresponding reaction products are named advanced lipoxidation end products (ALEs) when the modifying moiety derives from lipids, and advanced glycation end products (AGEs) when it comes from sugar.

From a chemical point of view, the RCS so far reported to react *in vivo* with proteins are quite heterogeneous and can be divided into the following groups: 1) α,β -unsaturated aldehydes; 2) di-aldehydes; 3) keto-aldehydes. The following paragraphs briefly describe the sources of RCS and their mechanism of reactions with proteins (please refer to the review by Vistoli et al. [2] for a more detailed description of RCS).

5 Carnosine and derivatives as inhibitors of protein covalent modifications induced by reactive carbonyl species

- Reactive carbonyl species are cytotoxic compounds generated by oxidative damage;
- Reactive carbonyl species can be formed either by lipid or sugar oxidation;
- Reactive carbonyl species react with proteins forming protein adducts that can induce cell damage;
- Reactive carbonyl species are involved in the pathogenesis of some oxidative based diseases;
- a strict correlation between the amount of RCS, of the corresponding protein adducts in tissues and fluids and disease states has been found in both animal and human subjects;
- a substantial amount of literature is now available reporting the molecular and cellular pathogenic mechanisms for the involvement of reactive carbonyl species in the onset and progression of various diseases, including atherosclerosis, diabetes and some neurological disorders;
- Reactive carbonyl species are detoxified by phase I and II metabolism forming unreactive metabolites;
- Carnosine reacts with reactive carbonyl species and is believed to take part to their detoxification;
- compounds effective as inhibitors of reactive carbonyl species or able to block their biological effects have been found to significantly ameliorate different oxidative based diseases.
- Reactive carbonyl species are now considered as promising drug targets

Tab. 1. This table lists the key facts or reactive carbonyl species (RCS) which are reactive by-products of lipids and sugars oxidation

5 Carnosine and derivatives as inhibitors of protein covalent modifications induced by reactive carbonyl species

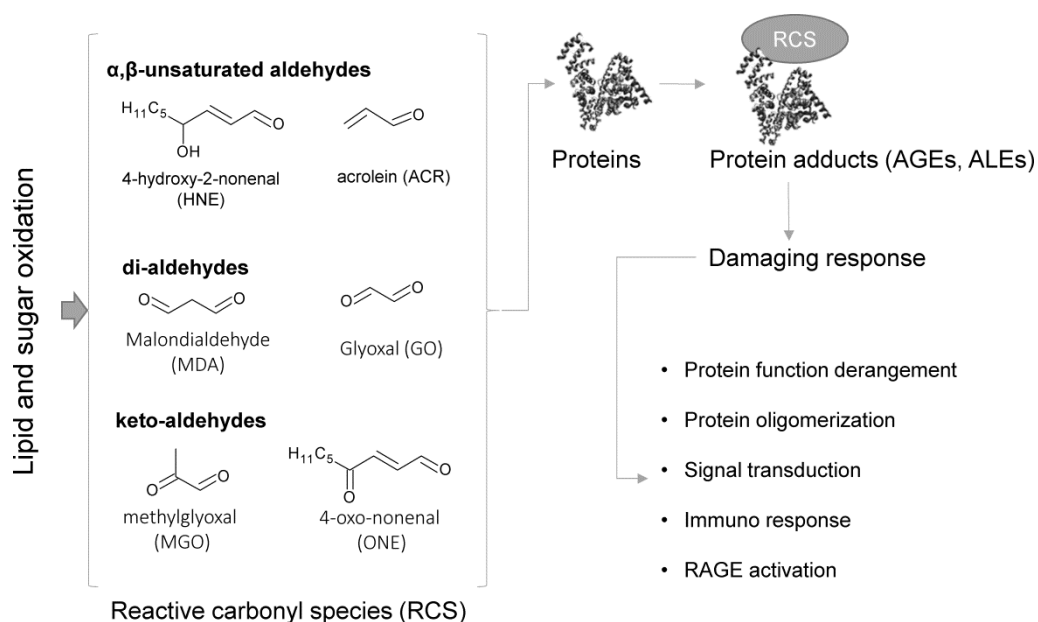


Fig. 1. Major classes and chemical structures of the most studied reactive carbonyl species (RCS). RCS are break-down products formed by the oxidative damage of lipids and sugars, belonging to different chemical classes including α,β -unsaturated aldehydes, di-aldehydes and keto-aldehydes. RCS are electrophilic compounds able to form covalent adducts with nucleophilic substrates such as proteins, forming adducts (AGEs and ALEs) that can elicit a damaging response.

5.1.1 α,β -unsaturated aldehydes

α,β -unsaturated aldehydes include hydroxylated (i.e. 4-hydroxynonenal [HNE], 4-hydroxyhexenal [HHE]) and non-hydroxylated (acrolein [ACR], crotonaldehyde, nonenal, hexenal) derivatives. They can have either endogenous or exogenous sources and different mechanisms of formation, although the lipid-peroxidation cascade involving free PUFAs or phospholipids represents the main pathway [2]. Acrolein is also generated in inflammatory condition by the degradation of threonine and of spermine and spermidine by myeloperoxidase and amine oxidase, respectively [3, 4].

The reactivity of the α,β -unsaturated aldehydes towards the nucleophilic sites of proteins (Lys, His, Cys, Arg and the terminal amino group) is regulated by their electrophilic nature, due to the carbonyl function which acts as an electron-withdrawing group, decreasing the electron-richness of the conjugated alkene group and making the alkene β -carbon atom electron deficient [5]. The Michael adduct represents the main reaction product and it is formed by the covalent reaction between the electrophilic β -carbon atom of the unsaturated aldehydes and the nucleophilic (electron-rich species) sites of the protein such as the thiolate anion of cysteines, the ϵ -amino group of lysines and the imidazolic ring of histidines (Figure 2). The α,β -unsaturated aldehydes can also generate a reversible Schiff base through the dehydration reaction between the aldehydic carbonyl group and the primary amino group of the protein (the ϵ -terminal group of Lys or the amino-terminus of the protein) (Figure 2).

5 Carnosine and derivatives as inhibitors of protein covalent modifications induced by reactive carbonyl species

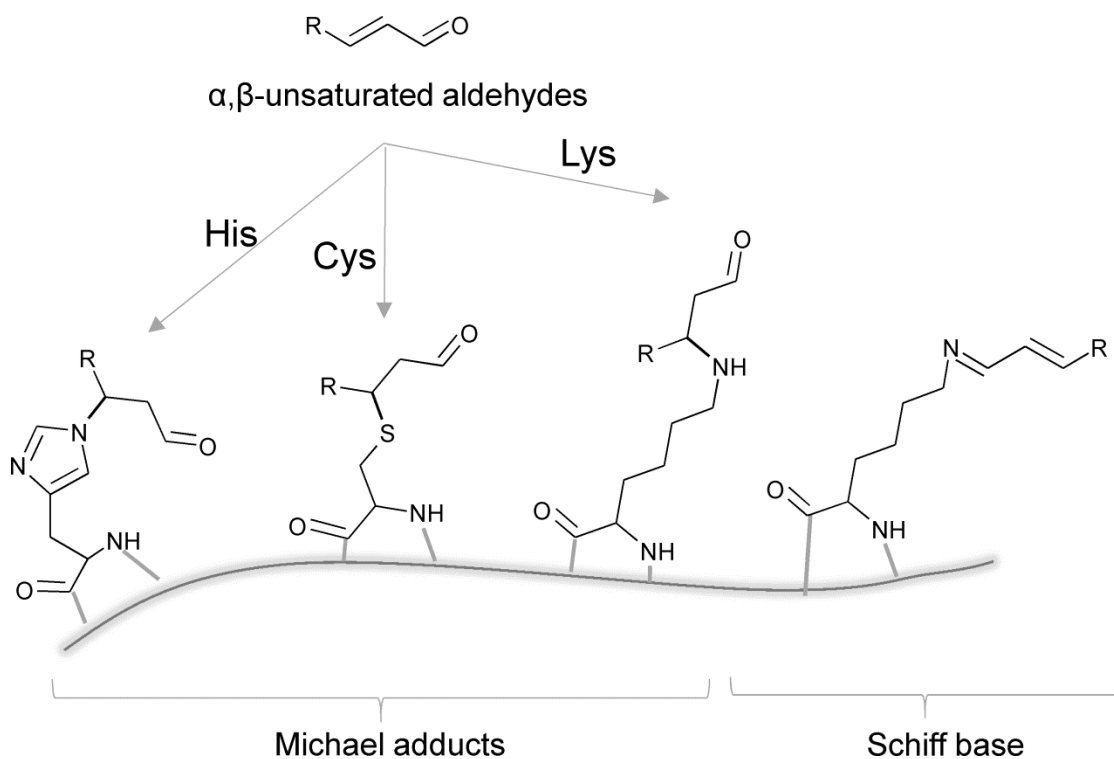


Fig. 2. Covalent addition of α,β -unsaturated aldehydes with nucleophilic sites of proteins. C3 of α,β -unsaturated aldehydes react with the nucleophilic sites of proteins (His, Cys and Lys) forming Michael adducts and with the ϵ -amino group of Lys forming the corresponding Schiff base.

5.1.2 Di-aldehydes

Malondialdehyde (MDA) and glyoxal (GO) are the two most studied di-aldehydes involved in the formation of protein adducts. The former is generated by the lipid peroxidation cascade involving PUFA and it reacts with both Lys and Arg, forming several protein adducts and cross-links. The protein covalent adduction of MDA is due to the non-dissociated enolate form (the β -hydroxyacrolein) which, by reacting with the ϵ -amino group of Lys, forms the $N\epsilon$ -(2-propenal)lysine (N-propenal-Lys), a reactive intermediate that can further react forming additional products (Figure 3).

Glyoxal has both exogenous and endogenous sources. Exogenous sources include cooked foods [6] and environment (combustion) [7]. Exogenous glyoxal is easily absorbed. At endogenous level, glyoxal can be generated by the oxidation of both lipids and sugars [8] as well as by the degradation of the Amadori products [9].

$N\epsilon$ -(carboxymethyl)lysine (CML) and S-(carboxymethyl)cysteine (CMC) represent the two main reaction products of GO with proteins. Glyoxal can also react with Arg forming imidazolinone derivatives and N-(carboxymethyl) arginine. Due to the presence of the two carbonyl groups, GO can also react with two nucleophilic sites forming cross-links named GOLD and GODIC, formed by the reaction of one molecule of glyoxal with two Lys or with one Lys and one Arg, respectively (Figure 3).

5 Carnosine and derivatives as inhibitors of protein covalent modifications induced by reactive carbonyl species

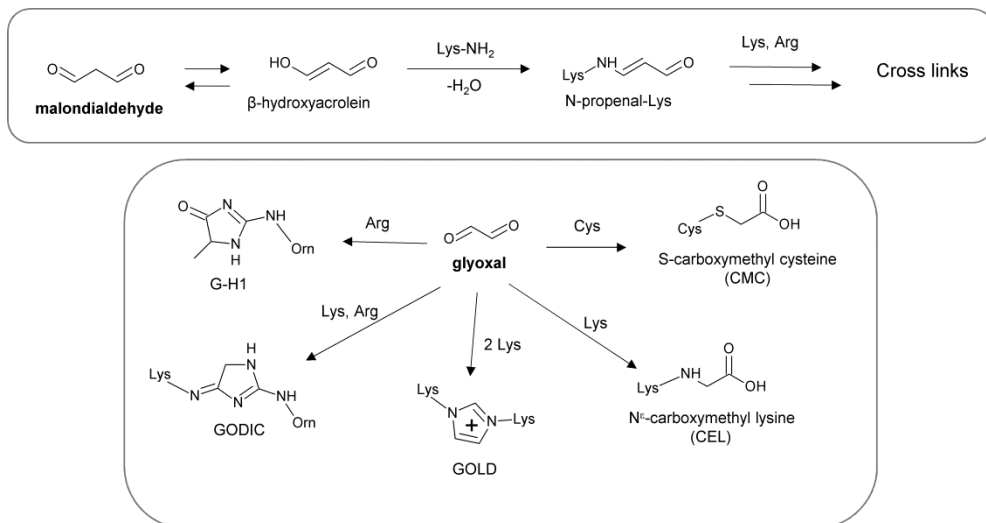


Fig. 3. Reaction mechanisms of formation for the malondialdehyde- (upper panel) and glyoxal-based adducts with nucleophilic sites. Upper panel – MDA, through the non-dissociated enolate form (the β-hydroxyacrolein) is able to react with the ε-amino group of Lys, forming the N-propenal-Lys, a reactive intermediate that can further react forming additional products.

Lower panel - Glyoxal can react with Lys and Cys forming Nε-(carboxymethyl)lysine (CML) and S-(carboxymethyl)cysteine (CMC) which represent the two main reaction products of GO with proteins. Glyoxal can also react with Arg forming imidazolinone derivatives and N-(carboxymethyl) arginine. Due to the presence of the two carbonyl groups, GO can also react with two nucleophilic sites forming cross-links named GOLD and GODIC, formed by the reaction of one molecule of glyoxal with two Lys or with one Lys and one Arg, respectively.

5.1.3 Keto-aldehydes

Methylglyoxal (MGO), 4-oxo-nonenal (ONE) and isoketals (also called levuglandins) are the most studied keto-aldehydes responsible of protein covalent modifications.

MGO has different exogenous and endogenous sources and several mechanisms of formation. At endogenous level, the main source is represented by the involvement of the enzymatic or non-enzymatic degradation of the triose phosphate intermediates originating from the glycolytic processes [10]. MGO reacts primarily with Arg and Lys forming imidazolinone derivatives and carboxyethyl-lysine (CEL) adduct, respectively. Similarly to GO, it can also form crosslinks involving Lys and Arg residues (Figure 4).

4-oxo-nonenal (ONE) is generated by the lipid-oxidation and it is more reactive than HNE towards nucleophilic sites. It forms Michael adducts by the reaction of C2 and C3 with His, Lys and Cys; moreover, it can form cross-links and Schiff base by reacting with Lys.

Isoketals are highly reactive γ -ketoaldehydes generated by the free radical mediated lipid peroxidation of H₂-isoprostanes. Isoketals react with the ϵ -amino group of Lys forming a reversible imine derivative or an irreversible pyrrol adduct through a pyrrolidine intermediate [11] (Figure 4).

5 Carnosine and derivatives as inhibitors of protein covalent modifications induced by reactive carbonyl species

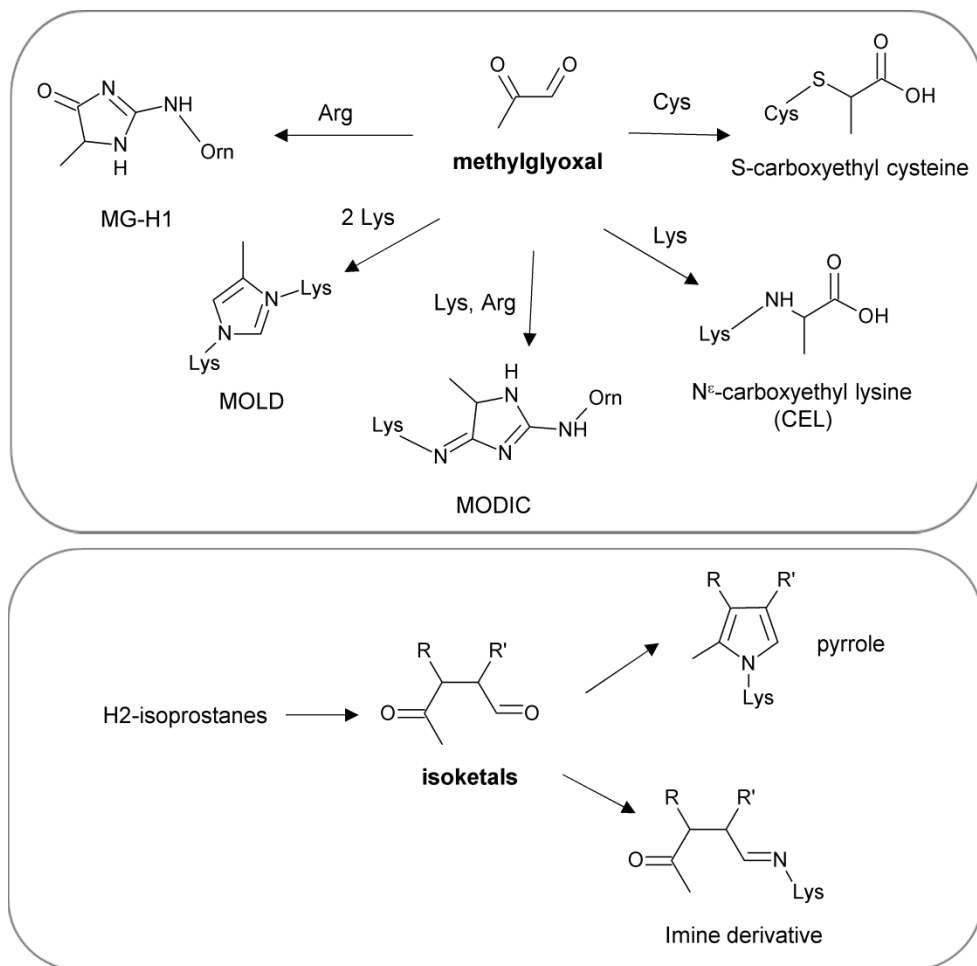


Fig. 4. Reaction mechanisms of formation for the methylglyoxal- (upper panel) and isoketals-based adducts with nucleophilic sites. Upper panel: reaction pathway of MGO. MGO reacts primarily with Arg and Lys forming imidazolinone derivatives and carboxyethyl-lysine (CEL) adduct, respectively. Similarly to GO, it can also form crosslinks involving Lys and Arg residues.

Lower panel: reaction pathway of isoketals. Isoketals are highly reactive γ -ketoaldehydes able to react with the ϵ -amino group of Lys forming a reversible imine derivative or an irreversible pyrrole adduct through a pyrrolidine intermediate.

5.2 Biological implications of RCS induced protein covalent modifications

In the past, RCS such as HNE and MDA and the corresponding protein adducts were mainly considered as biomarkers of oxidative damage [12-14]. Several assays for their measurement have been set-up and used extensively; among the most widespread, there is the TBARS assay, based on thiobarbituric acid, for measuring MDA and the assay based on the derivatizing agent 2,4-dinitrophenylhydrazine, to quantify protein carbonyl [15]. Later, several studies demonstrated that RCS and the corresponding protein adducts are also involved in the onset and progression of several oxidative-based diseases such as diabetes, atherosclerosis and some neurological disorders, therefore nowadays, RCS are widely studied as pathogenetic factors as well as drug targets [1, 16]. Several mechanisms have been considered to explain the biological effects induced by RCS and protein adducts, as summarized below.

5.2.1 Protein function derangement

When RCS react with a target protein, the function of the protein itself can be deranged due to several mechanisms, such as a conformational change or the impairment of the interaction with the natural substrate when the RCS bind the active site of the protein. Proteomic studies have identified several proteins highly susceptible to RCS modification and undergoing function derangement [17, 18]. In general, most of the target proteins are characterized by nucleophilic sites that are not only solvent accessible, but also characterized by a peculiar amino acid surrounding environment that stabilizes the most nucleophilic forms (the thiolate anion in the case of Cys or the uncharged ϵ -amino group in the case of Lys). Accordingly, as an example, we found that actin is a very susceptible cellular target of electrophilic agents due to the presence of several accessible

5 Carnosine and derivatives as inhibitors of protein covalent modifications induced by reactive carbonyl species

nucleophilic targets; among these Cys374 was found to be the most reactive [19]. The peculiar reactivity of Cys374 can be explained not only by considering its accessibility, but also by the presence of surrounding amino acids that stabilize the thiolate anion [19]. By using MS strategies we found that actin is the protein target of several electrophilic agents including HNE, ACR, [20] and 15-deoxy-delta 12,14-prostaglandin J2 (15d-PGJ₂) [21]. In the case of quite bulky electrophiles, such as 15d-PGJ₂, the function of actin was found compromised also at cellular level, due to a conformational change which induces a depolymerization process of fibrillar actin as well as the inhibition of actin polymerization, leading to cytoskeletal damage and cell death [21].

The liver fatty acid-binding protein (L-FABP) is another interesting example regarding the derangement of protein function induced by the covalent modification generated by RCS. L-FABP adduction by HNE, that has been found in several pathological conditions such as alcoholic liver disease, impairs its stability and ligand binding ability [22].

Other proteins whose functions are altered by RCS covalent adducts have recently been reviewed [23, 24].

5.2.2 The antigenic properties of RCS protein adducts

The antigenic properties of RCS protein adducts and the consequent inflammatory response represents an additional mechanism of oxidative damage. Circulating antibodies against epitopes formed by the reaction of RCS with proteins were found in the sera of patients affected by chronic obstructive pulmonary disease (COPD), as well as in a murine model of chronic ozone exposure [25]. HNE protein adduction was also proposed as a possible antigenic stimulus for systemic lupus erythematosus (SLE) autoantibodies. Alzolibani et al. recently demonstrated that the structural perturbation of histone-H2A by HNE makes the protein immunogenic and that the neo-epitope might play a role in the induction

5 Carnosine and derivatives as inhibitors of protein covalent modifications induced by reactive carbonyl species

of circulating autoantibodies in SLE [26]. Human serum albumin is another protein that, once modified by RCS such as HNE, increases the production of autoantibodies [27].

5.2.3 The damaging AGEs-RAGE axis

More recently, the role of the receptor RAGE has been widely considered as additional mechanism of oxidative damage. RAGE is a multiligand transmembrane receptor consisting of an extracellular region, which is composed of one ligand-binding V-type Ig domain and two Ig-like C-domains (C1 and C2), a short hydrophobic transmembrane-spanning region, and a signal-transducing cytoplasmic domain [28]. The RAGE receptor is activated by AGEs, in particular those generated by GO and MGO [29]. RAGE activation induces the transcription factor NF κ -B, leading to a pro-inflammatory and pro-fibrotic response [30]. The involvement of RAGE activation for some AGEs has been well documented in some animal models, although a clear structure affinity relationship between AGEs and RAGE is still missing.

5.2.4 The amyloidogenic properties of RCS protein adducts

RCS can induce oligomerization and aggregation of some target proteins. As an example, HNE covalently reacts with amyloid-beta peptides forming cross-links and promoting Alzheimer protofibril formation [31]. α -synuclein was reported as another RCS target; its covalent modification has been found to induce protein oligomerization [32] and an increase of dopaminergic toxicity [33].

5.3 Endogenous detoxification of RCS

RCS are efficiently detoxified to unreactive derivatives by both phase I and II metabolic pathways. Phase I metabolism is mainly mediated by aldehyde-oxidizing enzymes and by aldehyde-reducing enzymes, while phase II by glutathione-dependent enzymes, as reviewed by O'Brien et al. [8].

5.3.1 phase I metabolism

The oxidation of the carbonyl group to the corresponding carboxylic function is usually catalyzed by aldehyde dehydrogenase enzymes (ALDH) and NAD⁺ as cofactor. Different aldehyde-oxidizing enzymes, characterized by different levels of affinity towards RCS, have so far been reported. For example, ALDH2 efficiently oxidizes HNE [34], but not MGO, while α -oxoaldehyde dehydrogenase oxidizes MGO to pyruvate, but not glyoxal nor 3-deoxyglucosone [35].

The reduction of RCS to the corresponding aldehydes is catalyzed by enzymes belonging to three groups of enzymes: the alcohol dehydrogenase family, the aldo-keto reductase superfamily and the short-chain dehydrogenase/reductase family [8].

5 Carnosine and derivatives as inhibitors of protein covalent modifications induced by reactive carbonyl species

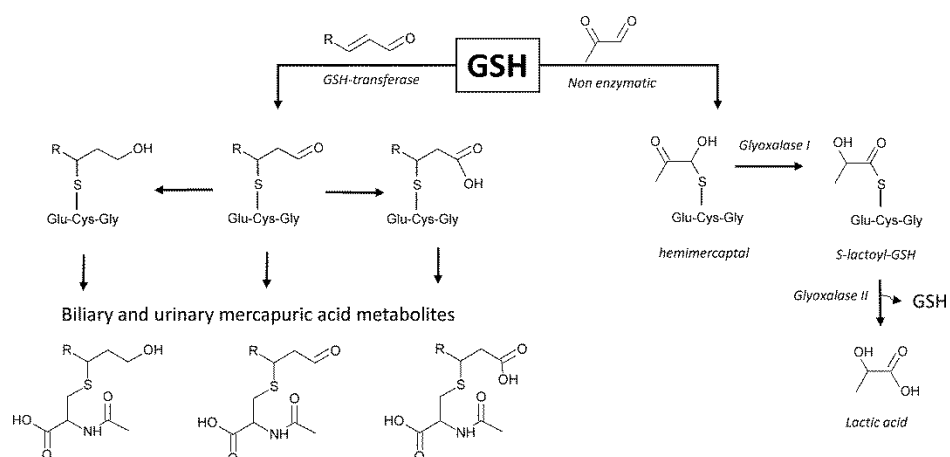


Fig. 5. GSH dependent metabolic pathways for the detoxification of α,β -unsaturated aldehydes (left) and oxoaldehydes (right).

GSH dependent detoxification of α,β -unsaturated aldehydes- The glutathione (GSH) transferases catalyze the conjugation of GSH with the C3 of α,β -unsaturated alkenals and hydroxyalkenals forming the corresponding Michael adducts that are further metabolized by ALDH or ADH to form the corresponding acid or alcohol derivatives. In the kidney, the GSH adducts are then hydrolyzed and acetylated forming the mercapturic acid derivatives, which are then excreted in the urine.

MG detoxification - The metabolic detoxification of MG starts with the GSH-methylglyoxal hemithioacetal that is formed by the non-enzymatic reaction between glutathione and MG; the metabolite is then isomerized to S-D-lactoylglutathione by glyoxalase 1 and is then converted to D-lactate and GSH by the enzyme glyoxalase 2.

5.3.2 phase II metabolism

Two main GSH-dependent enzymes are involved in the phase II metabolism of RCS: the glutathione transferases and the glyoxylase system.

The glutathione transferases (GSTs) catalyze the conjugation of GSH with the C3 of alkenals and hydroxyalkenals forming the corresponding Michael adducts. The adducts still maintain the aldehydic function and can be further metabolized by ALDH or ADH to form the corresponding acid or alcohol derivatives. In the kidney, the GSH adducts are then hydrolyzed and acetylated forming the mercapturic acid derivatives, which are then excreted in the urine [36] (Figure 5).

The glyoxylase system detoxifies oxoaldehydes, such as glyoxal and methylglyoxal, into the corresponding α -hydroxyacid; it consists of two enzymes, glyoxalase 1 and glyoxalase 2 and of GSH as a cofactor. As an example, the metabolic detoxification of MG starts with the GSH-methylglyoxal hemithioacetal that is formed by the non-enzymatic reaction between glutathione and MG; the metabolite is then isomerized to S-D-lactoylglutathione by glyoxalase 1 and is then converted to D-lactate and GSH by the enzyme glyoxalase 2 [37] (Figure 5).

5.3.3 Carnosine and histidine dipeptides as RCS sequestering agents

Carnosine (β -alanyl-L-histidine) is a physiological dipeptide present in large amounts in muscular and nervous tissues of vertebrate animals. Interest in this endogenous compound is due not only to its high concentrations in some tissues (spanning the millimolar range in the skeletal muscle), but also to the fact that its synthesis, modulation, transport, and degradation is regulated by a quite complex and energy-consuming molecular system [38]. After its discovery at the beginning of the XX century, its biological role remained obscure for many

5 Carnosine and derivatives as inhibitors of protein covalent modifications induced by reactive carbonyl species

decades, although several hypotheses have been proposed: among others, carnosine and derivatives such as anserine, balenine and homocarnosine (Figure 6) have been proposed as possible buffering agents, metal ion chelators, antioxidants and neuromodulators, as recently reviewed by Boldyrev et al. [38].

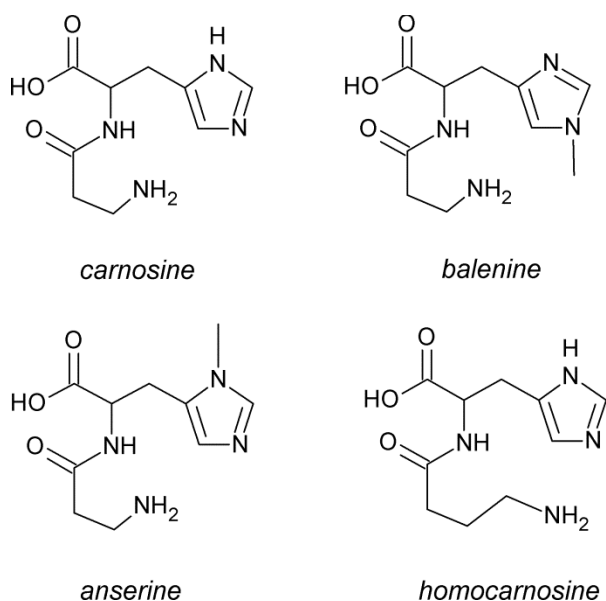


Fig. 6. Chemical structures of carnosine and its naturally occurring derivatives. Carnosine is a dipeptide, composed of beta-alanine and L-histidine. Carnosine is the archetype of a family of naturally-occurring derivatives including anserine, ophidine (balenine), the L-histidine methylated, and homocarnosine, in which beta-alanine is replaced by gamma-aminobutyric acid (GABA).

Moreover, carnosine was found to inhibit protein oxidation, glycation and covalent adduction induced by RCS. In this regard, the quenching activity (ability of a compound to react with RCS forming unreactive adducted metabolites) of carnosine and related histidine dipeptides towards the different classes of RCS has been studied *in vitro* and *in vivo* since the late 90's. Overall, these studies proposed carnosine, together with GSH, as the most important RCS sequestering

5 Carnosine and derivatives as inhibitors of protein covalent modifications induced by reactive carbonyl species

agents in vertebrate organisms, and suggested its role in preventing the formation of AGEs and ALEs [39]. Such mechanism has been tested in several *in vitro* and *in vivo* studies conducted by different research groups and besides contributing towards a better understanding of the biological role of the endogenous dipeptide, it also opened a growing interest towards carnosine derivatives as a novel class of bioactive compounds [40]. The *in vitro* and *in vivo* studies demonstrating the quenching activity of carnosine towards different RCS are summarized below.

5.4 In vitro studies

The first experiments demonstrating the *in vitro* ability of carnosine to react with RCS were performed by incubating the molecule in the presence of different RCS at physiological pH (generally pH 7.4) and temperature (37-40°C); the reactivity was then estimated by measuring the RCS disappearance by HPLC [41]. More complex experiments were then carried out, consisting of incubating pure proteins with RCS, and then estimating the effect of carnosine on the formation of protein carbonyls by observing the modulation of protein crosslinks and oligomers by electrophoresis [42, 43]. Later, molecular studies on the reaction between carnosine and α - β -unsaturated aldehydes were performed not only to characterize their reaction products, but also to elucidate their reaction mechanism [44, 45]. It should be noted that analyses aiming at the study of the reaction mechanisms of carnosine towards other classes of RCS, such as di-aldehydes and keto-aldehydes, are still missing; also the comparison of the quenching efficiency of carnosine in respect to the well-known RCS quenchers, such as aminoguanidine, hydralazine and pyridoxamine has not yet been reported.

5.4.1 α - β -unsaturated aldehydes

Carnosine was reported to quench *trans*-2-hexenal and 4-hydroxy-2-*trans*-nonenal (HNE) by measuring by HPLC their disappearance upon incubation with carnosine [41]. The quenching activity of carnosine was higher in respect to its constituent amino acids, β -alanine and histidine, as well as of other histidine-containing dipeptides such as leucyl-histidine, isoleucyl-histidine and valyl-histidine. Polyunsaturated aldehydes (*trans,trans*-2,4-decadienal and *trans,trans*-2,4-hexadienal) and the non-conjugated monounsaturated aldehyde *trans*-4-decenal reacted weakly with carnosine.

5 Carnosine and derivatives as inhibitors of protein covalent modifications induced by reactive carbonyl species

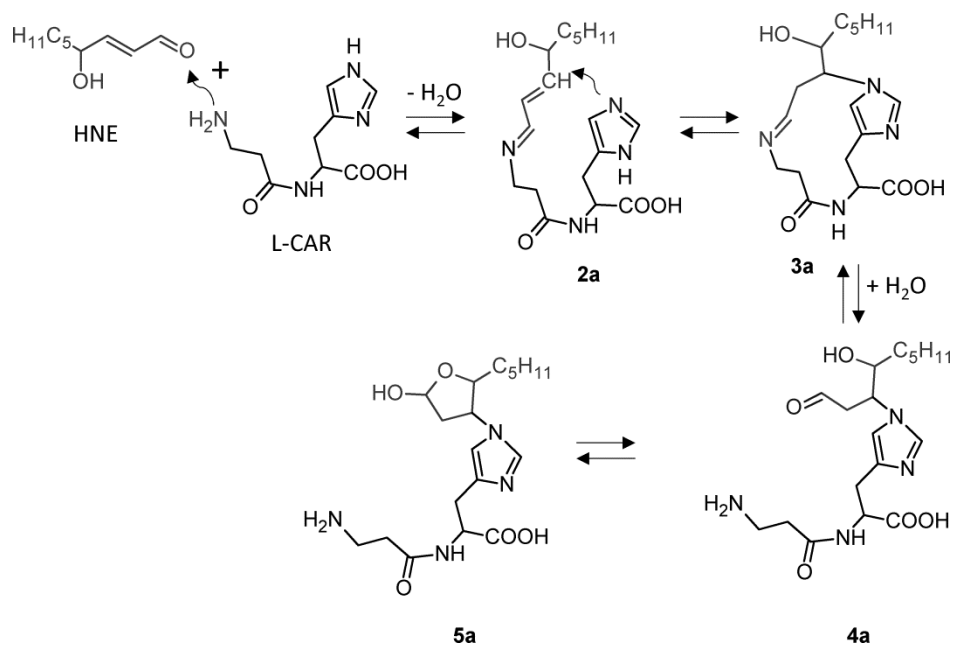


Fig. 7. Reaction mechanism of carnosine with HNE. With permission from Aldini, G., M. Carini, et al. (2002). CAR reacts with HNE through a two-steps mechanism. The reaction starts with the formation of a reversible Schiff base (an α,β -unsaturated imine, **2a**) to yield the macrocyclic adduct **3a** through an intramolecular Michael addition, which hydrolyzes to form the stable hemiacetal derivative **5a**

Further studies confirmed carnosine as effective quencher of HNE and identified and characterized the reaction products by MS [44]. In particular, two reaction products were identified by incubating HNE with carnosine: an imine macrocyclic derivative (**2a** in Figure 7) and a Michael adduct, stabilized as a 5-member cyclic hemiacetal (**5a**). The suggested adduction chemistry presents multiple steps: it begins with the formation of a reversible Schiff base (an α,β -unsaturated imine, **2a**) to yield the macrocyclic adduct **3a** through an intramolecular Michael addition, which hydrolyzes to form the stable hemiacetal derivative **5a** [44, 45]. Structural analyses were based on NMR and mass

5 Carnosine and derivatives as inhibitors of protein covalent modifications induced by reactive carbonyl species

spectrometry and were performed on carnosine and its analogues N-acetylcarnosine and anserine (a N^π-methyl derivative of carnosine). N-acetylation of the β-alanine amine group significantly reduced the quenching activity; this, together with the observation on the limited quenching capability of the two constitutive amino acids, suggested that both the amino group of the β-alanyl residue and the imidazole ring of L-histidine synergistically trap HNE. The two step reaction of carnosine with HNE also explains the selectivity of the dipeptide towards α,β-unsaturated aldehydes and that carnosine does not cross-react with physiological aldehydes, such as pyridoxal phosphate, a damaging mechanism quite common to well-known RCS scavenging agents such as hydralazine, aminoguanidine and edaravone [46].

The fact that HNE reacts with proteins mainly on Lys and His residues [47] suggests that carnosine may act as a detoxifying agent by mimicking the target amino acids of proteins.

5 Carnosine and derivatives as inhibitors of protein covalent modifications induced by reactive carbonyl species

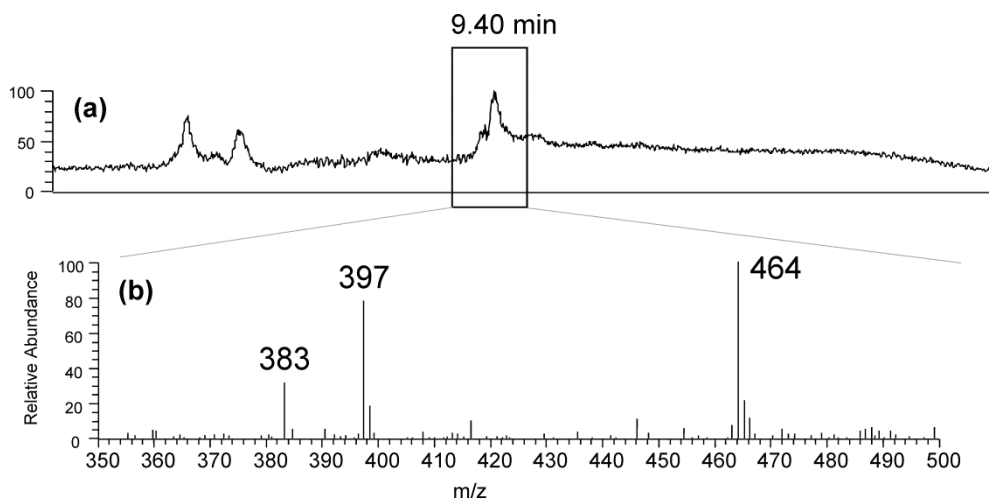


Fig. 8. LC/MS analysis (positive-ion mode) of skeletal muscle homogenate incubated with HNE (5 nmoles/mg protein).

The upper panel shows the total ion current (TIC); the lower panel shows the MS spectrum of the peak eluted at of 9.4 min. The ions at m/z 383, m/z 397 and m/z 464 correspond to Michael adducts of HNE with carnosine, anserine and GSH, respectively. Figure is adapted from Aldini, G., P. Granata, et al. (2002).

Such quenching activity was then demonstrated in tissue by detecting the carnosine-HNE Michael adduct **5a** in rat skeletal muscle homogenate (Figure 8) upon *in vitro* spontaneous oxidation in aerobic conditions [44] [48, 49], thereby confirming the RCS scavenging of carnosine in biological media and that carnosine-HNE can be considered as a biomarker of lipid peroxidation. In these studies, the anserine-HNE Michael adduct was observed for the first time in oxidized rat muscle, too (Figure 8). This finding is consistent with the fact that anserine is also present at high concentration in rat muscle and exerts quenching activity similar to carnosine *in vitro*.

Recently, the ability of carnosine and other carbonyl quenchers (hydralazine, aminoguanidine and pyridoxamine) to quench HNE was compared, using

5 Carnosine and derivatives as inhibitors of protein covalent modifications induced by reactive carbonyl species

ubiquitin as a model of protein undergoing RCS-induced carbonylation [50]. HNE covalently modified ubiquitin on lysine and histidine residues, to form Schiff base and Michael adducts: all tested compounds were found to dose-dependently inhibit ubiquitin carbonylation, but carnosine and hydralazine were the most effective quenchers.

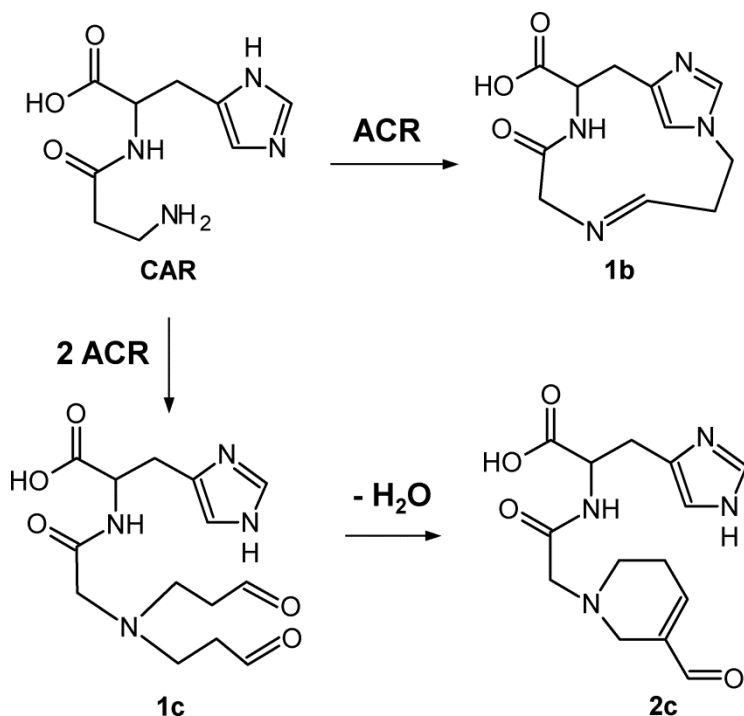


Fig. 9. Predominant reaction pathways of CAR with ACR. With permission from Carini, M., G. Aldini, et al. (2003). Carnosine reacts with ACR forming several molecular species, among which the predominant are: (a) the 14-membered macrocyclic derivatives, deriving from the formation of the iminic bond between the terminal amino group followed by intramolecular Michael addition of the C(3) of the ACR moiety to histidine; (b) the N^β -(3-formyl-3,4-dehydropiperidino) derivatives arising from the Michael addition of two acrolein molecules to the amino group of b-alanine, followed by an aldol condensation and dehydration.

5 Carnosine and derivatives as inhibitors of protein covalent modifications induced by reactive carbonyl species

In addition to HNE, the reaction between carnosine and acrolein was also described in detail[51]. The reaction products obtained *in vitro* were analyzed by mass spectrometry; several molecular species were detected, including macrocyclics deriving from the formation of the iminic bond between the terminal amino group followed by intramolecular Michael addition of the C3 of acrolein to histidine (Figure 9, **1c**). Additional reaction products were the N(β)-3-formyl-3,4-dehydropiperidinos (Figure 9, **2c**) deriving from the Michael addition of two acrolein molecules to the amino group of β -alanine, followed by aldol condensation and dehydration.

5.4.2 Di-aldehydes and ketoaldehydes

Besides α,β -unsaturated aldehydes, carnosine was reported to directly react with other reactive RCS [52], such as the di-aldehydes MDA and GO, the ketoaldehyde MGO as well as with reducing sugars [53]. Several analytical and biochemical methods were used to demonstrate the RCS quenching effect, although the reaction mechanisms as well as the reaction products have not yet been elucidated. For example, the reaction obtained *in vitro* between carnosine and methylglyoxal was observed by spectrophotometry: carnosine was found to inhibit methylglyoxal-mediated modification of ovalbumin, chosen as model protein [42]. Carnosine also reacts with MDA [43], as demonstrated by its effect in preventing MDA-induced protein cross-link and oligomerization. Carnosine was also found to protect cultured human and rat cells against the effects of toxic RCS such as formaldehyde, acetaldehyde, sugar-deriving AGEs and MDA itself. The *in vitro* studies carried out by Hipkiss [54] et al. mainly focused on the RCS quenching ability of carnosine and had a pioneering role in highlighting the protective role of carnosine against protein carbonylation in cells, promoting carnosine and related analogues as therapeutic targets for the treatment of

5 Carnosine and derivatives as inhibitors of protein covalent modifications induced by reactive carbonyl species

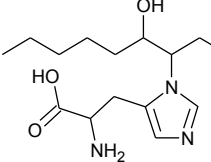
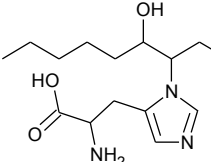
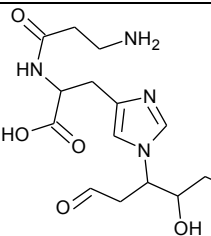
pathologies involving noxious RCS, such as secondary diabetic complications, inflammation and possibly Alzheimer's disease.

5.5 In vivo studies

GSH dependent conjugation represents the most efficient phase II detoxification reaction towards electrophilic compounds, including RCS, leading to urinary mercapturic acid metabolites. As above reported, *in vitro* studies carried out either in solution or in skeletal muscle homogenates indicate that carnosine and analogues can also act as nucleophilic agents able to detoxify RCS (in particular α,β -unsaturated aldehydes), forming unreactive conjugated metabolites. Such studies suggest that besides GSH, carnosine could also represent an important detoxification pathway of RCS, acting in particular areas, such as skeletal muscle, or when GSH is depleted. This important issue has been investigated, although not conclusively, in several *in vivo* studies, as reported in the present chapter.

One of the first pieces of evidence on the *in vivo* formation of covalent adducts between toxic endogenous aldehydes and histidine dipeptides was reported by Orioli et al in 2007 [55]. An analytical LC-MS method was developed and validated for the determination of RCS adducts with mercapturic acid and carnosine in the urine of obese Zucker rats. The Zucker rat was selected because it represents a well-established animal model of metabolic syndrome, since it is characterized by obesity, hyperlipidaemia, insulin resistance and renal injury; in this animal, the oxidative stress and lipid hydroperoxides lead to RCS and ultimately to protein carbonylation processes that are involved in the onset and progression of tissue damage [56]. The mass spectrometry method applied in this study was set to scan the molecules able to generate the immonium ion of histidine (m/z 110), which was used as a diagnostic marker of carnosine products; this method, based on the precursor ion scan (PIS) mode, allowed identifying the urinary metabolites of carnosine.

5 Carnosine and derivatives as inhibitors of protein covalent modifications induced by reactive carbonyl species

His containing metabolites		Urine		
		Lean Rats 4 week old	Lean Rats 6 months old	Zucker Rats
His-DHN (<i>m/z</i> 314)		Not found	Found	Found
His-HNA (<i>m/z</i> 328)		Not found	Not found	Found
CAR-HNE (<i>m/z</i> 383)		Not found	Found	Found

Tab. 2. RCS adducts metabolites containing histidine found in the rats' urine by precursor and product ion scan analyses. Two adducts were found in the old lean rats, three in the Zucker rats and none of the adducts were found in the young lean rats. Data are adapted from Orioli et al [55]

The method was applied to compare the urine of young lean rats (4 weeks old), old lean rats (6 months old) and Zucker rats. As reported in Table 2, three distinct precursor ions at *m/z* 314, 328 and 383 were identified in Zucker rats; none of them was identified in young lean rats, while two of them (*m/z* 314 and 383) were detected in old lean rats. The characterization of the three carnosine products by MS/MS led to the identification of His-1,4-dihydroxynonane (His-DHN, at *m/z* 314), His-1,4-hydroxynonanoic acid (His-HNA, at *m/z* 328) and the Michael

5 Carnosine and derivatives as inhibitors of protein covalent modifications induced by reactive carbonyl species

adduct carnosine-HNE (CAR-HNE, at m/z 383). These results confirm that RCS - and in particular HNE - is generated in physiological conditions, and that its formation is associated with aging and with the metabolic syndrome. Once identified and characterized, a validated Multiple Reaction Monitoring (MRM) method was set-up for their quantitation and to measure HNE-mercapturic acid metabolites, such as the 1,4 dihydroxynonane mercapturic acid (DHN-MA), with a good sensitivity.

His containing metabolites	Urine	
	Lean Rats (nmoles/24h)	Zucker Rats (nmoles/24h)
His-DHN (m/z 314)	0.9	3.8
DHN-MA (m/z 322)	16	60
CAR-HNE (m/z 383)	0.8	2

Tab. 3. Quantitative analysis of RCS metabolites containing His in lean and Zucker rat urine. Data are from Orioli et al. [55]

The results, summarized in table 3, well indicate that GSH and carnosine act as nucleophilic substrates in the detoxification of HNE, and that GSH is more reactive, highlighting the role of GSH as first-line defense against cytotoxic HNE. Upon a significant oxidative stress, GSH is likely to be consumed, therefore carnosine, due to the fact that it is quite stable towards oxidation (it has a poor antioxidant activity in respect to GSH), might acquire a crucial role in detoxifying cytotoxic RCS: this mechanism would suggest an interesting cooperation between the histidine dipeptides and GSH in RCS metabolism. It is still not clear whether the His-HNE metabolites detected in Zucker rats derive from carnosine-HNE adducts or from other sources, such as HNE-protein digestion.

5 Carnosine and derivatives as inhibitors of protein covalent modifications induced by reactive carbonyl species

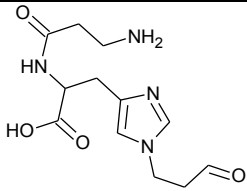
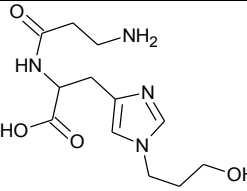
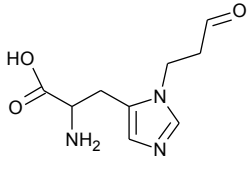
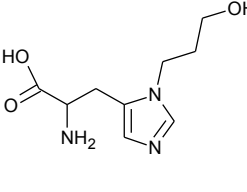
The ability of carnosine to form covalent adducts with HNE has been confirmed by different studies, which show that the formation of carnosine-HNE metabolites correlate with the inhibition of protein carbonyls formation and with a protective effect as well, suggesting that the pharmacological activity of carnosine can be mediated by the RCS detoxifying activity and by the prevention of ALEs formation. In particular, the chronic administration of L-carnosine and of its enantiomer, D-carnosine (β -alanyl-D-histidine), to Zucker obese rat significantly reduced the development of dyslipidemia, hypertension and renal injury, as demonstrated by urinary parameters and by microscope analysis of renal tissue biopsies [57]. Such a pharmacological effect was associated with an improved excretion of HNE, as carnosine-HNE and histidine-HNE, thereby reducing the accumulation of AGEs and protein carbonyls. These data suggest that the biological effect of endogenous L-carnosine is not based on a pro-histaminic effect, since D-carnosine does not undergo peptidic hydrolysis and therefore it is not a histidine precursor; conversely, a direct carbonyl quenching mechanism can explain, at least partially, the pharmacological effects of carnosine[57].

The protective and HNE quenching effect of carnosine was then confirmed in apoE null mice feeding a western and pro-atherogenic diet [58]. Treatment with D-carnosine octylester (a D-carnosine pro-drug, see chapter 5) attenuated atherosclerosis and renal diseases, an effect which was associated with increased urinary levels of HNE-carnosine adducts and reduced protein carbonylation, circulating and tissue ALEs, expression of receptors for these products, and systemic and tissue oxidative stress [58].

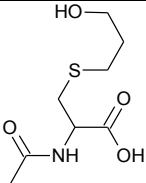
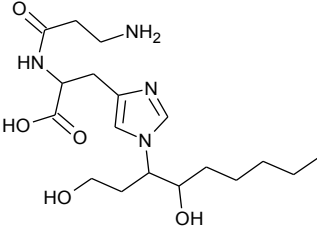
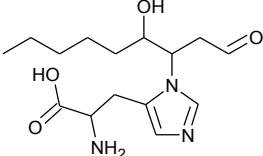
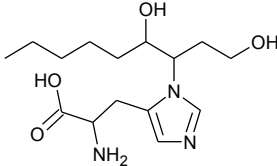
The RCS quenching ability and the anti-atherogenic effect of D-carnosine (given as octyl-ester) was confirmed and further characterized by an independent research group [59]. Oral treatment with the drug decreased atherosclerotic lesion formation in the aortic valves of apolipoprotein E-null mice. Such pharmacological activity was associated with a RCS scavenging effect of D-carnosine, determined by a decrease in the accumulation of the adducts protein-

5 Carnosine and derivatives as inhibitors of protein covalent modifications induced by reactive carbonyl species

acrolein, protein-4-hydroxyhexenal and protein-4-hydroxynonenal in atherosclerotic lesions and by a concomitant increase of urinary excretion of aldehydes as carnosine conjugates [59].

Adduct Urine Concentration (pmoles/mg creatine)		Urine
		Healthy Humans
Carnosine-propanal (<i>m/z</i> 283)		66 ± 17
Carnosine-propanol (<i>m/z</i> 285)		200 ± 75
Histidine-propanal (<i>m/z</i> 212)		227 ± 150
Histidine-propanol (<i>m/z</i> 214)		127 ± 84

5 Carnosine and derivatives as inhibitors of protein covalent modifications induced by reactive carbonyl species

Adduct Urine Concentration (pmoles/mg creatine)		Urine
		Healthy Humans
3-HPMA (<i>m/z</i> 220)		695 ± 213
Carnosine-DHN (<i>m/z</i> 385)		Found at trace levels
His-HNE (<i>m/z</i> 312)		2.7 ± 1
His-DHN (<i>m/z</i> 314)		2.9 ± 1

Tab. 4. Quantitative analysis of RCS adducted metabolites containing histidine in healthy humans. Acrolein adducts are the most abundant ones, in particular 3-HPMA, carnosine-propanol, histidine propanol. The concentration is reported as pmoles/mg creatine. The data are from [60].

5 Carnosine and derivatives as inhibitors of protein covalent modifications induced by reactive carbonyl species

The first paper reporting the identification of carnosine-RCS metabolites in humans was published by Baba et al [60]. Urine samples from healthy, non-smoker adults were analyzed by LC/MS with the aim of identifying carnosine-aldehyde metabolites. The most abundant metabolites identified by this study were carnosine-propanol (m/z 285), carnosine-propanal (m/z 283), histidine-propanol (m/z 214) and histidine-propanal (m/z 212), resulting from the acrolein adduction by carnosine followed by reduction and hydrolysis. The majority of the metabolites (75%) were in their reduced form, suggesting that the reduction of carnosine/histidine conjugates is an important step of their metabolism. The origin of the histidine conjugates is not clear, since they can arise either from the hydrolysis of the adducted carnosine, from the direct reaction between histidine and acrolein or from the hydrolysis of adducted histidines in proteins. HNE adducts were found as well, but in lower amounts than ACR metabolites; for example, the urinary concentration of His-HNE (m/z 310) was 75-fold lower than His-propanal concentration. Moreover, only trace levels of carnosine-HNE (m/z 383) and its reduced form carnosine-DHN (m/z 385) were detected. It is important to notice that these observations were made on samples obtained from healthy volunteers, while no data have been reported for pathological conditions, where a significant increase of HNE is expected⁶¹.

Taken together, the above mentioned studies indicate as follows: 1) carnosine and its analogues, together with GSH, represent an efficient endogenous detoxifying system for RCS and in particular for α,β -unsaturated aldehydes; 2) the metabolites arising from the adduction of carnosine/histidine and RCS are excreted in the urine mainly in their reduced form, both in healthy humans and rodents; 3) the carnosine adduction pathway seems a relevant metabolic fate of acrolein's overall metabolism; and finally that 4) in healthy rat and human urine only a low amount of HNE adducts were found: this can be explained by considering that in physiological conditions HNE is mainly detoxified by GSH and/or that HNE is degraded to generate other metabolites⁶⁰.

5 Carnosine and derivatives as inhibitors of protein covalent modifications induced by reactive carbonyl species

Concerning the reduction of RCS-carnosine adducts, Baba et al. [60] found that aldose reductase is the enzyme involved in the reducing reaction and that it is able to catalyse the reduction not only of carnosine-propanals but also of other histidine peptides conjugates such as homo-carnosine and anserine. Studies performed on mice lacking aldose reductase (KO mice) confirmed this observation, since no reduced metabolites were detected in the urine of these animals. The enzyme showed a limited catalytic activity on HNE conjugates; this can explain the low levels of the CAR-DHN adduct, in respect to its non-reduced form, in both rodent and human urines. Such limited activity was explained by considering that in HNE conjugates, HNE is in an hemiacetal form so that the aldehyde group is not available for the reducing reaction.

5.6 Carnosine derivatives as a novel class of bioactive compounds

Carnosine and the methyl derivatives anserine and ophidine (balenine) are dietary dipeptides found in significant amounts in red and white meat and in some fish such as tuna, salmon and trout.

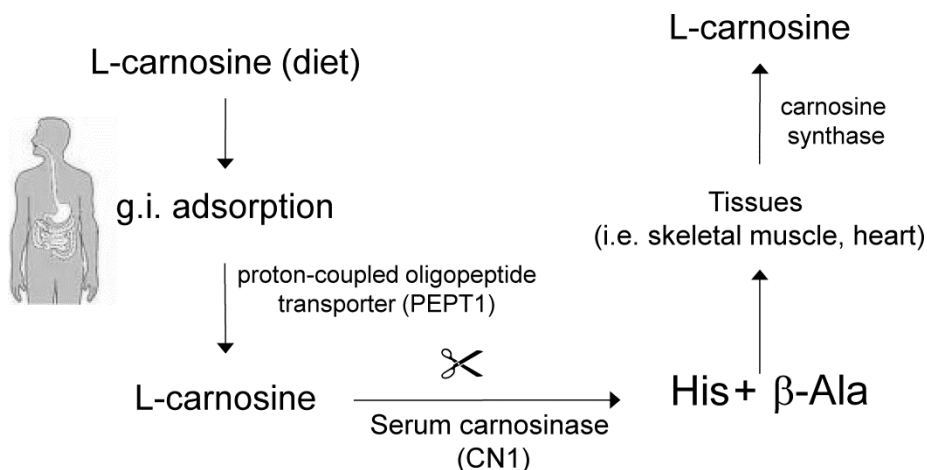


Fig. 10. Metabolic fate of carnosine orally ingested in humans.

Carnosine is absorbed in intact form, primarily in the jejunum, through an active transport, which is accomplished by the oligopeptide transporter 1 (PEPT1). Once absorbed, carnosine is hydrolyzed by serum carnosinase. The constitutive amino acids histidine and β -alanine are then absorbed from the serum to the tissues, where they are the substrates of the carnosine synthase that produces carnosine.

5 Carnosine and derivatives as inhibitors of protein covalent modifications induced by reactive carbonyl species

The dipeptides are absorbed in intact form, primarily in the jejunum, through an active transport, which is accomplished by the oligopeptide transporter 1 (PEPT1). In humans, once absorbed, carnosine and derivatives are efficiently hydrolyzed by specific hydrolytic enzymes, named carnosinase (Figure 10). Two forms of carnosinase have been identified so far: CN1, or serum carnosinase, and CN2, also named tissue carnosinase or cytosolic nonspecific dipeptidase [61]. CN1 is highly expressed in the serum of humans and causes the limited bioavailability of carnosine, as observed in intervention studies [62]. The constitutive amino acids histidine and β -alanine are then absorbed from the serum to the tissues, where they are the substrates of the carnosine synthase that produces carnosine [63]. By contrast CN1 is absent in non-primate mammals; this explains the bioavailability of such dipeptides in the rodents blood.

Considering the involvement of RCS in the pathogenetic mechanisms of several human diseases based on oxidative stress, serum RCS represents an important drug target for the discovery of bioactive compounds able to detoxify RCS [1, 16]. Such an innovative drug target has been validated by testing the efficacy of carnosine in several animal models of oxidative-stress based diseases, such as metabolic syndrome [57] and atherosclerosis [58, 59] - where RCS act as pathogenetic factors. The observed pharmacological activity of carnosine in animal models can be explained by considering that the absence of serum carnosinase in rodents allows carnosine to reach a plasma concentration able to trap circulating RCS, as evidenced by the detection of its adducts in plasma and urine. In humans, carnosine probably acts as endogenous detoxifying agent of RCS in those tissues where it is present in a high concentration such as skeletal muscle, brain and heart, but not in the blood stream due to the presence of carnosinase, even following treatment with oral doses of 60 mg/kg body [62, 64]. Evidence, although indirect, of the potential activity of carnosine, when bioavailable in serum, is given by genetic studies. Jansenn et al. first reported that diabetic patients with a decreased risk of developing diabetic nephropathy are

5 Carnosine and derivatives as inhibitors of protein covalent modifications induced by reactive carbonyl species

characterized by a polymorphism of the CNDP1 gene, leading to a reduced secretion of serum carnosinase [65]. The disease-protecting effect of lower serum carnosinase activity probably relies on the higher stability of carnosine in the blood stream or to a local effect of enhanced carnosine availability in the kidney, as commented by Boldyrev et al. [38].

All the evidence reported above prompted the design of carnosine derivatives that, on one hand, maintain or improve the RCS quenching efficacy and selectivity of carnosine, and on the other hand are characterized by improved bioavailability, as a result of being recognized by PEPT1, but not by carnosinase [40]. The first strategy used to obtain stable derivatives involved the inversion of the chiral center of histidine leading the enantiomer D-carnosine [57]. D-CAR was found to be stable in the plasma, since it is not recognized by carnosinase; its HNE quenching efficacy and selectivity were superimposable on those of L-carnosine. However, D-CAR is less recognized by PEPT-1 in respect to L-CAR, resulting in a lower absorption, thus reducing bioavailability despite its carnosinase stability. With the aim of improving the bioavailability of D-carnosine, a set of lipophilic pro-drugs have been designed and synthesized to be absorbed through a passive absorption [66]. Among these, the octyl ester of D-CAR was selected for *in vivo* studies; its pharmacokinetic profile confirmed the improved bioavailability and its efficacy was tested in several animal models, including obese Zucker rats and ApoE null mice fed with a Western diet (see above) [58, 59].

5.7 Conclusions

Several pieces of evidence indicate that carnosine, together with GSH, is an endogenous nucleophilic peptide able to detoxify cytotoxic RCS and in particular α,β -unsaturated aldehydes, such as HNE and ACR.

Michael adducts between carnosine and α,β -unsaturated aldehydes, in both reduced and non reduced form, represent the main metabolites so far identified in both human and rodent urine and plasma. However several questions remain open; in particular it is still not clear whether the carnosine detoxification pathway is catalysed by enzymes. Recent evidence indicates that aldose reductase is involved in reducing the carbonyl group of the Michael adducts, thus forming more stable and unreactive adducts [60]. However, the existence of an enzyme catalysing the formation of the Michael adduct and the biological function of these metabolites are still unexplored.

It is now well established that carnosine-mediated detoxification of RCS is associated with a protective effect in some animal models of oxidative-stress based diseases including atherosclerosis, diabetes, ischemia/reperfusion damage and metabolic syndrome. Such promising effects can be explained in rodents, where carnosine, due to the absence of serum carnosinase, is bioavailable and acts as detoxifying agent of circulating RCS.

The effect of carnosine in humans is not yet known, due to the absence of controlled intervention studies; what it is well established is the lack of carnosine bioavailability in serum due to the presence of carnosinase [62, 64].

Overall, taking into consideration the biological effect of carnosine as RCS detoxifying agent, its lack of bioavailability and the pathogenetic effects of circulating RCS, the design of novel carnosine derivatives stable to carnosinase represent a promising therapeutic approach [67] [40].

5.8 Summary points

- The chapter focuses on carnosine as detoxifying agent of reactive carbonyl species
- Reactive carbonyl species (RCS) are generated by lipid and sugar oxidation and belong to different chemical classes including α,β -unsaturated aldehydes, di-aldehydes and keto-aldehydes;
- RCS and the corresponding reaction products with proteins (AGEs and ALEs) are involved in the pathogenic mechanisms of several oxidative based pathologies, such as atherosclerosis and diabetes related diseases;
- Several mechanisms have been considered to explain the damaging effects of RCS and of the corresponding adducts, among these the protein function derangement, the antigenic properties of RCS protein adducts, the damaging AGEs-RAGE axis and the amyloidogenic properties of RCS protein adducts;
- RCS are recognized as important pathogenetic mediators and as innovative drug targets;
- RCS are detoxified by phase I and II metabolism;
- Carnosine is an endogenous histidine dipeptide of dietary source, presents in mM concentrations in some tissues but not in serum due to the presence of carnosinases that catalytically hydrolyze carnosine to its constitutive amino acids;
- Carnosine was found to be a selective RCS sequestering agent, in particular towards α,β -unsaturated aldehydes;
- Carnosine and its analogues, together with GSH, represent an efficient endogenous detoxifying system for α,β -unsaturated aldehydes;
- the metabolites arising from the adduction of carnosine with α,β -unsaturated aldehydes are excreted in urine mainly in their reduced form, both in healthy humans and rodents;

5 Carnosine and derivatives as inhibitors of protein covalent modifications induced by reactive carbonyl species

- the carnosine adduction pathway seems a relevant metabolic fate of acrolein's overall metabolism;
- By considering the reduced bioavailability of carnosine in human serum due to the presence of serum carnosinase, carnosine analogues resistant to carnosinases have been proposed and tested in animal models as detoxifying agents of circulating RCS;
- Carnosine derivatives represent a novel class of bioactive compounds.

5.9 Definitions of words and terms

Aldehyde dehydrogenases (ALDHs) are a group of phase I enzymes that catalyse the oxidation (dehydrogenation) of aldehydes to the corresponding carboxylic acids through a NAD(P)⁺ dependent reaction.

AGEs: acronym for Advanced Glycation End products. AGEs indicates a heterogeneous class of covalent adducts arising from the reaction between proteins and RCS generated from the oxidative degradation of sugars. AGEs can also be generated by the direct condensation between reducing sugars and Lys residues (also called glycation) via the so called Maillard reactions.

ALEs: acronym for Advanced Lipoxidation End products. ALEs indicates the covalent adducts arising from the reaction between protein and RCS generated from the oxidation degradation of lipids.

Carnosine is a β -alanyl-L-histidine dipeptide discovered in 1900 as an abundant non-protein nitrogen-containing compound of meat. The dipeptide is not only found in skeletal muscle, but also in other excitable tissues. Although the biological role of carnosine is still unknown, several biological activities have been proposed, among which the carbonyl quenching activity.

D-carnosine octylester is a new chemical entity synthesized to act as a pro-drug of D-carnosine. D-carnosine (β -alanyl-D-histidine) is the enantiomer of carnosine,

5 Carnosine and derivatives as inhibitors of protein covalent modifications induced by reactive carbonyl species

designed to be stable to carnosinases. D-carnosine octylester is absorbed through passive diffusion.

Glutathione (GSH) is an endogenous tripeptide (γ -L-Glutamyl-L-cysteinylglycine) acting as a substrate in both conjugation reactions (phase II reactions) and reduction reactions. GSH is the main endogenous antioxidant able to reduce oxidants and forming the oxidized form (GSSG). GSSG is reduced to GSH by glutathione reductase and using NADPH as an electron donor.

4-hydroxy-*trans*-nonenal (HNE) is an α,β -unsaturated aldehyde generated by the lipid-peroxidation of ω -6 polyunsaturated fatty acids such as arachidonic and linoleic acids. HNE is an electrophilic by-product able to form covalent adducts with nucleophilic substrates such as proteins, nucleic acids and phospholipids. It is metabolized through phase I and II reactions.

hPepT1 is a peptide transporter belonging to the POT (proton oligopeptide transporter) family. It modulates intestinal absorption and renal reabsorption of di- and tri-peptides in a proton dependent way, hence acting like as a cotransporter

Reactive carbonyl species (RCS) are break-down products formed by the oxidative damage to lipids and sugars. RCS are electrophilic compounds able to form covalent adducts with nucleophilic substrates and in particular with protein, nucleic acids and phospholipids.

Serum Carnosinase (CN2) is a hydrolytic metallo-enzyme found in plasma and responsible for the rapid and selective digestion of the absorbed carnosine. It is expressed also in CNS where it can hydrolyze homocarnosine thus modulating the release of GABA in the brain.

5.10 References

1. Aldini G, Dalle-Donne I, Facino RM, Milzani A, Carini M. Intervention strategies to inhibit protein carbonylation by lipoxidation-derived reactive carbonyls. *Medicinal Research Reviews*. 2007 Nov;27(6):817-68.
2. Vistoli G, De Maddis D, Cipak A, Zarkovic N, Carini M, Aldini G. Advanced glycoxidation and lipoxidation end products (AGEs and ALEs): an overview of their mechanisms of formation. *Free radical research*. 2013 2013-Aug;47 Suppl 1:3-27.
3. Stevens JF, Maier CS. Acrolein: sources, metabolism, and biomolecular interactions relevant to human health and disease. *Mol Nutr Food Res*. 2008 Jan;52(1):7-25.
4. Seiler N. Catabolism of polyamines. *Amino Acids*. 2004 Jun;26(3):217-33.
5. LoPachin RM, Gavin T, Petersen DR, Barber DS. Molecular Mechanisms of 4-Hydroxy-2-nonenal and Acrolein Toxicity: Nucleophilic Targets and Adduct Formation. *Chemical Research in Toxicology*. 2009 Sep;22(9):1499-508.
6. Degen J, Hellwig M, Henle T. 1,2-Dicarbonyl Compounds in Commonly Consumed Foods. *Journal of Agricultural and Food Chemistry*. 2012 Jul;60(28):7071-9.
7. Fu TM, Jacob DJ, Wittrock F, Burrows JP, Vrekoussis M, Henze DK. Global budgets of atmospheric glyoxal and methylglyoxal, and implications for formation of secondary organic aerosols. *Journal of Geophysical Research-Atmospheres*. 2008 Aug;113(D15).
8. O'Brien PJ, Siraki AG, Shangari N. Aldehyde sources, metabolism, molecular toxicity mechanisms, and possible effects on human health. *Critical Reviews in Toxicology*. 2005 Aug;35(7):609-62.
9. Thornalley PJ, Langborg A, Minhas HS. Formation of glyoxal, methylglyoxal and 3-deoxyglucosone in the glycation of proteins by glucose. *Biochem J*. 1999 Nov;344 Pt 1:109-16.
10. Kalapos MP. Methylglyoxal in living organisms - Chemistry, biochemistry, toxicology and biological implications. *Toxicology Letters*. 1999 Nov;110(3):145-75.

5 Carnosine and derivatives as inhibitors of protein covalent modifications induced by reactive carbonyl species

11. Davies SS, Amarnath V, Roberts LJ. Isoketals: highly reactive gamma-ketoaldehydes formed from the H-2-isoprostane pathway. *Chemistry and Physics of Lipids*. 2004 Mar;128(1-2):85-99.
12. Requena JR, Fu MX, Ahmed MU, Jenkins AJ, Lyons TJ, Thorpe SR. Lipoxidation products as biomarkers of oxidative damage to proteins during lipid peroxidation reactions. *Nephrol Dial Transplant*. 1996;11 Suppl 5:48-53.
13. Janero DR. Malondialdehyde and thiobarbituric acid-reactivity as diagnostic indices of lipid peroxidation and peroxidative tissue injury. *Free Radic Biol Med*. 1990;9(6):515-40.
14. Moore K, Roberts LJ. Measurement of lipid peroxidation. *Free Radic Res*. 1998 Jun;28(6):659-71.
15. Dalle-Donne I, Rossi R, Colombo R, Giustarini D, Milzani A. Biomarkers of oxidative damage in human disease. *Clin Chem*. 2006 Apr;52(4):601-23.
16. Aldini G, Dalle-Donne I, Colombo R, Facino RM, Milzani A, Carini M. Lipoxidation-derived reactive carbonyl species as potential drug targets in preventing protein carbonylation and related cellular dysfunction. *Chemmedchem*. 2006 Oct;1(10):1045-+.
17. Fedorova M, Bollineni RC, Hoffmann R. Protein carbonylation as a major hallmark of oxidative damage: Update of analytical strategies. *Mass Spectrom Rev*. 2014 Mar;33(2):79-97.
18. Colzani M, Aldini G, Carini M. Mass spectrometric approaches for the identification and quantification of reactive carbonyl species protein adducts. *J Proteomics*. 2013 Apr.
19. Aldini G, Dalle-Donne I, Vistoli G, Facino RM, Carini M. Covalent modification of actin by 4-hydroxy-trans-2-nonenal (HNE): LC-ESI-MS/MS evidence for Cys374 Michael adduction. *Journal of Mass Spectrometry*. 2005 Jul;40(7):946-54.
20. Dalle-Donne I, Carini M, Vistoli G, Gamberoni L, Giustarini D, Colombo R, et al. Actin Cys374 as a nucleophilic target of alpha,beta-unsaturated aldehydes. *Free Radical Biology and Medicine*. 2007 Mar;42(5):583-98.
21. Aldini G, Carini M, Vistoli G, Shibata T, Kusano Y, Gamberoni L, et al. Identification of actin as a 15-deoxy-Delta(12,14)-prostaglandin J(2) target in O6-neuroblastoma cells: Mass spectrometric, computational, and functional approaches to investigate the effect on cytoskeletal derangement. *Biochemistry*. 2007 Mar;46(10):2707-18.

5 Carnosine and derivatives as inhibitors of protein covalent modifications induced by reactive carbonyl species

22. Smathers RL, Fritz KS, Galligan JJ, Shearn CT, Reigan P, Marks MJ, et al. Characterization of 4-HNE modified L-FABP reveals alterations in structural and functional dynamics. *PLoS One*. 2012;7(6):e38459.
23. Madian AG, Regnier FE. Profiling carbonylated proteins in human plasma. *J Proteome Res*. 2010 Mar;9(3):1330-43.
24. Madian AG, Myracle AD, Diaz-Maldonado N, Rochelle NS, Janle EM, Regnier FE. Differential carbonylation of proteins as a function of in vivo oxidative stress. *J Proteome Res*. 2011 Sep;10(9):3959-72.
25. Kirkham PA, Caramori G, Casolari P, Papi AA, Edwards M, Shamji B, et al. Oxidative stress-induced antibodies to carbonyl-modified protein correlate with severity of chronic obstructive pulmonary disease. *Am J Respir Crit Care Med*. 2011 Oct;184(7):796-802.
26. Alzolibani AA, Al Robaee AA, Al-Shobaili HA, Rasheed Z. 4-Hydroxy-2-nonenal modified histone-H2A: a possible antigenic stimulus for systemic lupus erythematosus autoantibodies. *Cell Immunol*. 2013 Jul-Aug;284(1-2):154-62.
27. Khatoon F, Moinuddin, Alam K, Ali A. Physicochemical and immunological studies on 4-hydroxynonenal modified HSA: implications of protein damage by lipid peroxidation products in the etiopathogenesis of SLE. *Hum Immunol*. 2012 Nov;73(11):1132-9.
28. Fritz G. RAGE: a single receptor fits multiple ligands. *Trends Biochem Sci*. 2011 Dec;36(12):625-32.
29. Xue J, Rai V, Singer D, Chabierski S, Xie J, Reverdatto S, et al. Advanced glycation end product recognition by the receptor for AGEs. *Structure*. 2011 May;19(5):722-32.
30. Kierdorf K, Fritz G. RAGE regulation and signaling in inflammation and beyond. *J Leukoc Biol*. 2013 Jul;94(1):55-68.
31. Siegel SJ, Bieschke J, Powers ET, Kelly JW. The oxidative stress metabolite 4-hydroxynonenal promotes Alzheimer protofibril formation. *Biochemistry*. 2007 Feb;46(6):1503-10.
32. Näsström T, Fagerqvist T, Barbu M, Karlsson M, Nikolajeff F, Kasrayan A, et al. The lipid peroxidation products 4-oxo-2-nonenal and 4-hydroxy-2-nonenal promote the formation of α -synuclein oligomers with distinct biochemical, morphological, and functional properties. *Free Radic Biol Med*. 2011 Feb;50(3):428-37.
33. Xiang W, Schlachetzki JC, Helling S, Bussmann JC, Berlinghof M, Schäffer TE, et al. Oxidative stress-induced posttranslational modifications of

5 Carnosine and derivatives as inhibitors of protein covalent modifications induced by reactive carbonyl species

alpha-synuclein: specific modification of alpha-synuclein by 4-hydroxy-2-nonenal increases dopaminergic toxicity. *Mol Cell Neurosci*. 2013 May;54:71-83.

34. Siems W, Grune T. Intracellular metabolism of 4-hydroxynonenal. *Mol Aspects Med*. 2003 2003 Aug-Oct;24(4-5):167-75.

35. Izaguirre G, Kikonyogo A, Pietruszko R. Methylglyoxal as substrate and inhibitor of human aldehyde dehydrogenase: comparison of kinetic properties among the three isozymes. *Comp Biochem Physiol B Biochem Mol Biol*. 1998 Apr;119(4):747-54.

36. Alary J, Guéraud F, Cravedi JP. Fate of 4-hydroxynonenal in vivo: disposition and metabolic pathways. *Mol Aspects Med*. 2003 2003 Aug-Oct;24(4-5):177-87.

37. Thornalley PJ. The glyoxalase system: new developments towards functional characterization of a metabolic pathway fundamental to biological life. *Biochem J*. 1990 Jul;269(1):1-11.

38. Boldyrev AA, Aldini G, Derave W. Physiology and pathophysiology of carnosine. *Physiol Rev*. 2013 Oct;93(4):1803-45.

39. Aldini G, Facino RM, Beretta G, Carini M. Carnosine and related dipeptides as quenchers of reactive carbonyl species: From structural studies to therapeutic perspectives. *Biofactors*. 2005;24(1-4):77-87.

40. Vistoli G, Carini M, Aldini G. Transforming dietary peptides in promising lead compounds: the case of bioavailable carnosine analogs. *Amino Acids*. 2012 Jul;43(1):111-26.

41. Zhou S, Decker EA. Ability of carnosine and other skeletal muscle components to quench unsaturated aldehydic lipid oxidation products. *J Agric Food Chem*. 1999 Jan;47(1):51-5.

42. Hipkiss AR, Chana H. Carnosine protects proteins against methylglyoxal-mediated modifications. *Biochem Biophys Res Commun*. 1998 Jul;248(1):28-32.

43. Hipkiss AR, Worthington VC, Himsforth DT, Herwig W. Protective effects of carnosine against protein modification mediated by malondialdehyde and hypochlorite. *Biochim Biophys Acta*. 1998 Mar;1380(1):46-54.

44. Aldini G, Carini M, Beretta G, Bradamante S, Facino RM. Carnosine is a quencher of 4-hydroxy-nonenal: through what mechanism of reaction? *Biochemical and Biophysical Research Communications*. 2002 Nov;298(5):699-706.

5 Carnosine and derivatives as inhibitors of protein covalent modifications induced by reactive carbonyl species

45. Liu Y, Xu G, Sayre LM. Carnosine inhibits (E)-4-hydroxy-2-nonenal-induced protein cross-linking: structural characterization of carnosine-HNE adducts. *Chem Res Toxicol*. 2003 Dec;16(12):1589-97.
46. Aldini G, Vistoli G, Regazzoni L, Benfatto MC, Bettinelli I, Carini M. Edaravone Inhibits Protein Carbonylation by a Direct Carbonyl-Scavenging Mechanism: Focus on Reactivity, Selectivity, and Reaction Mechanisms. *Antioxidants & Redox Signaling*. 2010 Feb;12(3):381-92.
47. Nadkarni DV, Sayre LM. Structural definition of early lysine and histidine adduction chemistry of 4-hydroxynonenal. *Chemical Research in Toxicology*. 1995 Mar;8(2):284-91.
48. Aldini G, Granata P, Carini M. Detoxification of cytotoxic alpha,beta-unsaturated aldehydes by carnosine: characterization of conjugated adducts by electrospray ionization tandem mass spectrometry and detection by liquid chromatography/mass spectrometry in rat skeletal muscle. *Journal of Mass Spectrometry*. 2002 Dec;37(12):1219-28.
49. Orioli M, Aldini G, Beretta G, Facino RM, Carini M. LC-ESI-MS/MS determination of 4-hydroxy-trans-2-nonenal Michael adducts with cysteine and histidine-containing peptides as early markers of oxidative stress in excitable tissues. *Journal of Chromatography B-Analytical Technologies in the Biomedical and Life Sciences*. 2005 Nov;827(1):109-18.
50. Colzani M, Criscuolo A, De Maddis D, Garzon D, Yeum KJ, Vistoli G, et al. A novel high resolution MS approach for the screening of 4-hydroxy-trans-2-nonenal sequestering agents. *J Pharm Biomed Anal*. 2014 Jan;91C:108-18.
51. Carini M, Aldini G, Beretta G, Arlandini E, Facino RM. Acrolein-sequestering ability of endogenous dipeptides: characterization of carnosine and homocarnosine/acrolein adducts by electrospray ionization tandem mass spectrometry. *Journal of Mass Spectrometry*. 2003 Sep;38(9):996-1006.
52. Hipkiss AR, Brownson C, Carrier MJ. Carnosine, the anti-ageing, anti-oxidant dipeptide, may react with protein carbonyl groups. *Mech Ageing Dev*. 2001 Sep;122(13):1431-45.
53. Hipkiss AR, Michaelis J, Syrris P. Non-enzymatic glycosylation of the dipeptide L-carnosine, a potential anti-protein-cross-linking agent. *FEBS Lett*. 1995 Aug;371(1):81-5.
54. Hipkiss AR. Carnosine and its possible roles in nutrition and health. *Adv Food Nutr Res*. 2009;57:87-154.
55. Orioli M, Aldini G, Benfatto MC, Facino RM, Carini M. HNE Michael adducts to histidine and histidine-containing peptides as biomarkers of lipid-

5 Carnosine and derivatives as inhibitors of protein covalent modifications induced by reactive carbonyl species

derived carbonyl stress in urines: LC-MS/MS profiling in Zucker obese rats. *Anal Chem.* 2007 Dec;79(23):9174-84.

56. Dominguez JH, Wu P, Hawes JW, Deeg M, Walsh J, Packer SC, et al. Renal injury: similarities and differences in male and female rats with the metabolic syndrome. *Kidney Int.* 2006 Jun;69(11):1969-76.

57. Aldini G, Orioli M, Rossoni G, Savi F, Braidotti P, Vistoli G, et al. The carbonyl scavenger carnosine ameliorates dyslipidaemia and renal function in Zucker obese rats. *Journal of Cellular and Molecular Medicine.* 2011 Jun;15(6):1339-54.

58. Menini S, Iacobini C, Ricci C, Scipioni A, Fantauzzi CB, Giaccari A, et al. D-carnosine octylester attenuates atherosclerosis and renal disease in ApoE null mice fed a Western diet through reduction of carbonyl stress and inflammation. *British Journal of Pharmacology.* 2012 Jun;166(4):1344-56.

59. Barski OA, Xie Z, Baba SP, Sithu SD, Agarwal A, Cai J, et al. Dietary carnosine prevents early atherosclerotic lesion formation in apolipoprotein E-null mice. *Arterioscler Thromb Vasc Biol.* 2013 Jun;33(6):1162-70.

60. Baba SP, Hoetker JD, Merchant M, Klein JB, Cai J, Barski OA, et al. Role of aldose reductase in the metabolism and detoxification of carnosine-acrolein conjugates. *J Biol Chem.* 2013 Aug.

61. Teufel M, Saudek V, Ledig JP, Bernhardt A, Boularand S, Carreau A, et al. Sequence identification and characterization of human carnosinase and a closely related non-specific dipeptidase. *J Biol Chem.* 2003 Feb;278(8):6521-31.

62. Yeum KJ, Orioli M, Regazzoni L, Carini M, Rasmussen H, Russell RM, et al. Profiling histidine dipeptides in plasma and urine after ingesting beef, chicken or chicken broth in humans. *Amino Acids.* 2010 Mar;38(3):847-58.

63. Drozak J, Veiga-da-Cunha M, Vertommen D, Stroobant V, Van Schaftingen E. Molecular identification of carnosine synthase as ATP-grasp domain-containing protein 1 (ATPGD1). *J Biol Chem.* 2010 Mar;285(13):9346-56.

64. Everaert I, Taes Y, De Heer E, Baelde H, Zutinic A, Yard B, et al. Low plasma carnosinase activity promotes carnosinemia after carnosine ingestion in humans. *American Journal of Physiology-Renal Physiology.* 2012 Jun;302(12):F1537-F44.

65. Janssen B, Hohenadel D, Brinkkoetter P, Peters V, Rind N, Fischer C, et al. Carnosine as a protective factor in diabetic nephropathy: association with a leucine repeat of the carnosinase gene CNDP1. *Diabetes.* 2005 Aug;54(8):2320-7.

5 Carnosine and derivatives as inhibitors of protein covalent modifications induced by reactive carbonyl species

66. Orioli M, Vistoli G, Regazzoni L, Pedretti A, Lapolla A, Rossoni G, et al. Design, Synthesis, ADME Properties, and Pharmacological Activities of beta-Alanyl-D-histidine (D-Carnosine) Prodrugs with Improved Bioavailability. *Chemmedchem*. 2011 Jul;6(7):1269-82.

67. Aldini G, Carini M, Yeum KJ, Vistoli G. Novel molecular approaches for improving enzymatic and nonenzymatic detoxification of 4-hydroxynonenal: toward the discovery of a novel class of bioactive compounds. *Free Radic Biol Med*. 2014 Jan.

6 Intervention study of Carnosine in obese volunteers: bioavailability and reactive carbonyls species sequestering effect

Keywords: Carnosine, obesity, intervention study, bioavailability, RCS, sequestering effect

Abbreviations: 3-HPMA, 3 hydroxypropyl-mercaptopic acid; ACR, acrolein; AGEs, advanced glycation end-products; ALDH, aldehyde dehydrogenase enzymes; ALEs, advanced lipoxidation end-products; CAR, Carnosine; CAR-ACR-FDP, carnosine-formyl-dehydropiperidinyl acrolein derived adduct; CAR-ACR-SB, carnosine- schiff base acrolein derived adduct; CAR-DHN, carnosine dihydroxynonane; CAR-HNE-MA, carnosine 4-hydroxynonenal michael adduct; CAR-HNE-SB, carnosine 4-hydroxynonenal schiff base adduct; CEL, N^ε-(carboxyethyl)lysine; CML, N^ε-(carboxymethyl)lysine; ESI, Electrospray ionisation; GSTs, glutathione transferases; HNE, 4-hydroxynonenal; His-DHN, histidine dihydroxynonane; His-HNE, histidine 4-hydroxynonenal michael adduct; MA-DHN, mercapturic acid dihydroxynonane; MA-HNE, mercapturic acid 4-hydroxynonenal michael adduct; MA-HNE-SB, mercapturic acid 4-hydroxynonenal schiff base adduct; RCS, reactive carbonyl species; TSQ: Triple Stage Quadrupole;

6.1 Introduction

Reactive Carbonyl Species (RCS) are a class of highly electrophilic compounds that derives from the oxidation of lipids and sugars. RCS are toxic by-products, and due to their electrophilic nature, can covalently modify protein, nucleic acids and phospholipids, forming toxic adducts.

RCS, and the corresponding protein adducts, have been studied as biomarkers of oxidative damage but it is only in recent years that RCS have also been investigated as pathogenetic factors in several diseases such as diabetes, atherosclerosis, some neurological disorders and cancer and consequentely they are now considered as a potential drug target

In physiological conditions, RCS are efficiently detoxified by phase I and phase II metabolism. In particular aldehyde dehydrogenase enzymes (ALDH) are mainly involved in phase I, while GSH conjugating enymes have a pivotal role in phase II metabolism. More recently, the importance of histidine dipeptides as phase II detoxifying agents has also been recognized: CAR and derivatives such as anserine covalently react with RCS forming unreactive covalent adducts. The detoxifying efficacy of CAR and derivatives was firstly evaluated in vitro by incubating the target RCS with CAR and by monitoring the disappearance of RCS by HPLC-UV [1]. Then more complex experiments based on HPLC-UV and ESI-MS confirmed the CAR quenching activity towards ACR and HNE and the covalent unreactive adducts formed were then identified and characterized [2] [3]. Furthermore the quenching activity was also shown in oxidized rat muscle [4] , thereby confirming that the RCS scavenging activity of carnosine also occurs in biological media and that carnosine-HNE can be considered as a biomarker of lipid peroxidation. Finally, CAR and CAR derivatives were found to have a protective role against protein carbonylation induced by adding RCS to human and rat cell culture [5].

6 Intervention study of Carnosine in obese volunteers: bioavailability and reactive carbonyls species sequestering effect

Regarding *in vivo*/ *ex vivo* studies, CAR or CAR derivatives were tested in different animal models such as the Zucker rat, which is a well established model of metabolic syndrome where CAR-RCS adducts were identified, characterized and quantified by different MS approaches. It was found that CAR treatment was linked to an increase of CAR-HNE, CAR-DHN and 3-HPMA urinary excretion which was associated with a decrease of AGEs and ALEs [6].

The sequestering activity of CAR and derivatives designed to be stable to carnosinases was then confirmed in other animal models. [7, 8].

The first paper reporting the identification of carnosine-RCS metabolites in humans was published by Baba et al [9]. Urine samples from healthy, non-smoker adults were analyzed by LC/MS with the aim of identifying carnosine-aldehyde metabolites. The most abundant metabolites identified by this study were carnosine-propanol (m/z 285), carnosine-propanal (m/z 283), histidine-propanol (m/z 214) and histidine-propanal (m/z 212), resulting from acrolein adduction by carnosine, followed by reduction and hydrolysis. The majority of the metabolites (75%) were in their reduced form, suggesting that the reduction of carnosine/histidine conjugates is an important step of their metabolism. The origin of the histidine conjugates is not clear, since they can arise either from the hydrolysis of the adducted carnosine, from the direct reaction between histidine and acrolein or from the hydrolysis of adducted histidines in proteins. HNE adducts were found as well, but in lower amounts than ACR metabolites; for example, the urinary concentration of His-HNE (m/z 310) was 75-fold lower than His-propanal concentration. Moreover, only trace levels of carnosine-HNE (m/z 383) and its reduced form carnosine-DHN (m/z 385) were detected. It is important to note that these observations were made on samples obtained from healthy volunteers, while no data have been reported for pathological conditions, where a significant increase of HNE is expected [10]. Hence, on the basis of the above mentioned studies, there is compelling evidence that carnosine acts as a detoxifying agent of RCS, not only in rodents where it is bioavailable due to the lack of carnosinases but also in

6 Intervention study of Carnosine in obese volunteers: bioavailability and reactive carbonyls species sequestering effect

humans and that the reduction of RCS, leading to a decrease AGEs, ALEs and protein carbonylation, is associated with a beneficial effect.

Recent evidence links reactive carbonyl species and protein carbonylation to several human diseases including obesity and type 2 diabetes mellitus (T2DM). Proteomic studies indicate that obesity is accompanied by an increase in the carbonylation of a number of adipose-regulatory proteins that may serve as a mechanistic link between increased oxidative stress and the development of insulin resistance [11].

Considering these premises, and in particular that carnosine is an efficient dietary sequestering agent of RCS, that RCS are overproduced in obese subjects and that by reacting with proteins are linked to the obesity related diseases such as insulin resistance, a carnosine supplementation study in overweight/obese human subjects was set up. The end point of such an intervention study was to evaluate the bioavailability and metabolic fate of carnosine in obese subjects and to demonstrate the ability of CAR to detoxify RCS by a direct quenching mechanism by detecting and quantifying urinary CAR-RCS adducts. To our knowledge, this is the first intervention study of CAR in overweight/obese human subjects .

6.2. Materials and Methods

6.2.1. Chemicals and Reagents

HPLC-grade water was prepared with a Milli-Q water purification system of Millipore (Milan, Italy).

Acrolein, NFPA (nonafluoropentanoic acid), trichloroacetic acid, sulphosalicylic acid, formic acid, sodium phosphate dibasic and LC-grade and analytical-grade organic solvents were from Sigma-Aldrich (Milan, Italy). Carnosine (β -alanyl-L-histidine) and the internal standard (IS) H-Tyr-His-OH were a generous gift from Flamma S.p.A (Chignolo d'Isola, Bergamo, Italy). 4-hydroxy-2-nonenal (HNE) was prepared from synthesized 4-hydroxy-2-nonenal diethylacetal as previously described and quantitated by UV spectroscopy (λ_{\max} 224 nm; ϵ $13.75 \times 10^4 \text{ cm}^{-1} \text{ M}^{-1}$)[12]

6 Intervention study of Carnosine in obese volunteers: bioavailability and reactive carbonyls species sequestering effect

6.2.2. *Biological samples used as the matrix for calibration curves*

Calibration curves of carnosine were prepared in human plasma obtained from blood samples withdrawn from a 28 years old donor. Blood was collected by venipuncture with Terumo venosafe K₂EDTA tubes (CEA, Milan, Italy) and centrifuged for 10 min at 1000 g at 20 °C. Plasma aliquots were stored at -80 °C until their use. A 1.6 M aqueous solution (35 % w/v) of 5-sulfosalicylic acid was added to blood at a final concentration of 0.18 M (4% w/v) in order to precipitate proteins. Treated blood was kept for 5 minutes at 5 °C and then centrifuged at 14.000 g at 5 °C in a refrigerated centrifuge, Thermo Heraeus Megafuge (Thermo, Milan, Italy). The supernatant plasma was immediately separated from the precipitated red blood cells and stored at -80 °C until its use.

For the quantitative analysis of carnosine in urine, calibration curves were prepared by spiking carnosine in pooled human urines collected from 6 different volunteers, aged from 24 to 28 years old. Urines were kept at -80 °C until their use.

All the volunteers followed for one day a lacto-ovo-vegetarian diet before the collection.

6.2.3 *Supplementation study design*

This was a single-center randomized double blind placebo controlled intervention study of carnosine supplementation to overweight/obese individuals. The daily dose of carnosine was 2 g divided into two 1 g doses, administered orally in the morning and in the evening for 12 consecutive weeks. The study protocol was approved by the local Ethics committee of University Hospital Bratislava, and it conforms to the ethical guidelines of the Helsinki declaration from 2000. All individuals signed a written informed consent prior study entry. There was one

6 Intervention study of Carnosine in obese volunteers: bioavailability and reactive carbonyls species sequestering effect

drop-out from the study due to non-compliance. No side effects were reported in the course of the study.

The study population consisted of 31 overweight to obese non-vegetarian sedentary individuals, 8 females and 23 males, age 42,45 +/- 7,64 years; BMI 31,87 +/- 4,04 kg/m². Volunteers did not receive any regular medication nor food supplements and were asked to refrain from substantial changes in their lifestyle habits in the course of the study. Prior to blood sampling, participants were asked to abstain from strenuous exercise, alcohol and caffeine for 3 days. The samples of blood and urine were taken in the morning at 8.00 o'clock, after a 12-h overnight fast, before and after 12-week carnosine supplementation. The samples of urine were centrifuged for 10 min at 4°C, 400g. Plasma samples were taken into pre-cooled sample tubes containing EDTA and immediately spun down for 10 minutes, 1600g, at 4°C. All samples were stored at -80°C.

6.2.4. Carnosine-RCS adducts quantification in urine

6.2.4.1 Carnosine-RCS adducts preparation

10 mM carnosine (CAR) was incubated in 100 mM sodium phosphate dibasic buffer pH 7.4 at 37 °C with the target reactive carbonyl species (RCS) in a 10:1 molar ratio. After an overnight period a first aliquot of the reaction mixture was stored at -20 °C and a second aliquot was reduced with 100 mM NaBH₄ (final concentration), for 30 minutes at room temperature, in the dark. At the end of the incubation periods both the aliquots were diluted 1:50 with H₂O mq. and then analysed by LC-ESI-MS in order to assay the type of adducts and to perform a semi quantitative calculation of the adducts formed. The ion responses of the CAR-RCS-adducts were determined by measuring the peak areas in the selected ion chromatograms (SICs) reconstituted by using the corresponding [M_nH]ⁿ⁺ as filter

6 Intervention study of Carnosine in obese volunteers: bioavailability and reactive carbonyls species sequestering effect

ions. The peptide responses were normalized with respect to Tyr-His (TH) dipeptide, chosen as internal standard.

Afterwards both the aliquots were analysed by HPLC-UV to measure ACR and HNE consumption. These two RCS were determined by reverse-phase LC, using a Thermo-finnigan (Thermo, Milan, Italy) instrument, equipped with a quaternary pump system, an on-line degasser and a UV-Vis diode array programmable detector operating at 223 nm. Analyses were performed on a Agilent Zorbax SB-C18 (150 x 2.1 mm i.d., particle size 3.5 µm). The mobile phase (isocratic elution) was water/acetonitrile/orthophosphoric acid (6.6:3.4:0.001 v/v/v) delivered at a flow rate of 0.2 mL/min.

The concentration of the adducts were calculated on the basis of acrolein and HNE consumption (95 % and 93 % of consumption respectively) by using the semi quantitative values of each adducts calculated by ESI-MS spectra. In particular the reduced reaction mixture was evaluated in order to determine the adduct concentration, since the reduced adduct are chemically stabilised and the corresponding retro-reactions cannot occur. Stock solution of carnosine-RCS adducts were evaluated each time, before their use for the calibration curve, by means of LC-ESI-MS to ensure that the concentrations of the original solutions were within the limits of the maximum established error ($\leq 5\%$).

The semi-quantitative percent of each adducted derivative was calculated by the following equation: (normalized area of compound A / sum of the normalized areas of all the considered compounds)*100. All considered compounds are listed in table 1 and as an example the CAR-propanal adducts concentration was calculated as follows:

[CAR-propanal]= [(normalized area of CAR-propanal) / (\sum normalized areas of compounds listed in table 1)] * [RCS concentration used for the incubation * % of RCS consumption calculated by HPLC-UV]

[Car-propanal]= [(1.3 a.u. / 3.9 a.u.)] * [1 mM * 0.95] = 0.32 mM

6 Intervention study of Carnosine in obese volunteers: bioavailability and reactive carbonyls species sequestering effect

6.2.4.2 Carnosine-RCS calibration curves

Internal standard calibration curves were set up for carnosine-propanal (CAR-propanal) and carnosine-propanol (CAR-propanol) adducts.

Urine pool sample from six volunteers was used as blank urine to prepare positive control urine samples. This urine was checked by the applied analytical procedure to ensure it did not contain the selected adduct above the FDA prescribed limit, that is $\leq 20\%$ of the LLOQ area [13]. Calibration samples for adducts were prepared by spiking blank urine samples with each adduct working solution to provide the following final concentrations: 0.1, 0.8, 1.6, 4.8, 9.6 μM for carnosine propanal and 0.2, 1.6, 3.2, 9.6, 19.2 μM for carnosine-propanol. The internal Standard, TH, was added at a final concentration of 1 μM . Each sample was then treated as the ex vivo samples, as explained in the following paragraph. Calibration standards were analysed in duplicate in two independent runs. The calibration curves were constructed by least square linear regression analysis of the peak area ratios of each analyte to the IS against nominal analyte concentration.

6.2.4.3 Ex vivo urine samples preparation for CAR-RCS adducts detection and quantification

All the urine samples analysed in this study were treated as follows. 300 μL of urine were centrifuged at 14.000 g for 10 minutes by using a refrigerated centrifuge, Thermo Heraeus Megafuge (Thermo, Milan, Italy), in order to remove the particulate matter.

All the urinary supernatants was collected and then 10 μL of TH stock solution 30 μM was spiked into 290 μL of urine, in order to have a final TH concentration of 1 μM . Afterwards in order to remove the possible proteins present in the urine, it was filtered by Amicon centrifugal filter device with a molecular cut-off of 3 KDa (Millipore, Milan, Italy).

6 Intervention study of Carnosine in obese volunteers: bioavailability and reactive carbonyls species sequestering effect

The filtered urinary solution was then placed in a plate well, ready to be injected in the liquid chromatography system.

6.2.4.4 Liquid chromatography electrospray ionization mass spectrometry/mass spectrometry analysis (LC-ESI-MS/MS): LTQ Orbitrap XL mass spectrometer

All the filtered urine samples were separated by online liquid chromatography (nanoLC) and analyzed by electrospray tandem mass spectrometry (ESI-MS/MS); The chromatographic system was the UltiMate 3000 RSLCnano System (Dionex). An aliquot of 20 μ L of urines were loaded in a 20 μ L sample loop in full loop mode and then injected in a Phenomenex Polar analytical column, 4 μ m particle size, 2 mm i.d., 150 mm length, protected by a polar RP guard column 4 μ m particle size, 2 mm i.d., 4 mm length (Phenomenex, Italy). buffer A, H₂O mq containing 0.08 % nonafluoropentanoic acid (NFPA), and buffer B, pure acetonitrile, were used as mobile phases. For the initial 3 minutes the flow was diverted in the waste in order to perform on-line sample desalting. After 5 minutes of isocratic elution at 99 % buffer A, Gradient elution started from 99 % buffer A to 80% acetonitrile (B) in 24 min at a flow rate of 0.2 mL/min followed by a 5 min isocratic elution. The composition of the eluent was then restored to 100% A within 1 min, and the system was re-equilibrated for 5 min. The samples rack was maintained at 4 °C.

A LTQ Orbitrap XL mass spectrometer (Thermo Italia, Milan, Italy) with electrospray ionization (ESI) source was used for mass detection and analysis. Mass spectrometric analyses were performed in positive ion mode. ESI interface parameters were set as follows: middle position; capillary temperature 275 °C; spray voltage 4.5 k, tube lens voltage 100 V, capillary voltage 40 V. Nitrogen was used as nebulising gas at the following pressure: sheath gas 35 a.u.; auxiliary gas 10 a.u. MS conditions and tuning were performed by mixing through a T-connection the water-diluted stock solutions of analytes (flow rate 10 μ L/min), with the mobile phase maintained at a flow rate of 0.2 mL/min: the intensities of

6 Intervention study of Carnosine in obese volunteers: bioavailability and reactive carbonyls species sequestering effect

the $[M + H]^+$ ions were monitored and adjusted to the maximum by using the Quantum Tune Master software (Thermo, Milan, Italy). Two runs for each samples were performed, with the method here described.

6.2.4.4.1 Orbitrap data-dependent scan and targeted scan

During analysis, a LTQ-Orbitrap XL mass spectrometer continuously performed scan cycles in which first an high-resolution (resolving power 30.000, fwhm at m/z 400) full scan (150-1000 m/z) in profile mode was made by Orbitrap, after which MS2 spectra were recorded in centroid mode for the 3 most intense ions, using both CID and HCD modes (isolation width, 3 m/z ; normalized collision energy, 50 CID arbitrary units, 45 HCD arbitrary units). Protonated phthlates [dibutylphthlate (plasticizer), m/z 279.159086; bis(2- ethylhexyl)phthalate, m/z 391.284286] and polydimethylcyclosiloxane ions $[(Si(CH_3)_2O)_6 + H]^+$; m/z 445.120025] were used for real time internal mass calibration. Dynamic exclusion was enabled (repeat count, 2; repeat duration, 30 s; exclusion list size, 500; exclusion duration, 60 s; relative exclusion mass width, 10 ppm). Charge state screening and monoisotopic precursor selection was enabled, four times and unassigned charged ions were not fragmented.

Furthermore in the method was set a targeted ms/ms scan in which only the precursor ion listed in tab.1 were fragmented by CID collision (precursor ion m/z width: 10 ppm, isolation width 3 m/z ; normalized collision energy, 50 CID a. u.). The list of precursor ions as reported in table 1 was filled in by considering the known CAR-RCS adducts so far reported in the literature in in vitro and ex vivo studies.

6 Intervention study of Carnosine in obese volunteers: bioavailability and reactive carbonyls species sequestering effect

<i>m/z</i>	Analyte
156.07675	His
212.10296	His-propanal
214.11861	His-propanol
220.06380	3-HPMA
227.11387	CAR
265.12952	CAR-ACR-SB
267.14517	CAR-ACR-SB-red
283.14008	CAR-propanal
285.15573	CAR-propanol
302.14205	MA-HNE-SB
312.19178	His-HNE
314.20743	His-DHN
319.14008	Tyr-His (IS)
320.15262	HNE-MA
321.15573	CAR-ACR-FDP
322.16827	DHN-MA
323.17138	CAR-ACR-FDP-red
367.23398	CAR-HNE-SB-red
383.22890	CAR-HNE-MA
385.24455	CAR-DHN

Tab. 1. Precursor ions list corresponding to the main target compound of this study

6.2.5 Carnosine quantification in urine and plasma

The urine and plasma carnosine was measured by using an internal standard and a triple quadrupole (TSQ quantum ultra, Thermo, Milano, Italy) in MRM scan mode as mass analyzer.

6.2.5.1 Calibration curves in urine and plasma

Two different calibration curves were set up for carnosine quantification both in urine and plasma. Blank matrices for calibration curves set-up were obtained by pooling urine and plasma from six volunteers aged from 24 to 28 years old and following a lacto-ovo-vegetarian diet for one day before the collection. Before pooling, the biological fluids were analyzed to ensure they did not contain the selected adduct above the 20 % of limit of quantitation [2]. Calibration samples were prepared by spiking carnosine in blank matrices at the following final concentrations: 0.5, 1, 5, 25, 50, 100, 200 μM for urine and 0.1, 0.5, 1, 5, 10, 20, 50, 100 μM for plasma. The internal standard, TH, was added at a final concentration of 35 and 5 μM for urine and plasma, respectively. Samples were then treated as the ex vivo samples, using the analytical procedure reported in the following paragraph.

Three independent samples were prepared for each level of the calibration curve and each of them was analyzed in triplicate. The calibration curves were built by the least square linear regression analysis by plotting the ratios between the peak areas of the analyte and the IS against the analyte's nominal concentration.

6 Intervention study of Carnosine in obese volunteers: bioavailability and reactive carbonyls species sequestering effect

6.2.5.2 Ex vivo sample preparation for CAR quantification in urine and plasma

For LC-MS analysis the urine samples were treated as follows: aliquots of 150 μL were mixed with 150 μL of an aqueous solution of 4 % TCA (v/v) and the spiked with TH to reach a final concentration of 70 μM . The sample was then centrifuged at 14.000 g for 10 minutes by using a refrigerated centrifuge, Thermo Heraeus Megafuge (Thermo, Milan, Italy), in order to remove the particulate matter.

All the urinary supernatant was collected and then an aliquot was placed in a plate well, ready to be injected in the chromatography system.

Instead considering plasma samples an aliquot of 40 μL of deproteinized plasma was mixed with 360 μL of a solution consisted in 5 mM (0.08%) NFPA and 5.56 μM of TH in water. Afterwards it was centrifuged as done for the urine and placed in a plate well.

6.2.5.3 Liquid chromatography electrospray ionization multiple reaction monitoring analysis (LC-ESI-MRM): TSQ mass spectrometer

A Surveyor HPLC system (Thermo, Milan, Italy) equipped with a quaternary pump and a thermostated autosampler was employed for solvent and sample delivery. Separations were performed with a Phenomenex Polar analytical column, 4 μm particle size, 2 mm i.d., 150 mm length, protected by a polar RP guard column 4 μm particle size, 2 mm i.d., 4 mm length (Phenomenex, Italy). Buffer A, H_2O mq containing 0.08 % nonafluoropentanoic acid, and buffer B, pure acetonitrile, were used as mobile phases.

An aliquot of 10 μL of urine was loaded in a 20 μL sample loop, partial loop mode, and then injected in the analytical column. Instead for the plasma an aliquot of 50

6 Intervention study of Carnosine in obese volunteers: bioavailability and reactive carbonyls species sequestering effect

μL was loaded in a 100 μL sample loop, in partial loop loading mode. The gradient employed were the same for urine and plasma.

For the initial 3 minutes the flow was diverted in the waste in order to perform on-line sample desalting. The mobile phases were kept isocratic for five minutes at 99 % buffer A and 1 % buffer B. Then in one minute the buffer B increased to 30 % and it was kept constant for 3 minutes, afterwards in one minute the buffer B increased to 60 % and it was maintained for one minute. Then in one additional minute the mobile phases were restored at the initial conditions and the equilibration lasted 5 minutes.

A TSQ Quantum Ultra mass spectrometer (Thermo Italia, Milan, Italy) with electrospray ionization (ESI) source was used for mass detection and analysis. Mass spectrometric analyses were performed in positive ion mode. ESI interface parameters were set as follows: middle position; capillary temperature 275 °C; spray voltage 4.5 k, tube lens 100 V, skimmer lens 5 V, capillary 40 V. Nitrogen was used as nebulizing gas at the following pressure: sheath gas 35 a.u.; auxiliary gas 10 a.u. A MRM method was optimized in order to quantify Carnosine. The selected MRM transitions were for CAR: 227.1 \rightarrow 110.1 + 122.1, and for TH: 319.1 \rightarrow 110.1 + 156.1. The parameters influencing these transitions were optimized as follows: argon gas pressure in the collision Q2, 1.5 mbar; peak full width at half-maximum (FWHM), 0.50 m/z at Q1 and Q3; scan width for all MRM channels, 0.5 m/z ; scan rate (dwell time), 0.1 s/scan. Data processing was performed by the Xcalibur 2.0 software. Fragmentation was done using CID mode (isolation width, 0.5 m/z ; normalized collision energy, 28 CID arbitrary units).

MS conditions and tuning were performed by mixing through a T-connection the water-diluted stock solutions of analytes (flow rate 10 $\mu\text{L}/\text{min}$), with the mobile phase maintained at a flow rate of 0.2 mL/min: the intensities of the $[\text{M} + \text{H}]^+$ ions were monitored and adjusted to the maximum by using the Quantum Tune Master software

6.2.6 Intact protein analysis of plasma to profile human plasma albumin

Whole human plasma was analysed by ESI-MS intact protein analysis in order to profile human plasma albumin (HSA), in particular to determine the relative percentage content of mercapto-albumin (HSA-SH), cysteinylated albumin (HSA-S-S-Cys) and glycosylated albumin (HSA-N-Glc).

Human plasma was centrifuged at 14.000 g for 10 min at 4 °C for removal of particulate matter. Then the plasma was diluted 1:200 with denaturing buffer 70 % H₂O , 30 % CH₃CN and 0.2 % HCOOH.

An automated loop injection was used to carry the sample to the ESI source. The autosampler and the pump used were modules of a Surveyor HPLC (Thermo, Milano, Italy). The mobile phase employed was the denaturing buffer. An aliquot of 10 µL of plasma were loaded in a 20 µL sample loop, partial loop mode. A flow of 10 µL/min carried the sample towards the ESI source, coupled to a TSQ Quantum mass spectrometer, that operated in positive ion mode.

Analyses were carried out under the following instrumental conditions: full scan mode, mass range m/z 1400-1500, positive-ion mode, 3 microscan, peak full width at half-maximum (FWHM), 0.50 m/z at Q1 and Q3, capillary temperature 275°C , spray voltage applied to the needle 4.0 kV; capillary voltage 40 V ; tube lens voltage 200 V ; nebulizer gas (nitrogen) flow rate set 10 a.u. ; acquisition time 10 min. The percentage of each albumin isoform was calculated by semiquantitative mode: [(intensity of isoform A peak) / (sum of all the intensities considered)]*100

6.2.7 Fluorescence and UV-vis assays for urine samples quantification of total protein, Advanced Glycation End products (AGE) and creatinine.

Fluorescence and UV-vis assays were used to determine the content of Advanced Glycation End products (AGE), creatinine and protein in urine.

Concerning creatinine determination a colorimetric assay (Cayman, USA), based on Jaffe reaction, was employed to determine creatinine concentration in urine. The urine samples are diluted 1:10 with H₂O and then treated with an alkaline picrate solution. When the creatinine reacts with the picrate a yellow/orange coloration is formed. The color intensity is proportional to creatinine concentration and it is measured at 500 nm. The sample creatinine concentration is determined using a creatinine standard curve. The color derived by creatinine is then destroyed at acidic pH and the intensity is measured again as a factor of correction. The protocol followed is provided by the manufacturers and is based on a paper of Heinegard et al.[14]

Total protein concentration in urine was calculated by means of Bradford assay, following the procedure reported in Bradford and Zor papers. [15, 16]

Moreover in order to measure urinary AGE 50 μ L of urine of each sample were diluted with 950 μ L of physiological solution (0.9 % NaCl). Then the diluted sample was read with a fluorimeter, Perkin Elmer LS50B (Perkin Elmer, Lissone, Italy). The excitation λ was set at 370 nm with a slit of 5 nm, instead the emission λ was set at 440 nm with a slit of 5 nm.

6 Intervention study of Carnosine in obese volunteers: bioavailability and reactive carbonyls species sequestering effect

6.2.8 Fluorescence and UV-vis assays for plasma samples quantification of total protein, Advanced Glycation End products (AGE), Advanced Oxidation Protein Products (AOPP), Protein Carbonyls (PCO) and Carboxy Methyl Lysine (CML).

Total protein concentration in plasma was calculated by means of Bradford assay, following the procedure reported in [3, 4].

Furthermore AGE in plasma were measured as done for the urine, paragraph 6.2.7. The only difference was that an aliquot of 20 μL of each plasma sample was diluted with 980 μL of physiological solution (0.9 % NaCl).

AOPP were quantified following the protocol reported in Witko-Sarsat et al article [17]. Briefly an aliquot of plasma was fivefold diluted with PBS solution, then 200 μL of the diluted plasma was placed in a well and there were added 20 μL of concentrated acetic acid, then 10 μL of a 1.16 M potassium iodide solution, and finally 20 μL of concentrated acetic acid. The treated solution was read at a λ of 340 nm by a Wallac Victor² multilabel counter, Perkin Elmer (Perkin Elmer, Lissone, Italy).

Protein carbonyls were measured by a PCO assay based on 2,4-Dinitrophenylhydrazine (DNPH) reaction. The protocol followed is described in Levine et al article [18]

CML levels in plasma were quantified by OxiSelect™ N ϵ -(carboxymethyl) lysine (CML) Competitive ELISA Kit (Cellbiolabs, Milan, Italy) and the procedure followed is described in the paper of Reddy et al [19].

6.2.9 informatics

Graphpad prism 5.0 (Graphpad Software Inc, USA) was employed for ANOVA, t test analysis, outliers analysis and to display the graphs reported. Origin 6.0 (Originlab Corp, USA) was used for the Principal Component Analysis (PCA) of the data. The dataset considered is reported in tab 2.

Direct infusion ESI-MS spectra were deconvoluted using the software MagTran 1.02 [20].

6 Intervention study of Carnosine in obese volunteers: bioavailability and reactive carbonyls species sequestering effect

Short name	Pal	Pol	CAR	uAGE	Cre	Treatment
Long name	CAR-Propanal [μM]	CAR-Propanol [μM]	Carnosine [μM]	Urinary AGE [UF/mg]	Urinary Creatinine [μM]	1= treated 0= placebo
Sample #						
1.1	0.60	0.98	0.09	95016.23	3359.33	1
2.1	0.89	0.87	13.70	36248.38	10962.01	0
3.1	0.79	0.59	1.38	179178.50	8928.74	0
4.1	0.35	0.63	4.95	11607.98	10608.40	1
5.1	0.85	0.99	8.84	50900.38	12376.47	1
6.1	0.53	0.78	15.32	69441.75	14940.16	1
7.1	0.60	0.98	3.65	31596.34	22100.83	1
8.1	2.11	3.01	12.08	36506.03	17327.05	0
9.1	1.69	1.69	21.15	49801.15	18387.89	1
10.1	1.33	1.67	9.81	38852.83	20774.78	0
11.1	5.58	5.93	8.84	56676.64	18034.28	1
12.1	2.76	1.41	17.58	33252.95	18829.91	1
13.1	2.35	2.69	19.20	40689.36	11669.24	1
14.1	1.56	1.70	5.27	33021.29	28200.66	1
15.1	0.38	0.60	0.50	41767.84	2210.08	0
16.1	1.03	1.52	14.34	23034.14	20951.59	1
17.1	0.66	0.92	10.46	94474.03	10431.59	0
18.1	1.06	0.96	4.62	31868.90	19713.94	0
19.1	0.88	1.08	5.92	20511.83	14586.55	0
20.1	1.77	2.26	6.57	56482.91	25636.97	0
21.1	1.33	1.51	20.82	82519.63	27493.44	0
22.1	1.04	1.18	2.68	23565.11	9459.16	0
23.1	1.16	1.14	3.33	75835.34	14763.36	1
24.1	0.79	0.99	9.48	71383.66	12376.47	1
25.1	0.67	1.02	7.22	16241.13	12906.89	0
26.1	2.41	2.81	15.96	23539.91	35361.34	1
27.1	0.35	0.66	1.06	30647.07	4066.55	0
28.1	1.47	1.66	7.86	14332.35	12376.47	1
29.1	0.45	0.75	1.38	15338.17	9547.56	1
30.1	0.82	1.00	11.10	32018.84	23868.90	0
31.1	2.92	2.39	15.32	31039.78	23161.67	0
1.3	0.89	0.84	1.38	39736.23	6011.43	1
2.3	1.16	1.02	14.34	29490.38	17857.47	0
3.3	0.52	0.67	3.65	94568.77	13348.90	0

6 Intervention study of Carnosine in obese volunteers: bioavailability and reactive carbonyls species sequestering effect

Short name	Pal	Pol	CAR	uAGE	Cre	Treatment
Long name	CAR-Propanal [μM]	CAR-Propanol [μM]	Carnosine [μM]	Urinary AGE [UF/mg]	Urinary Creatinine [μM]	1= treated 0= placebo
Sample #						
4.3	1.14	0.77	11.10	77766.83	6011.43	1
5.3	0.64	0.78	7.54	19589.95	6983.86	1
6.3	0.66	0.66	45.77	40372.10	8044.70	1
7.3	0.89	0.84	13.05	30548.59	20597.98	1
8.3	2.55	2.80	12.40	61299.19	23868.90	0
9.3	1.86	1.04	306.58	43738.10	25106.55	1
10.3	n.d	n.d	n.d	n.d	n.d	0
11.3	0.61	0.83	0.74	13770.30	3536.13	1
12.3	2.43	1.68	25.68	28168.29	19448.73	1
13.3	5.49	4.05	350.00	34044.32	12906.89	1
14.3	3.39	1.75	33.13	31601.24	31117.98	1
15.3	0.65	0.77	3.98	24895.03	6630.25	0
16.3	1.80	1.40	31.51	35076.54	20951.59	1
17.3	0.83	0.89	7.54	147585.00	10077.98	0
18.3	1.16	1.04	5.60	25859.63	16619.83	0
19.3	1.06	1.23	4.62	18000.23	11669.24	0
20.3	1.20	1.06	1.38	93316.45	24752.93	0
21.3	1.00	1.00	6.89	87777.01	15382.18	0
22.3	0.67	0.84	1.38	22199.30	5481.01	0
23.3	1.65	1.44	8.19	74043.56	16177.81	1
24.3	3.74	2.47	52.90	64373.43	21482.01	1
25.3	0.56	1.13	6.89	78083.61	23868.90	0
26.3	4.81	3.47	19.53	22171.63	32355.62	1
27.3	3.01	1.25	9.16	31386.72	12553.27	0
28.3	1.61	1.25	146.86	52720.72	7160.67	1
29.3	1.88	1.56	12.72	24416.88	20421.17	1
30.3	0.57	0.80	5.27	24255.29	9635.96	0
31.3	1.53	1.36	9.48	41847.23	18211.09	0

Tab. 2. Urinary variables submitted to PCA analysis. In sample number column n.1 means before supplementation, n.3 means after supplementation

6.3 Results

6.3.1 Carnosine-RCS-adducts preparation and quantification

Table 3 shows the concentrations of the reduced forms of ACR and HNE carnosine adducts prepared in in vitro conditions. Reduction of the carbonyl adducts was carried out using in order to make the adducts more stable. Calibration curves built using the reduced forms were also used to estimate the amount of the non reduced derivatives.

When CAR was incubated in the presence of ACR, the following adducts were identified and are here ordered from the most to the least abundant: carnosine-formyl-dehydropiperidiny adduct (CAR-FDP), carnosine-alimine-adduct (CAR-SB-ACR), carnosine-propanol (CAR-propanol) and carnosine-methyl-pyridine adduct (CAR-MP).

Only two adducts were formed when carnosine was incubated with HNE, namely carnosine dihydroxynonane (CAR-DHN) and CAR-alimine-HNE (CAR-SB-HNE). Table 4 depicts the chemical structures of the above mentioned carnosine adducts.

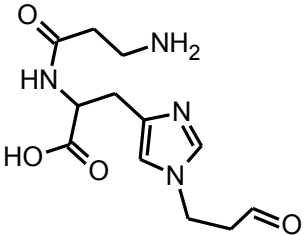
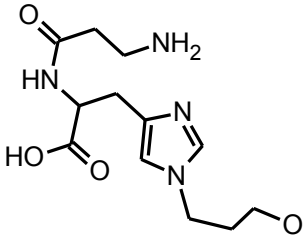
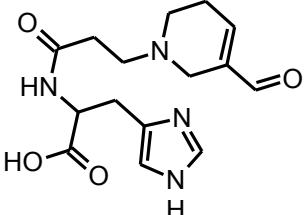
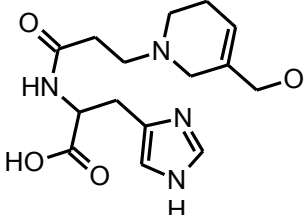
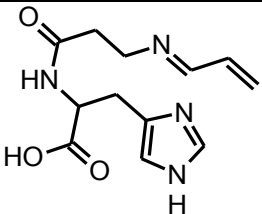
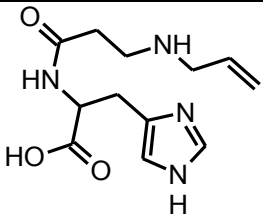
Carnosine adducts were then analyzed by LC-ESI-MS. Figure 1 shows the Single Ion Chromatograms (SIC) traces of the CAR-RCS adducts extracted by using the $[M+nH]^{n+}$ as filter ions (table 1) and using a mass tolerance of 5 ppm..

6 Intervention study of Carnosine in obese volunteers: bioavailability and reactive carbonyls species sequestering effect

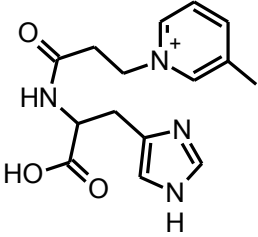
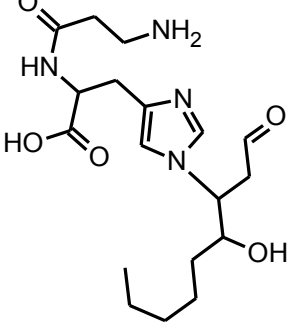
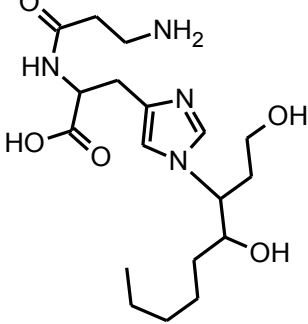
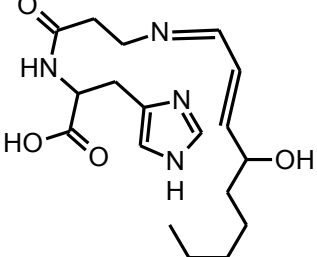
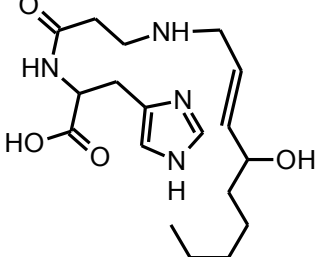
A) CAR 10:1 ACR				
Adduct	CAR-propanol	Car SB ACR-red	CAR FDP-red	CAR-MP
Concentration	230 uM	295 uM	415 uM	10 μM
B) CAR 10:1 HNE				
Adduct	CAR-DHN		CAR-SB-HNE-Red	
Concentration	497 uM		453 uM	

Tab. 3. The concentration of the various CAR-RCS adducts are reported. In A) section there are the CAR-ACR incubation derived adducts, instead in section B) there are the CAR-HNE incubation derived adducts.

6 Intervention study of Carnosine in obese volunteers: bioavailability and reactive carbonyls species sequestering effect

Not reduced	Reduced
<p>CAR-propanal (282 Da)</p> 	<p>CAR-propanol (284 Da)</p> 
<p>CAR-FDP (320 Da)</p> 	<p>CAR-FDP-red (322 Da)</p> 
<p>CAR-SB-ACR (264 Da)</p> 	<p>CAR-SB-ACR-red (266 Da)</p> 

6 Intervention study of Carnosine in obese volunteers: bioavailability and reactive carbonyls species sequestering effect

CAR-MP (303 Da)	
	
CAR-MA-HNE (382 Da)	CAR-DHN (384 Da)
	
CAR-SB-HNE (364 Da)	CAR-SB-HNE-red (366 Da)
	

Tab. 4. Structural formulas of the CAR-RCS adducts identified and quantified after incubation of CAR with ACR and HNE. For each compound the corresponding reduced form is displayed, except for CAR-MP that can't be reduced by NaBH_4

6 Intervention study of Carnosine in obese volunteers: bioavailability and reactive carbonyls species sequestering effect

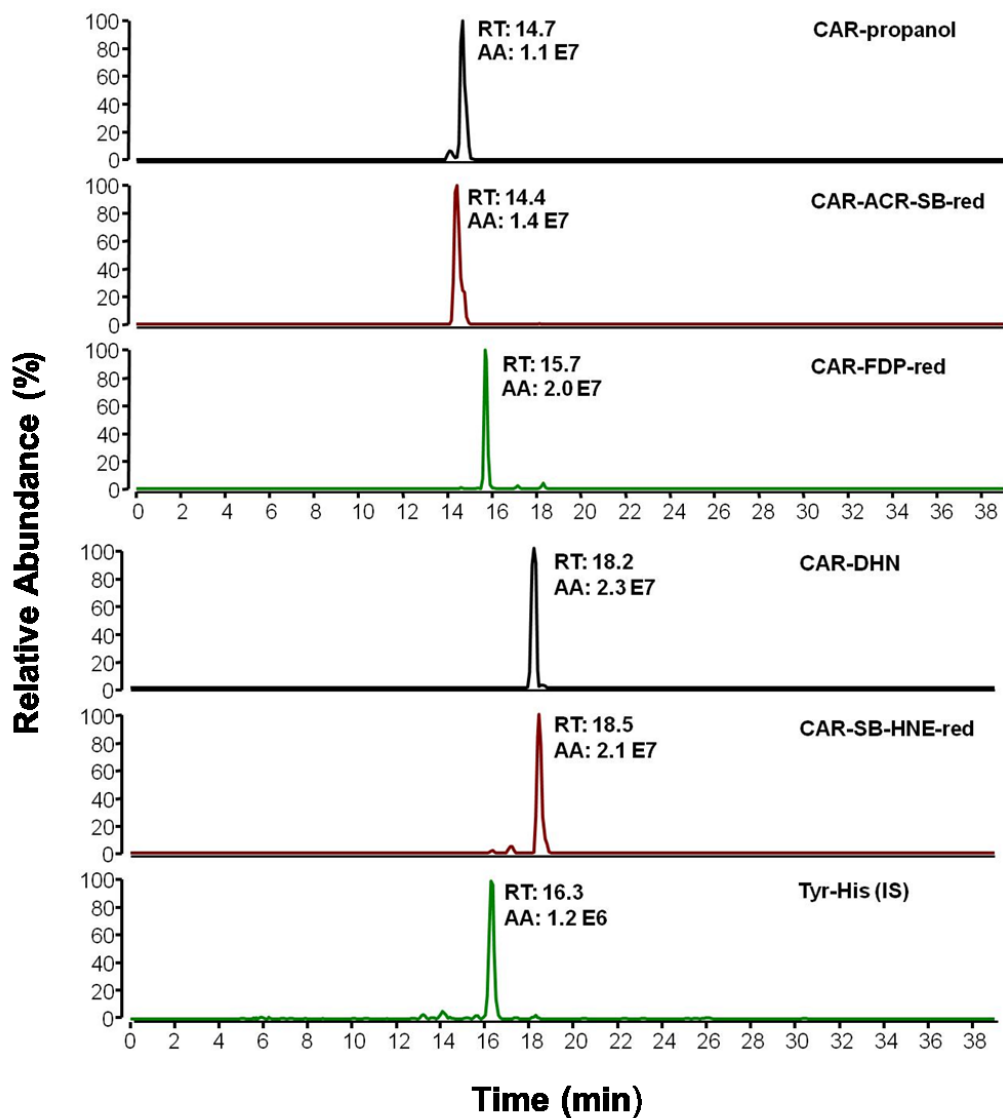


Fig.1. SIC traces of the adducts formed by incubating CAR with ACR (panel A) and HNE (panel B) followed by NaBH₄ reduction. . The bottom panel reports the SIC trace relative to the internal standard, Tyr-His.

6.3.2 Preliminary LC-Orbitrap-MS/MS analysis for adduct identification

Carnosine-RCS adducts were searched for in the urine samples by using LC-orbitrap as described in the methods section and using Tyr-His as internal standard. Among the searched for adducts, only CAR-propanal and CAR-propanol adducts were found. The presence of the two adducts was confirmed in all 31 patients both before and after carnosine supplementation. The SIC traces of both the adducts identified in urine samples are shown in Figures 2 and 4. Figure 2 relates to the SIC trace of carnosine propanal (ion current at m/z 283.14008 and a mass tolerance of 5 ppm) as identified in the urine of patient number four.

Identification of the CAR-propanal adduct was firstly based on the accurate mass and retention time; accurate mass showed a mass difference of only 0.14 ppm in respect to the simulated mass; the retention time at 14 ± 0.3 min was found superimposable in respect to that observed for the CAR-propanal standard. Final assignment of the structure was achieved by MS/MS experiments: the ion at m/z 283.1400 was fragmented and the acquired tandem mass spectrum is reported in figure 3 (upper panel). The lower panel shows the MS/MS spectrum of the CAR-propanal standard. The two MS spectra are almost superimposable, showing ten common fragment ions whose structural attribution is listed in tab.5.

Fig 4 shows the SIC trace of the ion at m/z 285.15573 relative to the urine of patient number four. The SIC shows a peak characterized by a retention time of 14.5 ± 0.3 min which can be attributed to the carnosine propanol adduct. The experimental m/z was 285.15588, characterized by a mass error of 0.53 ppm in respect to the theoretical mass. The tandem mass spectrum of the ion at m/z 285.15588 identified in the urine sample is shown in fig 5 (upper panel) and is characterized by a fragmentation pattern very similar to that recorded for the CAR-propanol standard (lower panel); nine diagnostic fragment ions were found in common in the two spectra and their structural attribution is summarized in tab.6.

6 Intervention study of Carnosine in obese volunteers: bioavailability and reactive carbonyls species sequestering effect

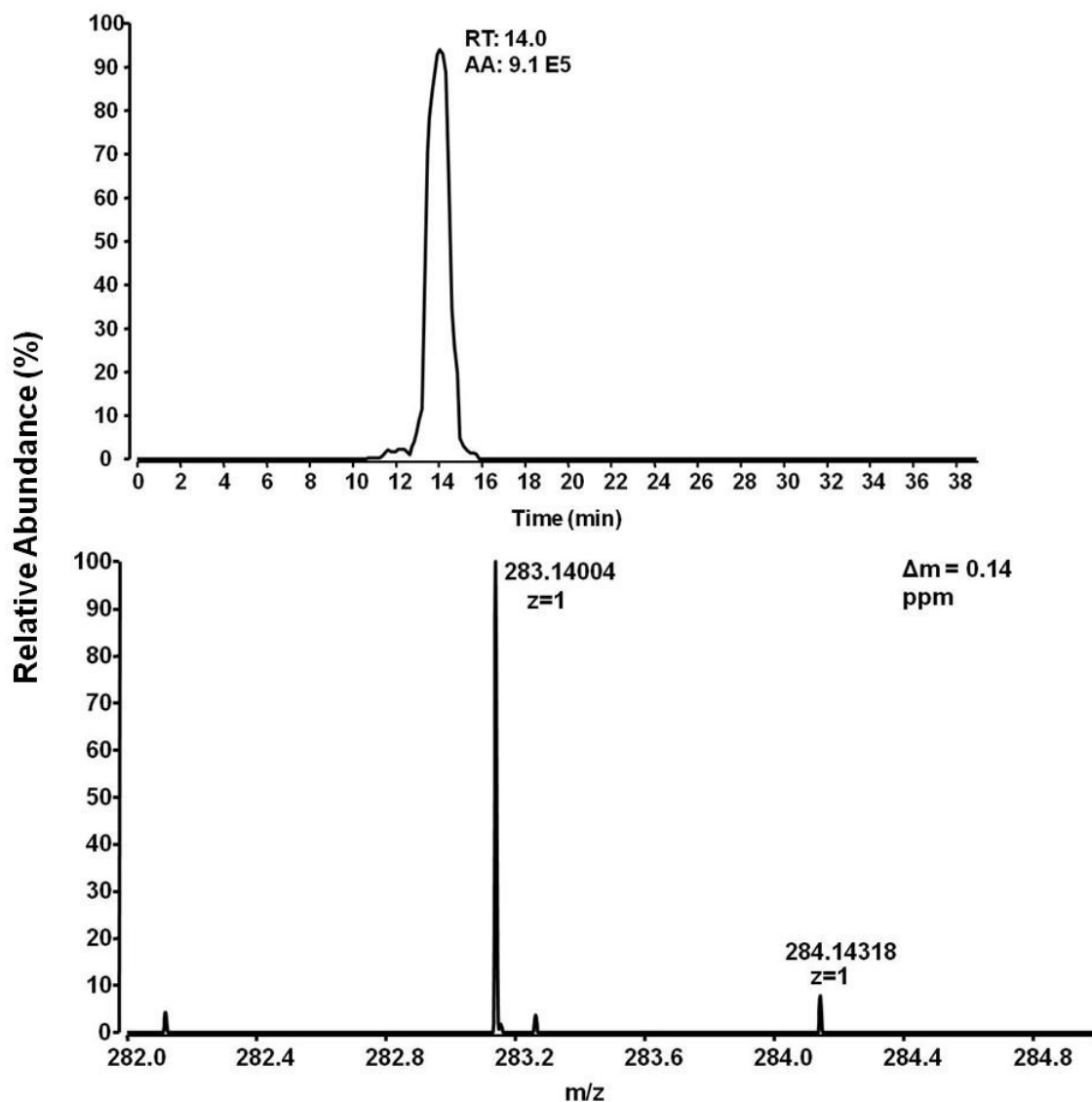


Fig. 2. Upper panel: SIC chromatogram reconstituted by setting the ion at m/z 283.14008 as filter ion and a 5 ppm tolerance. Lower panel: full mass spectrum relative to the peak at a retention time of 14.0 min and identified as CAR-propanal ion

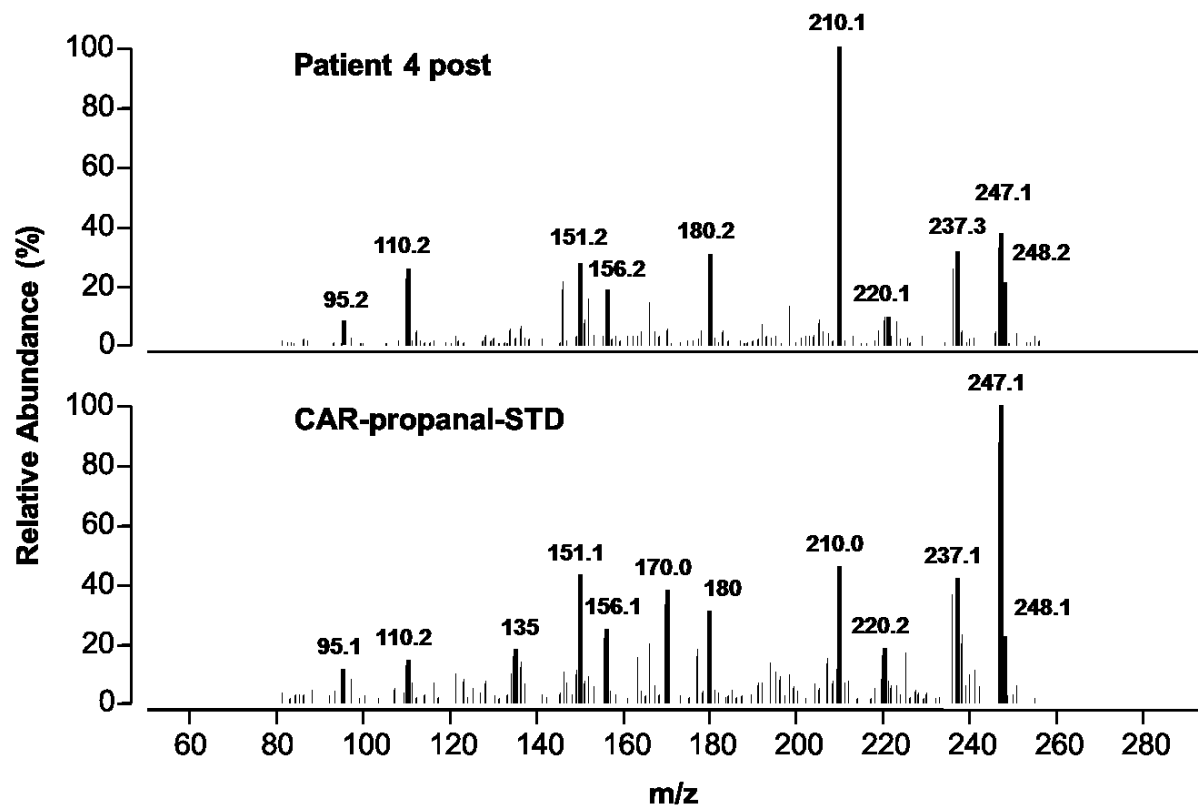
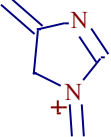
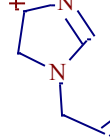
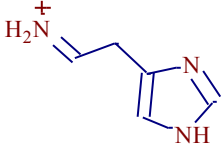
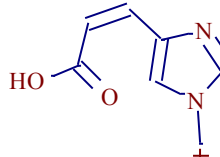
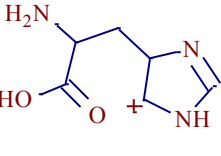
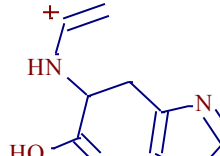

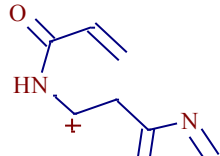
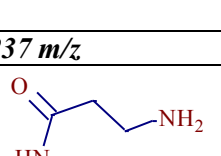
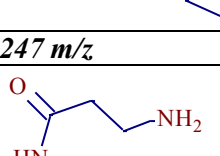


Fig. 3. Tandem mass spectrum of the ion at m/z 283.14004 identified in the urine sample. The lower panel shows the MS/MS spectrum of the carnosine-propanal standard. The attribution of the diagnostic fragments is reported in tab.5

6 Intervention study of Carnosine in obese volunteers: bioavailability and reactive carbonyls species sequestering effect

95 m/z	109 m/z
	
110 m/z	151 m/z
	
156 m/z	180 m/z
	
210 m/z	220 m/z
	
237 m/z	247 m/z
	

Tab. 5. Structure attribution of the fragment ions present in MS2 spectrum of car-propanal

6 Intervention study of Carnosine in obese volunteers: bioavailability and reactive carbonyls species sequestering effect

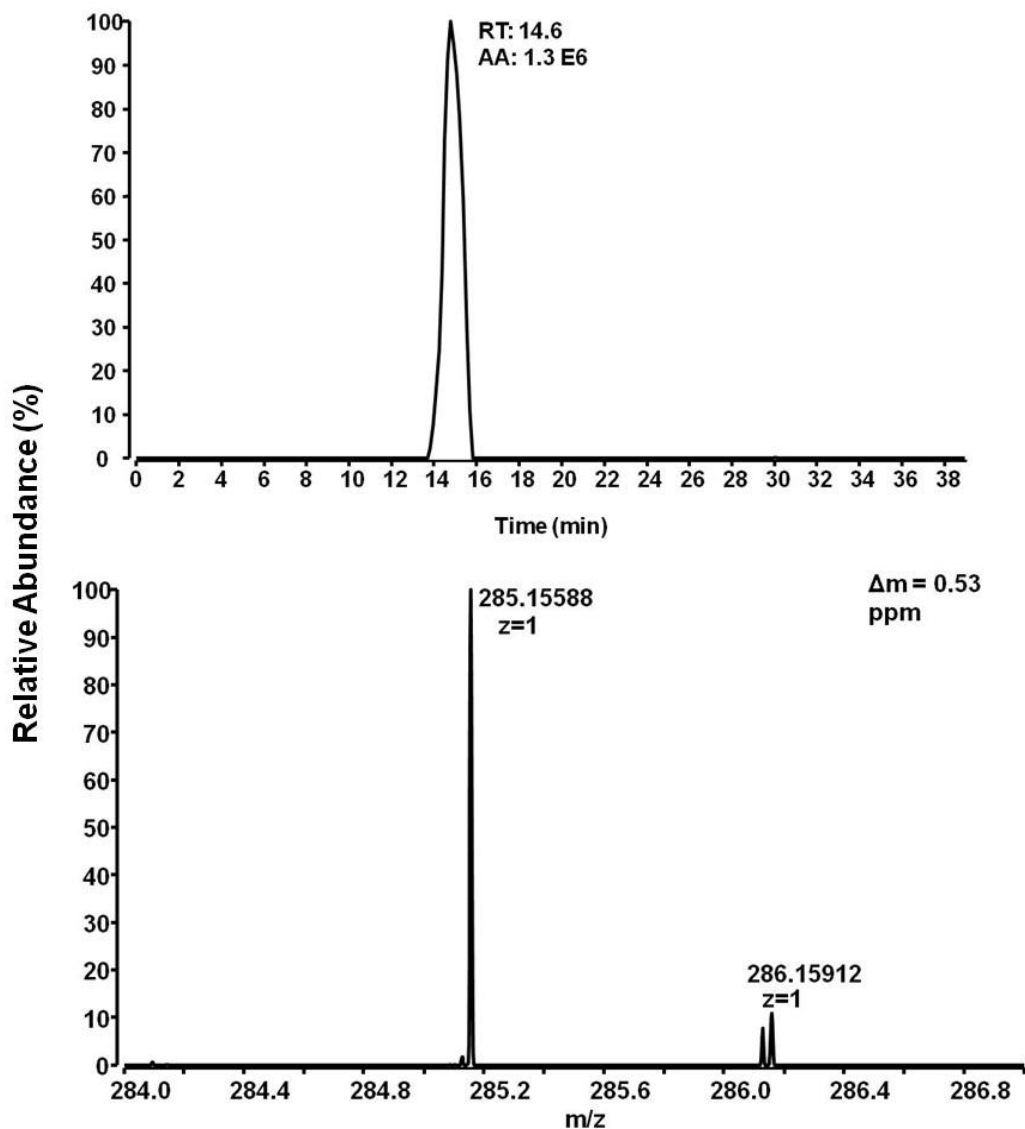


Fig. 4. In upper panel there is the SIC chromatogram of CAR-propanol ion based on m/z : 283.14008, extracted with 5 ppm of mass filter. Instead in the lower panel there is the corresponding full mass spectrum in which the top peak was identified as CAR-propanol ion

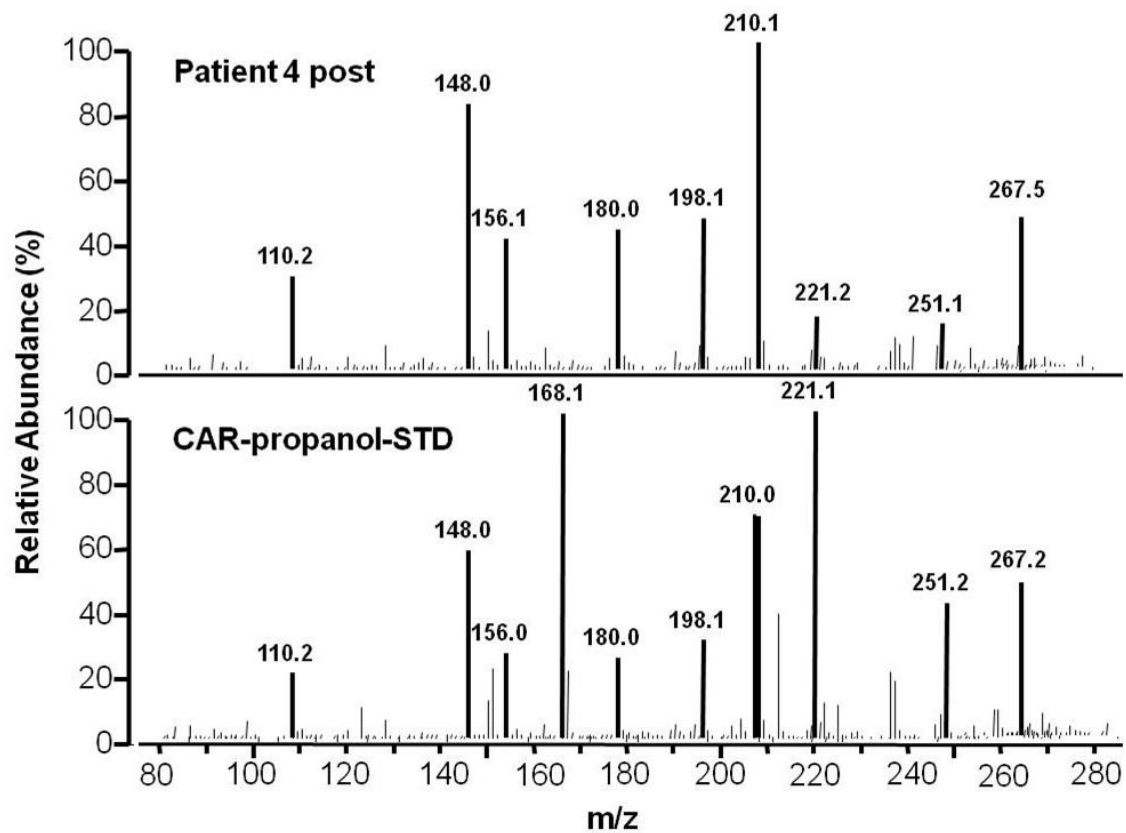
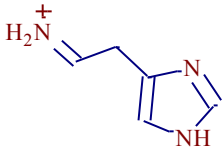
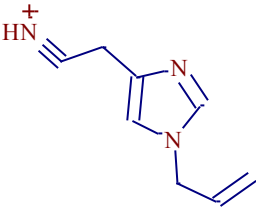
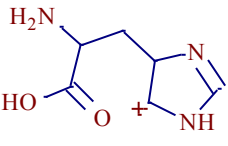
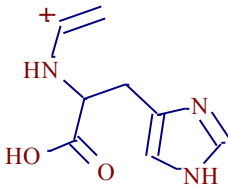
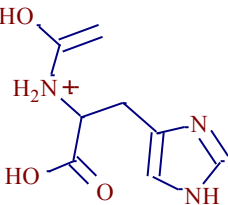
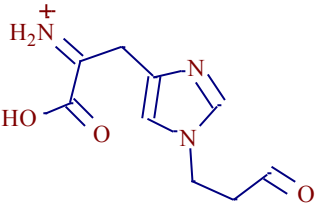
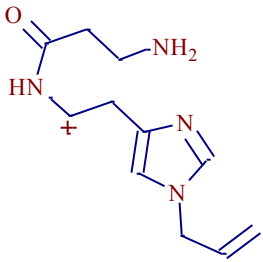
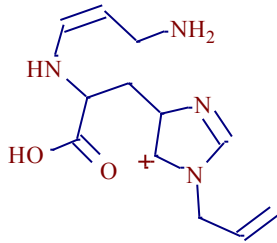
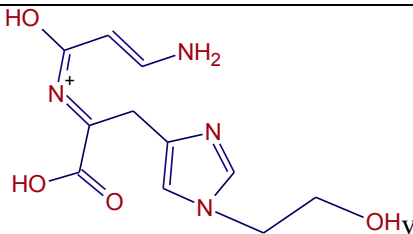


Fig. 5. Tandem mass spectrum of ion 285.15573. The corresponding fragments are reported in tab.6

6 Intervention study of Carnosine in obese volunteers: bioavailability and reactive carbonyl species sequestering effect

110 m/z	148 m/z
	
156 m/z	180 m/z
	
198 m/z	210 m/z
	
221 m/z	251 m/z
	
267 m/z	
	

Tab. 6. The fragment ions present in MS2 spectrum of car-propanol precursor ion are reported

6 Intervention study of Carnosine in obese volunteers: bioavailability and reactive carbonyls species sequestering effect

6.3.3 Carnosine propanal and Carnosine propanol calibration curves in urine.

Quantification of the carnosine adducts was carried out by using an internal standard calibration method. Urines of young volunteers were chosen as matrices to set-up the method and both the analytes were detected in such samples.

Samples were then spiked with the standards and the LLOQs were 0.10 μM for CAR-propanal and 0.20 μM for CAR-propanol; the LOD of both the analytes were of 0.03 μM .

The endogenous content of both the analytes was not quantified in the urine of young volunteers, since the area under the peak was 16 % and 18 % of the LLOQ peak for CAR-propanal and for CAR-propanol respectively. Fig.6 and 7 show the extracted single ion chromatograms (SICs) of CAR-propanal at m/z 283.14008 and CAR-propanol at m/z 285.15573. Each figure shows the SIC relative to the standard LLOQ (upper panel) and to the urine sample (lower panel). Tyr-His peptide was not detected (Fig 8).

The method was found specific, precise and accurate according to the FDA guidelines [2] : CV % range from 5 to 15 % and the bias didn't exceed $\pm 15\%$. FDA guidelines recommend both for precision and accuracy (CV % and bias respectively) a value below $\pm 15\%$, except for the LLOQ that is admitted also a value of $\pm 20\%$.

The equations relative to the calibration curve for carnosine-propanal and carnosine-propanol are as follows: $y = (0.3951 \pm 0.0070)x - (0.0029 \pm 0.0352)$ (fig.9 upper panel) and $y = (1.185 \pm 0.0176)x - (0.3879 \pm 0.1717)$ lower panel; for both the curves the r^2 is 0.99. Stability of the adducts and IS was assessed at 5 °C after 24 hours; since the areas of the analytes and of the

6 Intervention study of Carnosine in obese volunteers: bioavailability and reactive carbonyls species sequestering effect

IS decreased of a similar extent (12% and 14%, respectively) the content of the analytes determined with the internal std method was found constant.

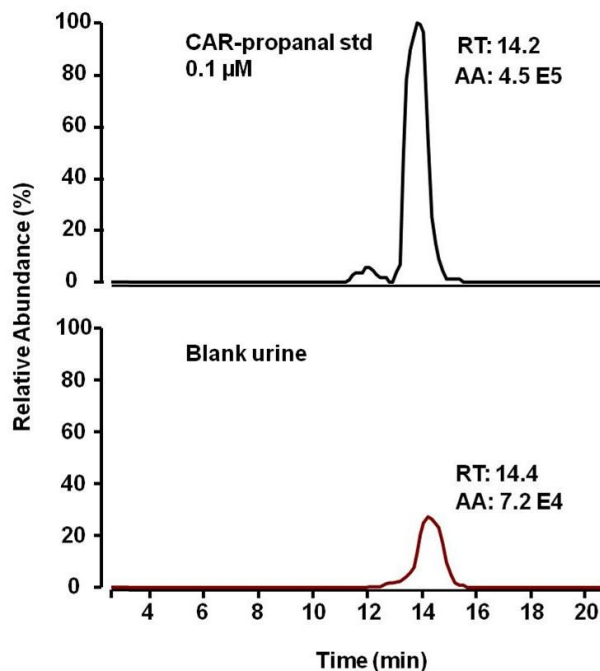


Fig. 6. In the upper panel there is the SIC trace of CAR-propanal of the LLOQ standard concentration spiked in blank urine. Instead in the lower panel it is reported the SIC trace of CAR-propanal extracted in blank urine sample. Its area is the 16 % of the LLOQ concentration area.

6 Intervention study of Carnosine in obese volunteers: bioavailability and reactive carbonyls species sequestering effect

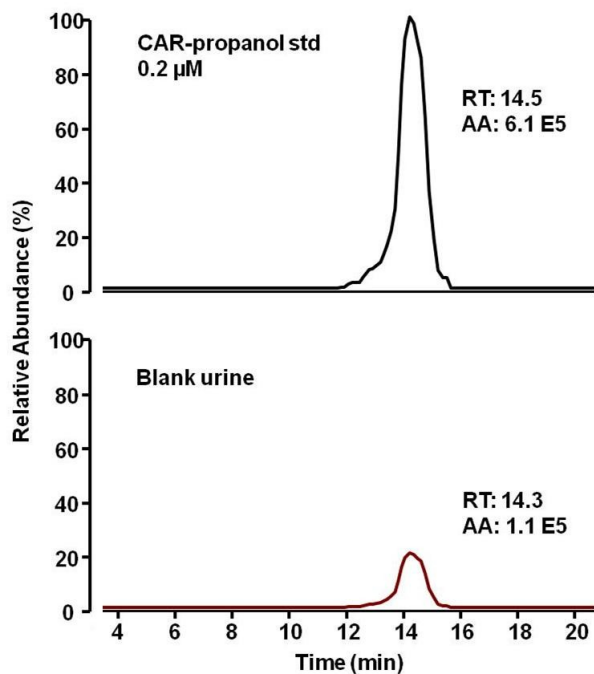


Fig. 7. In the upper panel there is the SIC trace of CAR-propanol of the LLOQ standard concentration spiked in blank urine. Instead in the lower panel it is reported the SIC trace of CAR-propanol extracted in blank urine sample. It is the 18 % of the LLOQ concentration area.

6 Intervention study of Carnosine in obese volunteers: bioavailability and reactive carbonyls species sequestering effect

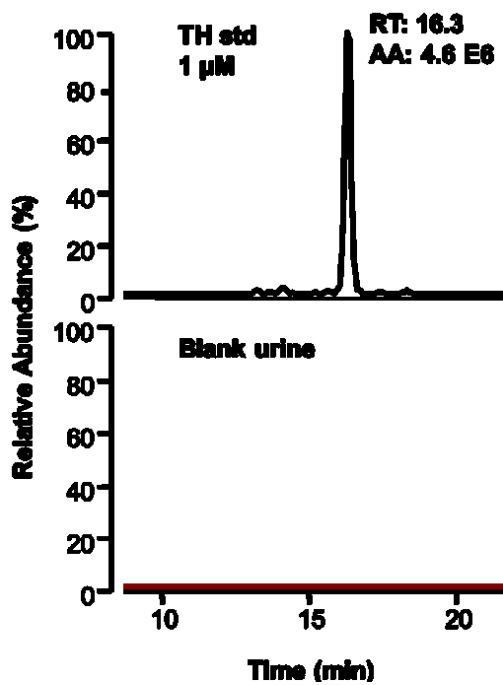


Fig. 8. In the upper panel it is reported the SIC trace of the internal standard (TH) spiked in blank urine, and TH it is not present in the blank urine used.

6 Intervention study of Carnosine in obese volunteers: bioavailability and reactive carbonyls species sequestering effect

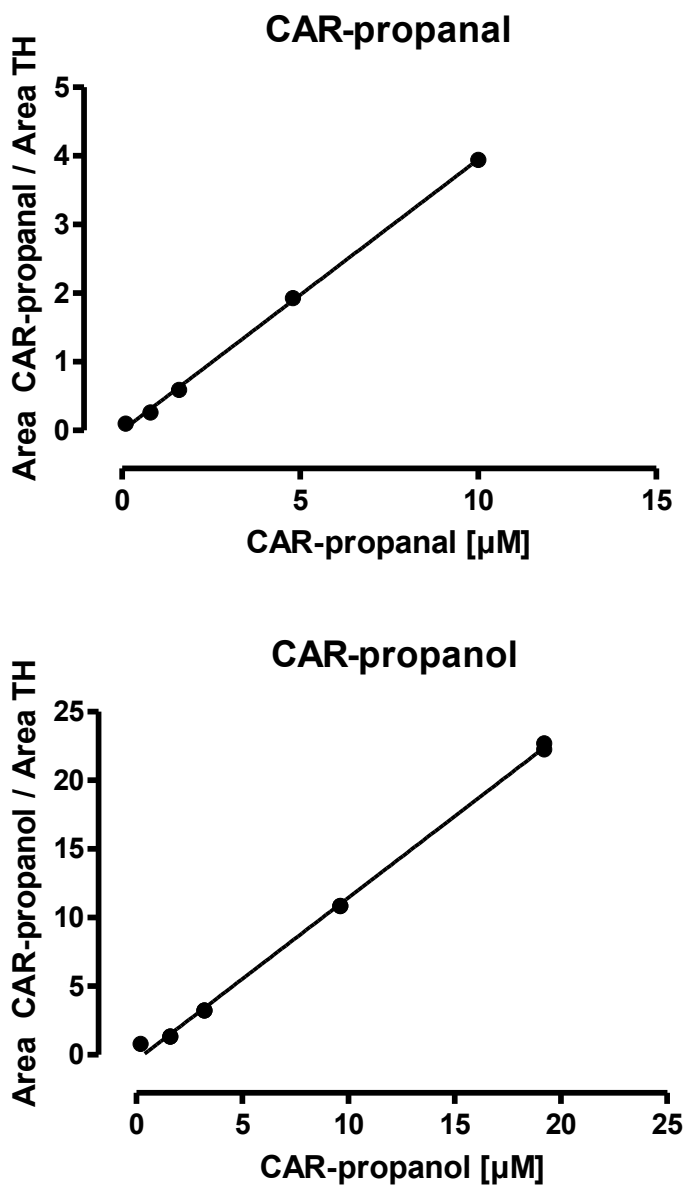


Fig. 9. in the upper panel it is reported the calibration curve of CAR-propanal, $y = (0.3951 \pm 0.0070)x - (0.0029 \pm 0.0352)$, $r^2 = 0.99$; Instead in the lower panel it is reported that of CAR-propanol, $y = (1.185 \pm 0.0176)x - (0.3879 \pm 0.1717)$ $r^2 = 0.99$

6 Intervention study of Carnosine in obese volunteers: bioavailability and reactive carbonyls species sequestering effect

6.3.4 Carnosine propanal and Carnosine propanol determination in urine samples of overweight/obese individuals

Table 7 reports the concentration of urinary CAR-propanal and CAR-propanol for each patient. The mean of CAR-propanal before CAR intake and in placebo was $1.2 \mu\text{M} \pm 0.7 \mu\text{M}$, ranging from $0.3 \mu\text{M}$ to $2.9 \mu\text{M}$, and increased to $1.7 \pm 1.3 \mu\text{M}$ in the supplemented group (ranging from $0.5 \mu\text{M}$ to $5.5 \mu\text{M}$).

The mean of CAR-propanol before CAR intake and in placebo subjects was $1.4 \pm 0.7 \mu\text{M}$, ranging from 0.6 to $3.0 \mu\text{M}$ and of $1.4 \pm 0.8 \mu\text{M}$ after the supplementation.

	PRE	POST	PRE	POST
Patient	Car-propanal [μM]	Car-propanal [μM]	Car-propanol [μM]	Car-propanol [μM]
1	0.60	0.89	0.98	0.84
2	0.89	1.16	0.87	1.02
3	0.79	0.52	0.59	0.67
4	0.35	1.14	0.63	0.77
5	0.85	0.64	0.99	0.78
6	0.53	0.66	0.78	0.66
7	0.60	0.89	0.98	0.84
8	2.11	2.55	3.01	2.80
9	1.69	1.86	1.69	1.04
10	1.33	n.d.	1.67	n.d
11	5.58	0.61	5.93	0.83
12	2.76	2.43	1.41	1.68
13	2.35	5.49	2.69	4.05
14	1.56	3.39	1.70	1.75

6 Intervention study of Carnosine in obese volunteers: bioavailability and reactive carbonyls species sequestering effect

	PRE	POST	PRE	POST
Patient	Car-propanal [μM]	Car-propanal [μM]	Car-propanol [μM]	Car-propanol [μM]
15	0.38	0.65	0.60	0.77
16	1.03	1.80	1.52	1.40
17	0.66	0.83	0.92	0.89
18	1.06	1.16	0.96	1.04
19	0.88	1.06	1.08	1.23
20	1.77	1.20	2.26	1.06
21	1.33	1.00	1.51	1.00
22	1.04	0.67	1.18	0.84
23	1.16	1.65	1.14	1.44
24	0.79	3.74	0.99	2.47
25	0.67	0.56	1.02	1.13
26	2.41	4.81	2.81	3.47
27	0.35	3.01	0.66	1.25
28	1.47	1.61	1.66	1.25
29	0.45	1.88	0.75	1.56
30	0.82	0.57	1.00	0.80
31	2.92	1.53	2.39	1.36

Tab. 7. CAR-propanal and CAR-propanol concentration for each patient both before (PRE) and after (POST) CAR or placebo intake. The number of the patient in bold type refers to the CAR treated patients, the italic type refers to the placebo group.

6.3.5 Carnosine determination in urine and plasma

A LC-MRM approach based on a triple quadrupole mass spectrometer was then developed in order to detect and quantify free carnosine in urine and plasma. TH was selected as internal standard and the method was found specific for this compound. Fig. 12 shows the SRM of TH in a blank urine sample and in urine spiked with TH at a final concentration of x μM .

The MRM approach was firstly applied to blank urine and plasma to measure the endogenous concentration of free carnosine. According to previous studies reporting that carnosine is an endogenous dipeptide present in urine but not in plasma, carnosine was detected but not quantified in the blank urine (the peak area was lower than 20 % the LLOQ, Fig. 10) and not detected in the blank plasma (Fig. 11).

The calibration curves for carnosine built in urine and plasma are displayed in fig.13 and the equation calculated in urine and plasma are as follows: $y = (0.01543 \pm 0.00039)x - (0.02865 \pm 0.03653)$, r^2 is 0.990 and $y = (0.11970 \pm 0.00155)x - (0.01417 \pm 0.00778)$, r^2 is 0.998

The LLOQs of carnosine was 0.5 μM in urine and 0.1 μM in plasma. The LLODs were as follows: 0.2 μM in urine and 0.05 μM in plasma

The intra and interday precision (CV%) and the accuracy of the method were determined on QC samples prepared separately from calibration standards, by analysing five replicates at three concentration levels, and data are reported in table 8.

Carnosine was found stable at 4 °C for at least for 18 hours both for CAR spiked in urine and plasma, instead after one freeze and thaw cycle, from -80 °C to room temperature, carnosine decreased by 4.5 % and 5.1 %, moreover after 3 freeze and thaw cycles carnosine decreased by 8.5 % in urine and 10.4 % in plasma.

6 Intervention study of Carnosine in obese volunteers: bioavailability and reactive carbonyls species sequestering effect

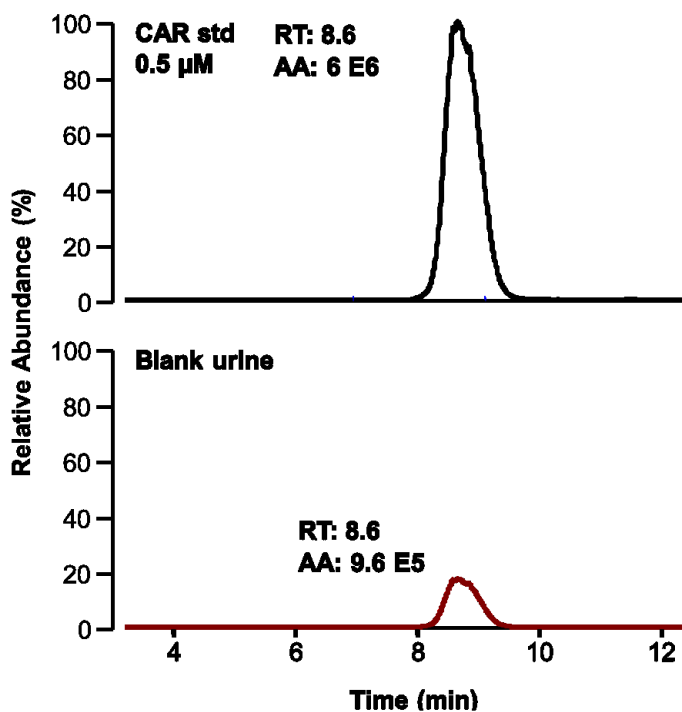


Fig. 10. Upper panel: SRM trace of CAR spiked in blank urine at the LLOQ; lower panel: SRM relative to CAR in blank urine: the peak area is 16 % in respect to the peak area of CAR spiked at the LLOQ.

6 Intervention study of Carnosine in obese volunteers: bioavailability and reactive carbonyls species sequestering effect

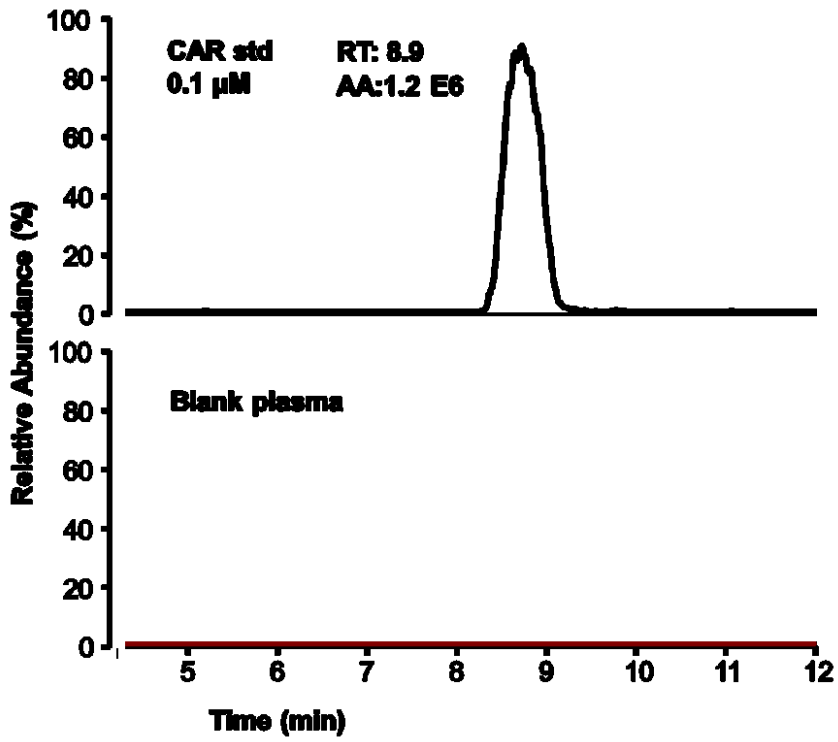


Fig. 11. Upper panel: SRM trace of CAR spiked at the LLOQ in blank plasma; lower panel: SRM trace of CAR in blank plasma.

6 Intervention study of Carnosine in obese volunteers: bioavailability and reactive carbonyls species sequestering effect

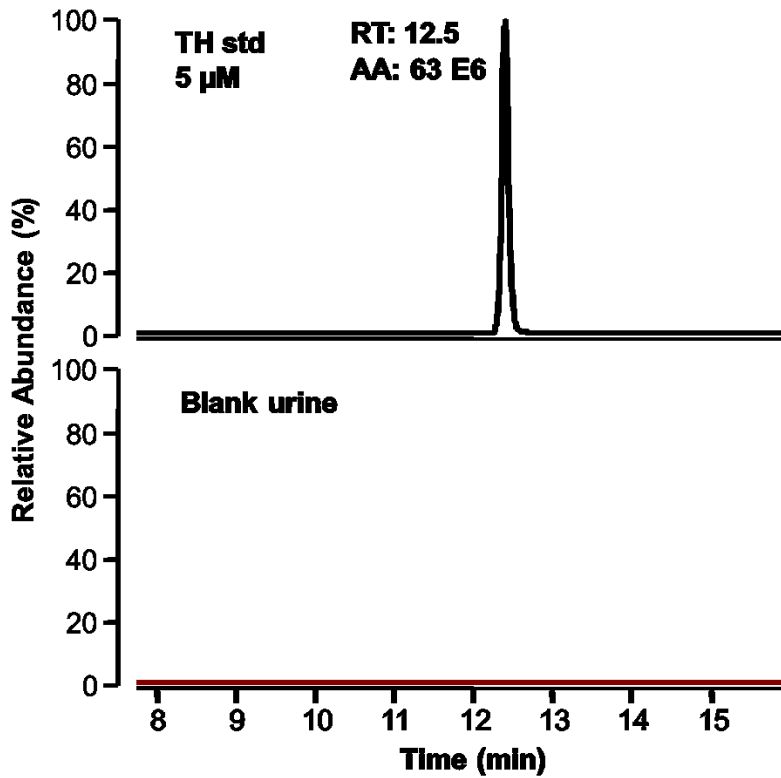


Fig. 12. Upper panel: SRM trace of TH as internal std spiked in blank plasma at a final concentration of 5 µM; lower panel, SRM trace of TH in a blank plasma. No peak are detected demonstrating the method's specificity.

6 Intervention study of Carnosine in obese volunteers: bioavailability and reactive carbonyls species sequestering effect

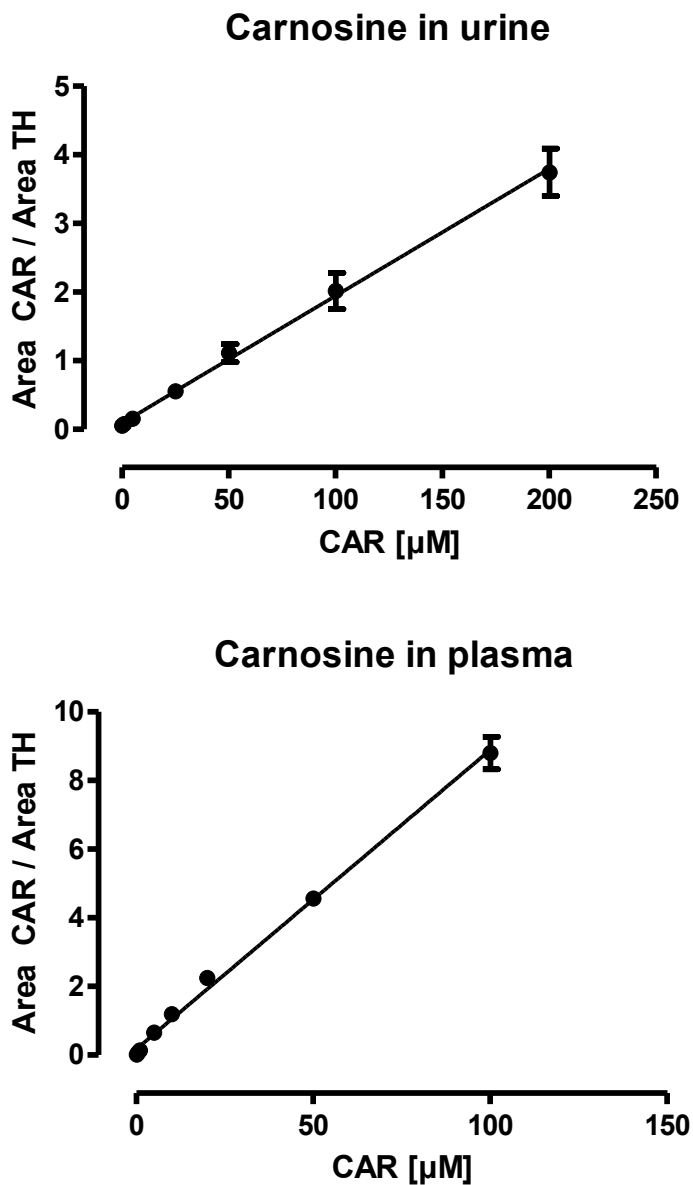


Fig. 13. Calibration curve of CAR in urine $y = (0.01543 \pm 0.00039)x - (0.02865 \pm 0.03653)$, $r^2 = 0.990$; lower panel - calibration curve of CAR in plasma $y = (0.11970 \pm 0.00155)x - (0.01417 \pm 0.00778)$ $r^2 = 0.998$

6 Intervention study of Carnosine in obese volunteers: bioavailability and reactive carbonyls species sequestering effect

analytical method for urine			
Concentration (μM)	Intraday (CV %)	Interday (CV%)	Accuracy
1	8.6	10.1	$\pm 9.3\%$
25	5.3	11.3	$\pm 5.1 \%$
200	6.1	6.8	$\pm 4.7\%$
analytical method for plasma			
Concentration (μM)	Intraday (CV %)	Interday (CV%)	Accuracy
0.5	9.7	12.3	$\pm 8.8\%$
10	6.6	10.5	$\pm 6.3 \%$
100	4.9	5.8	$\pm 4.1\%$

Tab. 8. Intra and interday precision and accuracy data for CAR in urine and CAR in plasma

Table 9 shows the data on urine CAR concentration for each patient. Before supplementation (PRE), carnosine ranged from 0.1 to 21 μM with a mean of $9 \pm 6.3 \mu\text{M}$. After the supplementation (POST), carnosine ranged from 1.4 μM to 350.0 μM and the mean raised to $40 \pm 85 \mu\text{M}$. The intra-run precision in terms of CV % was always below the 15 %.

6 Intervention study of Carnosine in obese volunteers: bioavailability and reactive carbonyls species sequestering effect

Urine	PRE	POST
Patient	CAR [μ M]	CAR [μ M]
1	0.1	1.4
2	13.7	14.3
3	1.4	3.7
4	4.9	11.1
5	8.8	7.5
6	15.3	45.8
7	3.7	13.0
8	12.1	12.4
9	21.1	306.6
<i>10</i>	9.8	n.d.
11	8.8	0.7
12	17.6	25.7
13	19.2	350.0
14	5.3	33.1
<i>15</i>	0.5	4.0

Urine	PRE	POST
Patient	CAR [μ M]	CAR [μ M]
16	14.3	31.5
<i>17</i>	10.5	7.5
<i>18</i>	4.6	5.6
<i>19</i>	5.9	4.6
<i>20</i>	6.6	1.4
<i>21</i>	20.8	6.9
<i>22</i>	2.7	1.4
23	3.3	8.2
24	9.5	52.9
<i>25</i>	7.2	6.9
26	16.0	19.5
<i>27</i>	1.1	9.2
28	7.9	146.9
29	1.4	12.7
<i>30</i>	11.1	5.3
<i>31</i>	15.3	9.5

Tab. 9. CAR concentration in urine for each patient before (PRE) and after (POST) CAR or placebo intake. CAR treated patients are recognized by the patient's number in bold, placebo subjects have the number in italic.

6 Intervention study of Carnosine in obese volunteers: bioavailability and reactive carbonyls species sequestering effect

6.3.6 Top down ESI-MS analysis of albumin's isoforms

Three main HSA isoforms are detected by ESI-MS intact protein analysis of human serum: mercapto-albumin (HSA-SH), cysteinylated-albumin (HSA-S-S-Cys) and glycated albumin (HSA-N-Glc). Figure 14 shows the full ESI-MS spectrum of HSA and the corresponding deconvoluted spectrum. The ESI-MS spectrum (upper panel) shows the +45, +46, +47 multicharged ions relative to the three isoforms. The corresponding deconvoluted spectrum is shown in the lower panel, characterized by a base peak at 66448 Da, corresponding to mercapto-albumin and differing of only 0.1 milli-mass unit (mmu) in respect to the theoretical mass (66454.6 Da).

In the spectrum there are two other minor peaks at 66565 Da (+117 Da) and 66610 Da (+162 Da) which are attributed to the cysteinylated and glycated forms, respectively, as previously reported [21]

Table 10 summarizes the relative percentage of the three isoforms for each patient, both before and after the supplementation. The intra-run precision in terms of CV % was always below the 15 %.

Patient	PRE			POST		
	HSA-SH	HSA-S-S-Cys	HSA-N-Glc	HSA-SH	HSA-S-S-Cys	HSA-N-Glc
1	58.9	22.6	18.5	60.6	21.9	17.6
2	59.9	22.6	17.4	60.1	23.2	16.7
3	55.4	27.0	17.6	58.2	24.7	17.1
4	56.8	24.3	18.9	59.3	22.9	17.7
5	61.0	21.1	17.9	61.4	21.9	16.7
6	58.4	22.5	19.1	58.2	24.1	17.7
7	53.9	28.2	17.9	55.0	25.6	19.4
8	59.4	23.1	17.5	60.0	22.8	17.3
9	62.4	21.3	16.3	59.5	24.1	16.4
10	58.8	23.5	17.7	n.d.	n.d.	n.d.

6 Intervention study of Carnosine in obese volunteers: bioavailability and reactive carbonyls species sequestering effect

	PRE			POST		
Patient	HSA-SH	HSA-S-S-Cys	HSA-N-Glc	HSA-SH	HSA-S-S-Cys	HSA-N-Glc
11	60.4	23.0	16.7	60.5	23.4	16.2
12	60.4	22.5	17.1	60.0	23.4	16.6
13	62.2	20.9	16.8	63.3	20.2	16.5
14	58.9	23.5	17.6	59.0	23.9	17.1
<i>15</i>	61.0	22.3	16.7	64.7	19.1	16.2
16	59.2	23.4	17.4	60.1	22.7	17.2
<i>17</i>	59.1	22.5	18.4	59.8	22.1	18.1
<i>18</i>	59.4	22.0	18.6	61.8	20.8	17.4
<i>19</i>	56.2	24.9	18.9	56.2	26.5	17.3
<i>20</i>	58.1	23.2	18.7	58.8	23.2	18.0
<i>21</i>	56.6	26.0	17.4	57.8	25.6	16.7
<i>22</i>	61.0	22.2	16.7	62.8	20.3	16.9
23	58.4	23.9	17.7	60.9	21.9	17.2
24	59.1	24.1	16.8	59.1	24.0	16.9
<i>25</i>	57.3	25.4	17.3	59.1	24.0	16.9
26	62.0	21.3	16.7	62.7	20.4	16.9
<i>27</i>	60.6	22.4	17.0	57.6	24.9	17.6
28	60.0	22.4	17.6	60.5	21.9	17.5
29	57.4	25.1	17.5	57.8	25.0	17.2
<i>30</i>	56.9	26.8	16.3	56.3	26.6	17.1
<i>31</i>	60.4	22.8	16.8	62.4	21.6	16.1

Tab. 10. For each patient the relative abundance of HSA-SH, HSA-S-S-Cys and HSA-N-Glc are reported. Green background refers to the relative values before the treatment (PRE), red background after treatment (POST). Treated patient numbers are in bold, placebo patient numbers are in italics.

6 Intervention study of Carnosine in obese volunteers: bioavailability and reactive carbonyls species sequestering effect

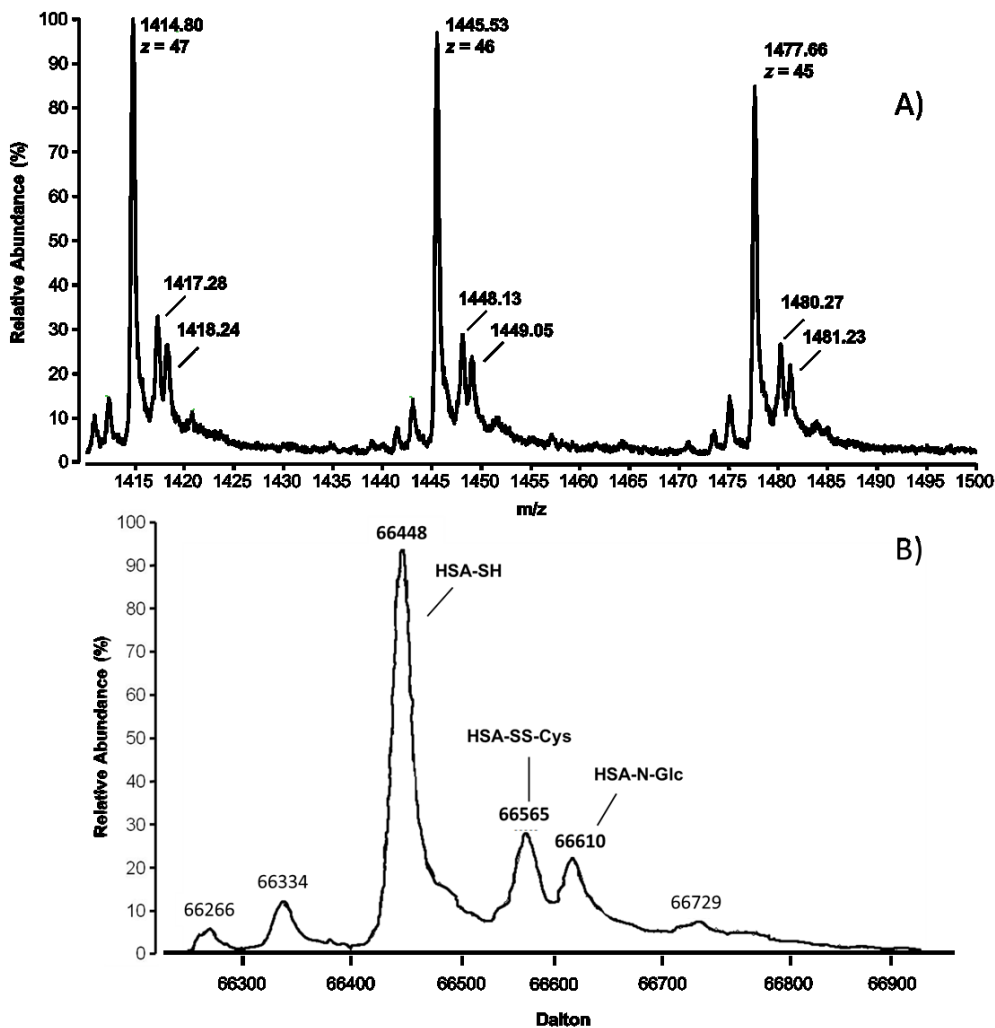


Fig. 14. Panel A: ESI full MS spectrum of HSA characterized by three intense multicharged ion series. Panel B: deconvoluted spectrum characterized by a base peak attributed to mercapto-albumin at 66448 (HSA-SH) and by two other less intense peaks referred to cysteinylated and glycated albumin at 66565 Da and 66610 Da, respectively

6 Intervention study of Carnosine in obese volunteers: bioavailability and reactive carbonyls species sequestering effect

6.3.7 Creatinine determination in urine

In table 11 the concentration of urinary creatinine is reported. The intra-run precision in terms of CV % was always below the 15 %.

Urine	PRE	POST
Patient	CRE [μ M]	CRE [μ M]
1	3359.3	6011.4
2	10962.0	17857.5
3	8928.7	13348.9
4	10608.4	6011.4
5	12376.5	6983.9
6	14940.2	8044.7
7	22100.8	20598.0
8	17327.1	23868.9
9	18387.9	25106.5
10	20774.8	n.d.
11	18034.3	3536.1
12	18829.9	19448.7
13	11669.2	12906.9
14	28200.7	31118.0
15	2210.1	6630.3

Urine	PRE	POST
Patient	CRE [μ M]	CRE [μ M]
16	20951.6	20951.6
17	10431.6	10078.0
18	19713.9	16619.8
19	14586.6	11669.2
20	25637.0	24752.9
21	27493.4	15382.2
22	9459.2	5481.0
23	14763.4	16177.8
24	12376.5	21482.0
25	12906.9	23868.9
26	35361.3	32355.6
27	4066.6	12553.3
28	12376.5	7160.7
29	9547.6	20421.2
30	23868.9	9636.0
31	23161.7	18211.1

Tab. 11. Urine creatinine concentration.

Treated patient numbers are in bold, placebo patient numbers are in italics.

6 Intervention study of Carnosine in obese volunteers: bioavailability and reactive carbonyls species sequestering effect

6.3.8 Advanced Glication End products (AGE) in urine and plasma

Urinary and plasma AGE levels are reported in table 12 and 13. The intra-run precision calculated as CV % was always below the 20 %

Urine	PRE	POST
Patient	AGE [UF/ mg protein]	AGE [UF/ mg protein]
1	95016.2	39736.2
2	36248.4	29490.4
3	179178.5	94568.8
4	11608.0	77766.8
5	50900.4	19590.0
6	69441.8	40372.1
7	31596.3	30548.6
8	36506.0	61299.2
9	49801.2	43738.1
10	38852.8	n.d.
11	56676.6	13770.3
12	33253.0	28168.3
13	40689.4	34044.3
14	33021.3	31601.2
15	41767.8	24895.0

Urine	PRE	POST
Patient	AGE [UF/ mg protein]	AGE [UF/ mg protein]
16	23034.1	35076.5
17	94474.0	147585.0
18	31868.9	25859.6
19	20511.8	18000.2
20	56482.9	93316.5
21	82519.6	87777.0
22	23565.1	22199.3
23	75835.3	74043.6
24	71383.7	64373.4
25	16241.1	78083.6
26	23539.9	22171.6
27	30647.1	31386.7
28	14332.4	52720.7
29	15338.2	24416.9
30	32018.8	24255.3
31	31039.8	41847.2

Tab. 12. Urinary AGE levels reported as fluorescence units per mg of protein.

6 Intervention study of Carnosine in obese volunteers: bioavailability and reactive carbonyls species sequestering effect

Plasma	PRE	POST
Patient	AGE [UF/ mg protein]	AGE [UF/ mg protein]
1	10.3	10.2
2	9.9	7.8
3	11.6	11.4
4	8.5	7.9
5	9.0	7.4
6	9.4	9.9
7	10.3	7.8
8	8.7	16.5
9	8.3	9.6
10	9.3	n.d.
11	12.7	11.9
12	13.2	9.4
13	8.6	7.5
14	16.8	20.9
15	8.4	7.8

Plasma	PRE	POST
Patient	AGE [UF/ mg protein]	AGE [UF/ mg protein]
16	10.3	9.6
17	11.8	11.1
18	9.9	10.2
19	11.4	11.7
20	12.2	13.6
21	8.9	12.1
22	26.6	13.1
23	7.4	12.2
24	11.5	16.0
25	7.2	8.7
26	8.3	9.2
27	8.9	9.8
28	9.6	11.2
29	14.8	13.6
30	8.8	12.4
31	8.4	9.6

Tab. 13. Plasma AGE levels are reported as fluorescence units per mg of protein. Treated patient numbers are in bold, placebo patient numbers are in italics.

6 Intervention study of Carnosine in obese volunteers: bioavailability and reactive carbonyls species sequestering effect

6.3.9 Carboxymethyl lysine (CML) in plasma

Table 14 reports the CML levels in plasma .

CML	PRE	POST
Patient	ng CML / mg protein	ng CML / mg protein
1	50.1	48.8
2	49.0	62.2
3	51.8	53.1
4	41.9	42.8
5	50.0	45.7
6	45.4	42.2
7	55.9	47.1
8	48.2	47.8
9	115.8	50.1
10	46.5	n.d.
11	47.4	46.0
12	53.2	42.3
13	79.4	54.5
14	50.2	42.0
15	43.5	44.9

CML	PRE	POST
Patient	ng CML / mg protein	ng CML / mg protein
16	45.1	42.5
17	42.7	42.2
18	42.5	52.2
19	52.1	51.5
20	45.7	46.1
21	44.0	45.0
22	122.9	41.8
23	42.8	45.2
24	41.4	62.6
25	50.6	52.5
26	46.3	46.0
27	45.4	45.6
28	40.9	49.7
29	46.4	54.0
30	38.4	39.1
31	55.3	53.8

Tab. 14. CML plasma levels reported as nanograms of CML per mg of protein. Treated patient numbers are in bold, placebo patient numbers are in italics.

6 Intervention study of Carnosine in obese volunteers: bioavailability and reactive carbonyls species sequestering effect

6.3.10 Advanced Oxidation Protein Products (AOPP) in plasma

Table 15 summarizes the plasma levels of AOPP.

AOPP	PRE	POST	AOPP	PRE	POST
Patient	nanomol / mg protein	nanomol / mg protein	Patient	nanomol / mg protein	nanomol / mg protein
1	5.3	3.7	16	4.1	4.4
<i>2</i>	1.9	4.6	<i>17</i>	4.3	8.4
<i>3</i>	2.8	3.9	<i>18</i>	6.2	4.9
4	5.2	4.6	<i>19</i>	6.2	6.0
5	2.7	2.4	<i>20</i>	6.2	6.5
6	2.5	3.9	<i>21</i>	4.2	6.0
7	4.9	3.3	<i>22</i>	24.9	7.7
<i>8</i>	3.4	4.2	23	5.8	8.5
9	4.9	3.5	24	10.1	6.0
<i>10</i>	3.1	n.d.	<i>25</i>	7.5	6.8
11	2.9	6.3	26	7.2	6.3
12	5.5	7.6	<i>27</i>	8.8	7.5
13	3.4	4.5	28	3.9	5.1
14	5.1	7.8	29	5.5	5.1
<i>15</i>	3.6	7.1	<i>30</i>	10.1	7.9
			<i>31</i>	3.8	8.0

Tab. 15. The plasma levels of AOPP are reported as nanograms per mg of protein. Treated patient numbers are in bold, placebo patient numbers are in italics.

6 Intervention study of Carnosine in obese volunteers: bioavailability and reactive carbonyls species sequestering effect

6.3.11 Protein Carbonyl (PCO) in plasma

Table 16 shows the plasma PCO levels in plasma.

PCO	PRE	POST
Patient	nanomol/mg protein	nanomol/mg protein
1	1.52	1.80
2	1.61	1.99
3	2.23	1.85
4	2.52	1.71
5	2.33	1.69
6	2.21	1.66
7	2.60	1.46
8	2.10	1.63
9	2.22	1.72
10	3.18	1.50
11	2.61	1.68
12	2.32	1.53
13	0.91	1.67
14	1.25	1.89
15	0.85	1.63

PCO	PRE	POST
Patient	nanomol/mg protein	nanomol/mg protein
16	1.53	1.96
17	1.35	1.12
18	0.90	1.42
19	1.06	1.44
20	1.00	1.36
21	0.97	1.88
22	3.67	1.56
23	1.32	2.05
24	1.82	1.58
25	1.68	1.82
26	1.90	1.80
27	1.80	1.72
28	2.02	1.56
29	2.04	1.74
30	2.38	2.00
31	2.33	1.81

Tab. 16. The plasma levels of PCO are reported as ng per mg of protein. Treated patient numbers are in bold, placebo patient numbers are in italics.

6.3.12 Statistical Analysis: T test

As already mentioned at the beginning of the results section, free carnosine, CAR-propanol and CAR-propanal were found in all the 31 patients urine, both before and after carnosine supplementation. Considering these results different statistical tests were applied in order to determine if CAR treatment significantly changes the urinary levels of both free carnosine and CAR-ACR-adducts as well as the other parameters measured. Patient n° 10 was excluded by all the statistical analysis since it was a drop out subject and we couldn't analyze his samples after the treatment.

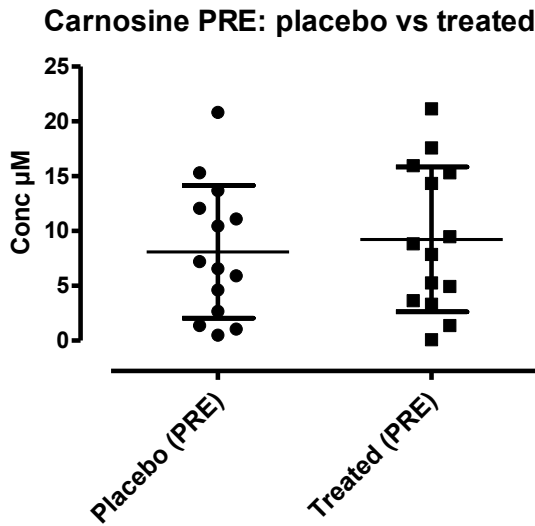
ANOVA test was firstly launched and it didn't indicate any significant difference for any groups and parameters considered. Hence unpaired t test was applied for all the analytes considered and between the different groups. For each considered analyte, there was no significant difference between the placebo and treated groups before starting the CAR supplementation thus indicating the homogeneity at the starting point between the two groups. The placebo and treated group after CAR intake as well as the treated group before and after the treatment were then matched and analysed by t-test in order to assess any possible significant variation induced by the treatment. The placebo group before and after the treatment was then analyzes in order to recognize any placebo effect after the supplementation. The t test revealed significant variations only in the case of free carnosine and carnosine propanal, unfortunately for all the other parameters reported above we couldn't find any significant variation.

6 Intervention study of Carnosine in obese volunteers: bioavailability and reactive carbonyls species sequestering effect

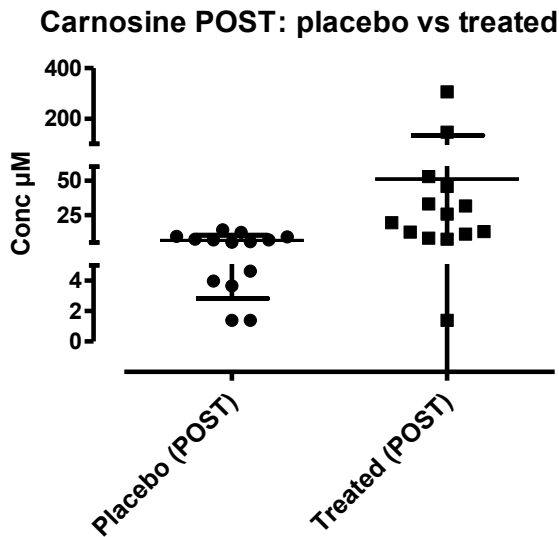
6.3.12.1 Free carnosine t test results

As shown in graph 1, placebo and treated groups were homogeneous in terms of urinary content of carnosine before CAR supplementation (P value = 0.46). After three months of CAR intake, the urinary CAR levels were significantly higher in the treated group than in placebo (P value ≤ 0.05) (graph 2). The effect of carnosine intake on the urinary levels was then confirmed by analysing the treated group before and after supplementation (p <0.05, graph 4). By contrast, placebo treatment was found not able to affect carnosine excretion (p=0.44, graph 3).

6 Intervention study of Carnosine in obese volunteers: bioavailability and reactive carbonyls species sequestering effect

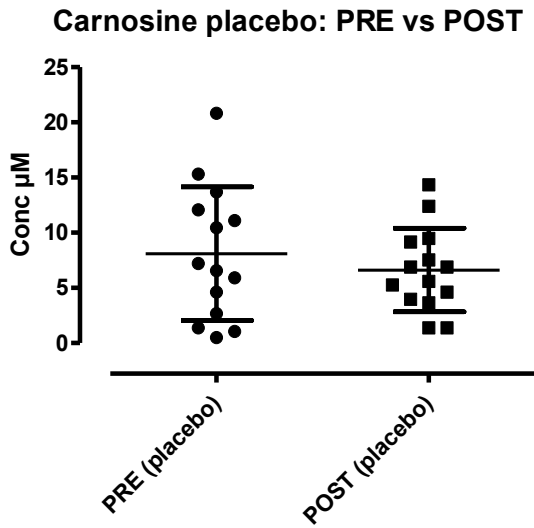


Graph 1. Scatter plot that compares the urinary content of CAR between placebo and treated group before the treatment (PRE).

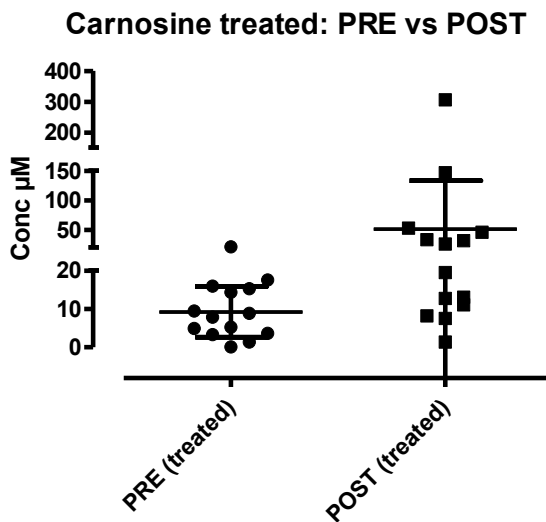


Graph 2. Scatter plot that compares the CAR concentration between placebo and treated group after the treatment (POST).

6 Intervention study of Carnosine in obese volunteers: bioavailability and reactive carbonyls species sequestering effect



Graph 3. Scatter plot that compares the CAR concentration of the placebo group before and after the placebo supplementation



Graph 4. Scatter plot that compares the CAR concentration of treated group before and after CAR supplementation

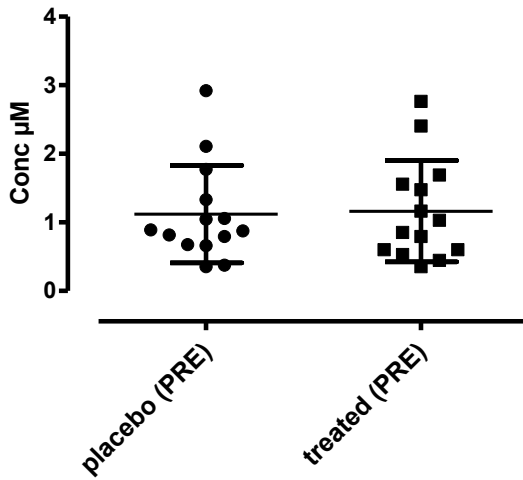
6 Intervention study of Carnosine in obese volunteers: bioavailability and reactive carbonyls species sequestering effect

6.3.12.2 CAR-propanal t test results

Similarly to carnosine, the urinary levels of CAR-propanal in placebo and treated groups were homogeneous before CAR supplementation (P value = 0.33, graph 5). After three months of treatment, the urinary CAR-propanal levels were significantly higher in the treated group than in placebo (P value ≤ 0.05 , graph 5). The result was confirmed by considering the effect of each treatment for each group, placebo did not change the levels of the adduct (p= 0.83, graph 7) while CAR treatment was significantly effective (p< 0.05, graph 8). Patient 11 and 13 were excluded by this t test analysis since the instrumental response had sensibility problem considering CAR-propanal for those samples.

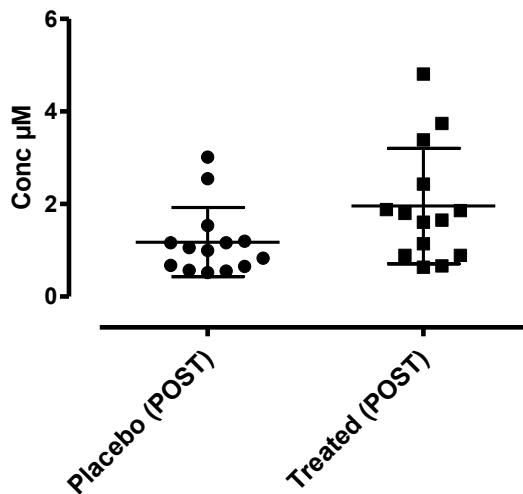
6 Intervention study of Carnosine in obese volunteers: bioavailability and reactive carbonyls species sequestering effect

Car-propanal PRE: placebo vs treated



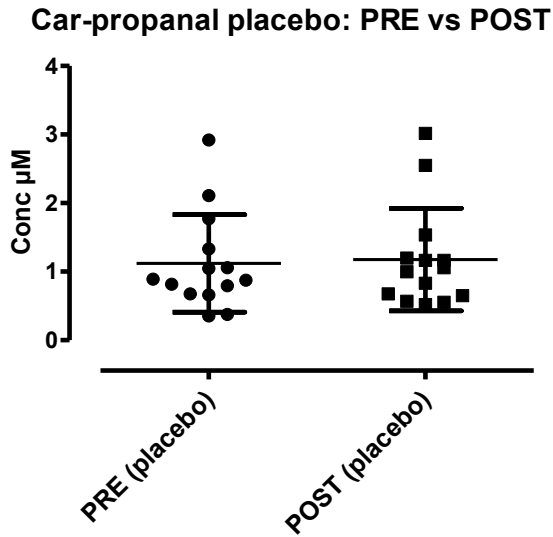
Graph 5. Scatter plot that compares the CAR-propanal concentration between placebo and treated group before the treatment (PRE).

Car-propanal POST: placebo vs treated

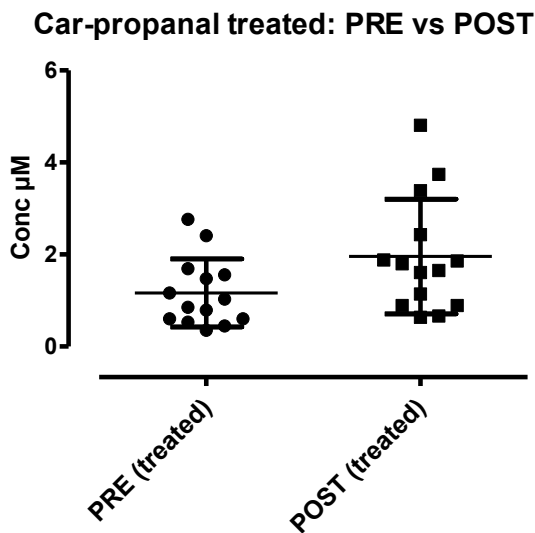


Graph 6. Scatter plot that compares the CAR-propanal concentration between placebo and treated group after the treatment (POST).

6 Intervention study of Carnosine in obese volunteers: bioavailability and reactive carbonyls species sequestering effect



Graph 7. Scatter plot that compares the CAR-propanal concentration of the placebo group before and after the placebo supplementation



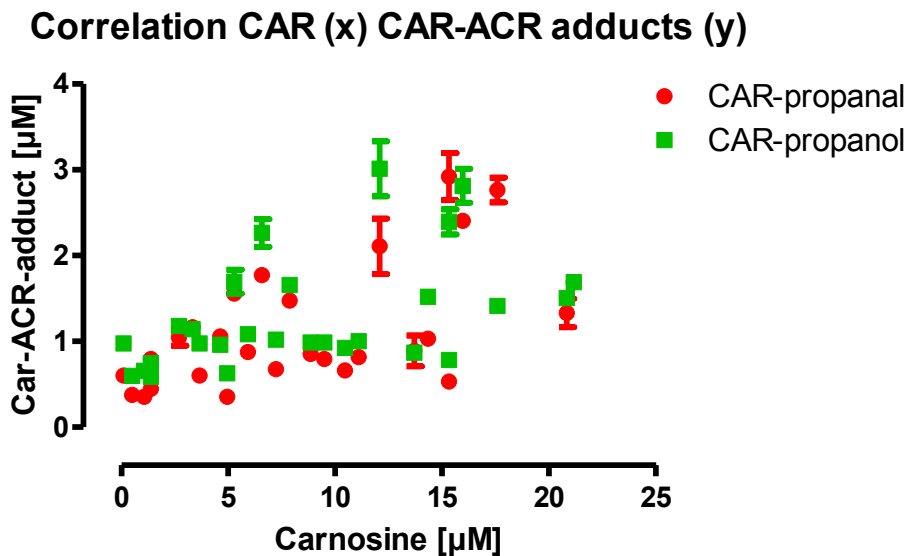
Graph 8. Scatter plot that compares the CAR-propanal concentration of the treated group before and after the placebo supplementation

6 Intervention study of Carnosine in obese volunteers: bioavailability and reactive carbonyls species sequestering effect

6.3.12.3 Correlation between CAR-ACR adducts and CAR concentration in urine

We then found that the increase of free carnosine in urine is associated to an increase of CAR-ACR adducts formation. In particular we observed a significant positive correlation between CAR-ACR adducts (CAR-propanal and CAR-propanol) and free carnosine in urine (graph 9).

Data regarding the parametric correlation, the Pearson r , the P value and the r^2 for each adduct are reported in tab. 17.



Graph 9. Points graph that shows the correlation between CAR.ACR adduct urinary concentration and CAR urinary concentration. The red dots refer to CAR-propanal, instead the green squares refer to CAR-propanol

6 Intervention study of Carnosine in obese volunteers: bioavailability and reactive carbonyls species sequestering effect

Parametric correlation	CAR-propanal	CAR-propanol
Pearson r	0.58	0.49
P value	0.0013	0.0085
r²	0.33	0.24

Tab. 17. Parametric correlation coefficients regarding CAR-propanal and CAR-propanol correlation with CAR.

6.3.13 Statistical analysis: Principal Component Analysis (PCA)

The data set was then analyzed by the Principal Component Analysis (PCA), a data simplification technique used in the field of the multivariate statistics. PCA convert a set of possibly correlated variables into a set of values of linearly uncorrelated variables called principal components. Each principal component explain a percentage of the total variance of the data. PCA was applied separately to the analytes measured in urine and in plasma, moreover the pre-treatment group was separated from the post-treatment group. No significant results were observed when PCA was applied to the data set regarding plasma parameters either considering the pre and post treatment groups.

By contrast, when PCA analysis was applied to urine, significant results were observed as reported in the following paragraph.

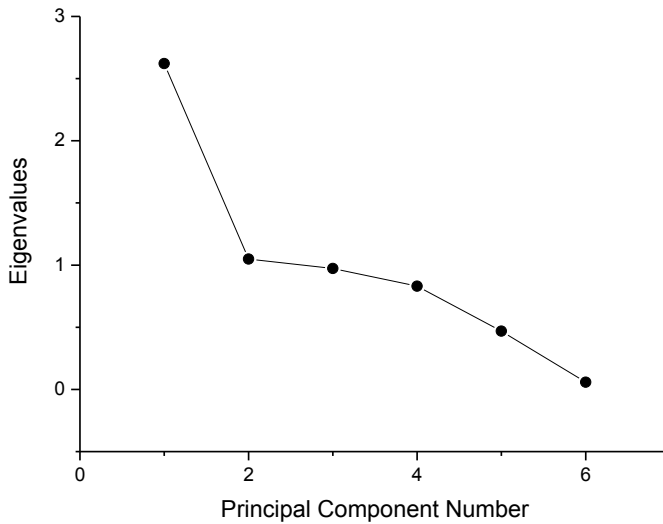
6 Intervention study of Carnosine in obese volunteers: bioavailability and reactive carbonyls species sequestering effect

6.3.13.1 PCA on urinary analytes before carnosine administration:

Graph 10 reports the loading plot reporting the eigenvalues on the y axis and the principal component number on the x axis. Each principal component found by the analysis have its own eigenvalue and describes a percentage of variance. As shown in figure 10, two principal components have an eigenvalues above 1: the principal component 1 (PC1) that have an eigenvalue of 2.6 and reporting the 43 % of data variance and the principal component 2 (PC2) which describes the 17 % of data variance; globally PC1 and PC2 account for 61.2 % of the variance. This two component were chosen also because their coefficients were consistent and logical in respect to the biological meaning of the experiment.

6 Intervention study of Carnosine in obese volunteers: bioavailability and reactive carbonyls species sequestering effect

Loading plot:



Graph 10. The Loading plot reports on the y axis the eigenvalues of each component and on the x axis the principal component number. PC1 and PC2 have an eigenvalue higher or equal to 1.

	Eigenvalue	Percentage of Variance	Cumulative
1	2.62084	43.68%	43.68%
2	1.04886	17.48%	61.16%
3	0.97245	16.21%	77.37%
4	0.83096	13.85%	91.22%
5	0.46914	7.82%	99.04%
6	0.05775	0.96%	100.00%

Tab. 18: Each derived component is reported. There are six principal components but component 1 and 2 describe the 43% and 17% of data variance, respectively.

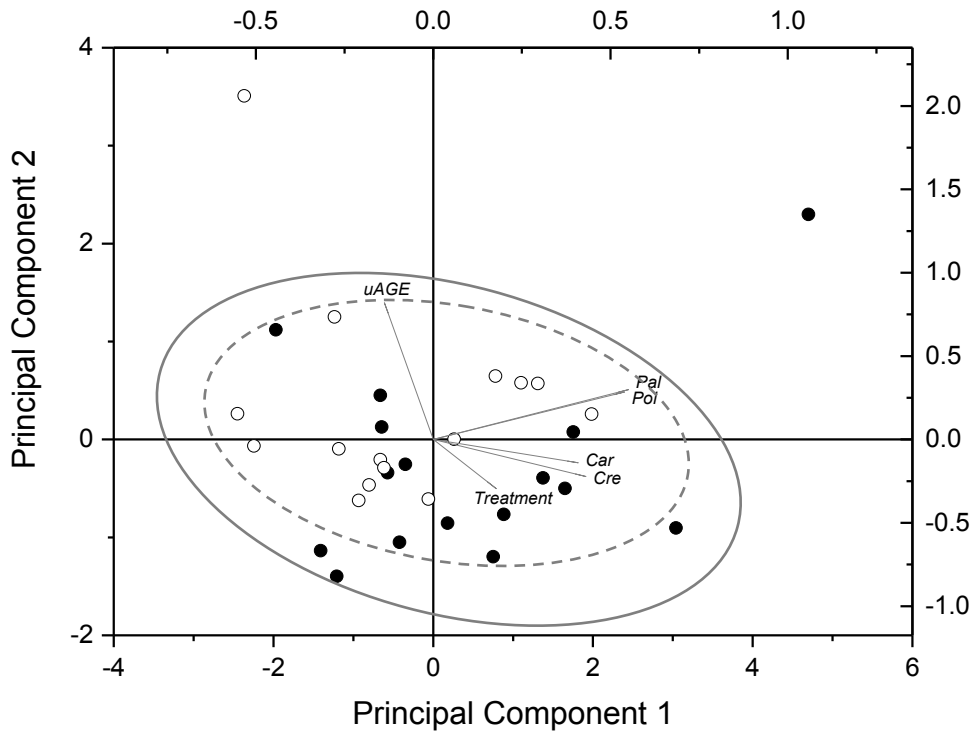
6 *Intervention study of Carnosine in obese volunteers: bioavailability and reactive carbonyls species sequestering effect*

	Coefficients of PC1	Coefficients of PC2
Pal	0.55164	0.29915
Pol	0.53993	0.285
CAR	0.4093	-0.14005
uAGE	-0.13799	0.82036
Cre	0.43121	-0.22215
Treatment	0.17796	-0.29552

Tab. 19. The coefficients of PC1 and PC2 are reported. Pa stand for CAR-propanal, Po for CAR-propanol, CAR for Carnosine, uAGE for urinary AGE, Cre for Creatinine.

Table 19 reports the coefficients of PC1 and PC2. Each component have different coefficients for all the variables taken into account. The value of the coefficient is related to the importance of the variable for the corresponding principal component. The variables are positively related when they have the same sign, negatively when characterized by an opposite sign. The strength of the correlation depends on the value of the coefficients, higher the value, higher the correlation. The first component (PC1) describes a positive covariance of Carnosine (CAR), Carnosine adducts (Pal, Pol) and Creatinine (Cre). The second component (PC2) is strongly associated to the urinary AGE concentration (uAGE).

6 Intervention study of Carnosine in obese volunteers: bioavailability and reactive carbonyls species sequestering effect



Graph 11. Biplot of PC1 against PC2. Subjects treated for CAR supplementation are visualized as filled dots and solid line, instead subjects chosen for placebo treatment are represented in empty dots, dashed line.

Graph 11 reports the PCA analysis applied to the set of data related to the subjects before the carnosine treatment. In particular the biplot of principal components (PC1 vs PC2) (graph 11) shows that subjects chosen for Carnosine administration (filled dots, solid line) and subjects chosen for placebo treatment (empty dots, dashed line) are quite evenly distributed on the biplot space thus demonstrating the homogeneity of the two groups.

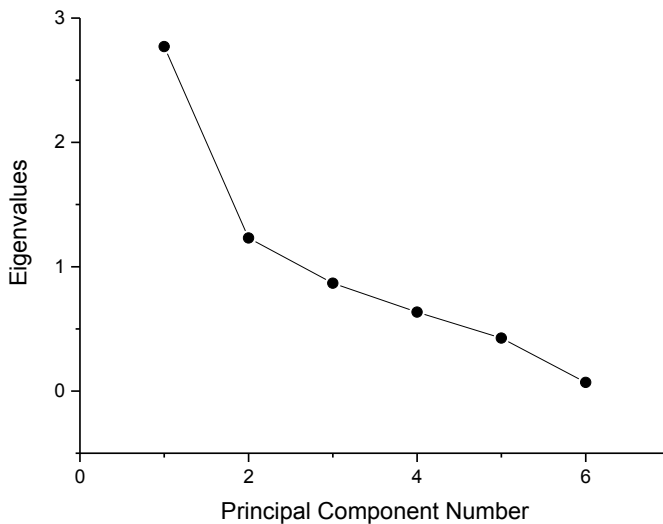
6 Intervention study of Carnosine in obese volunteers: bioavailability and reactive carbonyls species sequestering effect

6.3.13.2 PCA on urinary analytes after carnosine administration:

PCA was then performed to the data set after Carnosine administration. Graph 12 reports the loading plot and two principle components characterized by a value higher than 1 were observed, which explains almost the 67 % of the variance.

In particular component 1 and 2 describe the 46% and 20% of data variance, respectively. Notably, the percentage of variance of samples described by PCA after treatment is higher than before treatment.

Loading plot:



Graph 12. The loading plot is almost similar to previous graph 10. PC1 and PC2 eigenvalues are slightly higher than previous analysis on pre treatment group.

6 *Intervention study of Carnosine in obese volunteers: bioavailability and reactive carbonyls species sequestering effect*

	Eigenvalue	Percentage of Variance	Cumulative
1	2.77071	46.18%	46.18%
2	1.2308	20.51%	66.69%
3	0.86783	14.46%	81.16%
4	0.63524	10.59%	91.74%
5	0.42633	7.11%	98.85%
6	0.06909	1.15%	100.00%

Tab 19. Each derived component is reported. There are six principal components but component 1 and 2 describe the 46.2 % and 20.5 % of data

	Coefficients of PC1	Coefficients of PC2
Pal	0.56702	0.11224
Pol	0.54314	0.18071
CAR	0.38613	-0.21844
uAGE	-0.14401	0.61481
Cre	0.34189	0.50698
Treatment	0.31107	-0.52155

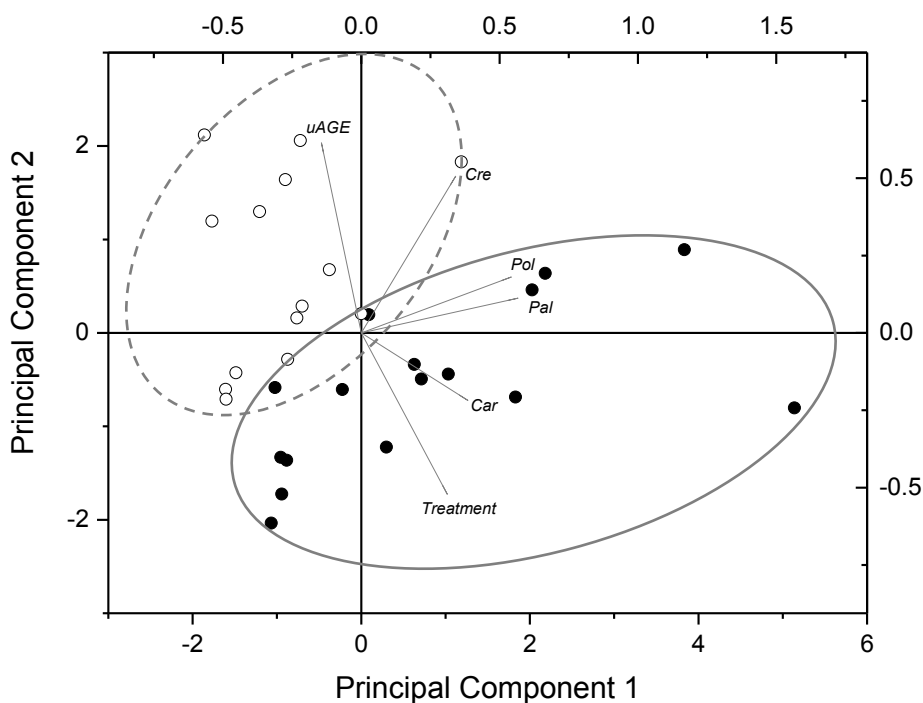
Tab. 20. The coefficients of PC1 and PC2 are reported. Pa stand for CAR-propanal, Po for CAR-propanol, CAR for Carnosine, uAGE for urinary AGE, Cre for Creatinine. It is remarkable that in PC2 uAGE and the treatment are negative correlated.

Similarly to the results of samples analyzed before treatment, the PC1 describes a positive covariance of carnosine (CAR), carnosine adducts (Pal, Pol) and Creatinine (Cre), while PC2 is more related to the increase of urinary AGE (uAGE) and Creatinine (Cre). However, treated subjects (i.e. subject administered with carnosine) show a positive covariance in PC1 which is higher than that observed before treatment (see above, tab 20) as well as a strong, negative

6 Intervention study of Carnosine in obese volunteers: bioavailability and reactive carbonyls species sequestering effect

covariance in PC2. This can be interpreted as an increased excretion of carnosine and related adduct, along with a decrease in the excretion of AGEs in carnosine administered subjects.

In particular the biplot of principal components (graph 13) (PC1 vs PC2) shows that PCA quite completely separates carnosine treated subjects (filled dots, solid line) from placebo subjects (empty dots, dashed line). Urinary creatinine is positively related to both components indicating that it has a random variability within the subjects tested. This variability is probably due to the broad concentration range detectable using a single time urine sampling as it was in the protocol used for urine collection.



Graph 13. Biplot of PC1 against PC2. CAR treated subjects are displayed as filled dots and solid line, placebo subjects in empty dots, dashed line. The treated and placebo group are separated by a strong negative correlation between uAGE and treatment and also CAR.

6.4 Discussion and conclusions

To our knowledge this is the first intervention study based on CAR supplementation in overweight/obese individuals. The bioavailability of carnosine and its effect on the oxidative stress and AGE/ALEs formation has been evaluated in both urine and serum samples and in particular the following biomarkers have been evaluated: AGEs (urine and plasma), CML (plasma), PCO (plasma), AOPP (plasma), HSA isoforms (plasma), CAR (urine) and CAR-RCS adducts (urine).

In serum, no significant differences (ANOVA or t test) were observed among the different experimental groups and for any of the considered parameters. Moreover, serum carnosine was not detected in any subject (LOD= 0.1 μM) accordingly to previous studies [22] and this is well explained by considering the presence of human carnosinases that rapidly hydrolyses the dipeptide. Serum carnosine can be detected only at high doses of supplemented carnosine (i.e. 6 gr as reported by x) which is able to induce a saturating effect of the hydrolytic enzyme.

By contrast, urine carnosine was detected in all the 31 patients either before and after CAR intake. It should be noted that free CAR, in particular after CAR supplementation, is characterized by an high variation among the subjects of the same group and this can be due to different reasons such as differences in carnosinases activity/content among the subjects, collection of the urine that was at one time point, no ovo-lacto-vegetarian diet assumed by the subjects during the intervention study. Normalization of the data on the basis of creatinine content did not reduce the variability.

The presence of CAR in urine but not in serum can be explained by the fact that a certain amount of carnosine, lower than the LLOD, is reached at serum level and that it is excreted as such in the urine where it is accumulated reaching a detected amount. Another explanation can be due considering that CAR is synthesized in

6 Intervention study of Carnosine in obese volunteers: bioavailability and reactive carbonyls species sequestering effect

the kidney starting from the two constitutive aa that are formed in circulation by the hydrolytic effect of carnosinase on the dipeptide. Although the large variability of CAR within each group, we observed that carnosine treatment significantly increased the urinary content of carnosine.

Two CAR-ACR adducts were detected in all the 31 patients both before and after the supplementation: CAR-propanal and CAR-propanol. CAR-propanal derives from the Michael addition of acrolein (ACR) to carnosine, while CAR-propanol is formed by the reduction of the carbonyl group belonging to CAR-propanal to the corresponding alcohol derivative. It is noteworthy that these adducts were found also before CAR supplementation, suggesting that carnosine acts as an endogenous detoxifier of acrolein.

The identification of the two CAR-ACR adducts confirm the data previously published by Baba et al [10], reporting that CAR-propanal and CAR-propanol were found as the most abundant CAR adducts in the urine of healthy non-smoker volunteers. Moreover Baba et al found other CAR adducts and metabolites such as histidine-propanal, histidine-propanol and low levels of histidine-HNE and histidine-DHN. We identified such adducts in previous animal studies but not in the current human study and this can be due to several reasons such as the differences in terms of the CAR treatment in the volunteers (acute vs chronic), analytical methods and urine collection (single spot vs 24 hours collection).

Furthermore we found that before the supplementation 55 % of the adduct was in the reduced form, CAR-propanol; after the treatment the reduced form decreased to 46 %. For sake of comparison Baba et al found in reduced form 75 % of carnosine conjugates of acrolein.

Then it is to take in account that in the urine of six young volunteers we could detect only a very low amount of CAR-propanal and CAR-propanol, that was roughly 160 nM and 360nM respectively. It is to remark that these subjects were set on a ovo-lacto-vegetarian diet in order to considerably decrease CAR excretion in urine. Since we've found a positive correlation between CAR

6 Intervention study of Carnosine in obese volunteers: bioavailability and reactive carbonyls species sequestering effect

excretion and CAR-ACR-adducts excretion it could be proposed that a withdrawal of carnosine could decrease also the CAR-ACR adducts levels.

As already reported in the results chapter, we performed ANOVA test between all the possible groups with all the urinary and serum parameters evaluated, but eventually we could not find any significant difference between treated and placebo groups neither between pre and post treatment groups. However, by means of t test previously reported, we found a significant increase trend of free CAR and CAR-propanal adduct in the treated group after 3 months of CAR intake. Unfortunately considering CAR-propanol a significant variation between treated and placebo group wasn't find, but more interestingly a positive parametric correlation between the excretion of CAR and CAR-ACR-adducts was identified. Based on these evidences it could be suggested that, also in vivo, CAR effectively detoxify RCS like acrolein by a direct quenching mechanism that leads to the formation of unreactive CAR-adducts. This detoxifying metabolic pathway based on histidine dipeptides have been already evaluated and confirmed both in vitro and in vivo studies, both in healthy lean humans and rodents.

These ex vivo findings support previous in vitro studies, published by our research group, that confirmed an efficient acrolein sequestering ability of CAR by means of HPLC-UV studies and moreover all possible CAR-ACR adducts formed after in vitro incubation were characterized by ESI-MS analysis [3]. In this framework it is important to point out that acrolein is the most reactive electrophilic compound among RCS and it is neurotoxic, furthermore ACR, besides endogenous sources, acrolein is also generated by the processing of several foods and it is present in tobacco smoke and automobile exhaust [23]. hence it is noteworthy that CAR can efficiently quench ACR also in vivo.

Moreover concerning in animal models of metabolic syndrome and atherosclerosis, carnosine treatment induced a significant protective effect, which was associated with a reduction of RCS-modified proteins (ALEs and AGEs) and with the excretion of carnosine-RCS adducts both in APO E null mice and Zucker

6 Intervention study of Carnosine in obese volunteers: bioavailability and reactive carbonyls species sequestering effect

obese rats [7] [8]. However it is still not clear if this protective effect, mediated by histidine dipeptides, is related only to a direct quenching mechanism or it involves other pathways such as interaction with AGE receptor.

PCA analysis was then performed in order to find some relationship between all the parameters measured in urine and plasma. PCA was taken in account because multiple regression analysis such as ANOVA requires that the parameters considered should be orthogonal, ie they cannot be mutually related [24]. An ANOVA performed on mutually related parameters could give limited reliability results. In the context of this study the various parameters measured are in reality mutually interact, as in the case of many biological variables.

Principle component analysis is a statistical procedure that reduce the dimensionality of the original possibly correlated variables and convert them in principal components. These principal components (PC) are calculated by finding a linear combination of those variables that explains most of the variability within the data-set considered. The resulting principal components are linearly uncorrelated variables and each PC explain a percentage of the variance of the data.

This kind of statistical analysis have been recently used to perform clinical data analysis concerning breast cancer [25] but also to develop a single parameter screening tool for metabolic syndrome [26]. Hence PCA could represent an alternative to classical regression analysis of multivariable dataset.

Concerning the serum parameters we couldn't find any correlation or discrimination of the results, but more interestingly remarkable and consistent results were found by the analysis of urinary parameters.

As reported in the corresponding results paragraph it was shown, from the first component, that both before and after the CAR intake, the levels of free CAR and CAR-ACR-adducts as well as creatinine positively correlate thus corroborating the direct quenching mechanism of CAR. Moreover the second component shown that the urinary AGE levels were strongly negative correlated with the treatment

6 Intervention study of Carnosine in obese volunteers: bioavailability and reactive carbonyls species sequestering effect

and mildly negative correlated with CAR concentration in urine. In particular the treated and placebo groups after the treatment are completely separated on the basis of this negative covariance between treatment and urinary AGE. Therefore it is logical to suppose that carnosine can detoxify RCS by a direct quenching mechanism and this could lead to reduced levels of RCS, thus attenuating RCS induced cellular injury as well as tissue inflammation.

In the light of these results it appears noteworthy continuing to study the in vivo RCS detoxifying action induced by histidine dipeptides in order to gain a deeper understanding of their mechanism of action and to once more demonstrate that this class of compounds are promising preventing and therapeutic agents concerning RCS based diseases.

6.5 References

1. Zhou S, Decker EA. Ability of carnosine and other skeletal muscle components to quench unsaturated aldehydic lipid oxidation products. *J Agric Food Chem.* 1999 Jan;47(1):51-5.
2. Aldini G, Carini M, Beretta G, Bradamante S, Facino RM. Carnosine is a quencher of 4-hydroxy-nonenal: through what mechanism of reaction? *Biochem Biophys Res Commun.* 2002 Nov;298(5):699-706.
3. Carini M, Aldini G, Beretta G, Arlandini E, Facino RM. Acrolein-sequestering ability of endogenous dipeptides: characterization of carnosine and homocarnosine/acrolein adducts by electrospray ionization tandem mass spectrometry. *J Mass Spectrom.* 2003 Sep;38(9):996-1006.
4. Aldini G, Granata P, Carini M. Detoxification of cytotoxic alpha,beta-unsaturated aldehydes by carnosine: characterization of conjugated adducts by electrospray ionization tandem mass spectrometry and detection by liquid chromatography/mass spectrometry in rat skeletal muscle. *J Mass Spectrom.* 2002 Dec;37(12):1219-28.
5. Hipkiss AR. Carnosine and its possible roles in nutrition and health. *Adv Food Nutr Res.* 2009;57:87-154.
6. Orioli M, Aldini G, Benfatto MC, Facino RM, Carini M. HNE Michael adducts to histidine and histidine-containing peptides as biomarkers of lipid-derived carbonyl stress in urines: LC-MS/MS profiling in Zucker obese rats. *Anal Chem.* 2007 Dec;79(23):9174-84.
7. Aldini G, Orioli M, Rossoni G, Savi F, Braidotti P, Vistoli G, et al. The carbonyl scavenger carnosine ameliorates dyslipidaemia and renal function in Zucker obese rats. *J Cell Mol Med.* 2011 Jun;15(6):1339-54.
8. Menini S, Iacobini C, Ricci C, Scipioni A, Blasetti Fantauzzi C, Giaccari A, et al. D-Carnosine octylester attenuates atherosclerosis and renal disease in ApoE null mice fed a Western diet through reduction of carbonyl stress and inflammation. *Br J Pharmacol.* 2012 Jun;166(4):1344-56.
9. Baba SP, Hoetker JD, Merchant M, Klein JB, Cai J, Barski OA, et al. Role of aldose reductase in the metabolism and detoxification of carnosine-acrolein conjugates. *J Biol Chem.* 2013 Aug.
10. Baba SP, Hoetker JD, Merchant M, Klein JB, Cai J, Barski OA, et al. Role of aldose reductase in the metabolism and detoxification of carnosine-acrolein conjugates. *J Biol Chem.* 2013 Sep;288(39):28163-79.

6 Intervention study of Carnosine in obese volunteers: bioavailability and reactive carbonyls species sequestering effect

11. Grimsrud PA, Picklo MJ, Griffin TJ, Bernlohr DA. Carbonylation of adipose proteins in obesity and insulin resistance: identification of adipocyte fatty acid-binding protein as a cellular target of 4-hydroxynonenal. *Mol Cell Proteomics*. 2007 Apr;6(4):624-37.
12. Aldini G, Granata P, Orioli M, Santaniello E, Carini M. Detoxification of 4-hydroxynonenal (HNE) in keratinocytes: characterization of conjugated metabolites by liquid chromatography/electrospray ionization tandem mass spectrometry. *J Mass Spectrom*. 2003 Nov;38(11):1160-8.
13. FDA. Guidance for industry: bioanalytical method validation. *Food and Drug Administration, Center for Drug Evaluation and Research (CDER), Center for Veterinary Medicine (CV)* 2001.
14. Heinegård D, Tiderström G. Determination of serum creatinine by a direct colorimetric method. *Clin Chim Acta*. 1973 Feb;43(3):305-10.
15. Bradford MM. A rapid and sensitive method for the quantitation of microgram quantities of protein utilizing the principle of protein-dye binding. *Anal Biochem*. 1976 May;72:248-54.
16. Zor T, Selinger Z. Linearization of the Bradford protein assay increases its sensitivity: theoretical and experimental studies. *Anal Biochem*. 1996 May;236(2):302-8.
17. Witko-Sarsat V, Friedlander M, Capeillère-Blandin C, Nguyen-Khoa T, Nguyen AT, Zingraff J, et al. Advanced oxidation protein products as a novel marker of oxidative stress in uremia. *Kidney Int*. 1996 May;49(5):1304-13.
18. Levine RL, Williams JA, Stadtman ER, Shacter E. Carbonyl assays for determination of oxidatively modified proteins. *Methods Enzymol*. 1994;233:346-57.
19. Reddy S, Bichler J, Wells-Knecht KJ, Thorpe SR, Baynes JW. N epsilon-(carboxymethyl)lysine is a dominant advanced glycation end product (AGE) antigen in tissue proteins. *Biochemistry*. 1995 Aug;34(34):10872-8.
20. Zhang Z, Marshall AG. A universal algorithm for fast and automated charge state deconvolution of electrospray mass-to-charge ratio spectra. *J Am Soc Mass Spectrom*. 1998 Mar;9(3):225-33.
21. Aldini G, Gamberoni L, Orioli M, Beretta G, Regazzoni L, Maffei Facino R, et al. Mass spectrometric characterization of covalent modification of human serum albumin by 4-hydroxy-trans-2-nonenal. *J Mass Spectrom*. 2006 Sep;41(9):1149-61.

6 Intervention study of Carnosine in obese volunteers: bioavailability and reactive carbonyls species sequestering effect

22. Yeum KJ, Orioli M, Regazzoni L, Carini M, Rasmussen H, Russell RM, et al. Profiling histidine dipeptides in plasma and urine after ingesting beef, chicken or chicken broth in humans. *Amino Acids*. 2010 Mar;38(3):847-58.
23. Aldini G, Orioli M, Carini M. Protein modification by acrolein: relevance to pathological conditions and inhibition by aldehyde sequestering agents. *Mol Nutr Food Res*. 2011 Sep;55(9):1301-19.
24. Larson MG. Analysis of variance. *Circulation*. 2008 Jan;117(1):115-21.
25. Buciński A, Bączek T, Krysiński J, Szoszkiewicz R, Załuski J. Clinical data analysis using artificial neural networks (ANN) and principal component analysis (PCA) of patients with breast cancer after mastectomy. *Reports of Practical Oncology & Radiotherapy*. 2007 1//;12(1):9-17.
26. Chang CH, Yen CH, Chen MY. Using principal component analysis to develop a single-parameter screening tool for metabolic syndrome. *BMC Public Health*. 2010;10:708.

7 Conclusions

Non enzymatic protein covalent modifications are involved in the toxic effects induced by xenobiotics and endogenous electrophilic compounds. Once the protein is covalently modified, the corresponding protein function is deranged due to several mechanisms such as the direct modification of the active site, the change of protein conformation and protein oligomerization and aggregation. Covalently modified proteins can also be toxic by acting as antigens, eliciting an immuno based response, and as ligands of RAGE receptors inducing an inflammatory response.

By considering that covalently modified proteins are involved in many human diseases and toxic responses but are poorly analytically characterized, the aim of the Ph.D thesis was to set up novel mass spectrometric strategies in order to identify, characterize and quantify protein adducts in vitro as well as in ex vivo conditions.

Mass spectrometric hyphenated techniques have greatly improved the study of protein covalent modification, and this is due to the development of soft ionization techniques, such as ESI and MALDI, along with the advent of commercially available high resolution analysers such as TOF reflectron and Orbitrap. Before the establishment of MS based techniques, immunochemistry analysis such as RIA, EIA and SDS-PAGE or 2D-electrophoresis analysis were the most used. Even though these techniques are still used, they are limited because they do not permit full characterization of the adduct (site of modification, identity of the protein undergoing modification, structure of the adducted moiety) or quantify it.

The results reported in the present Ph.D thesis have clearly shown the importance of novel high resolution mass spectrometric strategies in obtaining molecular insights into protein covalent modifications.

7 Conclusions

The MS strategies were applied to two different applications: elucidation of amoxicillin protein haptation and covalent binding of peptides by endogenous electrophilic compounds. In both studies MS strategies were applied to both in vitro and ex vivo samples.

Amoxicillin (AX), a β lactam antibiotic widely prescribed in Europe and the USA, is very often involved in drug allergic reactions due to protein haptation. Identification of Amoxicillin target protein and the reaction mechanism represents one aim of the present research program.

Human serum was incubated with AX at different concentrations and Western blotting analyses identified human serum albumin (HSA), transferrin and immunoglobulin as AX protein target. HSA was found as the most reactive target and 5 Lys residues were found to be covalently modified by AX, namely Lys 190, Lys 199, Lys 541, Lys351 and Lys432. Moreover molecular modelling was used in order to determine the key features of modified Lys and it was found that low basicity, reduced surface accessibility to solvent and the interaction of AX with the surrounding residues are crucial for Lys reactivity. An index of reactivity was also drawn and Lys 190 was the most reactive residue, followed by Lys 199 and the other three residues, namely Lys 541, 351 and 432. This index of reactivity was then confirmed by an ex vivo study that identified Lys 190 as the only modification site in volunteers orally treated with AX. This noteworthy result was obtained by setting-up a customized MS analysis carried out by a high resolution mass spectrometer, LTQ Orbitrap XL, and then confirmed by using different analytical strategies based on Western blotting, triple quadrupole MRM scan.

It should be noted that the residues found modified in this work were the same as those found by other research groups involving other β -lactam antibiotics such as penicillin [1], flucloxacillin [2] and piperacillin [3], confirming the reactivity of recurrent Lys residue towards this class of drug.

7 Conclusions

Another important issue evidenced by this study is that the AX protein adducts were detected in non AX allergic patients. Hence it is logical to suppose that there are concomitant factors that are required for the allergic reaction, such as danger signals or concurrent diseases. Hence future studies will be aimed correlating AX protein adducts and allergic reactions.

In summary, a highly sensitive mass spectrometric strategy for the detection and identification of AX-protein adducts was firstly applied to an *in vitro* study and this permitted the identification of the main protein targets of AX. The analytical approach was then applied to an *ex vivo* study permitting to identify albumin Lys 190 as the modified site after AX oral intake. These studies represent a starting point to characterize other AX binding proteins such as transferrin and immunoglobulin G and more in general for the untargeted identification and quantification of penicillin-protein adducts.

So it could be stated that HRMS based analytical approaches concur to better understand the protein haptentation mechanism and to design more relevant and specific antigens to be used in diagnostic tests.

Since MS-hyphenated techniques can provide a broad range of information about the covalent modification of proteins and peptides, this analytical strategy was also used to evaluate the direct quenching mechanism of reactive carbonyl species by carnosine (CAR). CAR was supplemented to overweight and obese individuals and both urine and plasma samples were analyzed to study the metabolic fate of carnosine as RCS quencher. Carnosine RCS adducts were searched for in the urine by LC-MS/MS analysis and using a high resolution Orbitrap mass spectrometer employed in a customised data dependent scan.

CAR and two CAR-acrolein adducts, CAR-propanal and CAR-propanol, were detected, identified and quantified. It is interesting to point out that the two adducts as well as CAR were detected both before and after carnosine supplementation, as well as in the placebo group, thus demonstrating that carnosine acts as an endogenous detoxifier of acrolein.

7 Conclusions

CAR and CAR-propanal significantly increased after three months of CAR-intake and a parametric correlation showed that urinary CAR-ACR adducts directly correlate with CAR urinary levels. Considering these results it could be stated that CAR effectively detoxifies ACR by a direct quenching mechanism in obese subjects.

Moreover, thanks to principle component analysis (PCA) a positive correlation between urinary CAR and CAR-ACR adducts was confirmed and that the urinary AGE levels were negative correlated with CAR treatment.

These results are notable since they demonstrate the sequestering ability of CAR towards ACR which is a neurotoxic intermediate and the most reactive compound among RCS [4]. Nonetheless, these results confirm previous studies on animal models of metabolic syndrome diseases in which CAR treatment increased CAR-RCS adducts in urines and decreased AGEs and ALEs levels [5, 6].

In conclusion, the development of dedicated MS strategies have enhanced the knowledge of CAR metabolism and the detoxifying role of CAR in *ex vivo* context and once again confirmed the importance of high resolution MS strategies in the study of protein covalent modification.

7.1 References

1. Yvon M, Anglade P, Wal JM. Identification of the binding sites of benzyl penicilloyl, the allergenic metabolite of penicillin, on the serum albumin molecule. *FEBS Lett.* 1990 Apr;263(2):237-40.
2. Jenkins RE, Meng X, Elliott VL, Kitteringham NR, Pirmohamed M, Park BK. Characterisation of flucloxacillin and 5-hydroxymethyl flucloxacillin haptenated HSA in vitro and in vivo. *Proteomics Clin Appl.* 2009 Jun;3(6):720-9.
3. Whitaker P, Meng X, Lavergne SN, El-Ghaiesh S, Monshi M, Earnshaw C, et al. Mass spectrometric characterization of circulating and functional antigens derived from piperacillin in patients with cystic fibrosis. *J Immunol.* 2011 Jul;187(1):200-11.
4. Carini M, Aldini G, Beretta G, Arlandini E, Facino RM. Acrolein-sequestering ability of endogenous dipeptides: characterization of carnosine and homocarnosine/acrolein adducts by electrospray ionization tandem mass spectrometry. *J Mass Spectrom.* 2003 Sep;38(9):996-1006.
5. Menini S, Iacobini C, Ricci C, Scipioni A, Blasetti Fantauzzi C, Giaccari A, et al. D-Carnosine octylester attenuates atherosclerosis and renal disease in ApoE null mice fed a Western diet through reduction of carbonyl stress and inflammation. *Br J Pharmacol.* 2012 Jun;166(4):1344-56.
6. Aldini G, Orioli M, Rossoni G, Savi F, Braidotti P, Vistoli G, et al. The carbonyl scavenger carnosine ameliorates dyslipidaemia and renal function in Zucker obese rats. *J Cell Mol Med.* 2011 Jun;15(6):1339-54.

8 Scientific activity during the PhD course

List of publications

1. On the self-condensation of aminoguanidine leading to 1, 1, 4, 10, 10-pentaamino-2, 3, 5, 6, 8, 9-hexaazadeca-1, 3, 5, 7, 9-pentaene (structure elucidation through X-ray powder diffraction)

Tasso B, Pirisino G, Novelli F, Garzon D, Fruttero R, Sparatore F, Colombo V, Sironi A.

Tetrahedron 2014 Oct 28

2. Mass spectrometric strategies for the identification and characterization of human serum albumin covalently adducted by amoxicillin: ex vivo studies.

Garzon D, Ariza A, Regazzoni L, Clerici R, Altomare A, Sirtori FR, Carini M, Torres MJ, Pérez-Sala D, Aldini G.

Chem. Res. Toxicol 2014 Sep 14

3. Standardization of solvent extracts from *Onopordum acanthium* fruits by GC-MS, HPLC-UV/DAD, HPLC-TQMS and ¹H-NMR and evaluation of their inhibitory effects on the expression of IL-8 and E-selectin in immortalized endothelial cells (HUVEctert).

Daci A, Gold-Binder M, Garzon D, Patea A, Beretta G

Nat. Prod. Commun 2014 Jul 9

4. A novel high resolution MS approach for the screening of 4-hydroxy-trans-2-nonenal sequestering agents.

Colzani M, Criscuolo A, De Maddis D, Garzon D, Yeum KJ, Vistoli G, Carini M, Aldini G.

J Pharm Biomed Anal 2014 Mar 25

5. A rapid profiling of gallotannins and flavonoids of the aqueous extract of *Rhus coriaria* L. by flow injection analysis with high-resolution mass spectrometry assisted with database searching.

Regazzoni L, Arlandini E, Garzon D, Santagati NA, Beretta G, Maffei Facino R.

J Pharm Biomed Anal 2013 Jan 18

6. Protein haptentation by amoxicillin: high resolution mass spectrometry analysis and identification of target proteins in serum.

Ariza A, Garzon D, Abánades DR, de los Ríos V, Vistoli G, Torres MJ, Carini M, Aldini G, Pérez-Sala D.

J Proteomics 2012 Dec 21

Book chapters

1. Carnosine and derivatives as inhibitors of protein covalent modifications induced by reactive carbonyl species

Colzani M, Garzon D and Aldini G

Imidazole Dipeptides: Chemistry, Analysis, Function, and Effects

Victor Preedy

Royal Society of Chemistry, ISBN 9781849738903, 2015

Communication to national and international congresses

Oral Communication

1. High resolution mass spectrometric strategies for detection of proteins and peptides covalently modified by electrophilic xenobiotics and endogenous intermediates

Garzon D

Summer School in Pharmaceutical Analysis SSPA 2014

September 23-25, 2014 Rimini (RN) Italy

2. Mass spectrometric strategies for studying albumin covalent modifications induced by xenobiotics and endogenous electrophilic cytotoxic compounds

Garzon D, Colzani M., Cannizzaro L., Carini M. and Aldini G.

Nuove Prospettive in Chimica Farmaceutica NPCF 7

May 29-31, 2013 Savigliano (CN) Italy

Poster

1. A new high resolution mass spectrometry application for the comprehensive analysis of the ligand binding properties of RAGE

De Maddis D, Degani G, Pancotti A, Garzon D, Vistoli G, Romeo S, Carini M, Popolo L, Aldini G

Nuove Prospettive in Chimica Farmaceutica NPCF 6

April 15-17, 2012 Riccione (RN) Italy

2. Reactive carbonyl species quenching ability and selectivity of a bioavailable carnosine peptidomimetic (FL-926-A16) in respect to L-carnosine and selected reference compounds

Regazzoni L, De Maddis D, Garzon D, Carini M, Aldini G

International Congress on " Carnosine in exercise and disease"

July 10-12, 2011 Ghent (Belgium)